On the Propagation of Scale-Dependent Macroeconomic Shocks into Asset Prices

Georgios Xyngis

A thesis submitted for the degree of

Doctor of Philosophy

University of East Anglia

Faculty of Social Sciences

December 2016

Declaration & Copyright

This thesis represents solely my own work and it does not include any co-authored material. Likewise, all errors are mine. Replication files & codes for all results are available upon request.

The total number of words is 56,443.

Abstract

This thesis focuses on the propagation of scale-specific (i.e., horizon-dependent) macroeconomic shocks into asset prices. In particular, chapter 1 provides an introduction to the theory and methods necessary for understanding scale-dependencies in financial economics. First, I present the multiresolution-based decompositions for weakly stationary time series of Ortu et al. (2013) and discuss its connection with other techniques in the literature. Next, I analyse the power and size properties of multi-scale variance ratio tests that distinguish a white noise process from a process whose scale-dependent components are serially correlated. Finally, I present an extension of the framework of Bandi et al. (2016) for scale-specific predictability. In chapter 2, I show that a single factor that captures assets' exposure to business-cycle variation in macroeconomic uncertainty can explain the level and cross-sectional differences of asset returns. In addition, I find that - in contrast with previous studies in the literature - macro uncertainty is not a valid risk factor under the ICAPM. Chapter 3 provides an empirical assessment of Epstein-Zin preferences in the frequency domain. I demonstrate that the strict conditions implied by the spectral decomposition of recursive-preferences are not empirically satisfied. That is, macroeconomic shocks with frequencies lower than the business-cycle are not robustly priced in asset prices.

Acknowledgements

I am greatly indebted to Andrea Tamoni for kindly providing code & help when I started working on this area for my dissertation. Also, I would like to thank Christine Mallin, Peter Moffatt and Anastasiya Shamshur for helpful comments and suggestions and Karina Nielsen for valuable support. Partial funding from the Faculty of Social Sciences of the University of East Anglia is acknowledged.

Chapter 2 has improved from comments by three anonymous reviewers, Jules van Binsbergen, Martijn Boons, George Constantinides, Wayne Ferson, Sergey Gelman (EFMA discussant), Klaus Grobys (PFMC discussant), conference participants at the 2016 European Financial Management Conference, the 2016 Royal Economic Society PhD Meeting, the 2015 Paris Financial Management Conference and seminar participants at Queen's Management School and Swansea Management School. Chapter 2 was shortlisted for the John A. Doukas PhD Best Paper Award at the 2016 EFMA Conference. Chapter 3 has improved from comments by two anonymous reviewers, Christian Gourieroux, John Doukas, Stefano Giglio, conference participants at the 48th Money, Macro and Finance Research Group Annual Conference, the 2016 Portsmouth-Fordham Conference on Banking & Finance and participants at the 2016 SoFiE Summer School.

Contents

List of Figures

List of Tables

Introduction to Thesis

In this thesis, I explore the link between financial markets and the macroeconomy. In particular, I examine how scale-specific (i.e., horizon-dependent) macroeconomic shocks propagate to asset prices. The core intuition behind this work is that shocks that affect an economy can be classified along two dimensions. That is, on the basis of their arrival time as in the standard Wold decomposition (see the early studies of Slutzky 1937; Yule 1927; Frisch 1933[1], for a theoretical systematization see Wold, 1938 and for a review Diebold, 1998) and across their level of resolution (i.e., scale) as measured by their half life in line with Ortu et al. (2013, 2016) and Bandi et al. (2016).

For instance, consider a zero-mean, weakly-stationary (purely non-deterministic) stochastic process $\{g_t\}_{t\in\mathbb{Z}}$. In line with the standard Wold decomposition the process g_t can be written as a linear combination of lagged values of a white noise process. That is, g_t has an infinite moving average MA(∞) representation[2] of the following form

$$g_t = \sum_{k=0}^{\infty} \alpha_k \varepsilon_{t-k}$$

where $\sum_{k=0}^{\infty} \alpha_k^2 < \infty, \alpha_0 = 1$ and ε_t is a white noise process. In contrast, in the generalized (i.e., multi-scale) Wold type decomposition of Bandi et al. (2016) the process can be represented

[1] Slutzky (1937) and Yule (1927) are the first to demonstrate that a moving average of a random series can generate oscillations and periodicities when no such movements exist in the original data. The Slutzky-Yule effect led to the formalization of ARMA processes.

[2] For classic text-book level treatments of time-series concepts see Hamilton (1994); Hayashi (2000) or Brockwell and Davis (2009).

(assuming again for simplicity and without any loss of generality that the process is zero-mean and for a fixed $J \leq \log_2 T$ where T is the length of g_t) as

$$g_t = \sum_{j=1}^{J} \sum_{k=0}^{\infty} \alpha_{j,k} \varepsilon_{t-k\times 2^j}^{(j)}$$

where the shocks $\varepsilon_t^{(j)}$, $t = k \times 2^j, k \in \mathbb{Z}$ that drive the time-series are now scale-specific (i.e., they depend on both time t and scale j). This modelling approach implies that the scale-specific shocks may carry unique information (i.e., *scale-wise heterogeneity*) and hence provides strong motivation to analyze the relation between macroeconomic fluctuations and asset prices on a scale-by-scale basis. More specifically, in this thesis I address the following questions:

- Are all macro uncertainty shocks created equal? In other words, do they have the same information content across different horizons and scales? If not, what are the value implications of macroeconomic shocks localized at a specific level of resolution?
- How do risk prices and risk exposures with respect to measures of macroeconomic activity change as we alter the investment horizon (i.e., across different time scales)?
- Are the strict conditions implied by Epstein-Zin preferences in the frequency domain empirically satisfied? That is, are low-frequency macro shocks robustly priced in asset prices?

Moreover, from a more technical perspective:

- How easy it is to detect persistent components of a time-series localized at low frequencies?
- Under what conditions does scale-specific predictability translate into long-horizon predictability?

The remainder of this thesis is structured as follows: Chapter 1 presents the econometric framework necessary to understand scale-dependencies in financial economics. I concentrate on the properties of multi-scale variance ratio tests for serially correlated decimated components and on the link

between scale-specific predictability and long-horizon aggregation. Chapters 2 and 3 provide two (robust) empirical studies linking macroeconomic fluctuations to asset prices. Specifically, chapter 2 focuses on business-cycle macro uncertainty while chapter 3 looks on both moments of macroeconomic activity (i.e., growth and volatility). A brief summary of the thesis along with a general appendix are available at the end.

Chapter 1

Understanding Scale-Dependencies in Financial Economics: Theory and Methods

1.1 Introduction

This chapter serves as an introduction to time series modelling with multiple scales and scale-wise heterogeneity. The theory and methods presented here provide the necessary background for the empirical work in chapters 2 and 3. In particular, section 1.2 presents a persistence-based decomposition for weakly stationary time series based on the work of Ortu, Tamoni, and Tebaldi (2013) while section 1.3 discusses its connection with other techniques in the literature. Section 1.4 introduces the econometric process of decimation which yields an alternative decimated decomposition by using only a finite-number of non-overlapping points. Section 1.5 describes the generalized (time and scale) Wold representation implied by the decomposition of Ortu et al. (2013). Section 1.6 demonstrates that standard portmanteau tests for serial correlation fail to detect components localized at a specific level of persistence. Section 1.7 discusses the multi-scale variance ratio test of Gençay and Signori (2015) for the white noise hypothesis and the modified version of Ortu et al. (2013) for a process whose decimated components are serially correlated. Section 1.8 analyzes the size and power properties of the modified variance ratio test through Monte Carlo simulations. Sec-

tion 1.9 discusses the link between scale-specific predictability and predictability upon aggregation. Finally, section 1.10 presents the novel framework of Bandi and Tamoni (2016) for the analysis of risk compensations on a scale-by-scale basis (i.e., across investment horizons) and section 1.11 concludes.

1.2 The Persistence-based Decomposition of Ortu et al. (2013)

Consider a weakly-stationary time series $\{g_t\}_{t\in\mathbb{Z}}$. Let $g_t^{(j)}$ denote fluctuations of the series with half-life in the interval $[2^{j-1}, 2^j)$, that is

$$g_t^{(j)} = \frac{\sum_{i=0}^{2^{(j-1)}-1} g_{t-i}}{2^{(j-1)}} - \frac{\sum_{i=0}^{2^j-1} g_{t-i}}{2^j} = \pi_t^{(j-1)} - \pi_t^{(j)} \tag{1.1}$$

where $j \geq 1$, $\pi_t^{(0)} \equiv g_t$ and the element $\pi_t^{(j)}$ satisfies the recursion

$$\pi_t^{(j)} = \frac{\pi_t^{(j-1)} + \pi_{t-2^{j-1}}^{(j-1)}}{2}. \tag{1.2}$$

For any $1 \leq J \leq \log_2 T$, the series $\{g_t\}$ can be written as

$$g_t = \sum_{j=1}^{J} \left\{ \pi_t^{(j-1)} - \pi_t^{(j)} \right\} + \pi_t^{(J)} = \sum_{j=1}^{J} g_t^{(j)} + \pi_t^{(J)}, \tag{1.3}$$

i.e. the series can be decomposed into a sum of components with half-life belonging to a specific interval plus a long-run average. For instance, for $J = 2$ the time series of interest is given by

$$g_t = \underbrace{\frac{g_t - g_{t-1}}{2}}_{g_t^{(1)}} + \underbrace{\frac{g_t + g_{t-1} - g_{t-2} - g_{t-3}}{4}}_{g_t^{(2)}} + \underbrace{\frac{g_t + g_{t-1} + g_{t-2} + g_{t-3}}{4}}_{\pi_t^{(2)}}. \tag{1.4}$$

Note that this decomposition is non-anticipative and can be computed using only past observations (i.e., not subject to look-ahead bias).

Nested within the MODWT family

The decomposition of Ortu et al. (2013) is identical to a multi-resolution based decomposition via the Maximum Overlap Discrete Wavelet Transform (MODWT) where the extraction is based on the Haar filter $\{h_l\}_0^1 = (1/2, -1/2)$. The difference is that the MODWT can accommodate several other filters (for instance Daubechies and Coiflet filters). That is, the decomposition of Ortu et al. (2013) is nested within the MODWT family. Below I illustrate this relationship. **Most of my discussion in this section closely follows the work of Percival and Walden (2000) and especially Gençay, Selçuk, and Whitcher (2001, chapter 4) - I refer the interested reader to these textbooks and the references therein for more information**. For empirical applications of wavelet analysis in finance and economics see Ramsey (1999) and Crowley (2007).

The MODWT[3] consists of a set of linear filters which, given a time series $\mathbf{y} = \{y_t\}_{t\in\mathbb{Z}}$ to be filtered, generate a collection of vectors of the same length that capture the characteristics of the original series at different time scales. In particular, a vector $\{h_l\} = (h_0, \ldots, h_{L-1})$ in $\mathbb{R}^L$ gives rise to a linear time invariant filter by means of the convolution operation. The convolution of $\{h_l\}$ and $\{y_t\}$ is the sequence

$$h * y_t = \sum_{l=-\infty}^{l=\infty} h_l y_{t-1}, \quad \forall t \tag{1.5}$$

where $h_l = 0$ for all $l < 0$ and $l \geq L$. A wavelet filter $\{h_l\}$ of length L satisfies the following three basic properties:

$$\sum_{l=0}^{L-1} h_l = 0, \quad \sum_{l=0}^{L-1} h_l^2 = 1/2 \quad \text{and} \quad \sum_{l=-\infty}^{\infty} h_l h_{l+2n} = 0 \quad \text{for all integers } n \neq 0. \tag{1.6}$$

The first property (i.e., zero sum) ensures that h_l is associated with a differencing operation and

[3]It is a common practice in the wavelet literature to distinguish the objects related to the Maximum Overlap Discrete Wavelet Transform from those related to the Discrete Wavelet Transform (DWT) by using a tilde ($\sim$) in the first case. Since I only refer to the MODWT in this section I do not follow this convention. The MODWT is also refereed to as the stationary DWT (Nason and Silverman, 1995), the translation-invariant DWT (Coifman and Donoho, 1995) and the time-invariant DWT (Pesquet et al., 1996).

thus identifies changes in the data. The second property states that its L^2 distance is 1/2. The third property ensures that it is orthogonal to its even shifts. The natural complement to the wavelet filter is the scaling filter $\{g_l\}$ defined by the quadrature mirror relationship[4]

$$g_l = (-1)^{l+1} h_{L-1-l} \tag{1.7}$$

for $l = 0, \ldots, L-1$. Similarly to Equation (1.6), the scaling filter satisfies the following properties:

$$\sum_{l=0}^{L-1} g_l = 1, \quad \sum_{l=0}^{L-1} g_l^2 = 1/2 \quad \text{and} \quad \sum_{l=-\infty}^{\infty} g_l g_{l+2n} = 0 \quad \text{for all integers } n \neq 0. \tag{1.8}$$

In other words, instead of differencing consecutive blocks of observations the scaling filter averages them.

The MODWT of level M for a given time series $\{y_t\}_{t=1}^T$ can be organized into $M+1$ vectors of length T

$$\mathbf{w} = \left(\mathbf{w}_1^{'}, \ldots, \mathbf{w}_M^{'}, \mathbf{v}_M^{'}\right)^{'} \tag{1.9}$$

where $M_{max} \leq \log_2 T$. In practice, the MODWT is computed recursively through a pyramid algorithm (see Mallat, 1989a,b). For each iteration of the pyramid algorithm three objects are required: the data vector, the wavelet filter h_l and the scaling filter g_l. The first steps begins by filtering[5] (convolving) the data with the wavelet and scaling filters to obtain the first level wavelet and scaling coefficients:

$$w_{1,t} = \sum_{l=0}^{L-1} h_l y_{t-1 \bmod T} \quad \text{and} \quad v_{1,t} = \sum_{l=0}^{L-1} g_l y_{t-1 \bmod T} \tag{1.10}$$

[4]The quadrature mirror relationship between the filters means that approximately perfect reconstruction of the series is possible.

[5]Periodic boundary conditions are imposed on $\{y_t\}$, that is $y_t \equiv y_t \, mod \, T$. Note that given two positive numbers α (the dividend) and β (the divisor), $\alpha \, modulo \, \beta$ (abbreviated as $\alpha \, mod \, \beta$) is the remainder of the Euclidean division of α by β .

for all $t = 1, \ldots, T$. In the second step, the filtering operations are applied to the scaling coefficients $v_{1,t}$ from the first iteration to obtain the second level wavelet and scaling coefficients:

$$w_{2,t} = \sum_{l=0}^{L-1} h_l v_{1,t-1 \bmod T} \quad \text{and} \quad v_{2,t} = \sum_{l=0}^{L-1} g_l v_{1,t-1 \bmod T} \tag{1.11}$$

for all $t = 1, \ldots, T$. Likewise, the mth step consists of applying the filtering operations as above to obtain the mth level of wavelet and scaling coefficients:

$$w_{m,t} = \sum_{l=0}^{L-1} h_l v_{m,t-1 \bmod T} \quad \text{and} \quad v_{m,t} = \sum_{l=0}^{L-1} g_l v_{m,t-1 \bmod T} \tag{1.12}$$

for all $t = 1, \ldots, T$. Keeping all vectors of wavelet coefficients and the level M scaling coefficients yields the expression in (1.9).

In matrix notation, the MODWT can be represented as $\mathbf{w} = \mathcal{W}\mathbf{y}$ where $\mathcal{W}$ is the $(M+1)\,T \times T$ matrix composed of the wavelet and scaling coefficients arranged on a row-by-row basis, that is

$$\mathcal{W} = \begin{pmatrix} \mathcal{W}_1 \\ \mathcal{W}_2 \\ \vdots \\ \mathcal{W}_M \\ \mathcal{V}_M \end{pmatrix}. \tag{1.13}$$

Let $\mathbf{d}_j = \mathcal{W}_j^\top \mathbf{w}_j$ for $j = 1, \ldots, M$ define the jth level wavelet detail associated with changes in $\{y_t\}$ at scale j where $\mathbf{w}_j = \mathcal{W}_j \mathbf{y}$. For a decomposition level $M = \log_2 T$ the final wavelet detail $\mathbf{d}_{M+1}$ is equal to the sample mean of the observations. A multiresolution analysis can now be defined as

$$y_t = \sum_{j=1}^{M} d_{j,t} + d_{M+1,t} \quad t = 1, \ldots, T. \tag{1.14}$$

where each observation y_t is a linear combination of wavelet detail coefficients.

For instance, consider the Haar wavelet filter of length $L = 2$ given by $\{h_l\}_0^1 = (h_0, h_1) =$

$(1/2, -1/2)$ and the corresponding scaling filter $\{g_l\}_0^1 = (g_0, g_1) = (1/2, 1/2)$. The first level wavelet and scaling coefficients of a time series $\{y_t\}$ are given by

$$w_{1,t} = \frac{1}{2}(y_t - y_{t-1}) \quad \text{and} \quad v_{1,t} = \frac{1}{2}(y_t + y_{t-1}) \tag{1.15}$$

for $t = 1, \ldots, T$. Note that $w_{1,t}$ is equivalent to $g_t^{(1)}$ and $v_{1,t}$ to $\pi_t^{(1)}$ in Equation (1.3). The use of the Haar filter $\{h_l\}_0^1 = (1/2, -1/2)$ is particular helpful since it relates scale-wise predictability to aggregation (see section 1.9 for further discussion).

1.3 Comparison with Other Techniques

Financial economists have long been interested in extracting different frequency components of a time series. For instance, business cycle theory is primarily concerned with understanding fluctuations in the range from 1.5 to 8 years. However, conventional methods for business cycles analysis tend to sweep low-frequency oscillations into the trend. As a result, significant information is removed form the analysis and thus lost (see also Comin and Gertler, 2006). Below I present three popular filtering methods:

- Beveridge-Nelson (BN) decomposition

Beveridge and Nelson (1981) provide a model-based method for decomposing a non-stationary time series into a permanent (i.e., trend) and a transitory (i.e., cyclical) component. In particular, assume that the univariate time series y_t is an $I(1)$ process with Wold representation given by

$$\Delta y_t = \mu + \psi(L)\epsilon_t \tag{1.16}$$

where $\Delta = 1 - L$ and ϵ_t are $i.i.d.$ $(0, \sigma^2)$ one-step-ahead forecast errors. The BN decomposition defines the stochastic trend as the limiting forecast of the level of the series minus any deterministic components given the current information set, that is

$$\tau_t^{BN} \equiv \lim_{J\to\infty} E\left[y_{t+J} - J\mu|\mathcal{F}_t\right] = \mu + \tau_{t-1}^{BN} + \psi\left(1\right)\epsilon_t \tag{1.17}$$

where $\mathcal{F}_t$ represents conditioning information available at time t. Note that the permanent component is a pure random walk with drift μ and variance $\sigma^2\psi\left(1\right)^2$. The remaining movements in the series are the $I\left(0\right)$ transitory component, i.e. $c_t^{BN} = y_t - \tau_t^{BN}$. In comparison with the BN decomposition, the persistence-based decomposition of Ortu et al. (2013) allows for J "transitory" components with different levels of (calendar-time) persistence operating at different frequencies. Furthermore, within the framework of Ortu et al. (2013) the shocks are functions of both time and scale.

- Hodrick-Prescott (HP) Filter

Hodrick and Prescott (1997) propose a procedure for representing a time series as the sum of a smoothly varying growth (i.e., trend) component and a cyclical component. In particular, a given time series $\{y_t\}_{t=1}^T$ can be written as

$$y_t = \tau_t + c_t \quad t = 1, \ldots, T \tag{1.18}$$

where the decomposition is obtained by solving the following minimization problem:

$$\underset{\{\tau_t\}}{min} \left\{ \sum_{t=1}^{T} \left(y_t - \tau_t\right)^2 + \lambda \sum_{t=1}^{T} \left[\left(\tau_{t+1} - \tau_t\right) - \left(\tau_t - \tau_{t-1}\right)\right]^2 \right\}. \tag{1.19}$$

The parameter $\lambda > 0$ penalizes variability in the growth component series. The larger the value of λ the less fluctuations are present in the growth component. As $\lambda \to \infty$, τ_t becomes a linear deterministic trend. For quarterly data, Hodrick and Prescott (1997) propose to set $\lambda = 1600$. Moreover, Ravn and Uhlig (2002) suggest that the parameter λ should be adjusted by multiplying it with the fourth power of the observation frequency ratios, i.e. λ should equal 6.25 for annual data and 129,600 for monthly data. The HP filter is criticized on the basis that it distorts the dynamics of the original time series (for instance, see Cogley and Nason, 1995 and Cogley, 2001) and induces

spurious cycles if the original time series is difference stationary (see Harvey and Jaeger, 1993).

- Baxter-King (BK) Filter

Baxter and King (1999) propose a finite moving-average approximation of an ideal band-pass filter[6]. The BK filter is designed to extract the components of a time series with fluctuations in a particular frequency range while removing higher and lower frequencies,

$$y_t^f = \sum_{i=-K}^{K} w_i y_{t-i} = w(L)\, y_t \tag{1.20}$$

where L is the lag operator. The weights can be derived from the inverse Fourier transform of the frequency response function under the constraint that the filter gain is zero at zero frequency. This restriction implies that the sum of the moving-average coefficients must be zero. For quarterly data Baxter and King (1999) recommend a lead-lag length of $K = 12$ while for annual data $K = 3$. Note that the components of the BK filter fail to capture a significant fraction of the variability in business-cycle frequencies (see Murray, 2003 and Guay and St.-Amant, 2005).

1.4 Decimation

The persistence-based decomposition in Equation (1.3) generates spurious serial correlation across different scales due to the mechanical overlapping of the moving averages that define the components $g_t^{(j)}$, for $j = 1, \ldots, J$. Following Renaud et al. (2005) this representation of the original time series $\{g_t\}_{t\in\mathbb{Z}}$ can be characterized as redundant. Ortu et al. (2013) and Bandi and Tamoni (2016) define an alternative decimated representation by selecting only the essential scale-wise information contained in the extracted components. Through the process of decimation the original time series can be summarized by a finite number of non-overlapping points

$$\left\{ g_t^{(j)}, t = k \times 2^j, k \in \mathbb{Z} \right\} \tag{1.21}$$

[6] An ideal band-pass filter removes the frequency components of a time series that lie within a particular range of frequencies

and

$$\left\{\pi_t^{(j)}, t = k \times 2^j, k \in \mathbb{Z}\right\} \tag{1.22}$$

referred to as decimated components. This approach resembles the work of Müller and Watson (2008) who extract the low-frequency dynamics of a time series by computing a finite number of weighted averages of the original data. However, within the framework of Ortu et al. (2013) the components are scale-specific.

The result above follows from the fact that for any level of persistence $J \geq 1$ a linear, invertible operator[7] $\mathcal{T}^{(J)}$ can be defined that maps uniquely the decimated components into the time series $\{g_t\}_{t\in\mathbb{Z}}$ (see Mallat, 1989a,b). For instance consider the simple case for $J = 2$. Assume the following vector of decimated components

$$\left[\pi_t^{(2)}, g_t^{(2)}, g_t^{(1)}, g_{t-2}^{(1)}\right]^\top \tag{1.23}$$

built on a block of length 2^2 of the original series where

$$\pi_t^{(2)} = \frac{1}{4}\left(g_t + g_{t-1} + g_{t-2} + g_{t-3}\right) \tag{1.24}$$

$$g_t^{(2)} = \frac{1}{2}\left(\frac{g_t + g_{t-1}}{2} - \frac{g_{t-2} + g_{t-3}}{2}\right) \tag{1.25}$$

$$g_t^{(1)} = \frac{1}{2}\left(g_t - g_{t-1}\right) \tag{1.26}$$

$$g_{t-2}^{(1)} = \frac{1}{2}\left(g_{t-2} - g_{t-3}\right) \tag{1.27}$$

and define the transformation (Haar) matrix

[7] For the construction of $\mathcal{T}^{(J)}$ in the general case see Daubechies (1990).

$$\mathcal{T}^{(2)} = \begin{pmatrix} \frac{1}{4} & \frac{1}{4} & \frac{1}{4} & \frac{1}{4} \\ \frac{1}{4} & \frac{1}{4} & -\frac{1}{4} & -\frac{1}{4} \\ \frac{1}{2} & -\frac{1}{2} & 0 & 0 \\ 0 & 0 & \frac{1}{2} & -\frac{1}{2} \end{pmatrix}. \tag{1.28}$$

In terms of matrix operations, the following relation holds

$$\begin{pmatrix} \pi_t^{(2)} \\ g_t^{(2)} \\ g_t^{(1)} \\ g_{t-2}^{(1)} \end{pmatrix} = \mathcal{T}^{(2)} \begin{pmatrix} g_t \\ g_{t-1} \\ g_{t-2} \\ g_{t-3} \end{pmatrix}. \tag{1.29}$$

Ortu et al. (2013) and Bandi and Tamoni (2016) show that $\mathcal{T}^{(2)}$ is orthogonal that is $\Lambda^{(2)} \equiv \mathcal{T}^{(2)} \left(\mathcal{T}^{(2)}\right)^{\top}$ is diagonal. In addition, the diagonal elements of the matrix $\Lambda^{(2)}$ are non-vanishing[8] (i.e., $\lambda_1 = \lambda_2 = 1/4$ and $\lambda_3 = \lambda_4 = 1/2$) so that $\left(\mathcal{T}^{(2)}\right)^{-1} = \left(\mathcal{T}^{(2)}\right)^{\top} \left(\Lambda^{(2)}\right)^{-1}$ is well-defined and therefore

$$\begin{pmatrix} g_t \\ g_{t-1} \\ g_{t-2} \\ g_{t-3} \end{pmatrix} = \left(\mathcal{T}^{(2)}\right)^{-1} \begin{pmatrix} \pi_t^{(2)} \\ g_t^{(2)} \\ g_t^{(1)} \\ g_{t-2}^{(1)} \end{pmatrix}. \tag{1.30}$$

Equation (1.29) demonstrates how to define the decimated components and Equation (1.30) how to reconstruct uniquely the original time series $\{g_t\}_{t\in\mathbb{Z}}$ by letting t vary in $\left\{t = k \times 2^j, k \in \mathbb{Z}\right\}$.

[8] The diagonal elements of the matrix $\Lambda^{(J)}$ are $\lambda_1 = \lambda_2 = 1/2^J$ and $\lambda_k = 1/2^{J-j+1}$, $k = 2^{j-1}+1, \ldots, 2^j$, $j = 2, \ldots, J$

Translation invariance property of decimation

For any $h = 0, 1, \ldots, 2^{j-1}$ the decimated components can be rewritten as $\left\{g^{(j)}_{h+k\times 2^j}, k \in \mathbb{Z}\right\}$ and $\left\{\pi^{(j)}_{h+k\times 2^j}, k \in \mathbb{Z}\right\}$. In other words, the dynamics of the subseries are translation invariant. This is due to the fact that the matrix $\mathcal{T}^{(J)}$ is independent of the parameter h (i.e., the MODWT is shift invariant). Following Ortu et al. (2013) and without loss of generality, I let $h = 0$ when constructing the decimated components (i.e., they are sampled every 2^j times).

Modelling the dynamics of the decimated components

The decimated components can be represented as scale autoregressive processes (i.e., scale-wise AR) on the time domain defined by decimation, i.e.

$$g^{(j)}_{k\times 2^j+2^j} = \rho_j g^{(j)}_{k\times 2^j} + \varepsilon^{(j)}_{k\times 2^j+2^j} \tag{1.31}$$

where the parameter ρ_j captures scale-specific persistence. The persistence in the raw series is an increasing function of the dependence in scale ρ_j which can be significantly low (see Bandi et al., 2016 and for an application with macro uncertainty shocks chapter 2 - Table 2B.17). A similar dynamic structure for decimated components exists also in the work of Dijkerman and Mazumdar (1994) for multi-scale signal processing.

1.5 The Multi-scale Wold Decomposition of Bandi et al. (2016)

For a given level of persistence J, Equation (1.3) implies a Wold-type representation (understood in the mean-squared sense) of the following kind:

$$g_t = \sum_{j=1}^{J}\sum_{k=0}^{\infty} \alpha_{j,k}\varepsilon^{(j)}_{t-k\times 2^j} + \sum_{k=0}^{\infty} b_{J,k}\pi^{(J)}_{\varepsilon,t-k\times 2^J,t-(k+1)\times 2^J+1} \tag{1.32}$$

where

$$\varepsilon_t^{(j)} = g_t^{(j)} - \mathcal{P}_{\mathcal{M}_{j,t-2^j}} g_t^{(j)} \tag{1.33}$$

and $\mathcal{P}_{\mathcal{M}_{j,t-2^j}}$ is a projection mapping[9] onto the closed subspace $\mathcal{M}_{j,t-2^j}$ spanned by the sequence $\left\{g_{t-k\times 2^j}^{(j)}\right\}_{k\in\mathbb{Z}}$,

$$\alpha_{j,k} = E\left(g_t, \varepsilon_{t-k\times 2^j}^{(j)}\right), \tag{1.34}$$

$$b_{J,k} = E\left(g_t, \pi_{\varepsilon,t-k\times 2^J,t-(k+1)\times 2^J+1}^{(J)}\right) \tag{1.35}$$

and

$$\pi_{\varepsilon,t-k\times 2^J,t-(k+1)\times 2^J+1}^{(J)} = \sqrt{2^J}\left(\frac{\sum_{i=t-(k+1)\times 2^J+1}^{t-k\times 2^J}\varepsilon_i}{2^J}\right) \tag{1.36}$$

with $\varepsilon_t = g_t - \mathcal{P}_{\mathcal{M}_{t-1}} g_t$ satisfying $\mathrm{Var}(\varepsilon_t) = 1$. Note that each $\alpha_{j,k}$ is the coefficient obtained by projecting g_t on the linear subspace of $L^2(\Omega, \mathcal{F}, \mathcal{P})$ generated by $\varepsilon_{t-k\times 2^j}^{(j)}$ and that the sequence $\{\alpha_{j,k}\}$ is square-summable, that is $\sum_{k=0}^{\infty}(\alpha_{j,k})^2 < \infty$ for any $j \in \mathbb{N}$. In practice, the real coefficients $\alpha_{j,k}$ are scale-specific impulse response functions that capture the effect of shocks with specific persistence.

The multi-scale Wold decomposition[10] allows any variable g_t of a weakly stationary purely non-deterministic stochastic process to be represented as the sum of scale-specific innovations $\varepsilon_t^{(j)}$ defined on the grid $\left\{t - k \times 2^j : k\in\mathbb{Z}\right\}$. In other words, the time series can be thought as a combination of shocks classified on the basis of their arrival time and scale. Intuitively, this modelling approach of Bandi et al. (2016) generates a separation between scales in terms of their information content (i.e., shocks are scale-specific) - thereby giving meaning to economic and financial relations which may only be satisfied at certain frequencies alone. Moreover, if

[9] For an introduction to Hilbert spaces and techniques - like the projection theorem - see Brockwell and Davis (2009), Chapter 2.

[10] Similar multiresolution-based decompositions are available in Wong (1993).

$$\varepsilon_t^{(j)} = \sqrt{2^j}\left(\frac{\sum_{i=0}^{2^{j-1}-1}\varepsilon_{t-i}}{2^{j-1}} - \frac{\sum_{i=0}^{2^j-1}\varepsilon_{t-i}}{2^j}\right) \tag{1.37}$$

i.e. if scale-specific innovations are well-defined aggregates of high-frequency innovations, then the information contained at every scale is an aggregate of that contained at higher frequencies. Under this condition, Equation (1.32) will reduce to a classical Wold decomposition. However, this restriction[11] is not unique as it depends on the Haar filter $\{h_l\}_0^1 = (1/2, -1/2)$ used to extract the components. A different filter would give rise to an alternative expression (i.e., the expression is not economically motivated).

A proof of this result is available in Bandi et al. (2016). For completeness I present below the simple case for $J = 1$. For conciseness, I let $k = 0, 1, 2$. First, note that

$$\begin{aligned} g_t = a_{1,0}\varepsilon_t^{(1)} + a_{1,1}\varepsilon_{t-2}^{(1)} + a_{1,2}\varepsilon_{t-4}^{(1)} + \ldots + \\ + b_{1,0}\pi_{\varepsilon,t,t-1}^{(1)} + b_{1,1}\pi_{\varepsilon,t-2,t-3}^{(1)} + b_{1,2}\pi_{\varepsilon,t-4,t-5}^{(1)} + \ldots \end{aligned} \tag{1.38}$$

where

$$\begin{aligned} a_{1,0} &= E\left(g_t, \varepsilon_t^{(1)}\right) = E\left(g_t, \frac{\varepsilon_t}{\sqrt{2}} - \frac{\varepsilon_{t-1}}{\sqrt{2}}\right) = \frac{\psi_0}{\sqrt{2}} - \frac{\psi_1}{\sqrt{2}} \\ a_{1,1} &= E\left(g_t, \varepsilon_{t-2}^{(1)}\right) = E\left(g_t, \frac{\varepsilon_{t-2}}{\sqrt{2}} - \frac{\varepsilon_{t-3}}{\sqrt{2}}\right) = \frac{\psi_2}{\sqrt{2}} - \frac{\psi_3}{\sqrt{2}} \\ a_{1,2} &= E\left(g_t, \varepsilon_{t-4}^{(1)}\right) = E\left(g_t, \frac{\varepsilon_{t-4}}{\sqrt{2}} - \frac{\varepsilon_{t-5}}{\sqrt{2}}\right) = \frac{\psi_4}{\sqrt{2}} - \frac{\psi_5}{\sqrt{2}} \\ &\vdots \end{aligned}$$

[11] The standardization by $\sqrt{2^j}$ yields a unit variance for $\varepsilon_t^{(j)}$, that is

$$E\left[\left(\varepsilon_t^{(j)}\right)^2\right] = 2^j E\left[\left(\frac{\sum_{i=0}^{2^{j-1}-1}\varepsilon_{t-i}}{2^{j-1}} - \frac{\sum_{i=0}^{2^j-1}\varepsilon_{t-i}}{2^j}\right)^2\right] = 2^j\left(\left(\frac{1}{2^{2(j-1)}}\right)\sum_{i=0}^{2^{j-1}-1} E\left[\varepsilon_t^2\right] - \left(\frac{1}{2^{2j}}\right)\sum_{i=0}^{2^j-1} E\left[\varepsilon_t^2\right]\right) = 1.$$

$$b_{1,0} = E\left(g_t, \pi^{(1)}_{\varepsilon,t,t-1}\right) = E\left(g_t, \frac{\varepsilon_t + \varepsilon_{t-1}}{\sqrt{2}}\right) = \frac{\psi_0}{\sqrt{2}} + \frac{\psi_1}{\sqrt{2}}$$

$$b_{1,1} = E\left(g_t, \pi^{(1)}_{\varepsilon,t-2,t-3}\right) = E\left(g_t, \frac{\varepsilon_{t-2} + \varepsilon_{t-3}}{\sqrt{2}}\right) = \frac{\psi_2}{\sqrt{2}} + \frac{\psi_3}{\sqrt{2}}$$

$$b_{1,2} = E\left(g_t, \pi^{(1)}_{\varepsilon,t-4,t-5}\right) = E\left(g_t, \frac{\varepsilon_{t-4} + \varepsilon_{t-5}}{\sqrt{2}}\right) = \frac{\psi_4}{\sqrt{2}} + \frac{\psi_5}{\sqrt{2}}$$

with

$$\psi_j = E\left(g_t, \varepsilon_{t-j}\right).$$

Next, notice that

$$\psi_0\left(\frac{1}{\sqrt{2}}\varepsilon^{(1)}_t + \frac{1}{\sqrt{2}}\pi^{(1)}_{\varepsilon,t,t-1}\right) = \psi_0\varepsilon_t$$

$$\psi_1\left(-\frac{1}{\sqrt{2}}\varepsilon^{(1)}_t + \frac{1}{\sqrt{2}}\pi^{(1)}_{\varepsilon,t,t-1}\right) = \psi_1\varepsilon_{t-1}$$

$$\psi_2\left(\frac{1}{\sqrt{2}}\varepsilon^{(1)}_{t-2} + \frac{1}{\sqrt{2}}\pi^{(1)}_{\varepsilon,t-2,t-3}\right) = \psi_2\varepsilon_{t-2}$$

$$\psi_3\left(-\frac{1}{\sqrt{2}}\varepsilon^{(1)}_{t-2} + \frac{1}{\sqrt{2}}\pi^{(1)}_{\varepsilon,t-2,t-3}\right) = \psi_3\varepsilon_{t-3}$$

$$\psi_4\left(\frac{1}{\sqrt{2}}\varepsilon^{(1)}_{t-4} + \frac{1}{\sqrt{2}}\pi^{(1)}_{\varepsilon,t-4,t-5}\right) = \psi_4\varepsilon_{t-4}$$

$$\psi_5\left(-\frac{1}{\sqrt{2}}\varepsilon^{(1)}_{t-4} + \frac{1}{\sqrt{2}}\pi^{(1)}_{\varepsilon,t-4,t-5}\right) = \psi_5\varepsilon_{t-5}$$

which yields the standard Wold representation

$$g_t = \psi_0\varepsilon_t + \psi_1\varepsilon_{t-1} + \psi_2\varepsilon_{t-2} + \ldots. \tag{1.39}$$

Hence, the classical Wold decomposition for weakly-stationary processes can be viewed as a statistical and economic restriction resulting from the multi-scale. Most importantly, however, this result

clearly suggests that traditional econometric methods for the analysis of covariance-stationary time series (e.g., univariate ARMA models) fail to capture the sensitivity of economic and financial variables to shocks with heterogeneous persistence. For a thorough treatment in a univariate setting and an introduction to multi-scale impulse response functions see Ortu, Severino, Tamoni, and Tebaldi (2016). Finally while this decomposition is empirically appealing (i.e., the components are simply rescaled differences of variables g_t), a drawback is that correlation across components that refer to different scales cannot be ruled out. Ortu et al. (2016) develop an extended Wold decomposition for stationary time series that addresses this issue - an orthogonalized version of the decomposition discussed here - and allows infinite levels of persistence.

1.6 Scale-specific Persistence Versus White Noise: Replicating the example from Ortu et al. (2013)

Standard statistical tests[12] (Box and Pierce, 1970; Ljung and Box, 1978) fail to detect components localized at a specific level of persistence. In this section, I demonstrate this point by producing a time series that is judged as a white noise while it contains a persistent component by construction. **This example is a replication from Ortu et al. (2013) (see page 2882) and provides the basis for the Monte Carlo analysis later in this chapter**. In particular, following Ortu et al. (2013) I model directly the dynamics of the decimated components and for $t = k \times 2^j, k \in \mathbb{Z}$ I assume that

$$g_t^{(j)} = \varepsilon_t^{(j)}, \quad \forall j < J^*$$

[12]Given *i.i.d.* observations Box and Pierce (1970) show that the product between the number of observations and the sum of k sample autocovariances is asymptotically distributed as a Chi-squared distribution with k degrees of freedom. In other words, $Q = T \times \sum_{m=1}^{k} \hat{\tau}_m^2 \sim \chi_m^2$ where T is the sample size and $\hat{\tau}_m$ denotes the autocorrelation coefficient at lag m. In practice, the strict restriction of independence and homogeneity is violated leading to inaccurate statistical inference especially in small samples (see also Ljung and Box, 1978).

$$g_{t+2^{J^*}}^{(J^*)} = \rho_{J^*} g_t^{(J^*)} + \varepsilon_{t+2^{J^*}}^{(J^*)}, \tag{1.40}$$

$$\pi_t^{(J^*)} = \eta_t^{(J^*)}$$

where $\varepsilon_t^{(j)} \sim N\left(0, 2^{-j}\right), \forall j < J^*$, $\eta_t^{(J^*)} \sim N\left(0, 2^{-J^*}\right)$ and $\varepsilon_t^{(J^*)} \sim N\left(0, 2^{-J^*}(1-\rho_{J^*}^2)\right)$. Moreover, I assume that the decimated components are independent across levels of persistence (i.e., the innovations $\varepsilon_t^{(j)}, \varepsilon_t^{(j')}$ are uncorrelated for $j \neq j'$ and $\varepsilon_t^{(j)}$ is uncorrelated with $\eta_t^{(J^*)}$ for all j).

As Equation (1.40) demonstrates all decimated components are independent normal innovations except for one with an autoregressive structure. More specifically, the persistent component $g_t^{(J^*)}$ is an autoregressive process of order 1 in the dilated time of the corresponding scale and thus its long-run variance is given by

$$\text{Var}\left(g_t^{(J^*)}\right) = \frac{\text{Var}\left(\varepsilon_t^{(J^*)}\right)}{(1-\rho_{J^*}^2)} = 2^{-J^*}. \tag{1.41}$$

Furthermore, note that the unconditional variance of the process is set equal to 1 since

$$\text{Var}\left(g_t\right) = \sum_{j=1}^{J^*} \text{Var}\left(g_t^{(j)}\right) + \text{Var}\left(\pi_t^{(J^*)}\right) = \sum_{j=1}^{J^*} 2^{-j} + 2^{-J^*} = 1. \tag{1.42}$$

Therefore, in line with the approach of Ortu et al. (2013) the persistent component $g_t^{(J^*)}$ explains exactly a fraction 2^{-J^*} of the total variability of g_t.

First, I simulate the components using the dynamics in (1.40). I set $J^* = 4$ so that the persistent component accounts only for 6.25% for the total variance and let $\rho_{J^*} = 0.5$. Then, I use the inverse of the operator $\mathcal{T}^{(J)}$ to reconstruct the series. In particular, I obtain the original series from the following relation

$$\begin{pmatrix} g_t \\ g_{t-1} \\ g_{t-2} \\ g_{t-3} \\ g_{t-4} \\ g_{t-5} \\ g_{t-6} \\ g_{t-7} \\ g_{t-8} \\ g_{t-9} \\ g_{t-10} \\ g_{t-11} \\ g_{t-12} \\ g_{t-13} \\ g_{t-14} \\ g_{t-15} \end{pmatrix} = \left(\mathcal{T}^{(4)}\right)^{-1} \begin{pmatrix} \pi_t^{(4)} \\ g_t^{(4)} \\ g_t^{(3)} \\ g_{t-8}^{(3)} \\ g_t^{(2)} \\ g_{t-4}^{(2)} \\ g_{t-8}^{(2)} \\ g_{t-12}^{(2)} \\ g_t^{(1)} \\ g_{t-2}^{(1)} \\ g_{t-4}^{(1)} \\ g_{t-6}^{(1)} \\ g_{t-8}^{(1)} \\ g_{t-10}^{(1)} \\ g_{t-12}^{(1)} \\ g_{t-14}^{(1)} \end{pmatrix}. \tag{1.43}$$

Figure 1.1 depicts the time series for the constructed process g_t along with its autocorrelation and cumulative distribution functions. Note that g_t clearly resembles a Gaussian white noise. Figure 1.2 presents the simulated decimated components and their corresponding autocorrelation functions. Similar to an AR(1) process the persistent component $g_t^{(4)}$ has an autocorrelation function that decays toward zero exponentially.

Table 1.1 presents descriptive statistics for the simulated decimated components and the series g_t. Moreover, I use the Kolmogorov-Smirnov test statistic to check for normality and the Ljung-Box (1978) Q-test to check simultaneously for autocorrelation at multiple lags. The null hypothesis that the constructed series comes from a standard normal distribution cannot be rejected. In addition,

Figure 1.1: Constructed process g_t

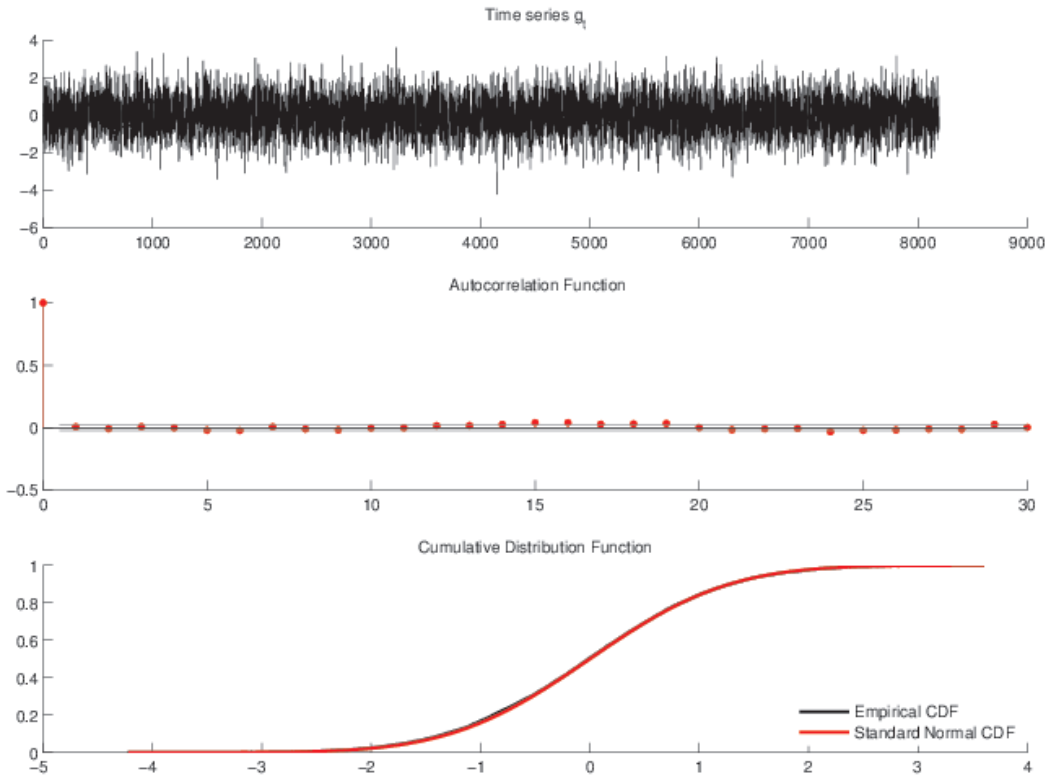

Notes: This figure plots the time-series and presents the autocorrelation function and the cumulative distribution function for the process $\{g_t\}$, which is constructed by applying the inverse transformation matrix $\left(\mathcal{T}^{(4)}\right)^{-1}$ in the simulated components from Equation (1.40) for $J^* = 4$ and $p_{J^*} = 0.5$.

I cannot reject the null that the first $k = 1, 2, \ldots, 5$ autocorrelation coefficients are jointly zero. Overall, this example illustrates the importance of this decomposition as a filtering procedure that disentangles layers of a process with heterogeneous levels of persistence. In section 1.7, I present a multi-scale variance ratio test that distinguishes a white noise process from a process whose decimated components are serially correlated.

Table 1.1: Descriptive statistics for the simulated components and the constructed series

Panel A	Constructed series	Decimated components				
	g_t	$g_t^{(1)}$	$g_t^{(2)}$	$g_t^{(3)}$	$g_t^{(4)}$	$\pi_t^{(4)}$
Mean	-0.0133	-0.0096	-0.0061	0.0166	0.0028	-0.0133
Variance	1.0222	0.5073	0.2560	0.1288	0.0631	0.0670
Skewness	-0.0071	-0.0036	-0.0433	0.0244	0.1544	-0.1073
Kurtosis	2.9274	3.0044	3.0487	2.9134	2.7945	3.0620
AC(1)	0.0057	-0.0282	-0.0504	-0.0076	0.5636	0.0842
# observations	8192	4096	2048	1024	512	512
Panel B						
Kolmogorov-Smirnov:	p-value	0.1151				
Ljung-Box Q-test:	lag	1	2	3	4	5
	p-value	0.6049	0.6202	0.7121	0.8432	0.4045

Notes: Panel A reports descriptive statistics for the decimated components whose dynamics are simulated according to Equation (1.40) and the constructed series g_t. I present the mean, variance, skewness, kurtosis as well as the autocorrelation coefficient for the first lag. Panel B reports the p-value of the Kolmogorov-Smirnov test for the null hypothesis that re-constructed series comes from a standard normal distribution. Also, it reports the p-values of the Ljung-Box (1978) Q-test for the null hypothesis that the first $k = 1, 2, \ldots, 5$ autocorrelation coefficients are jointly zero.

Figure 1.2: Simulated decimated components

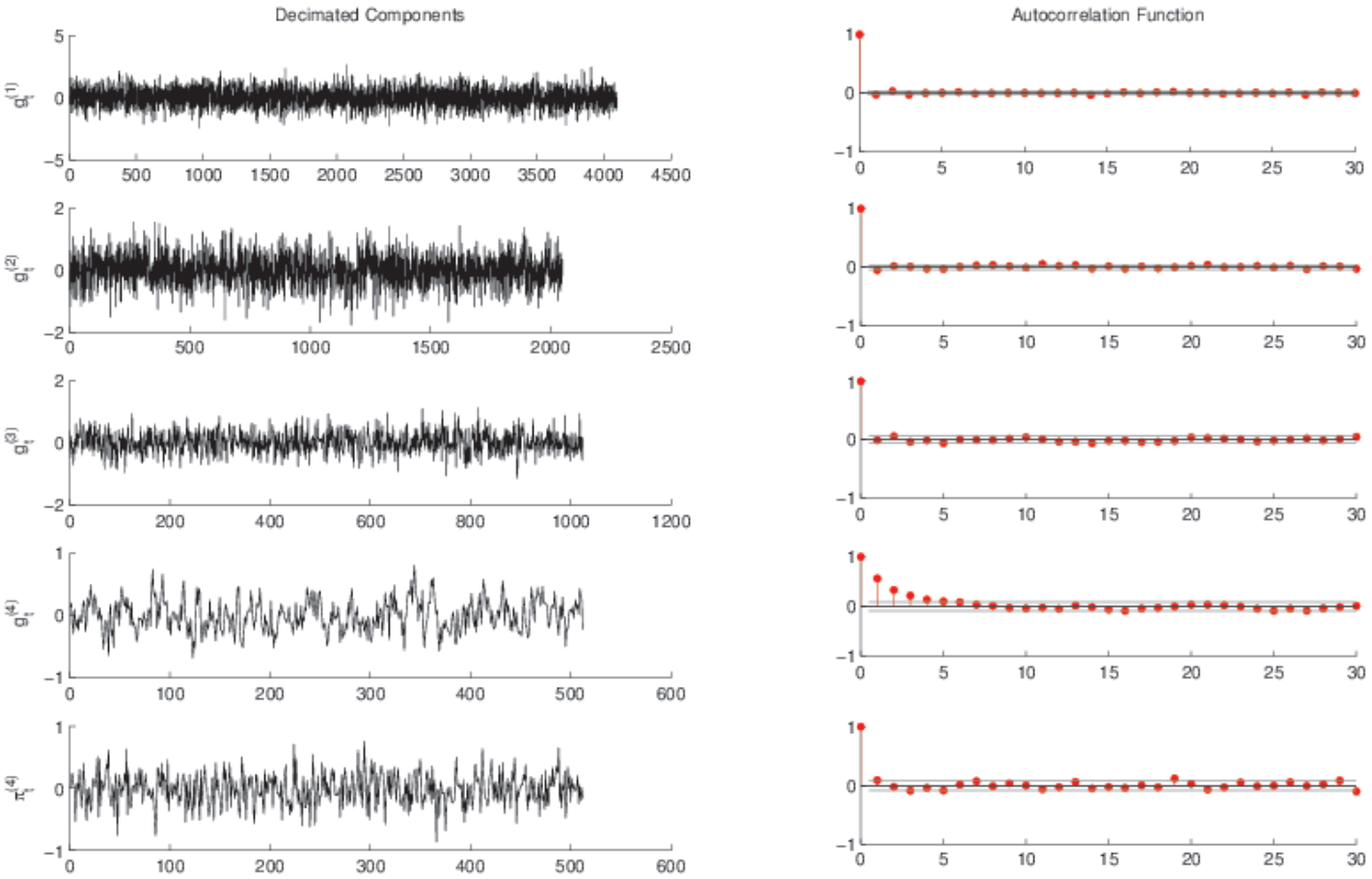

Notes: This figure presents the decimated components whose dynamics are simulated according to Equation (1.40) for $J^* = 4$ and $p_{J^*} = 0.5$ and their autocorrelation functions.

1.7 The Multi-scale Variance Ratio Tests of Gençay and Signori (2015)

Let $\{y_t\}_{t\in\mathbb{Z}}$ be a white noise process, i.e. $E(y_t)=0$, $\text{Var}(y_t)=\sigma_y^2$ and $\text{Cov}(y_t,y_s)=0$ for all $s\neq t$. Theorem 3 in Gençay and Signori (2015) states that the wavelet variance ratio for a stationary white noise process is given by

$$\mathcal{E}_m(y)\equiv\frac{\text{WVar}_m(y)}{\text{Var}(y)}=\frac{1}{2^m}. \tag{1.44}$$

That is, under the null of no serial correlation (i.e., $H_0:\ \text{Cov}(y_t,y_s)=0$ for all $s\neq t$ against $H_1:\ \text{Cov}(y_t,y_s)\neq 0$ for some $s\neq t$) the wavelet variance at scale m contributes a ratio of 2^{-m} to the total variance. This is because

$$\text{WVar}_m(y)\equiv\text{Var}(w_{m,t})=\int_{-1/2}^{1/2}S_m(f)\,df \tag{1.45}$$

where $w_{m,t}$ is the process obtained by applying the time invariant filter h_m to $\{y_t\}$. Gençay and Signori (2015) demonstrate that since $\{y_t\}$ is a zero-mean stationary process, the spectral density function of $w_{m,t}$ is $S_m(f)=|H_m(f)|^2S_y(f)$ where $H_m(f)$ is the discrete Fourier transform of the filter[13] and $S_y(f)=\sigma_y^2$. Also, $\int_{-1/2}^{1/2}|H_m(f)|^2df=||h_m||^2$ due to Parseval's identity. Hence, it follows that

$$\text{WVar}_m(y)=\int_{-1/2}^{1/2}|H_m(f)|^2S_y(f)\,df=\sigma_y^2\int_{-1/2}^{1/2}|H_m(f)|^2df=\sigma_y^2||h_m||^2=\sigma_y^2 2^{-m}. \tag{1.46}$$

Any departure from this benchmark provides the means to detect serial correlation. In particular,

[13] More specifically, let $\{y_t\}$ be a zero-mean stationary process with spectral density $f_y(\cdot)$ and $\{x_t\}$ be the process $x_t=\sum_{j=-\infty}^{\infty}\psi_j y_{t-j}$ where $\sum_{j=-\infty}^{\infty}|\psi_j|<\infty$. Then $\{x_t\}$ has a spectral density $f_x(\cdot)$ given by $f_x(\lambda)=|\psi(e^{i\lambda})|^2f_y(\lambda)$ where $\psi(e^{-i\lambda})=\sum_{j=-\infty}^{\infty}\psi_j e^{-ij\lambda}$. The operator $\psi(B)=\sum_{j=-\infty}^{\infty}\psi_j B^j$ applied to $\{y_t\}$ is a time-invariant linear filter with weights $\{\psi_j\}$ (see Brockwell and Davis, 2009 page 123).

by testing the implications resulting from Equation (1.44) Gençay and Signori (2015) introduce a family of test statistics[14] for the white noise hypothesis. First, they demonstrate that

$$\hat{\mathcal{E}}_{m,T}(y) \equiv \frac{\widehat{\mathrm{WVar}_m(y)}}{\widehat{\mathrm{Var}(y)}} = \frac{\sum_{t=1}^{T} w_{m,t}^2}{\sum_{t=1}^{T} y_{m,t}^2} \xrightarrow{p} \frac{1}{2^m} \tag{1.47}$$

is a consistent estimator of the wavelet variance ratio and that $\hat{\mathcal{E}}_{m,T}$ converges in probability to 2^{-m} even for (unconditionally) heteroskedastic white noise processes (i.e., for uncorrelated processes that may fail to be covariance stationary).

Then under mild restrictions, that is if $\{y_t\}$ is a white noise process whose cross-joint cumulants of order four are zero, they define the following test statistics

$$GS_m \equiv \sqrt{\frac{T}{a_m}}\left(\hat{\mathcal{E}}_{m,T} - \frac{1}{2^m}\right) \xrightarrow{d} \mathcal{N}(0,1) \tag{1.48}$$

with

$$a_m = \sum_{s \in Z} \sum_{i=i_{min}}^{i_{max}} \sum_{j>i}^{j_{max}} h_{m,i} h_{m,j} h_{m,i-s} h_{m,j-s},$$

where h_m is the wavelet filter used in the construction of $\hat{\mathcal{E}}_{m,T}$ and $i_{min} = max(0,s)$, $i_{max} = min(L_m, L_n + s) - 2$ and $j_{max} = min(L_m, Ln + s) - 1$. For instance, if h_m is the Haar filter $\left(\frac{1}{2}, -\frac{1}{2}\right)$ the test statistics for the scales 1 to 4 are given by

$$GS_1 = \sqrt{4T}\left(\hat{\mathcal{E}}_{1,T} - \frac{1}{2}\right), \; GS_2 = \sqrt{\frac{32}{3}T}\left(\hat{\mathcal{E}}_{2,T} - \frac{1}{4}\right)$$

$$GS_3 = \sqrt{\frac{256}{15}T}\left(\hat{\mathcal{E}}_{3,T} - \frac{1}{8}\right), \; GS_4 = \sqrt{\frac{2048}{71}T}\left(\hat{\mathcal{E}}_{4,T} - \frac{1}{16}\right)$$

respectively. Gençay and Signori (2015) show that each of these tests has strong power against specific alternatives. For instance, for $m = 1$ the test has significant power against $AR(1)$ and

[14] For wavelet-based tests for serial correlation see also Lee and Hong (2001) and Duchesne (2006). The simulation results in these studies indicate over-rejections and modest power in small samples.

$MA(1)$ alternatives.

Modified Multi-scale Variance Ratio Tests for Decimated Components

Ortu et al. (2013) propose a modified version of the test statistic in Equation (1.48) that distinguishes a white noise process from a process whose decimated components are serially correlated. Assume that $\{g_t\}_{t\in\mathbb{Z}}$ is weakly stationary with $E(g_t) = 0$ and $\text{Var}(g_t) = \sigma_g^2$. Denote with

$$\left(X_T^{(J)}\right)^\top = [g_T, g_{T-1}, \ldots, g_1] \tag{1.49}$$

the vector collecting the observations of g_t. Ortu et al. (2013) rely on the transformation matrix $\mathcal{T}^{(J)}$ to obtain the decimated components and build the variance decomposition of the series. Bandi and Tamoni (2016) use the same method to obtain a covariance decomposition between two series (see Section 1.11). In particular, similar to the simple case discussed in Section 1.2 it holds that

$$\mathcal{T}^{(J)} X_T^{(J)} = \begin{pmatrix} \pi_T^{(J)} \\ g_T^{(J)} \\ g_T^{(J-1)} \\ g_{T/2}^{(J-1)} \\ g_T^{(J-2)} \\ g_{3T/4}^{(J-2)} \\ g_{T/2}^{(J-2)} \\ g_{T/4}^{(J-2)} \\ \vdots \\ g_T^{(1)} \\ g_{T-2}^{(1)} \\ \vdots \\ g_2^{(1)} \end{pmatrix} \tag{1.50}$$

Letting now $\mathbf{g}^{(j)} = \left[g_{2^j}^{(j)}, \ldots, g_{k\times 2^j}^{(j)}, \ldots, g_T^{(j)}\right]^\top$, the sample variance of g_t can be computed as

$$\frac{\left(X_T^{(J)}\right)^\top X_T^{(J)}}{T} = \frac{\left(\left(\Lambda^{(J)}\right)^{-1/2}\mathcal{T}^{(J)}X_T^{(J)}\right)^\top\left(\left(\Lambda^{(J)}\right)^{-1/2}\mathcal{T}^{(J)}X_T^{(J)}\right)}{T} \tag{1.51}$$

$$= \frac{\sum_{j=1}^{J} 2^j \left(\mathbf{g^{(j)}}\right)^\top \mathbf{g^{(j)}}}{T} + 2^J \frac{\left(\pi_T^{(J)}\right)^\top \pi_T^{(J)}}{T} \tag{1.52}$$

$$= \frac{\sum_{j=1}^{J} 2^j \left(\mathbf{g^{(j)}}\right)^\top \mathbf{g^{(j)}}}{T} \tag{1.53}$$

Ortu et al. (2013) show that the equality in Equation (1.51) holds because the matrix $\left(\Lambda^{(J)}\right)^{-1/2}\mathcal{T}^{(J)}$ is orthogonal[15] (i.e., its columns are orthonormal) and hence the inner product $\left(X_T^{(J)}\right)^\top X_T^{(J)}$ is preserved. Equation (1.52) holds because the diagonal elements of the matrix $\Lambda^{(J)}$ are $\lambda_1 = \lambda_2 = 1/2^J$ and $\lambda_k = 1/2^{J-j+1}$,$k = 2^{j-1}+1, \ldots, 2^j, j = 2, \ldots, J$. Equation (1.53) exploits the fact that, given the stationarity assumption and for large samples, $\pi_T^{(J)}$ is an unbiased estimator of the population mean which is zero. In total, the above result shows that the variance of g_t can be expressed as the sum of the variances of its decimated components. The presence of the factor 2^j is justified on the basis that the decimated component $\mathbf{g}^{(j)}$ has $T/2^j$ observations.

The ratio of the sample variance of the decimated components at level of persistence j to the sample variance of the time series

$$\hat{\xi}_j = \frac{2^j \left(\mathbf{g^{(j)}}\right)^\intercal \mathbf{g^{(j)}}}{\left(X_T^{(J)}\right)^\intercal X_T^{(J)}} \tag{1.54}$$

can be used as test statistic. In particular, in order to test the null hypothesis of no serial correlation (i.e., $H_0: \rho_k \equiv \frac{\mathrm{Cov}(g_t, g_{t-k})}{\mathrm{Var}(g_t)} = 0$ for all $k \geq 1$ against $H_1: \rho_k \neq 0$ for some $k \geq 1$) Ortu et al. (2013)

[15] Note that

$$\left(\Lambda^{(J)}\right)^{-1/2}\mathcal{T}^{(J)}\left(\left(\Lambda^{(J)}\right)^{-1/2}\mathcal{T}^{(J)}\right)^\intercal = \left(\Lambda^{(J)}\right)^{-1/2}\mathcal{T}^{(J)}\left(\mathcal{T}^{(J)}\right)^\intercal\left(\Lambda^{(J)}\right)^{-1/2} = \left(\Lambda^{(J)}\right)^{-1/2}\Lambda^{(J)}\left(\Lambda^{(J)}\right)^{-1/2} = I$$

where I is the identity matrix.

employ the following test statistics which converge in distribution to a standard normal

$$\sqrt{\frac{T}{a_j}}\left(\hat{\xi}_j - \frac{1}{2^j}\right) \underset{\rightarrow}{d} \mathcal{N}(0,1). \tag{1.55}$$

The values of a_j for different resolution scales are given by

$$a_j = \frac{\binom{2^j}{2}}{2^j \times 2^{2(j-1)}}. \tag{1.56}$$

Finally, as Ortu et al. (2013) point out the existence of a maximum degree of persistence in the original series $\{g_t\}$ is equivalent to the existence of J such that the decimated component $\pi_t^{(J)}$ is white noise. In essence, the criterion to determine the optimal number of components to be extracted is based on a sequential analysis of the series $\pi_t^{(J)}$, $J = 1, 2, \ldots$ which incorporates fluctuations with persistence greater than 2^J periods.

1.8 Monte Carlo Simulations

I investigate by means of Monte Carlo simulations the power and size properties of the modified multi-scale variance ratio test of Ortu et al. (2013). I repeat the simulation exercise in Section 1.6 for $N = 5,000$ times and let ρ_{J^*} vary in the interval (0,1). For each simulation I compute the rescaled test statistics $\hat{\xi}_j$ for each level of persistence $j = 1, \ldots, 5$ and carry out a two-tailed test. Table 1.2 reports the probability of rejecting the null at a 5% level. The power of the test is size-adjusted. That is, for a given sample size the power is computed using the empirical critical values obtained from Monte Carlo simulations with 5,000 replications. The empirical critical values for different sample sizes are available in Table 1.5. Figures 1.3 and 1.4 plot simulated densities and quantile-quantile plots of the variance ratio test statistic.

Overall, the multi-scale variance ratio test statistics do not significantly over-reject or under-reject the null hypothesis. Moreover even though the deviations of Var $\left(g_t^{(4)}\right)$ from its large sample mean (i.e., $1/2^4 = 6.25\%$) are small in this framework, the test displays desirable power properties

at the time-scale at which the persistent component is localized (i.e., for $j = 4$). Also, as the sample size increases the power of the test increases steadily. Similar results hold for $J^* = 5$ and $J^* = 6$. However, as the level of resolution at which the persistent component is localized increases (i.e., J^*) the rejections rates decrease for $T = 256$. That is, it is harder to detect persistent components localized at low-frequencies in small samples.

A few comments are in order here. First, in comparison with the results of Ortu et al. (2013, see Table 1), the power of the test in my analysis is lower. This is because in their simulations Ortu et al. (2013) calibrate the variance of the simulated decimated components in line with actual consumption growth. In particular, the persistent component is localized at scale $J^* = 6$ and explains either 3%, 5% or 7% of the total variance. Within this setting, the test does display desirable properties. Intuitively, the deviation of $\text{Var}\left(g_t^{(6)}\right)$ from $1/2^6 \approx 1.56\%$ is large enough to increase the power of the test at this level of resolution without leading to significant over or under-rejections at the remaining time-scales. For more general applications, however, I argue that we need to be more cautious when interpreting the results of the test. For instance, when the test is applied to macro uncertainty - as in chapter 2 - the null of no serial correlation is rejected at multiple levels of resolution. This result does not mean that for all of the time-scales for which the test gives a rejection the uncertainty components are scale-wise AR(1) processes. Instead, it means that macro uncertainty contains a serially correlated decimated component in at least one of the time-scales. Deriving the joint asymptotic distribution of the modified variance ratio tests - in the spirit of Gençay and Signori (2015) - could allow us to gain power and potentially resolve these problems.

Table 1.2: Rejection rates under the null hypothesis, $J^* = 4$

	Panel A: $T = 256$					Panel B: $T = 512$				
	Persistence level					Persistence level				
$j =$	1	2	3	4	5	1	2	3	4	5
ρ_{J^*}										
0	0.0490	0.0460	0.0478	0.0426	0.0446	0.0510	0.0470	0.0494	0.0472	0.0512
0.1	0.0516	0.0490	0.0428	0.0522	0.0502	0.0458	0.0470	0.0530	0.0616	0.0478
0.2	0.0580	0.0578	0.0494	0.0536	0.0514	0.0506	0.0510	0.0500	0.0586	0.0518
0.3	0.0526	0.0492	0.0554	0.0632	0.0466	0.0512	0.0444	0.0488	0.0736	0.0436
0.4	0.0516	0.0482	0.0522	0.0764	0.0522	0.0500	0.0436	0.0480	0.0936	0.0468
0.5	0.0554	0.0502	0.0522	0.1012	0.0494	0.0586	0.0484	0.0520	0.1202	0.0498
0.6	0.0546	0.0498	0.0496	0.1340	0.0508	0.0568	0.0502	0.0518	0.1604	0.0494
0.7	0.0598	0.0512	0.0470	0.1830	0.0418	0.0624	0.0478	0.0566	0.2326	0.0482
0.8	0.0640	0.0528	0.0492	0.2912	0.0504	0.0690	0.0442	0.0584	0.3216	0.0476
0.9	0.0684	0.0556	0.0618	0.4543	0.0466	0.0808	0.0564	0.0544	0.5057	0.0506
	Panel C: $T = 1024$					Panel D: $T = 2048$				
	Persistence level					Persistence level				
$j =$	1	2	3	4	5	1	2	3	4	5
ρ_{J^*}										
0	0.0452	0.0516	0.0520	0.0508	0.0494	0.0538	0.0476	0.0508	0.0534	0.0516
0.1	0.0406	0.0520	0.0556	0.0460	0.0524	0.0484	0.0472	0.0504	0.0566	0.0500
0.2	0.0494	0.0582	0.0510	0.0522	0.0548	0.0470	0.0428	0.0434	0.0608	0.0458
0.3	0.0498	0.0568	0.0512	0.0722	0.0566	0.0518	0.0452	0.0450	0.0740	0.0560
0.4	0.0488	0.0480	0.0500	0.0766	0.0554	0.0478	0.0496	0.0526	0.0962	0.0538
0.5	0.0602	0.0542	0.0596	0.1208	0.0474	0.0568	0.0510	0.0498	0.1328	0.0526
0.6	0.0534	0.0544	0.0526	0.1566	0.0532	0.0606	0.0508	0.0510	0.1674	0.0530
0.7	0.0578	0.0566	0.0546	0.2232	0.0516	0.0602	0.0492	0.0524	0.2476	0.0476
0.8	0.0716	0.0614	0.0542	0.3330	0.0520	0.0740	0.0574	0.0524	0.3436	0.0504
0.9	0.0990	0.0706	0.0602	0.5053	0.0528	0.1068	0.0674	0.0538	0.5083	0.0540

Notes: This table reports rejection rates of the multi-scale variance ratio test at a nominal level of 5%. Five thousand replications have been used for all simulations.

Table 1.3: Rejection rates under the null hypothesis, $J^* = 5$

	Panel A: $T = 256$						Panel B: $T = 512$					
	Persistence level						Persistence level					
$j =$	1	2	3	4	5	6	1	2	3	4	5	6
ρ_{J^*}												
0	0.0490	0.0460	0.0478	0.0426	0.0464	0.0596	0.0510	0.0470	0.0494	0.0522	0.0452	0.0542
0.1	0.0516	0.0496	0.0420	0.0450	0.0542	0.0524	0.0450	0.0466	0.0528	0.0522	0.0480	0.0570
0.2	0.0574	0.0582	0.0492	0.0448	0.0524	0.0584	0.0510	0.0522	0.0508	0.0544	0.0522	0.0536
0.3	0.0502	0.0504	0.0548	0.0452	0.0570	0.0560	0.0488	0.0444	0.0494	0.0524	0.0614	0.0520
0.4	0.0500	0.0472	0.0516	0.0516	0.0744	0.0574	0.0502	0.0446	0.0484	0.0564	0.0780	0.0530
0.5	0.0520	0.0504	0.0520	0.0470	0.0814	0.0556	0.0582	0.0466	0.0506	0.0536	0.0984	0.0540
0.6	0.0510	0.0480	0.0506	0.0510	0.1108	0.0528	0.0516	0.0484	0.0518	0.0572	0.1406	0.0570
0.7	0.0558	0.0510	0.0458	0.0420	0.1600	0.0596	0.0524	0.0464	0.0562	0.0568	0.2048	0.0582
0.8	0.0530	0.0500	0.0476	0.0492	0.2374	0.0644	0.0592	0.0378	0.0562	0.0530	0.2894	0.0546
0.9	0.0540	0.0510	0.0570	0.0446	0.3896	0.0566	0.0562	0.0478	0.0526	0.0530	0.4633	0.0584
	Panel C: $T = 1024$						Panel D: $T = 2048$					
	Persistence level						Persistence level					
$j =$	1	2	3	4	5	6	1	2	3	4	5	6
ρ_{J^*}												
0	0.0452	0.0516	0.0520	0.0492	0.0548	0.0546	0.0538	0.0476	0.0508	0.0534	0.0478	0.0476
0.1	0.0396	0.0524	0.0562	0.0468	0.0494	0.0520	0.0490	0.0482	0.0500	0.0524	0.0526	0.0552
0.2	0.0494	0.0586	0.0510	0.0478	0.0592	0.0544	0.0466	0.0422	0.0428	0.0564	0.0556	0.0496
0.3	0.0490	0.0562	0.0510	0.0530	0.0762	0.0556	0.0516	0.0444	0.0440	0.0528	0.0682	0.0512
0.4	0.0466	0.0472	0.0502	0.0486	0.0876	0.0528	0.0488	0.0470	0.0528	0.0506	0.0890	0.0466
0.5	0.0560	0.0548	0.0594	0.0458	0.1184	0.0556	0.0554	0.0516	0.0500	0.0542	0.1304	0.0516
0.6	0.0514	0.0544	0.0538	0.0468	0.1754	0.0558	0.0568	0.0510	0.0512	0.0526	0.1644	0.0522
0.7	0.0536	0.0546	0.0542	0.0484	0.2428	0.0554	0.0546	0.0462	0.0524	0.0504	0.2420	0.0548
0.8	0.0564	0.0544	0.0502	0.0462	0.3346	0.0578	0.0622	0.0536	0.0486	0.0492	0.3416	0.0554
0.9	0.0714	0.0632	0.0560	0.0472	0.5033	0.0574	0.0814	0.0574	0.0540	0.0530	0.5103	0.0482

Notes: This table reports rejection rates of the multi-scale variance ratio test at a nominal level of 5%. Five thousand replications have been used for all simulations.

Table 1.4: Rejection rates under the null hypothesis, $J^* = 6$

	Panel A: $T = 256$							Panel B: $T = 512$						
	Persistence level							Persistence level						
$j =$	1	2	3	4	5	6	7	1	2	3	4	5	6	7
ρ_{J^*}														
0	0.0490	0.0460	0.0478	0.0426	0.0440	0.0536	0.0540	0.0510	0.0470	0.0494	0.0522	0.0438	0.0540	0.0532
0.1	0.0516	0.0502	0.0422	0.0452	0.0504	0.0538	0.0544	0.0464	0.0470	0.0518	0.0520	0.0498	0.0560	0.0518
0.2	0.0568	0.0574	0.0496	0.0448	0.0496	0.0580	0.0530	0.0506	0.0516	0.0508	0.0534	0.0494	0.0614	0.0512
0.3	0.0492	0.0496	0.0542	0.0454	0.0510	0.0674	0.0566	0.0484	0.0454	0.0486	0.0520	0.0486	0.0762	0.0490
0.4	0.0500	0.0464	0.0512	0.0514	0.0434	0.0674	0.0494	0.0498	0.0426	0.0488	0.0562	0.0458	0.0836	0.0522
0.5	0.0522	0.0482	0.0520	0.0464	0.0514	0.0790	0.0512	0.0560	0.0488	0.0504	0.0532	0.0452	0.1052	0.0490
0.6	0.0476	0.0476	0.0504	0.0512	0.0420	0.0904	0.0472	0.0496	0.0458	0.0520	0.0562	0.0504	0.1332	0.0524
0.7	0.0504	0.0498	0.0472	0.0418	0.0544	0.1144	0.0488	0.0480	0.0448	0.0548	0.0562	0.0492	0.1720	0.0504
0.8	0.0454	0.0486	0.0476	0.0506	0.0502	0.1452	0.0510	0.0538	0.0390	0.0536	0.0534	0.0466	0.2480	0.0494
0.9	0.0542	0.0496	0.0566	0.0432	0.0522	0.2794	0.0522	0.0480	0.0460	0.0504	0.0522	0.0508	0.4152	0.0502
	Panel C: $T = 1024$							Panel D: $T = 2048$						
	Persistence level							Persistence level						
$j =$	1	2	3	4	5	6	7	1	2	3	4	5	6	7
ρ_{J^*}														
0	0.0452	0.0516	0.0520	0.0492	0.0472	0.0538	0.0508	0.0538	0.0476	0.0508	0.0534	0.0514	0.0466	0.0452
0.1	0.0394	0.0520	0.0558	0.0470	0.0546	0.0518	0.0478	0.0486	0.0488	0.0506	0.0522	0.0550	0.0480	0.0434
0.2	0.0482	0.0574	0.0502	0.0476	0.0552	0.0566	0.0476	0.0468	0.0418	0.0426	0.0568	0.0498	0.0520	0.0454
0.3	0.0476	0.0548	0.0508	0.0528	0.0564	0.0714	0.0504	0.0526	0.0450	0.0440	0.0532	0.0530	0.0706	0.0492
0.4	0.0460	0.0470	0.0506	0.0486	0.0522	0.0858	0.0438	0.0492	0.0478	0.0534	0.0500	0.0474	0.0824	0.0504
0.5	0.0562	0.0540	0.0596	0.0466	0.0500	0.1084	0.0482	0.0526	0.0506	0.0480	0.0536	0.0514	0.1166	0.0454
0.6	0.0500	0.0534	0.0524	0.0472	0.0566	0.1528	0.0494	0.0542	0.0512	0.0500	0.0522	0.0532	0.1572	0.0450
0.7	0.0488	0.0540	0.0540	0.0482	0.0528	0.2162	0.0528	0.0500	0.0462	0.0530	0.0496	0.0540	0.2254	0.0496
0.8	0.0526	0.0520	0.0488	0.0462	0.0582	0.2910	0.0500	0.0536	0.0510	0.0488	0.0490	0.0500	0.3174	0.0448
0.9	0.0618	0.0568	0.0526	0.0464	0.0528	0.4611	0.0550	0.0660	0.0516	0.0498	0.0536	0.0502	0.4983	0.0458

Notes: This table reports rejection rates of the multi-scale variance ratio test at a nominal level of 5%. Five thousand replications have been used for all simulations.

Table 1.5: Empirical critical values for the multi-scale variance ratio test

	Persistence level						
$j =$	1	2	3	4	5	6	7
Panel A: $T = 256$							
0.025	-1.8637	-1.7996	-1.7711	-1.6422	-1.4639	-1.2403	-0.9758
0.975	2.0381	2.1194	2.1127	2.2840	2.4112	2.4037	2.6789
Panel B: $T = 512$							
0.025	-1.9437	-1.8501	-1.8223	-1.6988	-1.6208	-1.4420	-1.2483
0.975	1.9880	2.1963	2.0772	2.1396	2.3017	2.2829	2.4870
Panel C: $T = 1024$							
0.025	-1.9623	-1.8396	-1.8995	-1.8161	-1.6937	-1.6083	-1.4596
0.975	1.9931	2.0147	1.9985	2.1434	2.1657	2.1917	2.4173
Panel D: $T = 2048$							
0.025	-1.9798	-1.9023	-1.9523	-1.8439	-1.7929	-1.7277	-1.6358
0.975	1.9765	2.0992	1.9751	2.0251	2.1079	2.1688	2.2790

Notes: This table reports the empirical critical values of the distribution of the multi-scale variance ratio test for different sample sizes and $j = 1, \ldots, 7$ at percentiles 0.025 and 0.975.

Figure 1.3: Simulated densities of the multi-scale variance ratio test

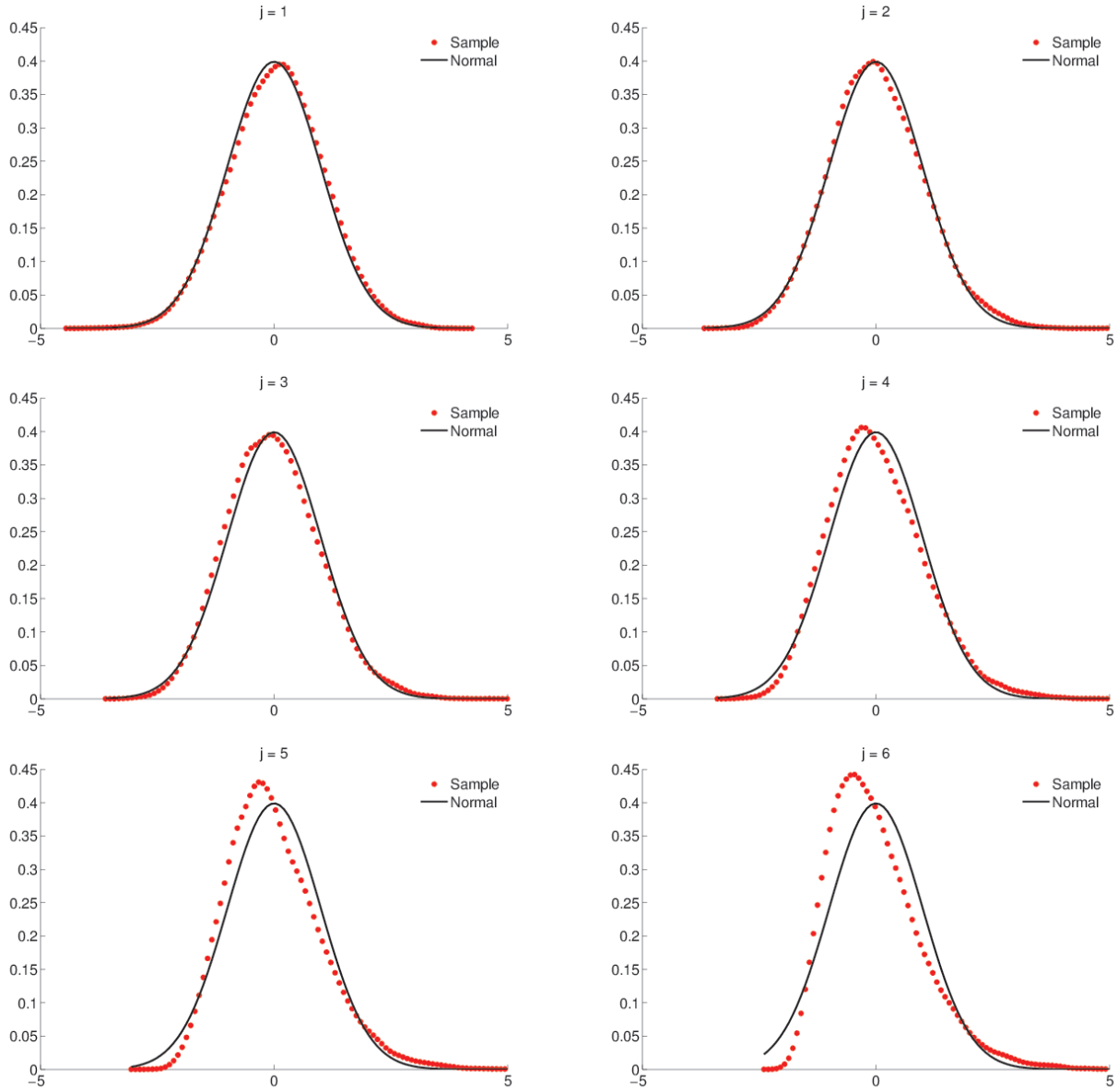

Notes: These figures plot simulated densities of the multi-scale variance ratio test statistic of Ortu et al. (2013) for $T = 512$ and $j = 1, \ldots, 6$. I implement 10,000 replications.

Figure 1.4: Quantile-quantile plots of the multi-scale variance ratio test

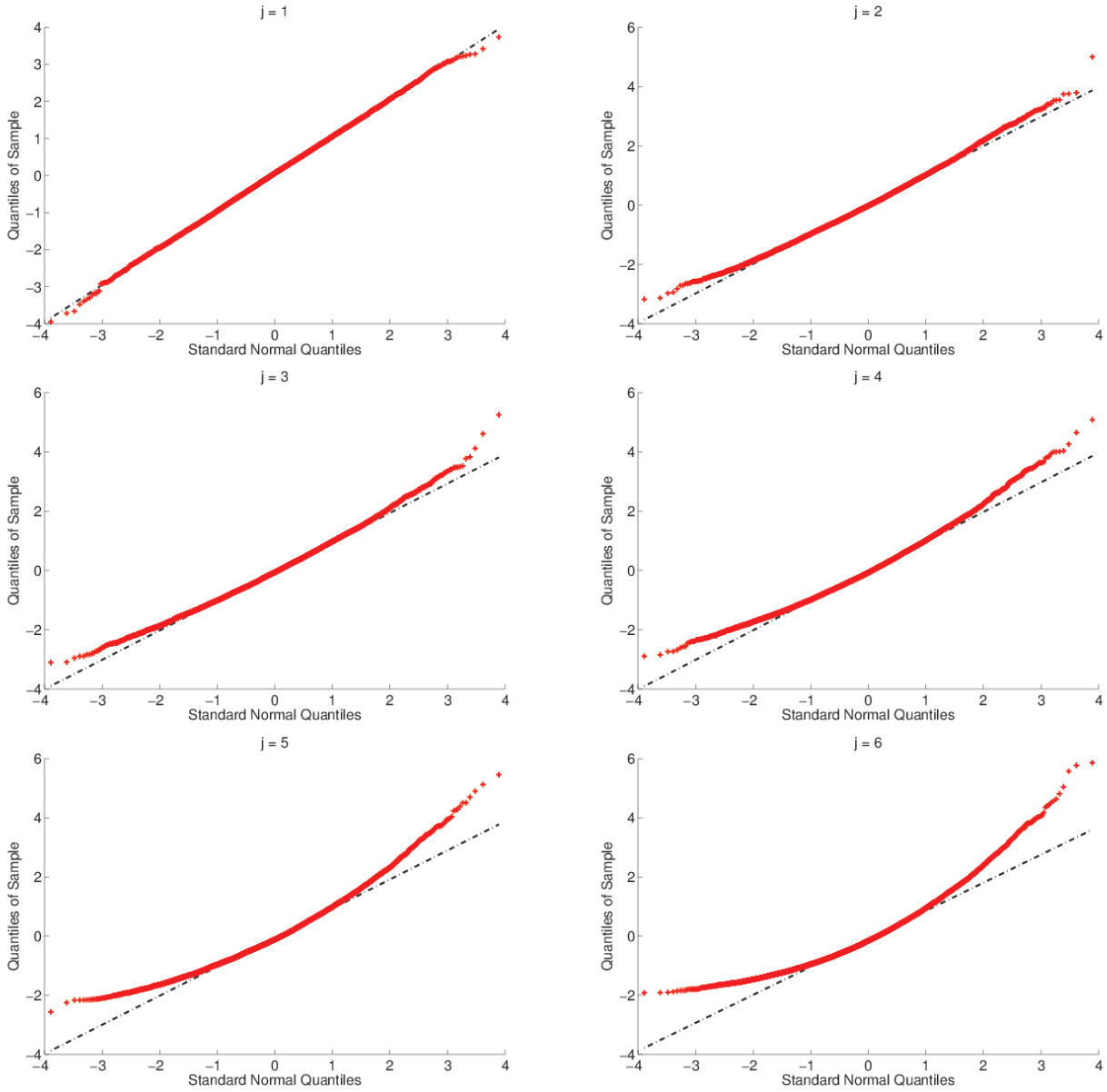

Notes: These figures plot quantile-quantile plots of the multi-scale variance ratio test statistic of Ortu et al. (2013) for $T = 512$ and $j = 1, \ldots, 6$. I implement 10,000 replications.

1.9 On the Properties of Scale-specific Predictability

I present an extension of the framework for scale-specific predictability of Bandi et al. (2016). In particular, I demonstrate theoretically and via simulations that predictability on the decimated components of two series translates into predictability upon two-way (forward for the regressand, backward for the regressor) adaptive aggregation of the series irrespective of the properties of the scale-wise regressor. **My work is motivated by the empirical relation between excess market returns and macro uncertainty as documented in chapter 2**.

First, consider the following scale-specific predictive system defined in Bandi et al. (2016). For $j = j^*$ with $j^* \in \{1, \ldots, J\}$, let

$$x^{(j^*)}_{k\times 2^{j^*}+2^{j^*}} = \beta_{j^*} g^{(j^*)}_{k\times 2^{j^*}} \tag{1.57}$$

$$g^{(j^*)}_{k\times 2^{j^*}+2^{j^*}} = \rho_{j^*} g^{(j^*)}_{k\times 2^{j^*}} + \varepsilon^{(j^*)}_{k\times 2^{j^*}+2^{j^*}} \tag{1.58}$$

while for $j \neq j^*$ assume that

$$x^{(j)}_{k\times 2^{j}} = u^{(j)}_{k\times 2^{j}} \tag{1.59}$$

$$g^{(j)}_{k\times 2^{j}} = \varepsilon^{(j)}_{k\times 2^{j}} \tag{1.60}$$

where $k \in \mathbb{Z}$ and the shocks $u^{(j)}_t, \varepsilon^{(j)}_t$ satisfy $\text{Corr}\left(u^{(j)}_t, \varepsilon^{(j)}_t\right) = 0$, $\forall t, j$. Equations (1.57)-(1.60) define a predictive system on scale j^*. Bandi et al. (2016) show that a predictive relation localized around the $j^{*\text{th}}$ scale produces patterns of slope coefficients and R^2s which have a peak for aggregation levels corresponding to the horizon 2^{j^*} (i.e., hump-shaped dynamics).

However, hump-shaped structures arise naturally upon aggregation irrespective of the dynamics of the regressor. That is, Equation (1.58) is not a necessary condition. For instance, consider the following scale-specific predictive system for $j^* \in \{1, \ldots, J\}$

$$x^{(j^*)}_{k\times 2^{j^*}+2^{j^*}} = \beta_{j^*} g^{(j^*)}_{k\times 2^{j^*}} \tag{1.61}$$

$$g^{(j^*)}_{k\times 2^{j^*}} = \sigma_{j^*} \varepsilon^{(j^*)}_{k\times 2^{j^*}} \tag{1.62}$$

where $k \in \mathbb{Z}$ and σ_{j^*} denotes scale-specific variance, while for $j \in \{1, \ldots, J\}$ with $j \neq j^*$

$$x^{(j)}_{k\times 2^{j}} = u^{(j)}_{k\times 2^{j}} \tag{1.63}$$

$$g^{(j)}_{k\times 2^{j}} = \varepsilon^{(j)}_{k\times 2^{j}}. \tag{1.64}$$

This system differs from the one in Bandi et al. (2016) in the sense that the scale-wise regressor is not an AR(1) process but a white noise-process. Simply put, two scale-localized white noise processes - one of which predicts the other - can also yield statistically significant economic relations upon aggregation.

Theoretical Example: For simplicity, I assume that $T = 8$, $j^* = 1$, $J = 2$ and I set all decimated components in Equations (1.63)-(1.64) equal to zero (i.e., $\left\{x^{(j)}_{k\times 2^{j}}, g^{(j)}_{k\times 2^{j}}\right\} = 0$). Using the inverse Haar transformation matrix I construct the raw series x_t and g_t. In particular, the time series g_t is equal to

$$\begin{pmatrix} g_8 \\ g_7 \\ g_6 \\ g_5 \\ g_4 \\ g_3 \\ g_2 \\ g_1 \end{pmatrix} = \begin{pmatrix} g_8^{(1)} \\ -g_8^{(1)} \\ g_6^{(1)} \\ -g_6^{(1)} \\ g_4^{(1)} \\ -g_4^{(1)} \\ g_2^{(1)} \\ -g_2^{(1)} \end{pmatrix}. \tag{1.65}$$

Next, I aggregate the series over a horizon $q = 2^{j^*} = 2$. The aggregated series are

$$\begin{aligned} g_{1,2} &= 0 & x_{1,2} &= 0 \\ g_{2,3} &= \left(g_2^{(1)} - g_4^{(1)}\right)/2 & x_{2,3} &= \left(x_2^{(1)} - x_4^{(1)}\right)/2 \\ g_{3,4} &= 0 & x_{3,4} &= 0 \\ g_{4,5} &= \left(g_4^{(1)} - g_6^{(1)}\right)/2 & x_{4,5} &= \left(x_4^{(1)} - x_6^{(1)}\right)/2 = \beta_1 g_{2,3} \\ g_{5,6} &= 0 & x_{5,6} &= 0 \\ g_{6,7} &= \left(g_6^{(1)} - g_8^{(1)}\right)/2 & x_{6,7} &= \left(x_6^{(1)} - x_8^{(1)}\right)/2 = \beta_1 g_{4,5} \\ g_{7,8} &= 0 & x_{7,8} &= 0 \end{aligned}$$

Based on a basic block of 2 elements the predictive regression of $x_{t+1,t+2}$ on $g_{t-1,t}$ yields

$$\widetilde{\beta} = \frac{Cov\left(x_{4,5}, g_{2,3}\right)}{Var\left(g_{2,3}\right)} = \beta_1 \tag{1.66}$$

and $R^2 = 100\%$. That is, there is a close one-to-one mapping between scale-specific predictability and two-way aggregation irrespective of whether the scale-wise regressor is autoregressive. Note that the addition of noise for $j \neq j^*$ (i.e., if $\left\{x_{k\times 2^j}^{(j)}, g_{k\times 2^j}^{(j)}\right\} \neq 0$ - for instance, if $g_{k\times 2^j}^{(j)}$ is a scale-wise AR process) leads to a blurring of the relation upon aggregation.

Moreover, the contemporaneous regression of $x_{t+1,t+2}$ on $g_{t+1,t+2}$ yields an inconsistent slope

estimate since

$$\widetilde{\beta} = \frac{Cov\left(x_{4,5}, g_{4,5}\right)}{Var\left(g_{4,5}\right)} = \beta_1 \frac{Cov\left(g_{2,3}, g_{4,5}\right)}{Var\left(g_{4,5}\right)} = -\beta_1 \frac{Var\left(g_4^{(1)}\right)}{Var\left(g_4^{(1)}\right) + Var\left(g_6^{(1)}\right)}. \tag{1.67}$$

That is, $\widetilde{\beta}$ has a wrong sign and is attenuated.

Simulations: I simulate scale-specific predictability by modelling the dynamics of the decimated components of excess market returns and macro uncertainty according to Equations (1.61)-(1.64). The relation is at scale $j^* = 6$ with $\beta_{j^*} = 5$. For $j \neq 6$, $u_{k\times 2^j}^{(j)} \sim \mathcal{N}(0, \sigma_u^{(j)})$ and $\varepsilon_{k\times 2^j}^{(j)} \sim \mathcal{N}(0, \sigma_\varepsilon^{(j)})$. That is, the decimated components are white noise shocks. The variances of the decimated components (i.e., $\sigma_u^{(j)}$ and $\sigma_\varepsilon^{(j)}$) are calibrated to the data. I set $T = 512$ and implement 2,500 simulations. For each simulation, I run forward/backward regressions

$$x_{t+1,t+h} = \alpha_h + \beta_h g_{t-h+1,t} + z_{t,t+h} \tag{1.68}$$

where $x_{t+1,t+h} = \sum_{i=1}^{h} x_{t+i}$ and $g_{t-h+1,t} = \sum_{i=1}^{h} g_{t-i+1}$ are (forward/backward) aggregates over a horizon of length h. In addition, I run the equivalent contemporaneous regressions

$$x_{t+1,t+h} = \alpha_h + \beta_h g_{t+1,t+h} + z_{t,t+h}. \tag{1.69}$$

Finally, I also consider forward/backward regressions under the null of absence of scale-specific predictability. That is, I set $\beta_{j^*} = 0$ and let white noise shocks drive the decimated components at scale j^*.

Table 1.6 presents the simulation results. I report the median of the slope estimates, rejection probabilities at the 1%, 5% and 10% levels associated with Valkanov's (2003) rescaled $t/\sqrt{T}$ statistic[16] and the median of the adjusted R^2 statistics. In Panel A of Table 1.6 I run linear regressions

[16] As Bandi and Perron (2008) demonstrate, under the null of no dependence (i.e., $\beta_h = 0$ in Equation 1.68) the slope estimator is super-consistent. However, the standard t-statistic diverges with T leading to over-rejections of the null of zero-slope. Similarly, the R^2 converges to a random variable whose mean increases with the overlap.

(with an intercept) of forward/backward aggregates over a horizon of length h. In Panel B I run linear regressions (with an intercept) of contemporaneous aggregates over a horizon of length h and in Panel C I run linear regressions (with an intercept) of forward/backward aggregates under the null of absence of scale-specific predictability. An R^2 of 11.99% is achieved for a level of aggregation corresponding to $2^{j^*} = 64$ periods. Before and after, the predictive slopes and the R^2s display a hump-shaped behavior (see also Figure 1.5). This hump-shaped structure in both the predictive slopes and the R^2s is a significant feature of the assumed data generating process. If aggregation led to spurious predictability - by generating stochastic trends for instance - such patterns would be prevented. Furthermore, in line with the theoretical predictions the contemporaneous regression yields an inconsistent slope estimate with wrong sign for a level of aggregation corresponding to $2^{j^*} = 64$ periods. Under the null of absence of scale-specific predictability there is not a statistically significant relation upon aggregation.

1.10 Risk Decomposition Across Time-scales

Finally, I demonstrate how to decompose risk as proxied by the covariance between a risky factor $\{f_t\}_{t=1}^T$ and the returns of an asset $\{r_t\}_{t=1}^T$ on a scale-by-scale basis and investigate scale-specific risk compensations. **The framework presented here is based on the work of Bandi and Tamoni (2016).** Let $r_T^{(J)}$ and $f_T^{(J)}$ denote the vectors collecting the $T = 2^J$ observations of the series $\{r_t\}$ and $\{f_t\}$ respectively, that is

$$r_T^{(J)} = [r_T, r_{T-1}, \ldots, r_1]^\top \quad \text{and} \quad f_T^{(J)} = [f_T, f_{T-1}, \ldots, f_1]^\top . \tag{1.70}$$

Similarly to Section 1.7, the sample covariance between r_t and f_t can be expressed as the sum of the covariances of the decimated components

Table 1.6: Simulation of scale-specific predictability

	Horizon											
$h =$	8	16	32	48	56	64	72	80	88	96	112	128
Panel A	forward/backward regressions											
Median β_h	-0.0254	-0.0200	-0.0472	0.4057	0.5759	0.7320	0.6509	0.5592	0.4675	0.3595	0.2380	0.1448
1%	0.0072	0.0040	0.0036	0.0092	0.0160	0.0584	0.0324	0.0192	0.0140	0.0124	0.0028	0.0136
5%	0.0448	0.0292	0.0188	0.0348	0.0764	0.1444	0.1040	0.0760	0.0612	0.0480	0.0384	0.0796
10%	0.0992	0.0640	0.0408	0.0872	0.1388	0.2172	0.1716	0.1312	0.1072	0.1068	0.0892	0.1320
Median Adj.R^2(%)	0.482%	0.948%	1.683%	4.764%	8.002%	11.992%	11.315%	10.842%	10.273%	9.885%	11.680%	17.103%
Panel B	contemporaneous regressions											
Median β_h	-0.0256	-0.0433	-0.0839	-0.1181	-0.1586	-0.1964	-0.1297	-0.0838	-0.0386	0.0011	0.0057	0.0460
1%	0.0668	0.0404	0.0192	0.0168	0.0180	0.0196	0.0148	0.0132	0.0128	0.0124	0.0060	0.0140
5%	0.1596	0.1104	0.0756	0.0596	0.0612	0.0696	0.0656	0.0572	0.0576	0.0584	0.0496	0.0712
10%	0.2376	0.1808	0.1296	0.1244	0.1220	0.1220	0.1112	0.1020	0.1000	0.1052	0.0980	0.1292
Median Adj.R^2(%)	1.055%	1.782%	3.132%	4.487%	5.604%	6.940%	7.105%	7.704%	8.710%	9.750%	11.966%	17.326%
Panel C	forward/backward regressions - **absence of scale-specific predictability**											
Median β_h	-0.0001	-0.0056	-0.0040	-0.0213	-0.0249	-0.0186	-0.0119	-0.0124	-0.0143	-0.0051	-0.0222	-0.0203
1%	0.0032	0.0096	0.0080	0.0064	0.0060	0.0056	0.0072	0.0116	0.0108	0.0108	0.0064	0.0108
5%	0.0220	0.0368	0.0456	0.0312	0.0312	0.0412	0.0436	0.0520	0.0536	0.0568	0.0572	0.0532
10%	0.0580	0.0788	0.0848	0.0740	0.0684	0.0776	0.0980	0.1008	0.1008	0.1048	0.1060	0.1048
Median Adj.R^2(%)	0.333%	1.010%	2.352%	3.609%	4.155%	5.028%	6.561%	7.522%	9.094%	10.057%	11.759%	14.846%

Notes: I simulate scale-specific predictability by modelling the dynamics of the decimated components of excess market returns and macro uncertainty according to Equations (1.61)-(1.64). The relation is at scale $j^* = 6$ with $\beta_{j^*} = 5$ and the variances of all decimated components are calibrated to the data. I set $T = 512$ and implement 2,500 simulations. For each regression, the table reports the median of the slope estimates, rejection probabilities at the 1%, 5% and 10% levels associated with Valkanov's (2003) rescaled $t/\sqrt{T}$ statistic and the median of the adjusted R^2 statistics. Panel A: I run linear regressions (with an intercept) of forward/backward aggregates over a horizon of length h. Panel B: I run linear regressions (with an intercept) of contemporaneous aggregates over a horizon of length h. Panel C: I run linear regressions (with an intercept) of forward/backward aggregates over a horizon of length h under the null of absence of scale-specific predictability (i.e., I set $\beta_{j^*} = 0$ and let white noise shocks drive the decimated components at scale j^*).

Table 1.7: Tails of $t/\sqrt{T}$ at various percentiles for the simulation exercise

		Horizon											
$h =$		8	16	32	48	56	64	72	80	88	96	112	128
	0.005	-0.3252	-0.4597	-0.6856	-0.8742	-0.9637	-1.0643	-1.1560	-1.2215	-1.2732	-1.3657	-1.6679	-1.8180
$\rho = 0.9863$	**0.025**	-0.2371	-0.3475	-0.4981	-0.6320	-0.6911	-0.7540	-0.8336	-0.8979	-0.9697	-1.0475	-1.1601	-1.2835
	0.050	-0.1971	-0.2862	-0.4129	-0.5169	-0.5699	-0.6318	-0.6792	-0.7397	-0.7983	-0.8508	-0.9511	-1.0464
	0.950	0.2142	0.2932	0.4379	0.5556	0.6365	0.6864	0.7410	0.7876	0.8384	0.8896	0.9832	1.1185
$\delta = -0.0792$	**0.975**	0.2529	0.3519	0.5235	0.6830	0.7455	0.8173	0.8906	0.9551	0.9891	1.0702	1.2340	1.3876
	0.995	0.3252	0.4726	0.6887	0.8867	0.9992	1.0674	1.2094	1.2957	1.3947	1.4749	1.8272	1.9682

Notes: This table reports the critical values of $t/\sqrt{T}$ at various percentiles (bold values). I simulate the distribution of $t/\sqrt{T}$ for samples of length $T = 512$. I implement 5,000 replications. The distribution depends on two nuisance parameters c and δ. The parameter $c = (\rho - 1)\, T$ measures deviations from unity in a decreasing (at rate T) neighbourhood of 1. The parameter δ measures the covariance of the innovations.

Figure 1.5: Dynamics of slope coefficients and R^2's under different simulation scenarios

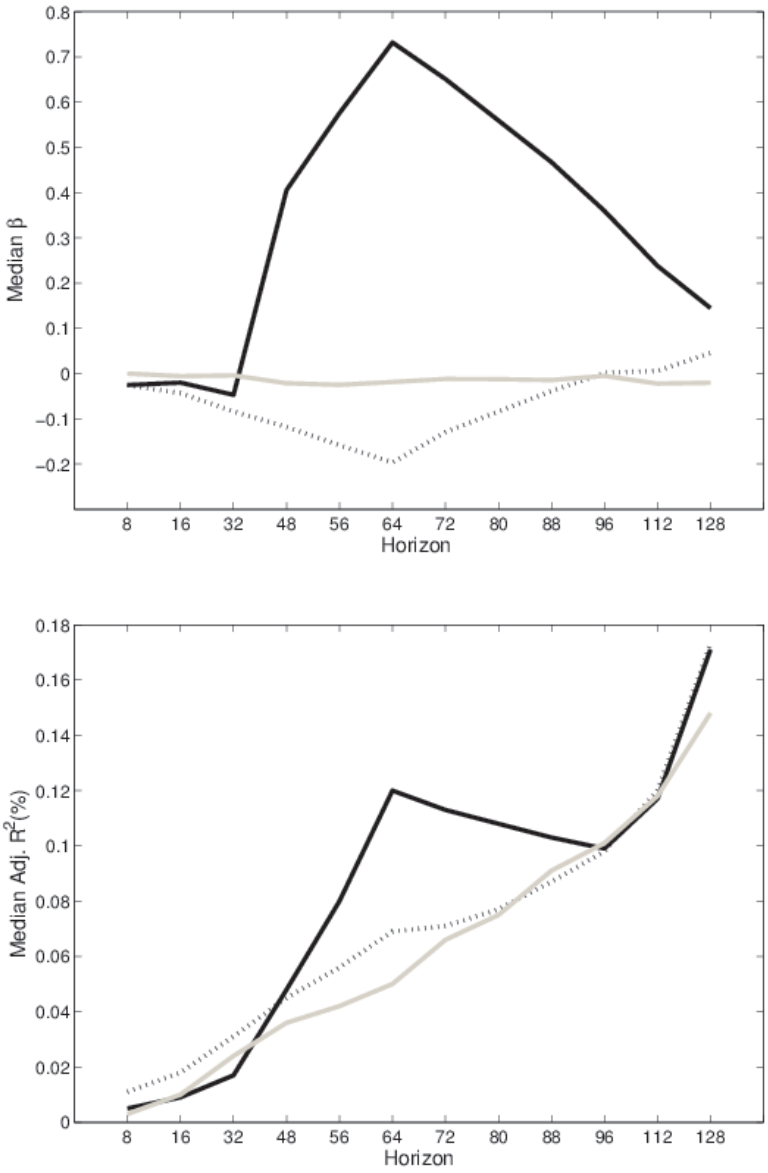

Notes: These figures plot the dynamics of the slope coefficients and R^2s across horizons under different simulation scenarios. The solid black lines represent the median of the slope estimates and the median of the adjusted R^2 statistics from regressions of forward-backward aggregates while the dotted line from contemporaneous regressions. The solid grey lines represent the median β_h and the median adj. R^2 from regressions of forward-backward aggregates under the null of absence of scale-specific predictability.

$$\boldsymbol{f}^{(\boldsymbol{j})} = \left[f_{2^j}^{(j)}, \ldots, f_{k\times 2^j}^{(j)}, \ldots, f_T^{(j)}\right]^\top \quad \text{and} \quad \boldsymbol{r}^{(\boldsymbol{j})} = \left[r_{2^j}^{(j)}, \ldots, r_{k\times 2^j}^{(j)}, \ldots, r_T^{(j)}\right]^\top. \tag{1.71}$$

In particular, the sample covariance is given by

$$\begin{aligned}
\operatorname{Cov}\left[r_t, f_t\right] &= \frac{\sum_{t=1}^T r_t f_t}{T} - \frac{\sum_{t=1}^T r_t}{T}\frac{\sum_{t=1}^T f_t}{T} && (1.72)\\
&= \frac{\left(r_T^{(J)}\right)^\top \left(f_T^{(J)}\right)}{T} - \frac{\sum_{t=1}^T r_t}{T}\frac{\sum_{t=1}^T f_t}{T} && (1.73)\\
&= \frac{\left(\left(\Lambda^{(J)}\right)^{-1/2}\mathcal{T}^{(J)} r_T^{(J)}\right)^\top \left(\left(\Lambda^{(J)}\right)^{-1/2}\mathcal{T}^{(J)} f_T^{(J)}\right)}{T} - \frac{\sum_{t=1}^T r_t}{T}\frac{\sum_{t=1}^T f_t}{T} && (1.74)\\
&= \frac{\sum_{j=1}^J 2^j \left(\mathbf{r}^{(\mathbf{j})}\right)^\top \mathbf{f}^{(\mathbf{j})}}{T} + \underbrace{2^J \frac{\pi_r^{(J)}\pi_f^{(J)}}{T} - \frac{\sum_{t=1}^T r_t}{T}\frac{\sum_{t=1}^T f_t}{T}}_{=0} && (1.75)
\end{aligned}$$

and therefore

$$\operatorname{Cov}\left[r_t, f_t\right] = \sum_{j=1}^J \operatorname{Cov}\left[r_{k\times 2^j}^{(j)} f_{k\times 2^j}^{(j)}\right] \tag{1.76}$$

By using simple time-series techniques, Bandi and Tamoni (2016) provide a formal method to analyze risk exposures at different frequencies and subsequently study how the pricing of risk varies across investment horizons. Note that the covariance-decomposition can also be extended to the case where the components are not decimated, i.e.

$$\operatorname{Cov}\left[r_t, f_t\right] = \sum_{j=1}^J \operatorname{Cov}\left[r_t^{(j)} f_t^{(j)}\right] + \operatorname{Cov}\left[\pi_r^{(J)}\pi_f^{(J)}\right] \tag{1.77}$$

where the last term is the covariance of the long-run trends. **See chapter 2 and 3 for applications with macroeconomic uncertainty and macro growth and volatility risks respectively**. For similar wavelet-based variance/covariance decompositions that allow more general filters see also Gençay, Selçuk, and Whitcher (2001).

1.11 Conclusions and Contribution

I have provided an introduction to the econometric framework necessary to understand scale-dependencies in financial economics. **My explicit contribution to the current body of work is two-fold**: First, I present an analysis of the size and power properties of the multi-scale variance ratio test of Ortu et al. (2013) that can distinguish a white noise process from a process whose decimated components are serially correlated. More importantly, however, I show that scale-specific predictability translates into predictability upon two-way aggregation irrespective of whether the regressor is scale-autoregressive. To put it simply, two scale-localized white noise processes - one of which predicts the other - can yield statistically significant economic relations upon aggregation.

Chapter 2

Business-Cycle Variation in Macroeconomic Uncertainty and the Cross-Section of Expected Returns: Evidence for Scale-Dependent Risks

2.1 Introduction

In this chapter, I decompose macroeconomic uncertainty into components with heterogeneous degrees of persistence and investigate the price of risk and the uncertainty premia associated with each of these scale-dependent macroeconomic shocks. This approach allows me to identify a close link between macroeconomic uncertainty and portfolio expected returns at business-cycle frequencies which is not present in the raw series. I quantify aggregate uncertainty using the model-free index of Jurado et al. (2015) that measures the common variation in the unforecastable component of a large number of economic indicators. That is, in line with the core intuition of Jurado et al. (2015) I start my empirical work from the premise that what matters for consumption and investment decisions is not if the conditional volatility of a particular macroeconomic indicator has become more or less dispersed. Instead, what is important is whether the state of the economy is more or less predictable. To classify uncertainty shocks into layers with different levels of persistence (i.e., on the basis of their arrival time and scale) I rely on the multiresolution-based decomposition for weakly

stationary time series of Ortu et al. (2013). Moreover, my study is based on the novel framework for scale-based (i.e., horizon-specific) analysis of risk as proposed first in Bandi and Tamoni (2016) and extended later by Boons and Tamoni (2016).

I find that a single *business-cycle*[17] *uncertainty* factor that captures assets' exposure to low-frequency variation in aggregate uncertainty can help explain the level and the cross-sectional differences of asset returns. In particular, based on portfolio-level tests I show that uncertainty shocks with persistence ranging from 32 to 128 months carry a negative price of risk of about -2% annually. The price of risk for high-frequency fluctuations and for the innovations in the raw series of aggregate uncertainty (see Table 2A.1) is not significant. In addition, I demonstrate that equity exposures to macroeconomic uncertainty are also negative and hence uncertainty risk premia are positive. My results remain statistically significant after using a t-statistic cutoff of three as suggested by Harvey et al. (2016) and are quantitatively similar irrespective of whether uncertainty is derived from 1, 3 or 12 months ahead forecasts. Furthermore, while misspecification is an inherent feature of several prominent asset pricing models (for instance, see Kan et al., 2013 and Gospodinov et al., 2014) I show that the one-factor model with business-cycle macro uncertainty is correctly specified. This finding is an important contribution in the existing literature.

My work follows and builds upon the novel work of Boons and Tamoni (2016) that emphasizes the importance of low-frequency macro volatility shocks with persistence greater than 4 years in determining asset prices. In comparison with Boons and Tamoni (2016) I do not restrict[18] the price of risk across scales and hence my empirical results are more precise about the exact time-scale (i.e., horizon) over which macroeconomic uncertainty matters (i.e., 32 to 128 months). In particular, I document that only business-cycle variation in uncertainty drives asset prices. Fluctuations in macro uncertainty with persistence greater than 128 months are not consistently priced in the cross-section

[17] Business-cycle dynamics correspond to periods of roughly 2-8 years - see Burns and Mitchell (1946) and the survey of Diebold and Rudebusch (1996). More recently, Comin and Gertler (2006) argue that business cycles are more persistent phenomena and suggest modelling fluctuations beyond 8 years.

[18] Note that I estimate separately the price of risk for each time-scale (i.e. I analyze the entire term structure of risk prices). Boons and Tamoni (2016) focus on a more traditional (in the spirit of Beveridge and Nelson, 1981) separation of high versus low-frequency components, i.e. they estimate a restricted two-factor model.

of expected returns (see Tables 2B.5 - 2B.7). In addition, I show that the quarterly results for macro volatility risk in Boons and Tamoni (2016) are not robust to changes in the sampling frequency. Specifically, using monthly data I find that low-frequency shocks in the volatility of industrial production are not priced at the portfolio level (see Table 2B.8). On the contrary, my estimates for the price of risk are free from dependencies on any single economic indicators, numerically similar (i.e., -2%) and robust across different test assets including: the 25 Fama and French (1993) size and book-to-market portfolios, the 25 Fama and French (2015) size and investment portfolios, the 25 Fama and French (2015) book-to-market and operating profitability portfolios and the 25 Fama and French (2016) size and variance portfolios. Also, my results suggest that the uncertainty shocks at each scale carry unique information[19] (i.e., *scale-wise heterogeneity*). That is, in the spirit of Bandi et al. (2016) there is a simple statistical explanation of why the relation between macro uncertainty and returns is only present at certain time-scales.

Moreover, I examine for monotonicity in the low-frequency uncertainty betas. I find that the scale-specific risk loadings are increasing monotonically for portfolios sorted on size and investment. An increase in low-frequency uncertainty has a smaller effect on large firms and aggressive firms and hence these securities offer smaller risk compensations - consistent with the well-known size effect (i.e., one-period average returns decrease from small to big stocks) and the investment effect (i.e., one-period average returns decrease from conservative to aggressive stocks), respectively. Similarly, scale-specific risk exposures decrease monotonically across book-to-market and dividend-yield - consistent with the well-documented value and dividend-yield effects. Overall, I document a low-frequency risk-return trade-off for the valuation of portfolios exposed to fluctuations in macroeconomic uncertainty.

My work adds to a new strand of research that examines how horizon-dependent shocks propagate to asset prices. Bandi et al. (2016) introduce the novel notion of scale-specific predictability and demonstrate its significance as a channel through which economic relations may be valid at

[19] See Table 2B.17. Similar results can be seen in Bandi et al. (2016) for market variance and consumption variance.

particular horizons (i.e., levels of resolution) without having to be satisfied at all horizons. Ortu et al. (2013) decompose consumption growth into components with heterogeneous levels of persistence and analyze their implications within a Bansal and Yaron (2004) style economy. Bandi and Tamoni (2016) show that fluctuations in consumption growth between 2 and 8 years can explain the differences in risk premia across book-to-market and size-sorted portfolios in line with the Consumption CAPM. In a similar fashion, Kamara et al. (2015) study the pricing of Fama-French factors across investment horizons. Noteworthy contributions in this area also include Yu (2012) and Dew-Becker and Giglio (2016) who analyze the joint properties of returns and macroeconomic growth at different frequencies.

Furthermore, my work contributes to a voluminous literature that analyzes the determinants of the cross-section of stock returns. For surveys of empirical literature on cross-sectional asset pricing see Subrahmanyam (2010), Goyal (2012) and more recently Harvey et al. (2016). Within this body of work two main lines of research are related to my study. The first part seeks to explain the cross-sectional pattern in returns based on the insights of the long-run risks (LRR) model of Bansal and Yaron (2004) which combines consumption and dividend growth rate dynamics governed by persistent shocks and fluctuating economy uncertainty[20]. Notable factors motivated from this framework include: long-horizon consumption growth rate (Parker and Julliard, 2005), long-run consumption risk (Bansal et al., 2005) and fourth-quarter year over year (Q4-Q4) consumption growth (Jagannathan and Wang, 2007). In line with Boons and Tamoni (2016), my study focuses on the covariance of long-term returns with innovations in long-term uncertainty and hence is distinct from the LLR framework which quantifies assets' exposure to long-run risks using one-period returns.

The second branch of this literature relies on the intuition of Merton's (1973) intertemporal capital asset pricing model (ICAPM)[21] to test for pricing of macroeconomic factors. In a seminal

[20] Due to the resulting low-frequency properties of the time series of aggregate consumption and dividends this family of models is known as long-run risks models.

[21] Theoretical extensions of the ICAPM include Campbell (1993, 1996); Chen (2002); Brennan et al. (2004); Campbell et al. (2014).

paper, Merton (1973) demonstrates that in a multi-period economy investors have incentives to hedge against future stochastic shifts in the investment and consumption opportunity sets. This implies that state variables that are correlated with changes in investment opportunities play an important role in determining asset returns. For an overview of studies that explore the cross-sectional implications of ICAPM-motivated macroeconomic factors see Table 2A.3.

Recent studies suggest that macroeconomic uncertainty can also be thought of as a state variable within the context of the ICAPM proxying for future investment and consumption opportunities[22]. In particular, Ozoguz (2009) shows that investors' uncertainty about the state of the economy can help explain the time-series variation in stock returns and their cross-sectional properties. Bali et al. (2016) develop a simple extension of Merton's (1973) conditional asset pricing model with economic uncertainty and show that uncertainty betas can explain the dispersion in individual stock returns while Bali et al. (2014) demonstrate that macroeconomic risk is priced in the cross-section of hedge funds. My work adds to this line of research in the following ways: First, I extend the study of Bali et al. (2016) by demonstrating that only fluctuations in macroeconomic uncertainty with persistence ranging from 32 to 128 months are consistently priced in the cross-section of portfolio returns while short-lived fluctuations and the innovations in the raw series are not. Second, I document that future excess aggregate returns are positively correlated with past uncertainty and thus the negative price of risk for exposure to business-cycle macro uncertainty is inconsistent with the central economic intuition underlying the ICAPM. That is, in the spirit of Maio and Santa-Clara (2012) and Boons (2016) macroeconomic uncertainty is not a valid risk factor under the ICAPM.

The remainder of this chapter is organized as follows: Section 2.2 provides the empirical analysis, including the extraction of the persistent components and cross-sectional regressions. Section 2.3 contains robustness checks and additional tests while Section 2.4 examines the monotonicity of the scale-specific risk exposures. Section 2.5 concludes.

[22] Bloom et al. (2007), Bekaert et al. (2009), Chen (2010) and Bloom et al. (2012) also provide theoretical and empirical evidence linking macroeconomic shocks to investment dynamics. For a review of the literature see Bloom (2014).

2.2 Empirical Analysis

2.2.1 Data Description

To measure macroeconomic uncertainty I use the model-free index[23] of Jurado et al. (2015) that aggregates uncertainty in the economy derived from various sources into one summary statistic. Jurado et al. (2015) combine 132 macroeconomic series and 147 financial time series together into one large macroeconomic dataset[24] to provide a new measure of macroeconomic uncertainty defined as the common variation in the unforecastable components. The first dataset (also used in Ludvigson and Ng, 2009) represents a broad category of macroeconomic time series such as: real output and income, employment, consumer spending, bond and stock market indexes and foreign exchange measures. The second dataset (also used in Ludvigson and Ng, 2007) includes valuation ratios such as dividend-price ratio and earnings-price ratio, default and term spreads, yields on corporate bonds and a large cross-section of equity returns.

In particular, let $u_{i,t}(h)$ denote the $h-$period ahead uncertainty in the variable $y_{i,t} \in Y_t = (y_{1,t}, \ldots, y_{Ny,t})'$ defined as the conditional volatility of the unforecastable component of its future value, that is,

$$u_{i,t}(h) \equiv \sqrt{E\left[\left(y_{i,t+h} - E\left[y_{i,t+h}|I_t\right]\right)^2 |I_t\right]} \tag{2.1}$$

where I_t is the information set[25] available to investors at time t. Jurado et al. (2015) construct the index of macroeconomic uncertainty by aggregating individual uncertainty at each date, i.e. the $h-$period ahead aggregate uncertainty at time t is given by

[23] Previous studies have relied on proxies of uncertainty such as "uncertainty-related" key words in news publications (Baker et al., 2013), cross-sectional dispersion of survey-based forecasts (Bali et al., 2016) and implied or realized volatility of stock market returns (Bloom, 2009).

[24] The dataset is available from Sydney Ludvigson's website: http://www.econ.nyu.edu/user/ludvigsons/ .

[25] To estimate $E[\cdot|I_t]$ Jurado et al. (2015) form factors from a large set of predictors whose span is close to I_t and approximate $E[\cdot|I_t]$ using the method of diffusion index forecasting (see Stock and Watson, 2002).

$$u_t(h) \equiv \text{plim}_{Ny\to\infty} \sum_{i=1}^{Ny} w_i u_{i,t}(h) \equiv E_w[u_{i,t}(h)] \tag{2.2}$$

where $w_i = 1/N_y$ are aggregation weights. I rely on estimates of aggregate uncertainty derived from 1, 3 and 12 months ahead forecasts. Throughout the chapter I use the notation u_t for the time series proxying for macroeconomic uncertainty leaving h understood when there is no chance of confusion.

In Panel A of Table 2.1 I report descriptive statistics for the macroeconomic uncertainty index. In addition, I examine the persistence of the uncertainty index through a battery of testing procedures. I report the p-values of the Augmented Dickey-Fuller (ADF - Dickey and Fuller, 1979) and Phillips-Perron (PP - Phillips and Perron, 1988) tests for unit root and the values of the KPSS (Kwiatkowski et al., 1992) test statistic for the null hypothesis of stationarity whose critical values are 0.347, 0.463 and 0.739 at the 10%, 5% and 1% significance levels respectively. The null hypothesis of a unit root is rejected at the 5% level with the ADF and PP tests for all measures of uncertainty. Similarly, the results of a KPSS test confirm that the series is stationary for all $h = 1, 3, 12$. Panel B of Table 2.1 presents the mean and standard deviation for the equity risk premium[26], defined as the total rate of return on the stock market minus the prevailing short-term interest rate. Over the sample period it has a mean of 5.71% and a standard deviation of 15.02%. Figure 2.1 plots the index of macroeconomic uncertainty for $h = 1, 3, 12$. The shaded areas represent NBER recessions.

2.2.2 Scale-wise Heterogeneity in Aggregate Uncertainty

I begin by decomposing uncertainty into layers with heterogeneous levels of persistence using the multiresolution-based decomposition of Ortu et al. (2013). In particular, let $u_t^{(j)}$ denote fluctuations of the uncertainty series with half-life in the interval $[2^{j-1}, 2^j)$, that is

[26]The data for the equity risk premium and the default and term spread used in Section 2.2.4 are available from Amit Goyal's website: http://www.hec.unil.ch/agoyal/

$$u_t^{(j)} = \frac{\sum_{i=0}^{2^{(j-1)}-1} u_{t-i}}{2^{(j-1)}} - \frac{\sum_{i=0}^{2^j-1} u_{t-i}}{2^j} \equiv \pi_t^{(j-1)} - \pi_t^{(j)} \tag{2.3}$$

where $j \geq 1$, $\pi_t^{(0)} \equiv u_t$ and the moving averages $\pi_t^{(j)}$ satisfies the recursion

$$\pi_t^{(j)} = \frac{\pi_t^{(j-1)} + \pi_{t-2^{j-1}}^{(j-1)}}{2} \tag{2.4}$$

for $j = 1, 2, 3, \ldots$. The derived series $\left\{u_t^{(j)}\right\}_{t\in\mathbb{Z}}$ captures fluctuations that survive to averaging over 2^{j-1} terms but disappear when the average involves 2^j terms. For any $J \geq 1$, the original series u_t can be written as a sum of components with half-life belonging to a specific interval plus a long-run average, that is,

$$u_t = \sum_{j=1}^{J} u_t^{(j)} + \underbrace{u_t^{(>J)}}_{\equiv \pi_t^{(J)}} \tag{2.5}$$

where $u_t^{(>J)}$ incorporates fluctuations with persistence greater than 2^J periods. The decomposition of the time series is conducted using wavelet methods as in multiresolution analysis. In particular, the extraction is based on the one-sided, linear Haar filter. Moreover, the decomposition in Equation (2.5) uses information only up to time t and hence is not subject to look-ahead bias. In contrast, other popular filters for business cycle analysis are estimated over the full sample (for instance, see Hodrick and Prescott, 1997).

For my empirical analysis, I set $J = 7$ so that the maximum level of persistence corresponds to the upper bound of business cycle frequencies. An interpretation of the $j-$th persistence level in terms of the corresponding time spans in the case of monthly time series is available in Table 2.2. Figures 2.2a and 2.2b depict the persistent components filtered out of aggregate uncertainty. Note that due to the initialization of the filtering procedure I discard the first $2^j - 1$ observations for each scale.

Furthermore, I use the multi-scale variance ratio test of Ortu et al. (2013) to test for serial

correlation in the extracted uncertainty components $u_t^{(j)}$, $j = 1, 2, \ldots, 7$. This test is based on a new family of frequency-domain tests for serial correlation as introduced by Gençay and Signori (2015) and exploits the fact that for a serial correlated process each component contributes a different percentage to the variance of the process. Specifically, let $\hat{\xi}_j$ be the ratio of the sample variance of the uncertainty components at level of persistence j to the sample variance of the time series, i.e.

$$\hat{\xi}_j = \frac{2^j \left(\mathbf{u^{(j)}}\right)^{\intercal} \mathbf{u^{(j)}}}{\left(X_T^{(J)}\right)^{\intercal} X_T^{(J)}} \tag{2.6}$$

where $\left(X_T^{(J)}\right)^{\intercal} = [u_T, u_{T-1}, \ldots, u_1]$ is the vector collecting the observations of $\{u_t\}$ and $\mathbf{u^{(j)}} = \left[u_{2^j}^{(j)}, \ldots, u_{k\times 2^j}^{(j)}, \ldots, u_T^{(j)}\right]^{\intercal}$. That is, due to the overlapping of the moving averages that define $u_t^{(j)}$ the elements of each component are first sampled every $k \times 2^j, k \in \mathbb{Z}$ times and thus the sample variance is calculated from the decimated series. Under the null hypothesis of no serial correlation, the rescaled test statistic $\sqrt{\frac{T}{a_j}}\left(\hat{\xi}_j - \frac{1}{2^j}\right)$ where $a_j = \frac{\binom{2^j}{2}}{2^j 2^{2(j-1)}}$ converges in distribution to a standard normal. Ortu et al. (2013) suggest employing these rescaled test statistics to distinguish a white noise process from a process whose (decimated) scale-dependent components are serially correlated. Table 2.3 presents the results for the variance ratio test of Ortu et al. (2013) for different levels of persistence with bold values denoting rejection of the null at a 99% confidence level. A white noise model is strongly rejected at multiple levels of persistence. These results imply that at least one of the uncertainty components can be represented as a scale autoregressive process on the dilated time of the scale being considered. In other words, there exists $j^* \in \{1, \ldots, 7\}$ such that $u_{k\times 2^{j^*}+2^{j^*}}^{(j^*)} = \rho_{j^*} u_{k\times 2^{j^*}}^{(j^*)} + \varepsilon_{k\times 2^{j^*}+2^{j^*}}^{(j^*)}$ where $k \in Z$ and the parameter ρ_j captures scale-specific persistence - known as scale-wise AR. Estimation results of the multi-scale autoregressive system are available in Appendix 2B (see Table 2B.17).

In total, the empirical evidence in this section provide strong support for a data generating process in which low-frequency uncertainty shocks are not linear combinations of high-frequency

shocks. That is, in line with the generalized Wold representation of Bandi et al. (2016) the uncertainty shocks at each scale carry unique information (i.e., scale-wise heterogeneity) - *thereby giving meaning to economic relations which may be satisfied at certain time-scales alone.* Moreover, innovations for all scale-specific uncertainty components have to be computed before examining their asset pricing implications (i.e., only the unexpected part of the uncertainty components should command a risk premium).

2.2.3 Cross-sectional Implications

I test whether the innovations (i.e., $\Delta u_t^{(j)} \equiv u_t^{(j)} - u_{t-1}^{(j)}$) in the persistent components filtered out of the uncertainty index can help explain the cross-sectional variation in asset prices. This approach resembles empirical studies that test ICAPM-motivated macroeconomic factors by calculating innovations in state variables. To obtain the innovations for each scale j, I first extract the $j-$th component and then I first-difference it. Under the one-sided, linear Haar filter used in the extraction, first-differencing the component of a given time series is identical to taking components of the first-differenced series (see Bandi et al., 2016).

Macroeconomic risk as proxied by the covariance between innovations in uncertainty (i.e., Δu_t) and asset excess returns (i.e., $R_t^{e,i}$) can be decomposed across scales as follows (see the novel framework of Bandi and Tamoni, 2016 and Boons and Tamoni, 2016)

$$Cov\left[R_t^{e,i}, \Delta u_t\right] = \sum_{j=1}^{J} Cov\left[R_t^{e,i(j)}, \Delta u_t^{(j)}\right] + Cov\left[R_t^{e,i(>J)}, \Delta u_t^{(>J)}\right] \tag{2.7}$$

and hence the scale-wise (i.e., horizon-specific) risk exposures are defined as

$$\beta^{i(j)} \equiv \frac{Cov\left[R_t^{e,i(j)}, \Delta u_t^{(j)}\right]}{Var\left(\Delta u_t^{(j)}\right)} \quad \text{and} \quad \beta^{i(>J)} \equiv \frac{Cov\left[R_t^{e,i(>J)}, \Delta u_t^{(>J)}\right]}{Var\left(\Delta u_t^{(>J)}\right)}. \tag{2.8}$$

In particular, in line with Boons and Tamoni (2016) I first run for each asset i (of size T) the following time-series regression

$$R_t^{e,i(j)} = \beta_0^{(j)} + \beta^{i(j)} \Delta u_t^{(j)} + \varepsilon_t^{(j)} \quad t = 1, \ldots, T \text{ for each } j = 1, \ldots, 7, > 7, \tag{2.9}$$

where $R_t{}^{e,i(j)}$ denotes the components of asset excess returns associated with scale j at time t. Then I estimate a cross-sectional regression of average portfolio returns on the estimated scale-specific risk exposures $\beta^{i(j)}$

$$\overline{R^{e,i}} = \lambda_{0,j} + \lambda_j \beta^{i(j)} + \alpha_i \quad \text{for each } j = 1, \ldots, 7, > 7, \tag{2.10}$$

where $\overline{R^{e,i}}$ denotes the average time-series excess return for asset i, $\lambda_{0,j}$ is the zero-beta excess return associated with different uncertainty components, λ_j is the relative price of risk for $\beta^{(j)}$ (i.e., the scale-specific risk compensation)[27] and α_i is a pricing error. In essence, I am interested in the ability of scale-dependent uncertainty shocks to explain aggregate portfolio returns. In addition, I run Equations (2.9)-(2.10) for uncertainty shocks with persistence between 32 and 128 months (i.e., for a *business-cycle uncertainty* factor) where the corresponding beta for $j = 6:7$ is defined as

$$\beta^{i(6:7)} \equiv \frac{Cov\left[R_t^{e,i(6)} + R_t^{e,i(7)}, \Delta u_t^{(6)} + \Delta u_t^{(7)}\right]}{Var\left(\Delta u_t^{(6)} + \Delta u_t^{(7)}\right)} \simeq \beta^{i(6)} \varpi^{(6)} + \beta^{i(7)} \varpi^{(7)} \tag{2.11}$$

with $\varpi^{(6)} = \frac{Var\left(\Delta u_t^{(6)}\right)}{Var\left(\Delta u_t^{(6)}\right) + Var\left(\Delta u_t^{(7)}\right)}$ and $\varpi^{(7)} = \frac{Var\left(\Delta u_t^{(7)}\right)}{Var\left(\Delta u_t^{(6)}\right) + Var\left(\Delta u_t^{(7)}\right)}$. That is, $\beta^{(6:7)}$ can be viewed as a linear combination[28] of the betas associated with the factors $\Delta u_t^{(6)}$ and $\Delta u_t^{(7)}$ with weights depending on the relative contribution to total variance (see also Bandi and Tamoni, 2016 for a similar approach using decimated components).

Following Campbell et al. (2014) and in line with the theoretical work of Black (1972) and

[27] I verify empirically that for $j > 7$ and for all test portfolios, assets' exposure to uncertainty shocks with persistence greater than $2^7 = 128$ months is not important for pricing. The results are available in Appendix 2B (see Tables 2B.5, 2B.6 and 2B.7).

[28] Asymptotically, the components are uncorrelated across scales. In sample, however, multiresolution filters - like the Haar filter used for the extraction - only deliver *nearly-uncorrelated* components (see also Bandi and Tamoni, 2016 and Gençay et al., 2001) and therefore the relation in Equation (2.11) is not exact. For further discussion and a comparison of $\beta^{(6:7)}$ versus $\beta^{(6)}\varpi^{(6)} + \beta^{(7)}\varpi^{(7)}$ see Appendix 2B (see Figure 2B.2).

the evidence[29] in Krishnamurthy and Vissing-Jorgensen (2012) I leave the zero-beta risk-free rate unrestricted. To determine whether uncertainty shocks with level of persistence j can explain the cross-sectional variation in asset returns I look for an estimate $\hat{\lambda}_j$ that remains significant after using a t-statistic cutoff of three as suggested by Harvey et al. (2016), for an intercept that is small and statistically insignificant and a sample R^2 significantly different from zero.

Table 2.4 presents the first-pass beta estimates for the 25 Fama and French (1993) size and book-to-market portfolios along with their statistical significance. The initial sample period is 1960:07 to 2013:05. The betas are estimated component-wise from Equation (2.9), that is regressing the $j-$th component of returns on innovations in the $j-$ th component of aggregate uncertainty. Given the adopted time-series decomposition spurious autocorrelation at level of persistence j emerges as a result of the 2^j-1 overlapping data. Thus, I compute Newey-West (1987) heteroskedasticity and autocorrelation consistent (HAC) standard errors with 2^j-1 lags. To preserve space I only report results[30] for $j=6,7$ and $j=6:7$. The scale-specific risk exposures for the test portfolios are negative. The last rows of Table 2.4 show the Wald test-statistics and their corresponding p-values from testing the joint hypothesis that all scale-dependent exposures are equal to zero. For $j=6$ and $j=6:7$ the null hypothesis in the joint test of significance i.e. $H_0: \beta^{1(j)}=\ldots=\beta^{25(j)}=0$ is strongly rejected. Therefore, in the spirit of Kan and Zhang (1999) it is empirically sound to use these scale-dependent betas as factors in cross-sectional regressions. In contrast, for $j=7$ I cannot reject the null that the scale-specific risk exposures are jointly zero.

Table 2.5 reports the estimates for the zero-beta excess return and the price of risk for each scale for the 25 size and book-to-market portfolios along with the corresponding Fama-MacBeth[31] (1973) test statistics in parentheses. In addition, I normalize the scale-wise risk exposures and

[29] Krishnamurthy and Vissing-Jorgensen (2012) suggest that investors' demand for Treasury Bills is driven by liquidity and safety concerns and argue against the common practice of identifying the Treasury Bills as risk-free interest rates.

[30] For $j\in\{1,2,3,4,5\}$ the scale-specific risk exposures are jointly different from zero across all test assets (results available upon request).

[31] Given that the first-stage regressions are scale-wise, the Shanken correction (Shanken, 1992) is not directly applicable here. To deal with the error-in-variables problem (i.e., the estimation errors in the betas) I report bootstrapped confidence intervals for the second-pass estimates in Appendix 2B (Table 2B.14).

estimate the price of risk per unit of cross-sectional standard deviation in uncertainty in percent per year. I also report the p-value for the Kan et al. (2013) specification test of $H_0 : R^2 = 1$ denoted as $p\left(\mathrm{R}^2 = 1\right)$. After taking into consideration the data-mining adjusted rate for t-statistics of three, the lambda estimates for levels of persistence $j = 1, \ldots, 5$ are insignificant. The estimated price of risk for the innovations in the sixth uncertainty component $\hat{\lambda}_6$ is -0.69 with a t-statistic of -4.57 while the intercept is 0.14 and insignificant (t-stat = 0.59). The coefficient of determination for this factor is high and equal to 72.35% ($se(\widehat{\mathrm{R}^2_{(6)}}) = 0.138$)[32] and the mean absolute pricing error (MAPE) across all securities is 1.11% per year. A standard deviation increase in exposure to low-frequency uncertainty shocks leads to a decrease in portfolio returns by -2.30% annually. Moreover, the estimated price of risk for the innovations in the seventh uncertainty component is also negative with a t-statistic of -3.21. However the estimated zero-beta excess return for this case is significant at the 1% level (t-stat = 2.37). The performance of the *business-cycle uncertainty* factor (i.e., $\Delta u_t^{(6:7)}$) is similar to $\Delta u_t^{(6)}$ with a cross-sectional R^2 of 73.90% ($se(\widehat{\mathrm{R}^2_{(6:7)}}) = 0.123$) and MAPE equal to 1.11% per year. Finally, for each of the low-frequency factors the Kan et al. (2013) specification test does not reject the hypothesis that the model is correctly specified.

Since $\beta^{(6)} \times \lambda_6 > 0$ (or equivalently $\beta^{(6:7)} \times \lambda_{6:7} > 0$) low-frequency uncertainty shocks carry positive risk premia. My results are in contrast with the work of Campbell et al. (2014) who find that in the post-1963 period equities have positive volatility betas and therefore negative risk premia. However, my findings are in line with Boguth and Kuehn (2013), Bansal, Kiku, Shaliastovich, and Yaron (2014) and Tédongap (2015) who provide evidence of negative exposure of asset returns to alternative measures of volatility risk. In addition, my results are in agreement with Boons and Tamoni (2016) who first show that the price of low-frequency volatility risk is negative and assets have negative low-frequency volatility betas and thus long-run volatility risk premia are positive.

[32] When $0 < \mathrm{R}^2 < 1$, $\widehat{\mathrm{R}^2}$ is asymptotically normally distributed around its true value and thus I cannot use $\widehat{\mathrm{R}^2} \pm 1.96 \times se(\widehat{\mathrm{R}^2})$ to obtain a 95% confidence interval. One way to construct confidence intervals is by pivoting the cumulative distribution function (cdf) (see section 9.2.3 in Casella and Berger, 2002). Kan and Robotti (2009) and Kan and Robotti (2015) use the same method to construct confidence intervals for the Hansen-Jagannathan distance and the Hansen-Jagannathan bound respectively. To preserve space I only report confidence intervals in Table 2.12. The R^2 for the *business-cycle uncertainty* factor is significantly different from zero across all test assets.

Panel A of Figure 2.3 plots realized versus fitted average excess returns for the 25 size and book-to-market FF portfolios where the priced factor is $\Delta u_t^{(6:7)}$, that is, the innovations in low-frequency uncertainty shocks (derived from monthly forecasts) with persistence ranging from 32 to 128 months. Each two-digit number represents a separate portfolio. The first digit refers to the size quintile of the portfolio (1 being the smallest and 5 the largest), while the second digit refers to the book-to-market quintile (1 being the lowest and 5 the highest). If the fitted and the realized returns for each portfolio are the same then they should lie on the 45-degree line from the origin. Panel A visually confirms that the fit of the model is good. Similarly, Panel B shows that the factor $\Delta u_t^{(6:7)}$ is successful at explaining the size and value effects.

2.2.4 Relation with Business-Cycle Indicators and Macroeconomic Volatility Risk

Next, I examine the relation of the low-frequency uncertainty factor $u_t^{(6:7)}$ with macroeconomic variables linked to fluctuations of the business cycle such as the term spread and default spread. It is well-documented that these yield spreads are high around business-cycle troughs and low near peaks (for instance, see Fama and French, 1989; Estrella and Hardouvelis, 1991 and Hahn and Lee, 2006). In addition, the default spread and term spread are known to forecast macroeconomic activity (Boons, 2016) and have long been used as proxies for credit market conditions and the stance of monetary policy, respectively. Following Welch and Goyal (2008), the default spread is defined as the difference between BAA and AAA-rated corporate bond yields. Similarly, the term spread is defined as the difference between the long term yield on government bonds and the three-month Treasury-bill rates. The correlation between the term spread and $u_t^{(6:7)}$ is 0.11 and statistically significant at the 5% level. The correlation between the default spread and $u_t^{(6:7)}$ is 0.48 and statistically significant at the 1% level (see Figure 2.4). That is, an increase in low-frequency aggregate uncertainty is closely associated with the deterioration of credit market conditions.

Moreover, I examine the correlation of $u_t^{(6:7)}$ with the low-frequency macroeconomic volatility

risk factor of Boons and Tamoni (2016). To measure macro volatility I consider the following AR (1) − GARCH(1, 1) specification

$$IPG_t = \mu + \phi IPG_{t-1} + \nu_t, \tag{2.12}$$

$$\sigma_t^2 = \omega_0 + \omega_1 \nu_{t-1}^2 + \omega_2 \sigma_{t-1}^2 \tag{2.13}$$

where IPG_t is the (latest vintage) seasonally-adjusted industrial production growth rate from the FRED database of the St. Louis FED and $IPVOL = \widehat{\sigma_t}$. The correlation between uncertainty shocks with persistence between 32 and 128 months (i.e., $u_t^{(6:7)}$) and macro volatility shocks with persistence greater than 32 months (i.e., $IPVOL_t^{(>5)}$) is 0.74 and statistically significant at the 1% level (see Figure 2.4). In other words, there is a close link between long-run uncertainty about the state of the economy and low-frequency variation in the volatility of industrial production. However, the correlation between $\Delta IPVOL_t^{(>5)}$ and innovations in the *business-cycle uncertainty* factor is 0.48 (for $h = 1$) and reduces further to 0.38 (for $h = 12$).

2.3 Robustness Checks and Additional Tests

2.3.1 Alternative Test Assets

I confirm that my findings are robust by looking at alternative sets of test portfolios. I use the 25 Fama and French (2015) size and investment portfolios, the 25 Fama and French (2015) book-to-market and operating profitability portfolios and the 25 Fama and French (2016) size and variance portfolios. Below I discuss the cross-sectional estimates based on macroeconomic uncertainty derived from monthly forecasts (i.e., $u_t(1)$). The results for aggregate uncertainty derived from quarterly (i.e., $u_t(3)$) and annual (i.e., $u_t(12)$) forecasts are similar.

Tables 2.6 and 2.7 report the first-pass scale-wise exposures and the cross-sectional estimates for the 25 Fama and French (2015) size and investment portfolios, respectively. The initial sample period is 1963:07 to 2013:05. For $j = 6$ and $j = 6 : 7$ the null $H_0 : \beta^{1(j)} = \ldots = \beta^{25(j)} = 0$ is

strongly rejected while for $j = 7$ the component-wise exposures are not statistically different from zero. The estimated price of risk for the innovations in the sixth uncertainty factor is negative (-0.52) with a t-statistic of -3.05 and the estimate of $\hat{\lambda}_{0,6}$ is not significant (t-stat = 1.00). The cross-sectional R^2 is 51.52% ($se(\widehat{\mathrm{R}^2_{(6)}}) = 0.286$) and the MAPE across all securities is less than 1% per year. Innovations in low-frequency uncertainty with persistence ranging between 64 and 128 months are also priced (t-stat = -3.83). However, the estimate for the zero-beta excess return is significant at the 1% level (t-stat = 2.91). The pricing performance of the *business-cycle uncertainty* factor is considerably better among these test portfolios with a cross-sectional R^2 of 73.00% and the lowest sampling variability (i.e., $se(\widehat{\mathrm{R}^2_{(6:7)}}) = 0.092$). In addition, the null hypothesis that the model is correctly specified is not rejected. The price of risk per unit of cross-sectional standard deviation in $\Delta u_t^{(6:7)}$ is -2.21%.

Tables 2.8 and 2.9 present the scale-specific risk exposures and the cross-sectional estimates for the 25 Fama and French (2015) book-to-market and operating profitability portfolios. The initial sample period is 1963:07 to 2013:05. Consistent with the results for the previous test portfolios for $j = 7$ the hypothesis that all scale-dependent betas are zero is not rejected, that is, the proposed factor is independent of the portfolio returns. The estimated price of risk for $\Delta u_t^{(6)}$ is -0.48 with a t-statistic of -2.98 and the estimated zero-beta excess return is not significant (t-stat = 1.03). The cross-sectional R^2 is 39.20% ($se(\widehat{\mathrm{R}^2_{(6)}}) = 0.177$) and the MAPE across all assets is 2.14% annually. Furthermore, the estimated price of risk for $\Delta u_t^{(6:7)}$ is also significant (t-stat = -3.35) with a similar sample R^2 but smaller standard error ($se(\widehat{\mathrm{R}^2_{(6:7)}}) = 0.142$). The price of risk per unit of cross-sectional standard deviation in $\Delta u_t^{(6:7)}$ is -2.32%. It is worth emphasizing that for all scales the specification test rejects the hypothesis of a perfect fit.

Tables 2.10 and 2.11 provide the scale-specific risk exposures and the results from the cross-sectional regressions for the 25 Fama and French (2016) size and variance portfolios. The initial sample period is 1963:07 to 2013:05. The price of high-frequency uncertainty shocks (i.e., for $j = 1, \ldots, 5$) is small and insignificant. Low-frequency uncertainty with persistence between 32

and 64 months carries a negative price of risk of -0.50 with a t-statistic of -2.92 and the intercept is insignificant (t-stat = 0.85). The coefficient of determination is equal to 20.60% but is not significantly different from zero ($se(\widehat{\mathrm{R}^2_{(6)}}) = 0.190$). That is, using only the sample R^2 I cannot reject that the factor $\Delta u_t^{(6)}$ has essentially no explanatory power. In contrast, the cross-sectional R^2 for the *business-cycle uncertainty* factor is 54.84% ($se(\widehat{\mathrm{R}^2_{(6:7)}}) = 0.164$) and the null that the model is correctly specified is not rejected.

Figure 2.5 plots fitted versus realized average excess returns for the test portfolios of this section where the priced factor is $\Delta u_t^{(6:7)}$ derived from monthly forecasts. Figure 2.6 plots the fitted excess returns for the same portfolios. Finally, I repeat the analysis of the cross-sectional implications by using equal weighted returns for all test portfolios. The results - available upon request - are qualitatively and qualitatively similar.

2.3.2 Tests of Equality of Cross-Sectional R^2's

Next, I compare the two competing beta pricing models based on the factors $\Delta u_t^{(6)}$ and $\Delta u_t^{(6:7)}$ by asking whether they have the same population cross-sectional R^2. My analysis is similar in spirit with Kan et al. (2013). However, the sequential testing procedure suggested by Vuong (1989) and described in Kan et al. (2013) is not applicable here since the two models are non-nested and *distinct*[33]. Therefore, I perform directly the normal test of $H_0 : 0 < \mathrm{R}^2_{(6)} = \mathrm{R}^2_{(6:7)} < 1$, that is, I assume that both models are not perfectly specified (i.e., I check if the population R^2's are equal for some value less than one) and rule out the scenario that the two beta pricing models are completely irrelevant for explaining expected returns. Table 2.12 reports the results of the tests of equality of the cross-sectional R^2's where both models are estimated over the same period. There are no sufficient evidence across all test assets to reject the null hypothesis. Two observations emerge from

[33]For instance, consider two competing beta pricing models. Let f_{1t}, f_{2t} and f_{3t} be three sets of distinct factors at time t where f_{it} is of dimension $K_i \times 1$, $i = 1, 2, 3$. Assume that model 1 uses f_{1t} and f_{2t} as factors while model 2 uses f_{1t} and f_{3t}. When $K_2 = 0$ model 2 nests 1 as a special case. Similarly, when $K_3 = 0$ model 1 nests model 2. When $K_2 > 0$ and $K_3 > 0$ the two models are non-nested. Finally, when $K_2, K_3 > 0$ and $K_1 = 0$ the two models are non-nested and distinct.

the results in Table 2.12. First, the limited precision of the estimates makes it difficult to conclude whether one model consistently outperforms the other. That is, even cases of large R^2 differences do not give rise to statistical rejections due to the high sampling variability of the cross-sectional R^2's. Kan and Robotti (2009) and Kan et al. (2013) report similar problems in the comparison of linear asset pricing models using aggregate measures of pricing errors. Second, it is hard to distinguish between the two models since the relative contribution of $\Delta u_t^{(7)}$ in Equation (2.11) is small (i.e., $\varpi^{(6)} > \varpi^{(7)}$).

2.3.3 Benchmark Results & Controlling for Fama-French Factors

Furthermore, I present in Table 2.13 benchmark results for the Fama and French (1993) three-factor model (FF3) and the Fama and French (2015) five-factor model (FF5). The *business-cycle uncertainty* factor performs better than the Fama-French models in the cross-sections of the size and book-to-market and the size and investment portfolios. In particular, while the estimates of the cross-sectional R^2's are similar, the pricing performance of the FF3 and the FF5 model is driven by a statistical significant zero-beta excess return. In addition, both models are misspecified (i.e., the Kan et al., 2013 specification test of $H_0: R^2 = 1$ is strongly rejected). In contrast, the FF5 model explains significantly better the cross-sectional differences of assets sorted across book-to-market and operating profitability. Also, for these test assets the uncertainty factor does not survive in the presence of the profitability-based factor[34]. This finding is in line with Wang and Yu (2015) who demonstrate that the profitability premium (see Novy-Marx, 2013 and Hou et al., 2015) is not driven by macroeconomic risk.

2.3.4 Predictability of Aggregate Returns

Finally, I test the ability of the scale-dependent shocks filtered out of the index of macroeconomic uncertainty to predict the components of aggregate stock returns with the same time-scale with the

[34] To preserve space I report the results in Appendix 2B (see Table 3B.10).

following set of regressions

$$r^{e(j)}_{t+2^j} = \beta^{(j)}_0 + \beta^{(j)} u^{(j)}_t + \varepsilon^{(j)}_{t+2^j} \quad \text{for } j = 1, \ldots, 7 \tag{2.14}$$

where $r^{e(j)}_t$ denotes the components of market excess returns associated with scale j at time t and $\varepsilon^{(j)}_{t+2^j}$ are scale-specific forecast errors. The lag between the regressand and the regressor means that fluctuations of time-scale j forecast the next cycle of length 2^j periods. In addition, since scale-wise predictability implies predictability upon two-way (forward for the regressand, backward for the regressor) adaptive aggregation of the series (see the novel work of Bandi et al., 2016) I run the following regression

$$r^e_{t+1,t+q} = a_q + \beta_q u_{t-q+1,t} + \eta_{t+q} \tag{2.15}$$

where $r^e_{t+1,t+q} = \sum_{i=1}^q r^e_{t+i}$ denotes excess market returns between $t+1$ and $t+q$ and $u_{t-q+1,t} = \sum_{i=1}^q u_{t-i+1}$ past uncertainty. The regressor and regressand are aggregated over non-overlapping periods. Also, the regressor is adapted to time t information and therefore is non anticipative. The reason for aggregating both the regressand and the regressor in Equation (2.15) resides in the intuition of Bandi and Perron (2008) according to which economic relations may impact highly persistent components of the variables while being hidden by short term noise.

Panel A of Table 2.14 presents the results for the component-wise equity risk premium predictability[35]. I use Newey-West (1987) HAC standard errors with $2^j - 1$ lags and the Hansen-Hodrick (1980) estimator. The coefficient for the uncertainty component with degree of persistence $j = 6$ (i.e., the component that captures fluctuations in uncertainty between 32 and 64 months) is positive and statistical significant at the 1% level with a NW corrected t-statistic of 3.84 and a HH t-statistic of 3.45. For levels of persistence $j = 1, \ldots, 5$ and for $j = 7$ the uncertainty coefficients are insignificant. Due to the initialization of the filtering procedure and the lag between regressor and regressand the effective sample for $j = 7$ is reduced substantially and therefore the statistical

[35]For reviews of the literature on stock return predictability see Welch and Goyal (2008), Cochrane (2008) and more recently Lettau and Ludvigson (2010).

inferences are based on a smaller period.

Panel B of Table 2.14 shows the results from the long-horizon predictive regression. I rely on Newey-West (1987) corrected t-statistics[36] with $2 \times (q-1)$ lags to correct for serial correlation induced by the overlapping nature of the data. Also, to address any potential inferential problems that arise in predictive regressions with persistent regressors (for instance, see Ferson et al., 2003) I report Valkanov's (2003) rescaled test statistic[37]. To illustrate my findings, Figure 2.7 reports scatter plots of excess market returns and past uncertainty at four levels of aggregation, namely $q = 8, 32, 64$ and 128. In line with the framework of Bandi et al. (2016) aggregation begins to reveal predictability over a horizon between 32 and 64 months (i.e., scale-wise predictability applies for $j = 6$ and therefore $2^{6-1} = 32$ and $2^6 = 64$). Moreover, the slope of the forward/backward regression for a horizon equal to 64 months (i.e., $\beta_{q=64} = 2.81$) is numerically very close to the slope of the relevant scale-wise predictive regression (i.e., $\beta^{(j=6)} = 3.06$). However, dependence increases in the long-run and the R^2 for a horizon of 128 months is around 66%. In addition, there is a rough tent-shaped behavior in the predictive slopes and R^2's (see Figure 2.8). These results indicate that uncertainty shocks with persistence between 64 and 128 months are also positive correlated with future aggregate returns (i.e., if scale-wise predictability was present only for $j = 6$, the maximum R^2 would be achieved for a level of aggregation corresponding to $2^6 = 64$ months). My findings are in line with Bandi and Perron (2008) who report that future excess market returns and past market variance are positively correlated in the long-run (i.e., between 6 and 10 years). Similarly, I confirm the results of Bandi et al. (2016) who document a scale-specific risk-return trade-off in market returns, that is, shocks in consumption and market variance with persistence between 8 and 16 years forecast positively future excess market returns with the same periodicity.

Overall, I demonstrate that business-cycle macroeconomic uncertainty as a risk factor does not meet the restrictions proposed by Maio and Santa-Clara (2012) that prevent ICAPM from being a

[36] For arguments against the validity of standard econometric inference and the statistical pitfalls in long-run predictive regressions in finance see Ferson et al. (2003), Valkanov (2003), Lewellen (2004), Campbell and Yogo (2006) and Boudoukh et al. (2008).

[37] For the right-tail critical values of $t/\sqrt{T}$ at various percentiles see Appendix 2B (Table 2B.16).

"fishing license" for researchers. Specifically, the price of risk for exposure to business-cycle variation in aggregate uncertainty is negative and thus inconsistent[38] with how these shocks forecast aggregate returns in the time-series. For instance, consider the cross-section with the 25 FF size and book-to-market portfolios. The intertemporal hedging demand argument implies that the portfolio with the least negative covariance with low-frequency uncertainty (i.e., the portfolio of small firms with small book-to-market values - 11 in Figure 2.3) will be the least attractive as hedge and thus offer the highest expected return. In contrast, the portfolio with the highest expected return is the one with the most negative exposure (i.e., the portfolio of small firms with high book-to-market values - 15 in Figure 2.3).

To understand this point further, assume a candidate state variable z_t and consider a discrete-time approximation of the ICAPM in an unconditional form (see Maio and Santa-Clara, 2012 or Chapter 9 in Cochrane, 2005)

$$E\left(R_t^{e,i}\right) \approx \gamma Cov\left(R_t^i, R_{m,t}\right) + \gamma_z Cov\left(R_t^i, \Delta z_t\right) \tag{2.16}$$

where the first term on the right-hand side captures the market risk premium associated with the CAPM, Δz_t denotes the innovations in the variable and γ_z is the covariance risk premium associated with the candidate state variable. Assume that the state variable z_t is positively correlated with future aggregate returns i.e. $Cov\left(z_t, R_{m,t+1}\right) > 0$. Also, that the return on asset i is negatively correlated with the (innovation in the) variable (i.e., $Cov\left(R_t^i, \Delta z_t\right) < 0$) and thus negatively correlated with future aggregate returns. If the risk price γ_z is negative it holds that $\gamma_z Cov\left(R_t^i, \Delta z_t\right) > 0$. That is, even though the asset provides a hedge for reinvestment risk it earns a higher risk premium than an asset with $Cov\left(R_t^i, \Delta z_t\right) = 0$. The price of risk for z_t is inconsistent with the ICAPM. Thus, in contrast with the interpretation of Bali et al. (2014) and Bali et al. (2016) my results suggest that macro uncertainty is not a valid risk factor under the ICAPM. The central difference is that Bali et al. (2016) assume that "*an increase in economic uncertainty reduces future investment*

[38] I am indebted to Martijn Boons for pointing out this inconsistency in an earlier version of this draft.

and consumption opportunities" while my results document a long-run risk-return trade-off (i.e., future aggregate returns are positively correlated with past uncertainty).

2.3.5 Robustness Checks

In Appendix 2B I provide a battery of robustness checks. A brief summary is available here. Tables 2B.1 through 2B.4 present the estimates from the cross-sectional regressions using the same burn-in period for all components. The results for all test assets remain quantitatively similar. In addition, the model with the *business-cycle uncertainty* factor is correctly specified in the joint cross-section of the 5 industry portfolios and the 25 size and book-to-market portfolios (see Table 2B.9). The uncertainty factor $u_t^{(6:7)}$ remains statistically significant after controlling for the Fama-French factors (see Table 3B.10) and for exposure to momentum, short-term reversal, long-term reversal, liquidity and portfolio characteristics (see Tables 2B.11a and 2B.11b). Also, the results for the uncertainty factor are similar if I estimate the innovations as the residuals from an AR(1) model fitted to the factor (see Table 3B.1). Finally, I present bootstrapped confidence intervals for the first-pass scale-dependent betas (see Table 2B.13), the second-pass cross-sectional estimates (see Table 2B.14) and the scale-wise predictive regressions (see Table 2B.15) using the bias-corrected percentile method and the stationary bootstrap of Politis and Romano (1994).

2.4 Monotonicity in Scale-Specific Risk Exposures

In this section, I examine whether the scale-specific risk exposures with respect to the factors $\Delta u_t^{(6)}$ and $\Delta u_t^{(6:7)}$ are monotonically increasing (or decreasing) across portfolios using the monotonic relation (MR) test of Patton and Timmermann (2010). In essence, I look for monotonic patterns in the scale-wise factor loadings that match known patterns in average excess returns for portfolios sorted on various firm characteristics. The MR test is nonparametric and is easily implemented via bootstrap methods. To preserve the dependence in the original time-series I use the stationary bootstrap of Politis and Romano (1994) where observations are drawn in blocks whose starting

point and length are both random. The block length is drawn from a geometric distribution where the average block size is set equal to 27[39]. For all MR tests I use 5,000 bootstrap replications. Following Patton and Timmermann (2010) and in line with Hansen (2005) and Romano and Wolf (2005) I implement a studentized version of the bootstrap. The MR test is designed so that the alternative hypothesis is the one that the researcher hopes to prove - hence a monotonic relation is confirmed only if there is sufficient evidence in the data to reject the null (for more information see Appendix A).

Tables 2.15a and 2.15b present the scale-specific risk exposures for one-way[40] portfolio sorts and the corresponding monotonicity tests. I consider average excess returns on a range of portfolios sorted on security characteristics such as size (Panel A), long-term reversal (Panel B), short-term reversal (Panel C), book-to-market (Panel D), investment (Panel E) and dividend yield (Panel F). The first row in each panel reports average returns (in percent per month) for the test assets. The final column in each panel presents the p-value for the monotonic relation (MR) test. Similarly, the penultimate column presents the bootstrap p-value for the top-minus-bottom difference in the corresponding returns and scale-wise betas.

Panel A of Table 2.15a shows that the MR test rejects the null of a flat or weakly decreasing pattern across size in the risk loadings with respect to the factor $\Delta u_t^{(6)}$ for $h = 1, 3$ at the 10% level. Similarly, the evidence in Panel E of Table 2.15b provide strong support for a monotonically increasing relation in the scale-dependent risk exposures across investment. In particular, the MR test detects a monotonically increasing pattern which is significant at the 1% level for the risk exposures to the factor $\Delta u_t^{(6)}$ and at the 5% level for the risk exposures to $\Delta u_t^{(6:7)}$. Given that all risk loadings are negative these results mean that an increase in low-frequency uncertainty has a smaller effect on large firms and aggressive firms. Hence, consistent with the size and the investment effects these securities offer smaller risk compensations.

[39] Calculated based on the Politis and White (2004) estimator of the optimal average block length. Note that the estimator is corrected to deal with the error in Lahiri's (1999) calculation of the variance for the stationary bootstrap - see also Nordman (2009) and Patton et al. (2009).

[40] Additional results for two-way sorted portfolios are available upon request.

In addition, there is statistically significant evidence at the 10% level for a monotonically decreasing relation in the scale-specific risk loadings across book-to-market. This finding is in line with the value effect (i.e., one-period average returns increase from growth to value stocks). Also, it is consistent with the work of Hansen et al. (2008) who show that cash flows from value portfolios[41] are positively correlated with long-run shocks in the economy while cash flows from growth portfolios are not and hence investors holding value portfolios must be compensated for bearing the extra risk. Moreover, low-frequency uncertainty betas decrease monotonically across stocks sorted on dividend yield (the null is strongly rejected at the 1% level). Overall, these findings provide a clear economic explanation for the well-documented size, value, dividend-yield and investment effects based on exposures to low-frequency macro uncertainty. Finally, there is significant evidence for an increasing pattern in the risk exposures of securities sorted across long-term and short-term reversal. That is, the top-minus-bottom difference in the corresponding scale-wise betas is statistically significant at the 5% level with respect to all factors.

2.5 Conclusions

I study how the pricing of macroeconomic uncertainty varies across investment horizons. In particular, I decompose aggregate uncertainty into heterogeneous - in terms of their persistence and periodicity - components and investigate the risk compensations associated with each of these scale-dependent macroeconomic shocks. Macroeconomic uncertainty is quantified using the model-free index of Jurado et al. (2015) that measures the common variation in the unforecastable component of a large number of economic indicators. My study is based on the novel framework for scale-specific analysis of risk proposed in Bandi and Tamoni (2016) and Boons and Tamoni (2016).

I document that a single *business-cycle uncertainty* factor that captures assets' exposure to low-frequency variation in macroeconomic uncertainty can explain the level and the cross-sectional

[41] In a similar fashion, Kamara et al. (2015) find that the risk price for exposure to the HML factor of Fama and French (1993) (i.e., the factor that measures the difference between the returns on portfolios of high and low book-to-market stocks) peaks at a horizon of two to three years.

differences of asset returns. In particular, I find that macroeconomic fluctuations with persistence levels ranging from 32 to 128 months carry a negative price of risk about -2% annually. In addition, equity scale-specific risk exposures are negative and thus uncertainty risk premia are positive. The results are robust across different test assets including: the 25 Fama and French (1993) size and book-to-market portfolios, the 25 Fama and French (2015) size and investment portfolios, the 25 Fama and French (2015) book-to-market and operating profitability portfolios and the 25 Fama and French (2016) size and variance portfolios. Moreover, my findings remain statistically significant after using a t-statistic cutoff of three as suggested by Harvey et al. (2016) and are qualitatively and quantitatively similar irrespective of whether uncertainty is derived from monthly, quarterly or annual forecasts. Furthermore, unlike several prominent asset pricing models (e.g., FF3 and FF5) I demonstrate that the one-factor model with business-cycle macro uncertainty is correctly specified. In total, my study suggests that only business-cycle variation in uncertainty drives asset prices and hence provides useful insights for the long-run risks literature. That is, in the spirit of Dew-Becker and Giglio (2016) we should allow Epstein-Zin preferences to put more weight on business-cycle frequency fluctuations compared to the standard Bansal and Yaron (2004) calibration (for instance, see Ghosh and Constantinides, 2014).

Finally, I show that future excess aggregate returns are positively correlated with past uncertainty and thus the negative price of risk for exposure to (low-frequency) macro uncertainty is inconsistent with the central economic intuition underlying the ICAPM. In contrast, investors demand higher risk compensations to hold portfolios that exhibit greater negative comovement with low-frequency macroeconomic uncertainty, i.e. there is a low-frequency risk-return trade-off for the valuation of assets. Future research can expand my work in the cross-section of hedge fund and mutual fund returns.

Figure 2.1: Aggregate uncertainty

Notes: This figure plots the index of macroeconomic uncertainty of Jurado et al. (2015) for $h = 1, 3, 12$. Data are monthly and span the period 1960:07 - 2013:05. The shaded areas represent NBER recessions.

Figure 2.2a: Persistence-based decomposition of aggregate uncertainty

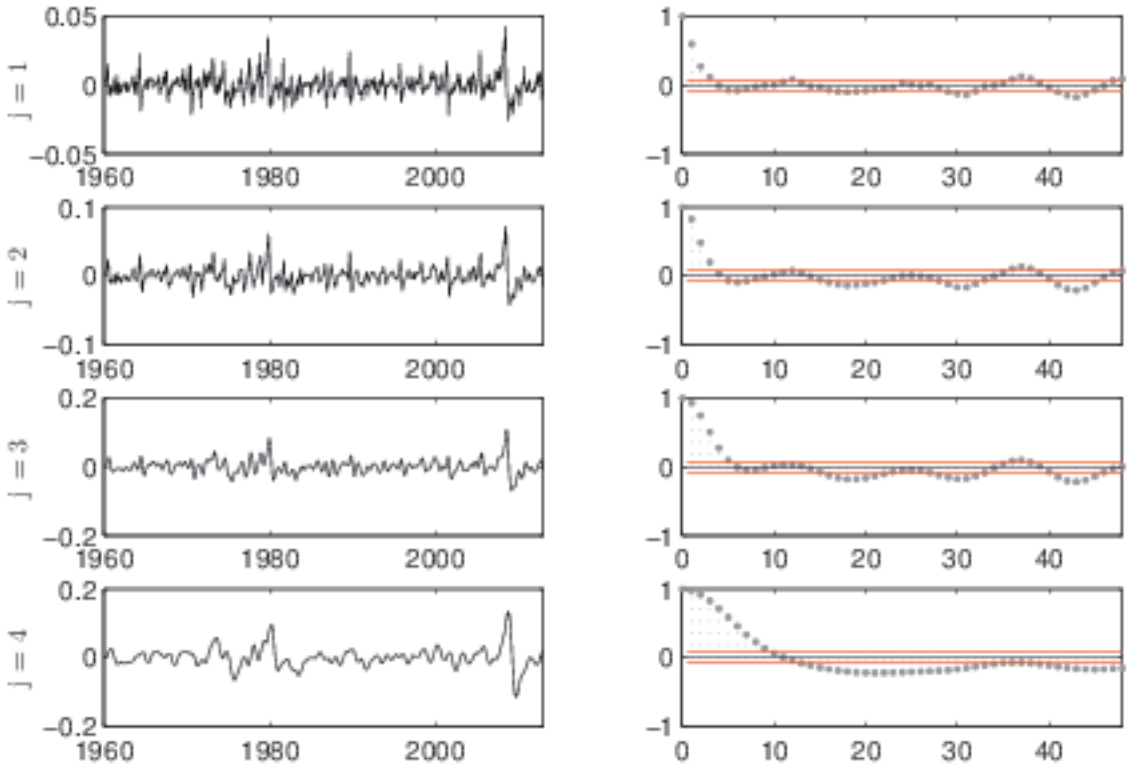

Notes: This figure plots the persistent components $u_t^{(j)}$ for $j = 1, \ldots, 4$ filtered out of aggregate uncertainty (derived from monthly forecasts - $h = 1$) and their corresponding sample autocorrelation functions. Data are monthly and span the period 1960:07 - 2013:05. In the empirical analysis, I discard the first $2^j - 1$ observations for each scale due to the initialization of the filtering procedure.

Figure 2.2b: Persistence-based decomposition of aggregate uncertainty

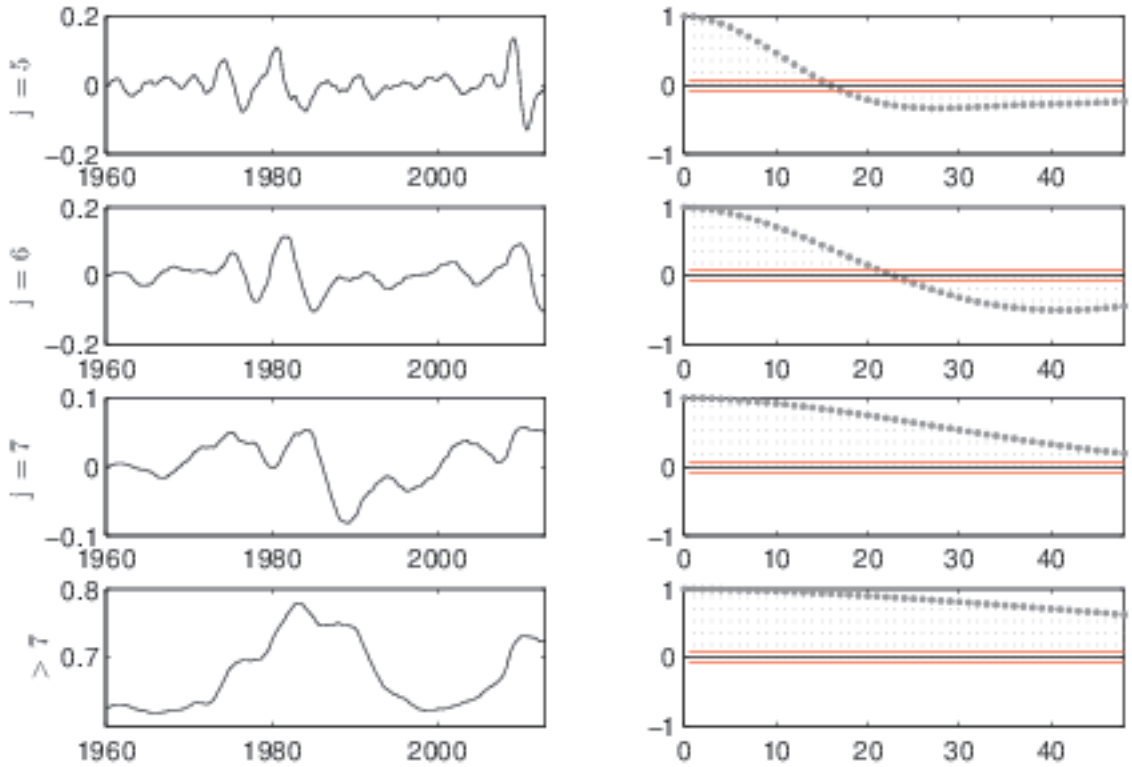

Notes: This figure plots the persistent components $u_t^{(j)}$ for $j = 5, 6, 7, > 7$ filtered out of aggregate uncertainty (derived from monthly forecasts - $h = 1$) and their corresponding sample autocorrelation functions. Data are monthly and span the period 1960:07 - 2013:05. In the empirical analysis, I discard the first $2^j - 1$ observations for each scale due to the initialization of the filtering procedure.

Figure 2.3: Cross-sectional fit - 25 FF size and book-to-market portfolios

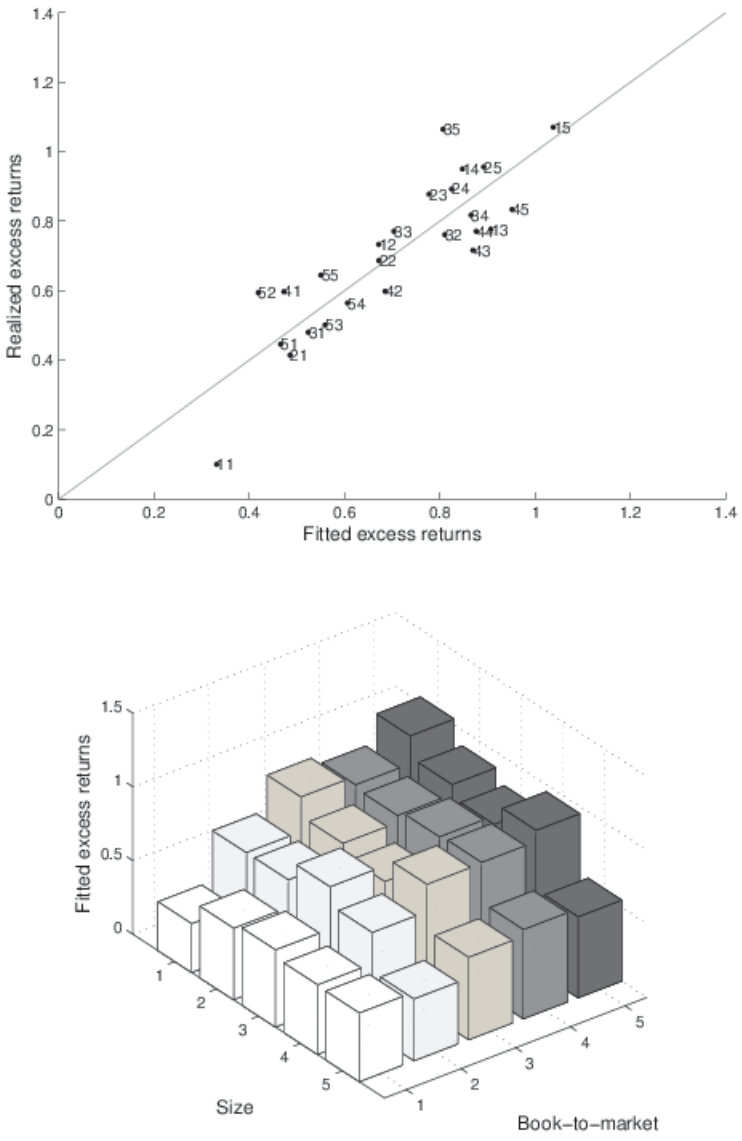

Notes: Panel A plots realized versus fitted excess returns for the 25 size and book-to-market Fama and French (1993) portfolios where the priced factor is $\Delta u_t^{(6:7)}$, that is, the innovations in low-frequency uncertainty shocks (derived from monthly forecasts) with persistence ranging from 32 to 128 months. Each two-digit number represents a separate portfolio. The first digit refers to the size quintile of the portfolio (1 being the smallest and 5 the largest), while the second digit refers to the book-to-market quintile (1 being the lowest and 5 the highest). The straight line is the 45-degree line from the origin. Panel B plots the fitted excess return for each portfolio.

Figure 2.4: Relation with default yield spread and macro volatility risk

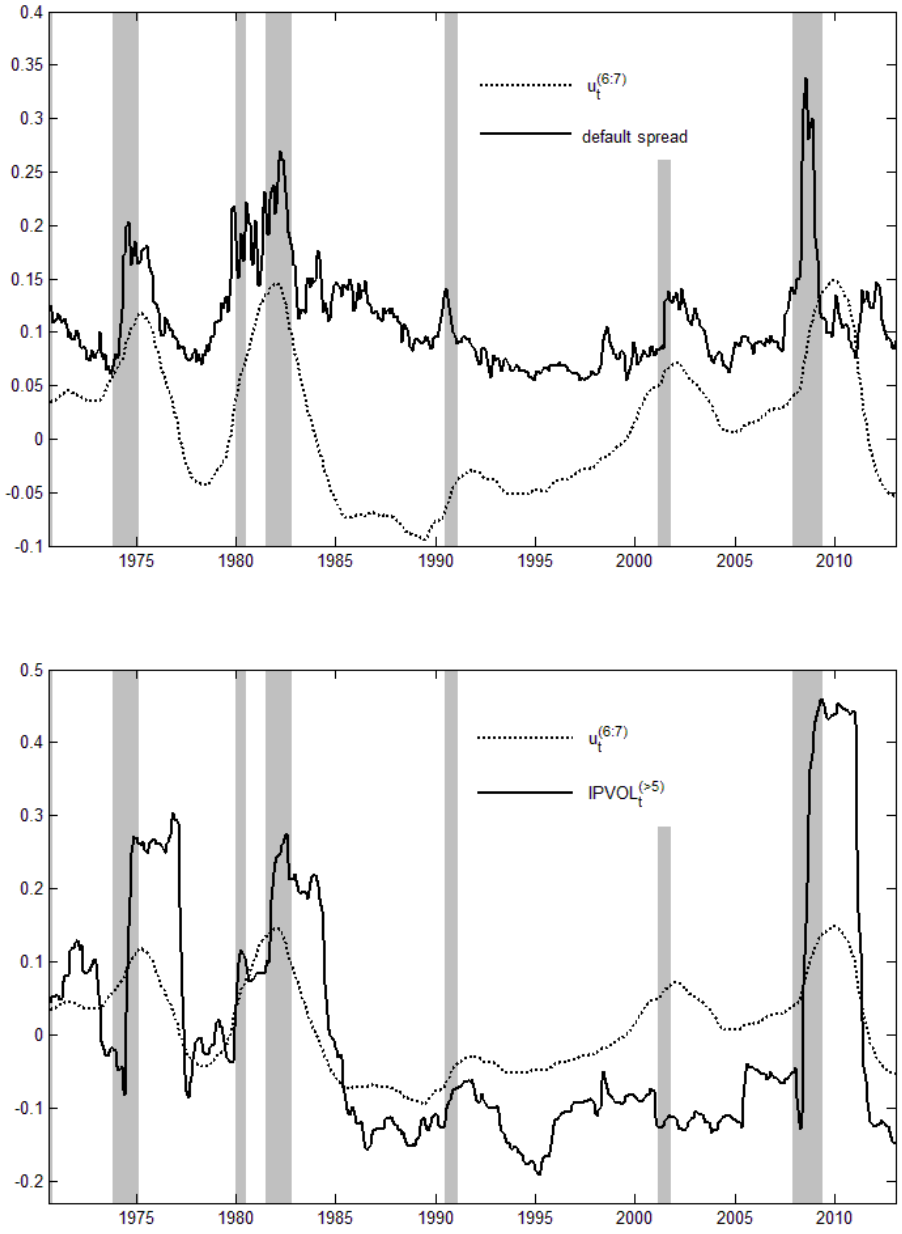

Notes: Panel A plots macroeconomic uncertainty shocks with persistence ranging between 32 and 128 months (i.e., $u_t^{(6:7)}$) along with the default yield spread which is defined as the difference between BAA and AAA-rated corporate bond yields. Panel B plots $u_t^{(6:7)}$ along with the macro volatility risk factor of Boons and Tamoni (2016) (i.e., macro volatility shocks with persistence greater than 32 months - $IPVOL_t^{(>5)}$). The shaded areas represent NBER recessions.

Figure 2.5: Realized versus fitted excess returns: Alternative test portfolios

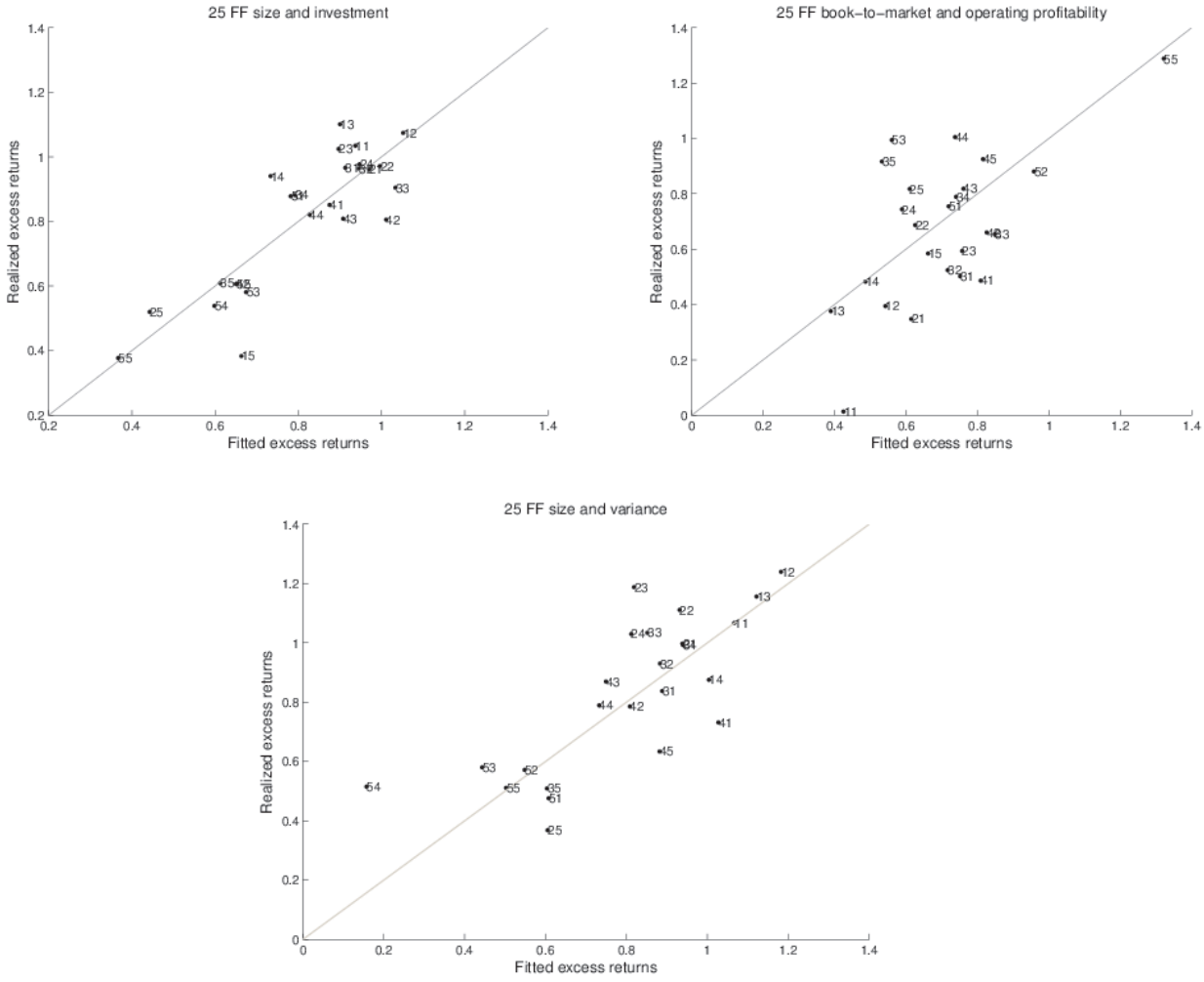

Notes: This figure plots realized versus fitted excess returns for the alternative test portfolios where the priced factor is $\Delta u_t^{(6:7)}$, that is, the innovations in low-frequency uncertainty shocks (derived from monthly forecasts) with persistence ranging from 32 to 128 months. The test assets include: the 25 FF size and investment portfolios (Panel A), the 25 FF book-to-market and operating profitability portfolios (Panel B) and the 25 FF size and variance portfolios (Panel C). Each two-digit number represents a separate portfolio. The straight line is the 45-degree line from the origin.

Figure 2.6: Fitted excess returns: Alternative test portfolios

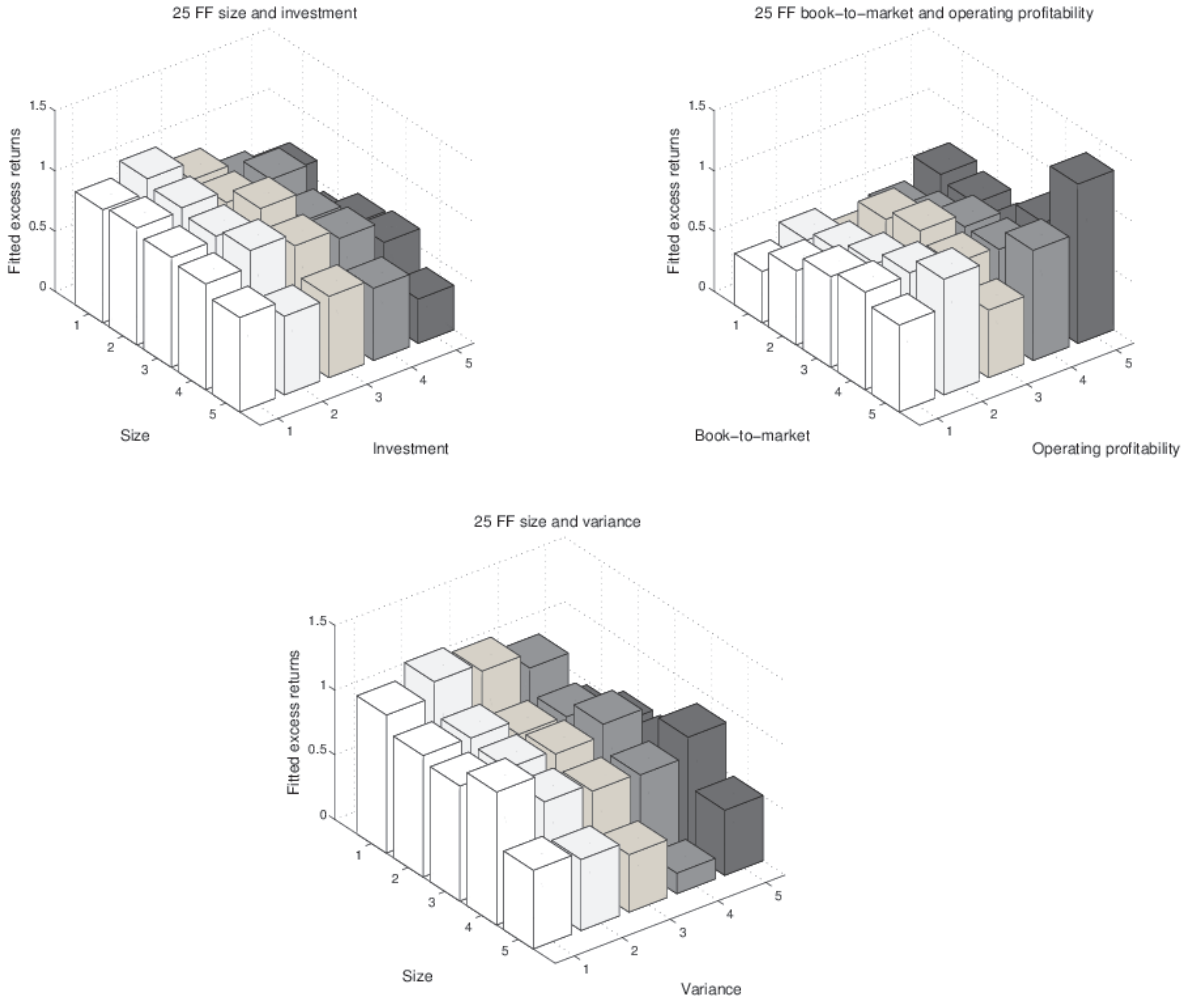

Notes: This figure plots the fitted excess returns for the alternative test portfolios where the priced factor is $\Delta u_t^{(6:7)}$, that is, the innovations in low-frequency uncertainty shocks (derived from monthly forecasts) with persistence ranging from 32 to 128 months. The test assets include: the 25 FF size and investment portfolios (Panel A), the 25 FF book-to-market and operating profitability portfolios (Panel B) and the 25 FF size and variance portfolios (Panel C).

Figure 2.7: Market returns and past uncertainty at different levels of aggregation

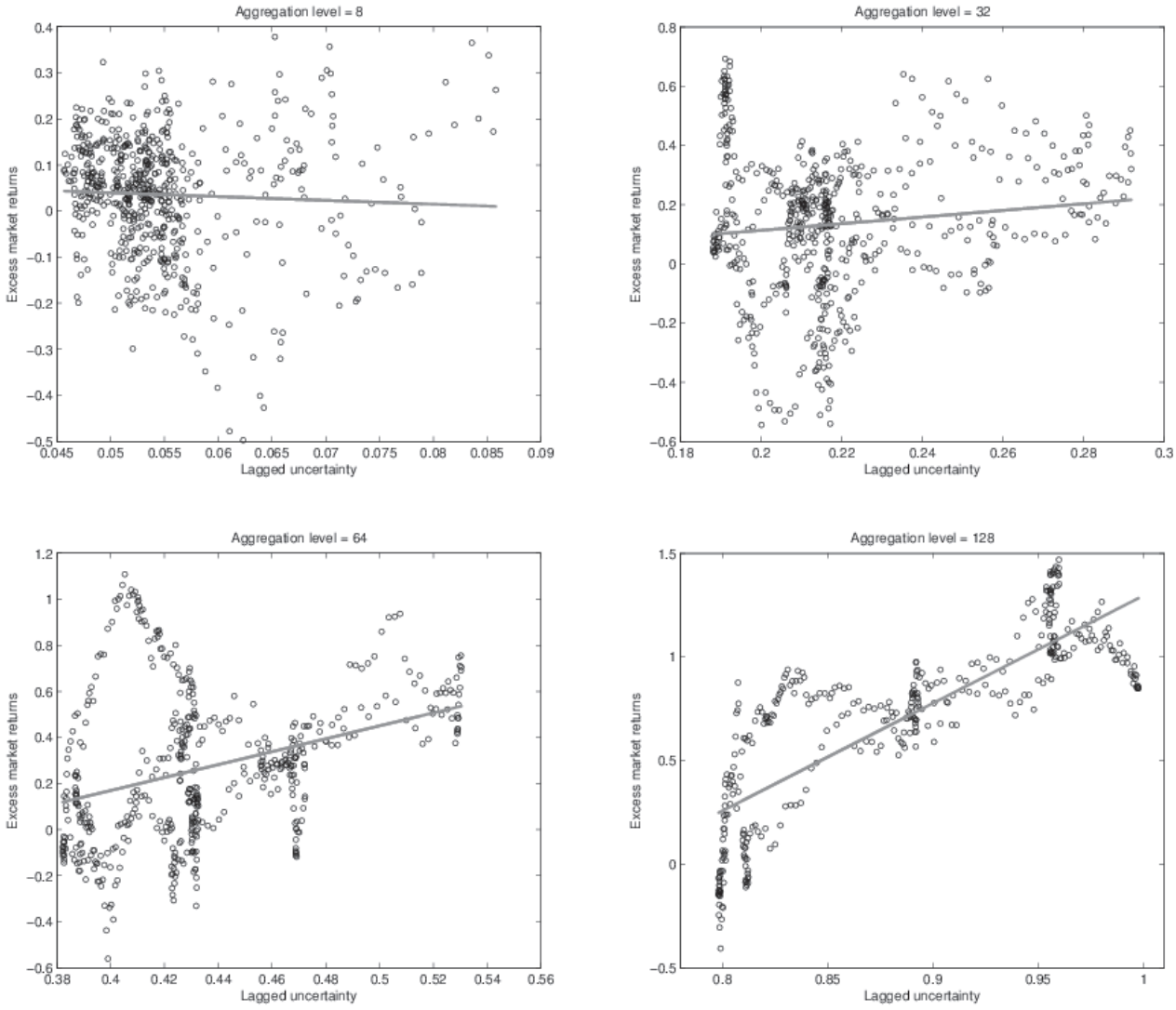

Notes: This figure reports scatter plots of excess market returns and past uncertainty at four levels of aggregation, namely $q = 8, 32, 64$ and 128.

Figure 2.8: Hump-shaped dynamics in slope coefficients and R^2's

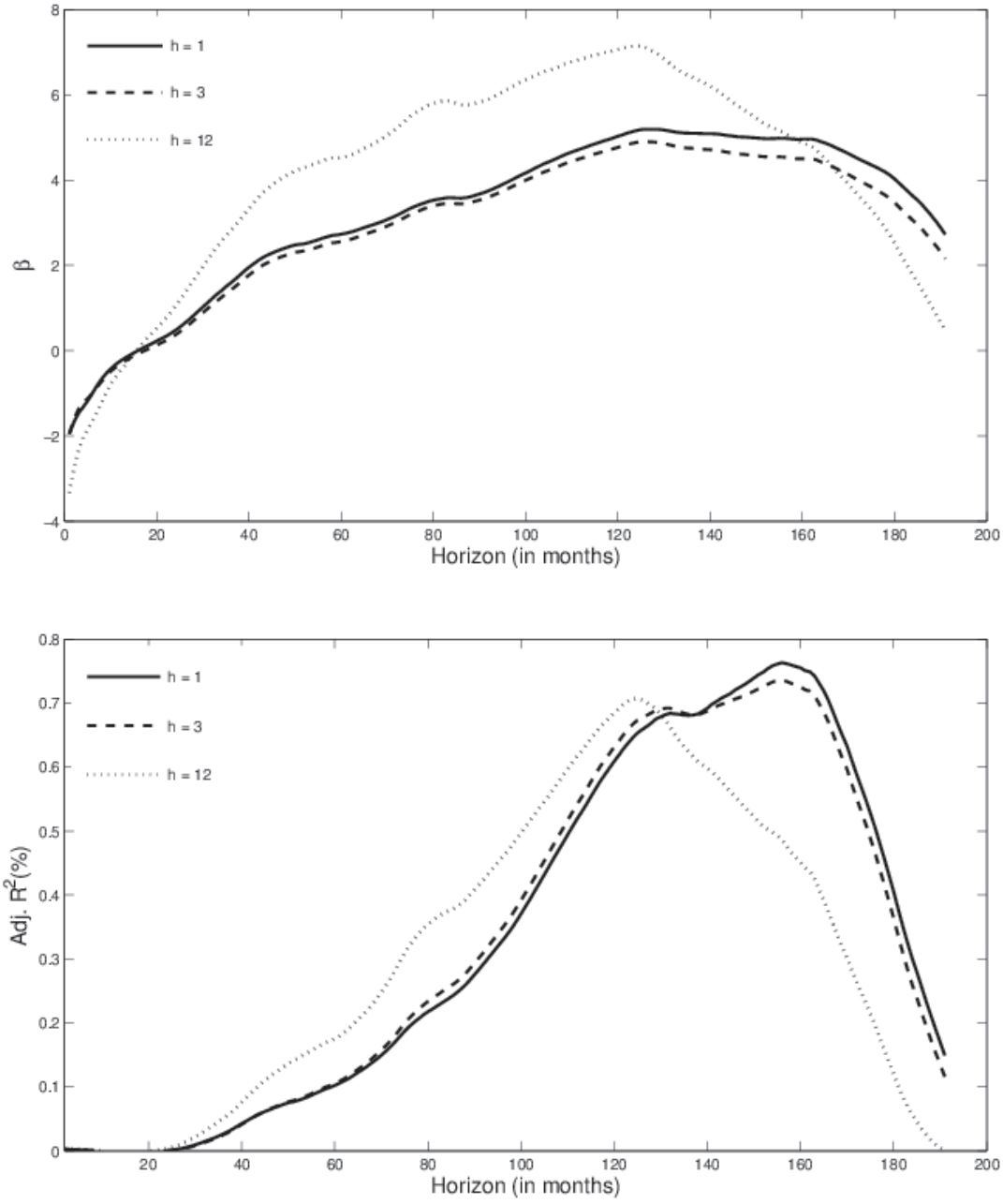

Notes: This figure reports slope coefficients and R^2's values obtained by regressing forward-aggregated excess market returns on backward-aggregated macro uncertainty.

Table 2.1: Descriptive statistics

Panel A	Aggregate uncertainty		
	$u_t(1)$	$u_t(3)$	$u_t(12)$
Mean	0.6871	0.8494	0.9591
Median	0.6655	0.8263	0.9509
Min	0.5635	0.7105	0.8467
Max	1.1344	1.3385	1.2052
St. Deviation	0.0949	0.1020	0.0668
Skewness	1.8179	1.7791	1.2918
Kurtosis	6.9444	6.7326	4.9931
JB	761.40	703.60	281.70
ADF	0.0057	0.0023	0.0396
PP	0.0190	0.0209	0.0475
KPSS	0.1930	0.2119	0.4043
AC(1)	0.9866	0.9891	0.9943
AC(2)	0.9578	0.9651	0.9811
Panel B	Equity risk premium		
	$r^e \equiv r_m - r_f$		
$E(r^e)$	5.71%		
$\sigma(r^e)$	15.02%		
# observations	635		

Notes: Panel A reports descriptive statistics for the model-free index of macroeconomic uncertainty of Jurado et al. (2015) for $h = 1, 3, 12$. I report the sample mean, median, minimum, maximum, standard deviation, skewness and kurtosis. In addition, I report the value of the Jarque-Bera (1980) normality test, the p-values of the Augmented Dickey-Fuller (ADF - Dickey and Fuller, 1979) and Phillips-Perron (PP - Phillips and Perron, 1988) tests for unit root, the values of the KPSS (Kwiatkowski et al., 1992) test statistic for the null hypothesis of stationarity whose critical values are 0.347, 0.463 and 0.739 at the 10%, 5% and 1% significance levels respectively as well as autocorrelation coefficients for the first and second lag. Panel B presents the mean and standard deviation for the equity risk premium.

Table 2.2: Frequency interpretation

Persistence level	Monthly-frequency resolution
$j = 1$	1 - 2 months
$j = 2$	2 - 4 months
$j = 3$	4 - 8 months
$j = 4$	8 - 16 months
$j = 5$	16 - 32 months
$j = 6$	32 - 64 months
$j = 7$	64 - 128 months
$j > 7$	$>$ 128 months

Notes: Frequency interpretation of the component $u_t^{(j)}$ at level of persistence j in the case of monthly time series. Each persistence level (or time-scale) is associated with a range of time horizons.

Table 2.3: Multi-scale variance ratio tests

$u_t\,(1)$	Persistence level						
$j =$	1	2	3	4	5	6	7
$\sqrt{\frac{T}{a_j}}\left(\hat{\xi}_j - \frac{1}{2^j}\right)$	**-15.7837**	**-8.5535**	**-3.9397**	1.4228	**12.0042**	**27.9433**	**29.4710**
$u_t\,(3)$	Persistence level						
$j =$	1	2	3	4	5	6	7
$\sqrt{\frac{T}{a_j}}\left(\hat{\xi}_j - \frac{1}{2^j}\right)$	**-15.8286**	**-8.6762**	**-4.1963**	1.3380	**12.4039**	**29.4475**	**29.9408**
$u_t\,(12)$	Persistence level						
$j =$	1	2	3	4	5	6	7
$\sqrt{\frac{T}{a_j}}\left(\hat{\xi}_j - \frac{1}{2^j}\right)$	**-15.9153**	**-8.9182**	**-4.8236**	0.3004	**11.4487**	**30.3735**	**33.4243**

Notes: This table presents the results of the multi-scale variance ratio test for the macroeconomic uncertainty series. The test statistic is given by

$$\hat{\xi}_j = \frac{2^j \left(\mathbf{u^{(j)}}\right)^{\intercal} \mathbf{u^{(j)}}}{\left(X_T^{(J)}\right)^{\intercal} X_T^{(J)}}$$

where $\left(X_T^{(J)}\right)^{\intercal} = [u_T, u_{T-1}, \ldots, u_1]$ is the vector collecting the observations of $\{u_t\}$ and $\mathbf{u^{(j)}} = \left[u_{2^j}^{(j)}, \ldots, u_{k\times 2^j}^{(j)}, \ldots, u_T^{(j)}\right]^{\intercal}$. Under the null hypothesis of no serial correlation, the rescaled test statistic $\sqrt{\frac{T}{a_j}}\left(\hat{\xi}_j - \frac{1}{2^j}\right)$ where $a_j = \frac{\binom{2^j}{2}}{2^j 2^{2(j-1)}}$ converges in distribution to a standard normal. Bold values reject the null hypothesis of no serial correlation at a 99% confidence level. These results imply that $\exists j^* \in \{1, \ldots, 7\}$ such that $u_{k\times 2^{j^*}+2^{j^*}}^{(j^*)} = \rho_{j^*} u_{k\times 2^{j^*}}^{(j^*)} + \varepsilon_{k\times 2^{j^*}+2^{j^*}}^{(j^*)}$.

Table 2.4: Scale-specific risk exposures: 25 FF size and book-to-market portfolios

Size	Book-to-market	$\beta^{(6)}$		$\beta^{(7)}$		$\beta^{(6:7)}$	
Small	LowBM	-0.5009	(-0.7619)	0.8891	(0.8479)	-0.3286	(-0.4172)
	2BM	-0.8292	(-1.7491)	-0.0996	(-0.1249)	-0.7378	(-1.3476)
	3BM	**-1.1794**	(-3.3176)	-0.4014	(-0.6297)	**-1.0207**	(-2.4147)
	4BM	**-1.0991**	(-3.1857)	-0.5002	(-0.7768)	**-0.9490**	(-2.3937)
	HighBM	**-1.3221**	(-3.5890)	-0.9179	(-1.3207)	**-1.1782**	(-2.8421)
2	LowBM	-0.5355	(-0.8820)	0.7294	(0.9866)	-0.5141	(-0.7595)
	2BM	-0.7527	(-1.8718)	0.0292	(0.0641)	-0.7381	(-1.7754)
	3BM	**-0.8812**	(-3.2527)	-0.6270	(-1.7518)	**-0.8648**	(-3.0858)
	4BM	**-1.0595**	(-3.6246)	-0.6058	(-1.6515)	**-0.9221**	(-3.1867)
	HighBM	**-1.1039**	(-3.8263)	-0.6804	(-1.6239)	**-1.0029**	(-3.4157)
3	LowBM	-0.4551	(-0.9432)	0.2801	(0.6001)	-0.5600	(-1.0819)
	2BM	**-0.9081**	(-2.6138)	-0.3593	(-0.9720)	**-0.9045**	(-2.6204)
	3BM	**-0.7960**	(-3.3909)	-0.4716	(-1.3342)	**-0.7760**	(-3.1721)
	4BM	**-1.0044**	(-3.6011)	**-0.7243**	(-2.2801)	**-0.9707**	(-3.4232)
	HighBM	**-0.9016**	(-3.5585)	**-0.8654**	(-2.3183)	**-0.8999**	(-3.2320)
4	LowBM	-0.3571	(-0.7628)	0.2956	(1.1102)	-0.4984	(-1.0381)
	2BM	-0.7447	(-1.8865)	-0.1957	(-0.5350)	-0.7538	(-1.9587)
	3BM	**-1.0108**	(-2.5861)	**-0.6028**	(-2.1452)	**-0.9759**	(-2.5932)
	4BM	**-1.0327**	(-4.0000)	**-0.6834**	(-2.3251)	**-0.9840**	(-4.0463)
	HighBM	**-1.0733**	(-3.6085)	**-0.8784**	(-3.2126)	**-1.0742**	(-4.0577)
Big	LowBM	-0.3370	(-1.4223)	0.0721	(0.1365)	-0.4900	(-1.8189)
	2BM	-0.4133	(-1.3696)	-0.1998	(-0.6944)	-0.4338	(-1.7910)
	3BM	-0.5888	(-1.7174)	-0.2065	(-0.7524)	-0.6023	(-1.7478)
	4BM	**-0.6579**	(-2.7198)	-0.3567	(-1.0614)	**-0.6590**	(-2.9868)
	HighBM	**-0.5883**	(-3.0566)	-0.5782	(-1.1847)	**-0.5917**	(-3.3996)
	Wald-stat	232.88		34.34		314.71	
	p-value	0.0000		0.1008		0.0000	

Notes: This table reports first-pass beta estimates for the Fama and French (1993) 25 size and book-to-market portfolios (indexed by Small to Big and LowBM to HighBM). The betas are estimated component-wise that is regressing low frequency components of returns on the low frequency components of aggregate uncertainty. The associated t-statistics are based on Newey-West standard errors with $2^j - 1$ lags. The last rows of the table present the Wald test-statistics and their corresponding p-values from testing the joint hypothesis that all component-wise exposures are equal to zero, i.e. $H_0 : \beta^{1(j)} = \ldots = \beta^{25(j)} = 0$ for $j = 6, 7$ and $j = 6 : 7$. The initial sample period is 1960:07 to 2013:05. Bold values denote statistically significant beta estimates at a 95% confidence level.

Table 2.5: Cross-sectional regression: 25 FF size and book-to-market portfolios

	Persistence level							
$j =$	1	2	3	4	5	6	7	6:7
$u_t(1)$								
$\lambda_{0,j}$	1.1321	0.9394	0.9242	0.3666	0.2484	0.1388	0.5814	0.0581
	(4.2639)	(4.0669)	(4.3238)	(1.7363)	(1.1258)	(0.5814)	(2.3717)	(0.2083)
λ_j	0.9062	0.3927	0.4412	-0.4048	-0.4815	-0.6867	-0.4016	-0.8315
	(1.3752)	(0.8124)	(0.9648)	(-1.3683)	(-1.9901)	(-4.5662)	(-3.2124)	(-4.3264)
price of risk	0.832%	0.534%	0.636%	-0.593%	-1.181%	-2.296%	-2.295%	-2.274%
R^2	9.861%	4.103%	5.734%	4.836%	19.080%	72.350%	75.271%	73.891%
$se(\widehat{R^2})$	0.1351	0.1034	0.1234	0.0815	0.2037	0.1378	0.2375	0.1224
$p\left(R^2=1\right)$	0.0074	0.0078	0.0087	0.0061	0.0102	0.2412	0.2956	0.3139
MAPE	2.075%	2.191%	2.199%	2.068%	1.818%	1.106%	1.156%	1.114%
$u_t(3)$								
$\lambda_{0,j}$	0.8821	0.9203	0.9129	0.3682	0.2189	0.1709	0.5836	0.1109
	(3.6045)	(3.7609)	(4.0607)	(1.4875)	(0.9945)	(0.7260)	(2.4041)	(0.4097)
λ_j	0.1843	0.2041	0.2946	-0.3428	-0.5189	-0.7172	-0.4259	-0.8476
	(0.5834)	(0.6652)	(0.8311)	(-1.0914)	(-2.1283)	(-4.5630)	(-3.3841)	(-4.3044)
price of risk	0.407%	0.455%	0.564%	-0.560%	-1.277%	-2.311%	-2.340%	-2.285%
R^2	2.365%	2.982%	4.507%	4.308%	22.305%	73.295%	78.251%	74.617%
$se(\widehat{R^2})$	0.0837	0.0915	0.1127	0.0899	0.2204	0.1399	0.2066	0.1311
$p\left(R^2=1\right)$	0.0062	0.0072	0.0080	0.0051	0.0117	0.2526	0.3255	0.3229
MAPE	2.177%	2.177%	2.197%	2.074%	1.758%	1.093%	1.075%	1.079%
$u_t(12)$								
$\lambda_{0,j}$	0.8354	0.9365	0.9217	0.2302	0.1801	0.2641	0.6407	0.2278
	(4.1869)	(4.1552)	(4.0731)	(0.9144)	(0.8476)	(1.1221)	(2.6882)	(0.8350)
λ_j	0.0951	0.1150	0.1318	-0.2364	-0.3230	-0.4253	-0.2284	-0.4856
	(0.5941)	(0.8194)	(0.8588)	(-1.5547)	(-2.5357)	(-4.5387)	(-2.9019)	(-4.0302)
price of risk	0.337%	0.561%	0.577%	-0.855%	-1.531%	-2.339%	-2.182%	-2.336%
R^2	1.615%	4.524%	4.709%	10.047%	32.070%	75.103%	68.037%	77.922%
$se(\widehat{R^2})$	0.0564	0.1135	0.1139	0.1446	0.2591	0.1226	0.2665	0.1147
$p\left(R^2=1\right)$	0.0037	0.0082	0.0083	0.0059	0.0187	0.2766	0.1920	0.3653
MAPE	2.192%	2.175%	2.187%	1.963%	1.608%	1.069%	1.315%	1.029%
# observ.	633	631	627	619	603	571	507	507

Notes: This table reports the estimates for the zero-beta excess return ($\lambda_{0,j}$) and the price of risk (λ_j) for each scale j along with the corresponding Fama-MacBeth (1973) test statistics in parentheses. In addition, I normalize the scale-wise risk exposures and estimate the price of risk per unit of cross-sectional standard deviation in exposure in percent per year. I also report the sample R^2 for each cross-sectional regression and its standard error, the p-value for the Kan et al. (2013) test of $H_0: R^2 = 1$ and the mean absolute pricing error (MAPE) across all securities expressed in percent per year.

Table 2.6: Scale-specific risk exposures: 25 FF size and investment portfolios

Size	Investment	$\beta^{(6)}$		$\beta^{(7)}$		$\beta^{(6:7)}$	
Small	LowINV	**-1.1200**	(-2.2307)	-0.1662	(-0.1765)	-0.8675	(-1.3650)
	2INV	**-1.1872**	(-3.2284)	-0.6092	(-0.9970)	**-1.0014**	(-2.3562)
	3INV	**-1.1366**	(-2.9889)	-0.3606	(-0.5467)	**-0.8248**	(-2.0585)
	4INV	**-0.9103**	(-2.2375)	-0.0737	(-0.0970)	-0.6303	(-1.3769)
	HighINV	-0.9164	(-1.5872)	0.5206	(0.5706)	-0.5485	(-0.8763)
2	LowINV	**-1.0506**	(-2.8382)	-0.2213	(-0.4769)	**-0.9057**	(-2.2926)
	2INV	**-1.1051**	(-3.6219)	-0.2644	(-0.7496)	**-0.9361**	(-3.1464)
	3INV	**-0.9175**	(-3.2796)	-0.5730	(-1.5613)	**-0.8206**	(-2.8159)
	4INV	**-1.0290**	(-2.8218)	-0.5773	(-1.5479)	**-0.8791**	(-2.7272)
	HighINV	-0.4554	(-0.8509)	0.6900	(1.0437)	-0.2919	(-0.5306)
3	LowINV	**-0.8943**	(-2.8294)	-0.5110	(-1.1239)	**-0.8393**	(-2.5474)
	2INV	**-0.9508**	(-4.3582)	-0.4117	(-1.5624)	**-0.8773**	(-3.8509)
	3INV	**-1.0130**	(-3.0823)	**-0.6046**	(-2.1461)	**-0.9796**	(-2.9490)
	4INV	**-0.7656**	(-2.3062)	-0.2933	(-0.9971)	**-0.6984**	(-2.2268)
	HighINV	-0.5589	(-1.2466)	0.2557	(0.4666)	-0.4893	(-1.1264)
4	LowINV	**-0.8714**	(-2.5750)	-0.1561	(-0.4289)	**-0.7953**	(-2.2618)
	2INV	**-0.9142**	(-2.8876)	**-0.8326**	(-5.9665)	**-0.9537**	(-3.5627)
	3INV	**-0.8657**	(-2.6096)	-0.4513	(-1.8898)	**-0.8334**	(-2.5484)
	4INV	**-0.7374**	(-2.2310)	-0.2962	(-1.0284)	**-0.7393**	(-2.3292)
	HighINV	-0.5138	(-0.9971)	0.3429	(0.9388)	-0.5362	(-1.0823)
Big	LowINV	**-0.6084**	(-2.0728)	-0.3640	(-1.3694)	**-0.6866**	(-2.4206)
	2INV	**-0.4469**	(-2.0689)	-0.2986	(-1.0654)	**-0.5334**	(-2.8270)
	3INV	**-0.4509**	(-2.1827)	-0.3037	(-0.6296)	**-0.5617**	(-2.8922)
	4INV	-0.3990	(-1.3400)	-0.0047	(-0.0089)	-0.4729	(-1.4432)
	HighINV	-0.0768	(-0.2104)	0.5503	(1.3040)	-0.2040	(-0.5535)
	Wald-stat	219.52		30.44		302.68	
	p-value	0.0000		0.2082		0.0000	

Notes: This table reports first-pass beta estimates for the Fama and French (2015) 25 size and investment portfolios (indexed by Small to Big and LowINV to HighINV). The betas are estimated component-wise that is regressing low frequency components of returns on the low frequency components of aggregate uncertainty. The associated t-statistics are based on Newey-West standard errors with $2^j - 1$ lags. The last rows of the table present the Wald test-statistics and their corresponding p-values from testing the joint hypothesis that all component-wise exposures are equal to zero, i.e. $H_0: \beta^{1(j)} = \ldots = \beta^{25(j)} = 0$ for $j = 6, 7$ and $j = 6:7$. The initial sample period is 1963:07 to 2013:05. Bold values denote statistically significant beta estimates at a 95% confidence level.

Table 2.7: Cross-sectional regression: 25 FF size and investment portfolios

	Persistence level							
$j =$	1	2	3	4	5	6	7	6:7
$u_t\,(1)$								
$\lambda_{0,j}$	1.0158	0.9535	0.9140	0.4723	0.2240	0.2322	0.7261	0.1923
	(6.5483)	(6.0353)	(5.6282)	(1.8269)	(0.8921)	(1.0019)	(2.9121)	(0.6872)
λ_j	0.6478	0.4381	0.3776	-0.2852	-0.4474	-0.5147	-0.4063	-0.8591
	(2.1639)	(1.2332)	(1.0184)	(-0.6915)	(-1.5581)	(-3.0417)	(-3.8261)	(-4.6799)
price of risk	0.869%	0.623%	0.571%	-0.429%	-1.064%	-1.757%	-1.927%	-2.212%
R^2	12.346%	6.233%	5.195%	2.940%	18.497%	51.221%	55.409%	73.006%
$se(\widehat{\mathrm{R}^2})$	0.1219	0.1108	0.1149	0.0903	0.2257	0.2858	0.2299	0.0922
$p\left(\mathrm{R}^2=1\right)$	0.0150	0.0092	0.0145	0.0033	0.0043	0.0529	0.0833	0.2508
MAPE	1.983%	2.064%	2.097%	2.039%	1.663%	0.924%	1.364%	0.985%
$u_t\,(3)$								
$\lambda_{0,j}$	0.7545	0.8693	0.8571	0.4515	0.2002	0.2605	0.7391	0.2531
	(3.5739)	(4.6675)	(5.0998)	(1.6789)	(0.8113)	(1.1360)	(3.0064)	(0.9309)
λ_j	0.0382	0.1630	0.1918	-0.2678	-0.4820	-0.5338	-0.4400	-0.8672
	(0.1269)	(0.5949)	(0.6432)	(-0.7210)	(-1.7000)	(-3.0814)	(-4.1403)	(-4.6254)
price of risk	0.082%	0.343%	0.377%	-0.467%	-1.168%	-1.775%	-2.028%	-2.227%
R^2	0.111%	1.895%	2.264%	3.476%	22.282%	52.221%	61.365%	74.027%
$se(\widehat{\mathrm{R}^2})$	0.0189	0.0697	0.0784	0.1015	0.2447	0.2854	0.2099	0.0934
$p\left(\mathrm{R}^2=1\right)$	0.0055	0.0063	0.0117	0.0031	0.0043	0.0565	0.1119	0.2645
MAPE	2.110%	2.126%	2.129%	2.021%	1.586%	0.915%	1.256%	0.963%
$u_t\,(12)$								
$\lambda_{0,j}$	0.9153	0.8810	0.8246	0.2888	0.1573	0.3194	0.8018	0.4021
	(5.7966)	(5.1554)	(4.9691)	(1.0854)	(0.6689)	(1.3954)	(3.3523)	(1.4791)
λ_j	0.1566	0.0895	0.0634	-0.2112	-0.3025	-0.3290	-0.2238	-0.4750
	(1.0985)	(0.7131)	(0.4990)	(-1.2331)	(-2.1389)	(-3.3864)	(-3.2885)	(-4.5760)
price of risk	0.539%	0.406%	0.287%	-0.832%	-1.448%	-1.867%	-1.771%	-2.166%
R^2	4.745%	2.647%	1.316%	11.031%	34.222%	57.812%	46.790%	70.012%
$se(\widehat{\mathrm{R}^2})$	0.0969	0.0812	0.0584	0.1772	0.2816	0.2693	0.2467	0.1424
$p\left(\mathrm{R}^2=1\right)$	0.0087	0.0094	0.0121	0.0021	0.0053	0.0843	0.0715	0.2089
MAPE	2.108%	2.114%	2.133%	1.878%	1.381%	0.849%	1.459%	1.078%
# observ.	598	596	592	584	568	536	472	472

Notes: This table reports the estimates for the zero-beta excess return ($\lambda_{0,j}$) and the price of risk (λ_j) for each scale j along with the corresponding Fama-MacBeth (1973) test statistics in parentheses. In addition, I normalize the scale-wise risk exposures and estimate the price of risk per unit of cross-sectional standard deviation in exposure in percent per year. I also report the sample R^2 for each cross-sectional regression and its standard error, the p-value for the Kan et al. (2013) test of $H_0: R^2 = 1$ and the mean absolute pricing error (MAPE) across all securities expressed in percent per year.

Table 2.8: Scale-specific risk exposures: 25 FF book-to-market and operating profitability portfolios

Book-to-market	OP	$\beta^{(6)}$		$\beta^{(7)}$		$\beta^{(6:7)}$	
LowBM	LowOP	-0.1602	(-0.2770)	0.8929	(1.6452)	-0.1982	(-0.2797)
	2OP	-0.2790	(-0.4899)	0.6963	(1.6806)	-0.3823	(-0.5860)
	3OP	-0.0074	(-0.0239)	0.4036	(1.1918)	-0.1426	(-0.4149)
	4OP	-0.0794	(-0.2298)	0.2298	(0.6090)	-0.2949	(-0.8174)
	HighOP	**-0.4692**	(-2.0722)	0.0888	(0.2289)	**-0.5698**	(-2.2028)
2	LowOP	-0.5683	(-1.3027)	0.5149	(1.5602)	-0.4956	(-1.0818)
	2OP	-0.4982	(-1.5679)	0.1717	(0.4596)	**-0.5130**	(-2.1381)
	3OP	-0.7042	(-1.8614)	-0.2990	(-0.9634)	-0.7192	(-1.8243)
	4OP	-0.4309	(-1.5860)	-0.2366	(-1.1351)	**-0.4553**	(-2.0486)
	HighOP	-0.5134	(-1.3984)	-0.2084	(-0.7791)	-0.4887	(-1.7064)
3	LowOP	-0.7152	(-1.8557)	-0.0756	(-0.2187)	-0.7105	(-1.6405)
	2OP	**-0.7224**	(-3.0868)	-0.3823	(-1.6974)	**-0.6556**	(-3.0527)
	3OP	**-0.8449**	(-2.2236)	**-0.5333**	(-2.5179)	**-0.8639**	(-2.3189)
	4OP	-0.7867	(-1.8388)	-0.2780	(-0.8720)	-0.6926	(-1.6636)
	HighOP	-0.5035	(-1.5997)	0.0093	(0.0362)	-0.3667	(-1.4344)
4	LowOP	**-0.9043**	(-4.9999)	-0.3856	(-1.6370)	**-0.8006**	(-4.8099)
	2OP	**-0.9072**	(-4.1810)	**-0.5199**	(-2.1765)	**-0.8270**	(-4.2185)
	3OP	**-0.8659**	(-1.9691)	-0.3979	(-1.0391)	-0.7247	(-1.6776)
	4OP	**-0.8016**	(-3.3689)	-0.2106	(-0.8644)	**-0.6879**	(-3.1197)
	HighOP	**-0.8364**	(-2.6551)	-0.5127	(-1.5724)	**-0.8108**	(-3.4822)
HighBM	LowOP	**-0.7207**	(-3.4777)	-0.4234	(-1.4925)	**-0.6597**	(-3.5634)
	2OP	**-1.1440**	(-4.8047)	**-0.7773**	(-3.7088)	**-1.0345**	(-5.0630)
	3OP	-0.5849	(-1.7228)	-0.1924	(-0.5618)	-0.4100	(-1.4220)
	4OP	**-1.2605**	(-3.7818)	-0.6525	(-1.4035)	**-0.9647**	(-3.0400)
	HighOP	**-1.6851**	(-2.9725)	-1.3934	(-1.6294)	**-1.6050**	(-2.3655)
	Wald-stat	109.40		27.32		136.18	
	p-value	0.0000		0.3399		0.0000	

Notes: This table reports first-pass beta estimates for the Fama and French (2015) 25 book-to-market and operating profitability portfolios (indexed by LowBM to HighBM and LowOP to HighOP). The betas are estimated component-wise that is regressing low frequency components of returns on the low frequency components of aggregate uncertainty. The associated t-statistics are based on Newey-West standard errors with $2^j - 1$ lags. The last rows of the table present the Wald test-statistics and their corresponding p-values from testing the joint hypothesis that all component-wise exposures are equal to zero, i.e. $H_0 : \beta^{1(j)} = \ldots = \beta^{25(j)} = 0$ for $j = 6, 7$ and $j = 6 : 7$. The initial sample period is 1963:07 to 2013:05. Bold values denote statistically significant beta estimates at a 95% confidence level.

Table 2.9: Cross-sectional regression: 25 FF book-to-market and operating profitability portfolios

	Persistence level							
$j =$	1	2	3	4	5	6	7	6:7
$u_t(1)$								
$\lambda_{0,j}$	1.3931	1.1400	0.6585	0.1557	0.3432	0.2438	0.6235	0.2989
	(4.8391)	(4.3727)	(3.6163)	(0.6980)	(1.6182)	(1.0298)	(2.7259)	(1.1748)
λ_j	1.8470	1.0794	0.1037	-0.5246	-0.2538	-0.4761	-0.4767	-0.6375
	(3.4545)	(2.2878)	(0.3355)	(-2.3075)	(-1.3845)	(-2.9832)	(-3.3816)	(-3.3535)
price of risk	1.625%	1.362%	0.171%	-1.118%	-0.760%	-2.101%	-2.806%	-2.322%
R^2	23.931%	16.801%	0.271%	11.607%	5.392%	39.193%	57.417%	39.300%
$se(\widehat{R^2})$	0.0647	0.1116	0.0174	0.0844	0.0785	0.1769	0.1781	0.1418
$p\left(R^2=1\right)$	0.0128	0.0041	0.0074	0.0146	0.0130	0.0236	0.0193	0.0151
MAPE	2.252%	2.496%	2.726%	2.519%	2.513%	2.140%	1.778%	2.231%
$u_t(3)$								
$\lambda_{0,j}$	1.3892	1.3460	0.7437	0.2136	0.3210	0.2632	0.6530	0.3255
	(5.4807)	(4.5328)	(3.9400)	(0.9783)	(1.4982)	(1.1230)	(2.8758)	(1.2899)
λ_j	0.9348	0.8626	0.1983	-0.3984	-0.2861	-0.5065	-0.4846	-0.6781
	(3.4858)	(2.3421)	(0.7393)	(-1.8920)	(-1.5146)	(-2.9861)	(-3.3262)	(-3.3478)
price of risk	2.070%	1.557%	0.417%	-0.919%	-0.846%	-2.120%	-2.788%	-2.376%
R^2	38.839%	21.961%	1.611%	7.841%	6.678%	39.899%	56.667%	41.156%
$se(\widehat{R^2})$	0.1442	0.1530	0.0460	0.0796	0.0859	0.1784	0.1823	0.1465
$p\left(R^2=1\right)$	0.0173	0.0046	0.0068	0.0132	0.0131	0.0229	0.0169	0.0137
MAPE	2.086%	2.418%	2.721%	2.579%	2.475%	2.138%	1.835%	2.190%
$u_t(12)$								
$\lambda_{0,j}$	1.0909	1.1320	0.8136	0.2038	0.2507	0.3190	0.6946	0.3887
	(4.5646)	(4.5708)	(4.3255)	(0.9213)	(1.1215)	(1.3921)	(3.0863)	(1.5558)
λ_j	0.4042	0.3133	0.1285	-0.2004	-0.2147	-0.3100	-0.2926	-0.4199
	(2.5614)	(2.1199)	(1.1203)	(-2.0143)	(-2.0058)	(-3.0097)	(-3.1887)	(-3.3174)
price of risk	1.217%	1.343%	0.645%	-1.002%	-1.167%	-2.179%	-2.735%	-2.499%
R^2	13.426%	16.329%	3.864%	9.321%	12.726%	42.155%	54.525%	45.510%
$se(\widehat{R^2})$	0.0834	0.1282	0.0712	0.0864	0.1070	0.1781	0.1882	0.1547
$p\left(R^2=1\right)$	0.0092	0.0049	0.0067	0.0131	0.0134	0.0231	0.0103	0.0110
MAPE	2.595%	2.554%	2.678%	2.558%	2.424%	2.116%	1.915%	2.083%
# observ.	598	596	592	584	568	536	472	472

Notes: This table reports the estimates for the zero-beta excess return ($\lambda_{0,j}$) and the price of risk (λ_j) for each scale j along with the corresponding Fama-MacBeth (1973) test statistics in parentheses. In addition, I normalize the scale-wise risk exposures and estimate the price of risk per unit of cross-sectional standard deviation in exposure in percent per year. I also report the sample R^2 for each cross-sectional regression and its standard error, the p-value for the Kan et al. (2013) test of $H_0: R^2 = 1$ and the mean absolute pricing error (MAPE) across all securities expressed in percent per year.

Table 2.10: Scale-specific risk exposures: 25 FF size and variance portfolios

Size	Variance	$\beta^{(6)}$		$\beta^{(7)}$		$\beta^{(6:7)}$	
Small	LowVAR	**-1.1606**	(-3.5863)	-0.7345	(-1.6874)	**-0.9466**	(-2.9859)
	2VAR	**-1.2850**	(-2.8327)	-0.4523	(-0.6993)	**-1.0397**	(-2.1856)
	3VAR	**-1.3079**	(-2.4115)	-0.0177	(-0.0230)	-0.9911	(-1.7242)
	4VAR	-1.2232	(-1.8982)	0.2793	(0.2828)	-0.8966	(-1.2095)
	HighVAR	-0.9090	(-1.2744)	0.7338	(0.5819)	-0.4671	(-0.5643)
2	LowVAR	**-0.9340**	(-4.3935)	**-0.7218**	(-2.5135)	**-0.8440**	(-4.3259)
	2VAR	**-1.0235**	(-2.6018)	-0.2386	(-0.5293)	**-0.8386**	(-2.1262)
	3VAR	**-0.9767**	(-2.3317)	-0.0206	(-0.0416)	-0.7478	(-1.8825)
	4VAR	-0.9362	(-1.5825)	0.4148	(0.5140)	-0.7424	(-1.1184)
	HighVAR	-0.7694	(-1.1172)	0.6201	(0.7757)	-0.5766	(-0.7060)
3	LowVAR	**-0.8350**	(-4.4499)	**-0.7499**	(-3.2149)	**-0.8037**	(-5.1894)
	2VAR	**-0.9104**	(-3.0623)	-0.3883	(-1.5002)	**-0.7994**	(-3.0519)
	3VAR	**-0.9149**	(-2.5530)	-0.1175	(-0.3102)	**-0.7744**	(-2.2277)
	4VAR	-0.9450	(-1.8311)	-0.0912	(-0.1553)	-0.8452	(-1.5384)
	HighVAR	-0.6686	(-1.0818)	0.5420	(0.6846)	-0.5754	(-0.8017)
4	LowVAR	**-0.9398**	(-5.0146)	**-0.7900**	(-4.0962)	**-0.9152**	(-7.2006)
	2VAR	**-0.8017**	(-3.0439)	**-0.4354**	(-2.9370)	**-0.7400**	(-3.6318)
	3VAR	**-0.7233**	(-2.1036)	-0.1906	(-0.8387)	**-0.6923**	(-2.1734)
	4VAR	-0.7092	(-1.4634)	0.0082	(0.0240)	-0.6789	(-1.4322)
	HighVAR	-0.7757	(-1.2303)	0.2322	(0.4126)	-0.7986	(-1.1640)
Big	LowVAR	**-0.5397**	(-4.9913)	-0.4779	(-1.1703)	**-0.5785**	(-6.2919)
	2VAR	-0.3767	(-1.5519)	-0.0298	(-0.0660)	**-0.5307**	(-2.2999)
	3VAR	-0.3656	(-1.6518)	-0.0278	(-0.0777)	**-0.4467**	(-2.1484)
	4VAR	-0.1042	(-0.2670)	0.2740	(0.7075)	-0.2174	(-0.5725)
	HighVAR	-0.3852	(-0.6956)	0.1239	(0.3307)	-0.4943	(-0.8780)
	Wald-stat	215.32		25.07		366.01	
	p-value	0.0000		0.4582		0.0000	

Notes: This table reports first-pass beta estimates for the Fama and French (2016) 25 size and variance portfolios (indexed by Small to Big and LowVAR to HighVAR). The betas are estimated component-wise that is regressing low frequency components of returns on the low frequency components of aggregate uncertainty. The associated t-statistics are based on Newey-West standard errors with $2^j - 1$ lags. The last rows of the table present the Wald test-statistics and their corresponding p-values from testing the joint hypothesis that all component-wise exposures are equal to zero, i.e. $H_0: \beta^{1(j)} = \ldots = \beta^{25(j)} = 0$ for $j = 6, 7$ and $j = 6:7$. The initial sample period is 1963:07 to 2013:05. Bold values denote statistically significant beta estimates at a 95% confidence level.

Table 2.11: Cross-sectional regression: 25 FF size and variance portfolios

	Persistence level							
$j =$	1	2	3	4	5	6	7	6:7
$u_t(1)$								
$\lambda_{0,j}$	1.0913	0.8877	0.8075	0.6649	0.7690	0.1962	0.7476	-0.1131
	(6.4114)	(5.3266)	(5.0955)	(3.4745)	(4.0675)	(0.8494)	(2.9177)	(-0.3569)
λ_j	0.8990	0.3657	0.2113	-0.0189	0.1029	-0.5079	-0.3932	-1.2460
	(1.5366)	(0.7471)	(0.4787)	(-0.0627)	(0.4269)	(-2.9246)	(-1.9058)	(-5.3519)
price of risk	1.380%	0.689%	0.460%	-0.063%	0.452%	-1.809%	-2.054%	-2.908%
R^2	13.822%	3.421%	1.524%	0.028%	1.423%	20.607%	27.355%	54.840%
$se(\widehat{R^2})$	0.1582	0.0912	0.0661	0.0098	0.0692	0.1898	0.1976	0.1644
$p\left(R^2=1\right)$	0.0002	0.0014	0.0017	0.0018	0.0017	0.0072	0.0004	0.0721
MAPE	2.825%	2.986%	3.008%	2.953%	3.008%	2.371%	2.595%	1.827%
$u_t(3)$								
$\lambda_{0,j}$	0.8787	0.8114	0.7996	0.6752	0.7336	0.2171	0.7602	-0.0194
	(4.7070)	(4.6350)	(4.9123)	(3.4839)	(3.9278)	(0.9437)	(3.0352)	(-0.0624)
λ_j	0.2011	0.1271	0.1406	-0.0070	0.0726	-0.5390	-0.4439	-1.2545
	(0.6176)	(0.4227)	(0.4273)	(-0.0263)	(0.2982)	(-2.9948)	(-2.0740)	(-5.1685)
price of risk	0.591%	0.396%	0.420%	-0.027%	0.313%	-1.844%	-2.186%	-2.918%
R^2	2.538%	1.128%	1.272%	0.005%	0.681%	21.427%	30.986%	55.231%
$se(\widehat{R^2})$	0.0828	0.0549	0.0615	0.0042	0.0479	0.1928	0.1940	0.1699
$p\left(R^2=1\right)$	0.0013	0.0014	0.0016	0.0017	0.0018	0.0079	0.0022	0.0711
MAPE	2.998%	2.992%	3.010%	2.959%	3.006%	2.342%	2.468%	1.832%
$u_t(12)$								
$\lambda_{0,j}$	0.6689	0.7507	0.7887	0.6118	0.6018	0.2404	0.8178	0.1788
	(5.1362)	(4.6092)	(4.8082)	(3.1967)	(3.2878)	(0.9901)	(3.5698)	(0.5214)
λ_j	-0.0194	0.0323	0.0544	-0.0316	-0.0284	-0.3763	-0.2151	-0.7293
	(-0.1144)	(0.2220)	(0.3802)	(-0.2502)	(-0.2128)	(-3.5909)	(-1.7500)	(-4.0420)
price of risk	-0.085%	0.199%	0.372%	-0.248%	-0.210%	-2.120%	-1.987%	-3.067%
R^2	0.052%	0.285%	0.999%	0.445%	0.307%	28.315%	25.623%	61.006%
$se(\widehat{R^2})$	0.0098	0.0271	0.0545	0.0395	0.0321	0.2013	0.2107	0.1278
$p\left(R^2=1\right)$	0.0031	0.0019	0.0016	0.0020	0.0021	0.0110	0.0004	0.0694
MAPE	2.914%	2.973%	3.007%	2.909%	2.921%	2.227%	2.654%	1.775%
# observ.	598	596	592	584	568	536	472	472

Notes: This table reports the estimates for the zero-beta excess return ($\lambda_{0,j}$) and the price of risk (λ_j) for each scale j along with the corresponding Fama-MacBeth (1973) test statistics in parentheses. In addition, I normalize the scale-wise risk exposures and estimate the price of risk per unit of cross-sectional standard deviation in exposure in percent per year. I also report the sample R^2 for each cross-sectional regression and its standard error, the p-value for the Kan et al. (2013) test of $H_0: R^2 = 1$ and the mean absolute pricing error (MAPE) across all securities expressed in percent per year.

Table 2.12: Tests of equality of cross-sectional R^2's

	$h=1$		$h=3$		$h=12$	
	$\Delta u_t^{(6)}$	$\Delta u_t^{(6:7)}$	$\Delta u_t^{(6)}$	$\Delta u_t^{(6:7)}$	$\Delta u_t^{(6)}$	$\Delta u_t^{(6:7)}$
Panel A						
R^2	62.416%	73.891%	63.443%	74.617%	67.543%	77.922%
$se(\widehat{R^2})$	0.2183	0.1224	0.2211	0.1311	0.2049	0.1147
2.5% CI (R^2)	0.1803	0.5167	0.2273	0.5103	0.2984	0.5616
97.5% CI (R^2)	1.0000	0.9701	1.0000	1.0000	1.0000	1.0000
difference	-0.1148		-0.1117		-0.1038	
$p\left(R^2_{(6)} = R^2_{(6:7)}\right)$	0.4089		0.3804		0.5598	
Panel B						
R^2	68.268%	73.006%	69.186%	74.027%	72.563%	70.012%
$se(\widehat{R^2})$	0.1968	0.0922	0.1942	0.0934	0.1742	0.1424
2.5% CI (R^2)	0.3267	0.5629	0.3403	0.5836	0.4144	0.4361
97.5% CI (R^2)	1.0000	0.9265	1.0000	0.9361	1.0000	0.9728
difference	-0.0474		-0.0484		0.0255	
$p\left(R^2_{(6)} = R^2_{(6:7)}\right)$	0.8115		0.7930		0.9196	
Panel C						
R^2	50.719%	39.300%	51.061%	41.156%	51.640%	45.510%
$se(\widehat{R^2})$	0.1454	0.1418	0.1477	0.1465	0.1522	0.1547
2.5% CI (R^2)	0.2384	0.1188	0.2391	0.1198	0.2457	0.1517
97.5% CI (R^2)	0.7846	0.6689	0.8047	0.6938	0.8269	0.7596
difference	0.1142		0.0991		0.0613	
$p\left(R^2_{(6)} = R^2_{(6:7)}\right)$	0.1482		0.1515		0.1950	
Panel D						
R^2	32.819%	54.840%	33.656%	55.231%	39.255%	61.006%
$se(\widehat{R^2})$	0.2250	0.1644	0.2260	0.1699	0.2201	0.1278
2.5% CI (R^2)	0.0000	0.2588	0.0000	0.2565	0.0000	0.3677
97.5% CI (R^2)	0.7946	0.8670	0.7975	0.9318	0.8191	0.8655
difference	-0.2202		-0.2158		-0.2175	
$p\left(R^2_{(6)} = R^2_{(6:7)}\right)$	0.1119		0.1220		0.3680	

Notes: This table reports tests of equality of the cross-sectional R^2's of the two competing models based on the factors $\Delta u_t^{(6)}$ and $\Delta u_t^{(6:7)}$ which are estimated over the same period (Panel A: #observ=507, Panels B-D: #observ=472). I report the sample cross-sectional R^2 and its standard error for each model, the 95% confidence interval for R^2 which is obtained by pivoting the cdf, the difference between the R^2's and the p-value for the (normal) test of $H_0 : 0 < R^2_{(6)} = R^2_{(6:7)} < 1$ denoted as $p\left(R^2_{(6)} = R^2_{(6:7)}\right)$. The reported p-values are two-tailed p-values. The test assets include: the 25 FF size and book-to-market portfolios (Panel A), the 25 FF size and investment portfolios (Panel B), the 25 FF book-to-market and operating profitability portfolios (Panel C) and the 25 FF size and variance portfolios (Panel D).

Table 2.13: Benchmark results

	λ_0	λ_{MKT}	λ_{SMB}	λ_{HML}	λ_{RMW}	λ_{CMA}	$\frac{\mathrm{R}^2}{se(\widehat{\mathrm{R}^2})}$	$p\left(\mathrm{R}^2=1\right)$
Panel A	25 FF size and book-to-market							
FF3	1.1103	-0.5860	0.1778	0.4138	-	-	66.560%	0.0001
	(3.7619)	(-1.6140)	(1.2666)	(3.0169)			0.1460	
	[3.3791]	[-1.4863]	[1.2722]	[3.0206]				
FF5	0.9421	-0.4611	0.2564	0.3687	0.5107	-0.0142	77.950%	0.0007
	(3.1163)	(-1.2548)	(1.8439)	(2.6944)	(2.7784)	(-0.0575)	0.1084	
	[2.5523]	[-1.0863]	[1.8403]	[2.5476]	[2.2142]	[-0.0359]		
Panel B	25 FF size and investment							
FF3	0.9590	-0.3379	0.2109	0.6055	-	-	74.415%	0.0023
	(3.2698)	(-0.9306)	(1.4811)	(3.3346)			0.1099	
	[2.7528]	[-0.8470]	[1.4717]	[3.1248]				
FF5	0.8245	-0.2109	0.2407	0.3824	0.1107	0.3576	75.834%	0.0004
	(2.4468)	(-0.5328)	(1.6776)	(1.6740)	(0.5787)	(3.6348)	0.1091	
	[1.9450]	[-0.4484]	[1.5803]	[1.2581]	[0.4088]	[3.5325]		
Panel C	25 FF book-to-market and operating profitability							
FF3	0.1686	0.3696	0.0247	0.5255	-	-	71.126%	0.0106
	(0.3580)	(0.7267)	(0.0874)	(3.3733)			0.1405	
	[0.2695]	[0.5638]	[0.0679]	[3.3014]				
FF5	0.7580	-0.2738	1.0895	0.2237	0.5063	-0.0583	93.405%	0.9534
	(1.4494)	(-0.4985)	(2.7552)	(1.4268)	(3.5418)	(-0.2933)	0.0532	
	[1.1686]	[-0.4125]	[2.2228]	[1.3061]	[2.9390]	[-0.2426]		
Panel D	25 FF size and variance							
FF3	0.1980	0.3438	-0.0091	0.9930	-	-	47.852%	0.0000
	(1.1010)	(1.2297)	(-0.0568)	(4.1240)			0.1593	
	[0.7195]	[1.0642]	[-0.0596]	[3.5421]				
FF5	1.1941	-0.5890	0.2995	-0.7029	1.4874	-1.6425	86.040%	0.0792
	(6.2037)	(-2.0752)	(1.9802)	(-2.4626)	(7.3199)	(-5.9008)	0.0644	
	[3.2846]	[-1.4610]	[1.7875]	[-1.4275]	[4.1041]	[-3.1551]		

Notes: This table reports the estimates for the zero-beta excess return and the price of risk for each factor in the Fama and French (1993) three-factor model (FF3) and the Fama and French (2015) five-factor model (FF5) along with the corresponding Fama-MacBeth (1973) test statistics in parentheses. The factors include the value-weight excess return on the market portfolio (MKT), the size factor (SMB, small minus big), the value factor (HML, high minus low book-to-market), the operating profitability factor (RMW, robust minus weak profitability) and the investment factor (CMA, conservative minus aggressive investment). In addition, I report the sample R^2 for each cross-sectional regression along with its standard error and the p-value for the Kan et al. (2013) specification test of $H_0: R^2 = 1$. Finally, I report the Kan et al. (2013) misspecification-robust test statistics in square brackets.

Table 2.14: Equity risk premium predictability

Panel A: scale-wise predictive regressions								
		Time-scale / Persistence level						
	j =	1	2	3	4	5	6	7
$u_t(1)$	β_j	17.0671	4.9732	-1.3015	1.2821	-1.4753	**3.0551**	0.3395
	NW t-stat	(1.2109)	(0.6536)	(-0.1805)	(0.3057)	(-0.5219)	(3.8358)	(0.1636)
	HH t-stat	(1.3849)	(0.6896)	(-0.1735)	(0.3544)	(-0.5445)	(3.4481)	(0.2996)
	Adj.R^2 (%)	[0.19%]	[0.08%]	[0.03%]	[0.10%]	[0.40%]	[**4.25%**]	[0.12%]
$u_t(3)$	β_j	14.4789	8.0920	-1.2110	1.5114	-1.4172	**2.8094**	0.4748
	NW t-stat	(0.9460)	(1.0158)	(-0.1697)	(0.3622)	(-0.5530)	(3.8691)	(0.2462)
	HH t-stat	(1.1196)	(1.0802)	(-0.1647)	(0.4063)	(-0.5929)	(3.2111)	(0.4812)
	Adj.R^2 (%)	[0.13%]	[0.21%]	[0.03%]	[0.16%]	[0.43%]	[**4.42%**]	[0.28%]
$u_t(12)$	β_j	12.8635	21.4342	-0.5482	3.2158	-1.2089	**4.2765**	1.2757
	NW t-stat	(0.3885)	(1.3916)	(-0.0440)	(0.4033)	(-0.2845)	(3.7904)	(0.4530)
	HH t-stat	(0.4795)	(1.7927)	(-0.0458)	(0.4490)	(-0.3339)	(3.0029)	(1.0020)
	Adj.R^2 (%)	[0.02%]	[0.34%]	[0.00%]	[0.23%]	[0.12%]	[**4.56%**]	[1.00%]
# observations		632	628	620	604	572	508	380

Panel B: long-horizon predictive regressions (forward/backward aggregates)								
		Horizon						
	q =	16	32	48	64	96	128	192
$u_t(1)$	β_q	-0.0515	1.1232	2.3776	2.8096	3.8981	**5.1908**	2.7207
	NW t-stat	(-0.0313)	(0.6605)	(1.3904)	(2.4831)	(4.4502)	(10.1284)	(4.4648)
	$t/\sqrt{T}$	{-0.0040}	{0.1158}	{0.2717}	{0.3597}	{0.6867}	{1.4034**}	{0.4223}
	Adj.R^2 (%)	[-0.16%]	[1.15%]	[6.73%]	[11.32%]	[31.99%]	[**66.35%**]	[14.90%]
$u_t(3)$	β_q	-0.1223	0.9830	2.2031	2.6418	3.7424	**4.8934**	2.1587
	NW t-stat	(-0.0810)	(0.6294)	(1.3859)	(2.4979)	(4.4820)	(10.1448)	(4.2962)
	$t/\sqrt{T}$	{-0.0103}	{0.1100}	{0.2739}	{0.3666}	{0.7174}	{1.4596**}	{0.3664}
	Adj.R^2 (%)	[-0.16%]	[1.03%]	[6.83%]	[11.71%]	[33.93%]	[**68.09%**]	[11.57%]
$u_t(12)$	β_q	-0.0663	2.1299	4.0386	4.6292	**6.0664**	**7.0527**	0.4706
	NW t-stat	(-0.0325)	(1.2430)	(2.8174)	(5.2286)	(6.0294)	(7.9741)	(1.0098)
	$t/\sqrt{T}$	{-0.0037}	{0.1672}	{0.3734}	{0.4871}	{0.9069*}	{1.5274**}	{0.0651}
	Adj.R^2 (%)	[-0.16%]	[2.56%]	[12.11%]	[19.08%]	[**45.12%**]	[**70.03%**]	[0.03%]

Notes: Panel A reports the results of scale-wise predictive regressions of the components of S&P 500 index excess returns on the components of macroeconomic uncertainty. For each regression, the table reports OLS estimates of the regressors, Newey-West (1987) and Hansen-Hodrick (1980) corrected t-statistics with $2^j - 1$ lags in parentheses and adjusted R^2 statistics in square brackets. Panel B presents the results of regressions (with an intercept) of forward/backward aggregates over a horizon q. Panel B reports OLS estimates of the regressors, Newey-West (1987) corrected t-statistics with $2 \times (q-1)$ lags in parentheses, Valkanov's (2003) rescaled test statistics in curly brackets and adjusted R^2 statistics in square brackets. Significance at the 5%, 2.5% and 1% level based on the rescaled t-statistic is indicated by *, ** and *** respectively.

Table 2.15a: Monotonicity tests for scale-specific risk exposures

Panel A		Size										Top−bottom	MR
		Low	2	3	4	5	6	7	8	9	High	p-value	p-value
Average Return		0.7570	0.7037	0.7728	0.7034	0.7372	0.6721	0.6812	0.6312	0.5724	0.4286	0.0670	0.3972
For returns - $H_0 : R_{10} \geq \ldots \geq R_1$ vs $H_1 : R_{10} < \ldots < R_1$							For risk-loadings - $H_0 : \beta_{10}^{(j)} \leq \ldots \leq \beta_1^{(j)}$ vs $H_1 : \beta_{10}^{(j)} > \ldots > \beta_1^{(j)}$						
$\beta^{(6)}$	$h = 1$	-1.0051	-0.9265	-0.8087	-0.7419	-0.7083	-0.7327	-0.7294	-0.6944	-0.5487	-0.3512	0.0606	0.0656
$\beta^{(6)}$	$h = 3$	-0.9136	-0.8385	-0.7296	-0.6654	-0.6301	-0.6572	-0.6498	-0.6194	-0.4770	-0.2764	0.0606	0.0906
$\beta^{(6)}$	$h = 12$	-1.2469	-1.1572	-0.9866	-0.8730	-0.8108	-0.8857	-0.8641	-0.8236	-0.5952	-0.2726	0.1010	0.2222
$\beta^{(6:7)}$	$h = 1$	-0.8207	-0.8314	-0.7332	-0.7339	-0.7175	-0.7697	-0.7221	-0.7677	-0.5903	-0.4568	0.2696	0.1416
$\beta^{(6:7)}$	$h = 3$	-0.7515	-0.7470	-0.6640	-0.6574	-0.6409	-0.6934	-0.6434	-0.6877	-0.5144	-0.3625	0.2530	0.1580
$\beta^{(6:7)}$	$h = 12$	-0.9683	-0.9940	-0.8915	-0.8734	-0.8424	-0.9727	-0.8778	-0.9557	-0.6915	-0.4531	0.3238	0.3178
Panel B		Long-term Reversal										Top−bottom	MR
		Low	2	3	4	5	6	7	8	9	High	p-value	p-value
Average Return		0.9069	0.7314	0.7297	0.6410	0.6397	0.6077	0.5806	0.5335	0.4058	0.4229	0.0139	0.0036
For returns - $H_0 : R_{10} \geq \ldots \geq R_1$ vs $H_1 : R_{10} < \ldots < R_1$							For risk-loadings - $H_0 : \beta_{10}^{(j)} \leq \ldots \leq \beta_1^{(j)}$ vs $H_1 : \beta_{10}^{(j)} > \ldots > \beta_1^{(j)}$						
$\beta^{(6)}$	$h = 1$	-1.3095	-0.7870	-0.9055	-0.7816	-0.6135	-0.4687	-0.4758	-0.3173	-0.1509	-0.0635	0.0014	0.4644
$\beta^{(6)}$	$h = 3$	-1.2286	-0.7282	-0.8301	-0.7010	-0.5419	-0.4071	-0.4061	-0.2596	-0.0881	0.0081	0.0012	0.4094
$\beta^{(6)}$	$h = 12$	-1.8966	-1.0688	-1.2519	-0.9897	-0.7372	-0.5128	-0.4981	-0.2578	0.0839	0.3111	0.0018	0.4962
$\beta^{(6:7)}$	$h = 1$	-1.1734	-0.7088	-0.9100	-0.8408	-0.6730	-0.4944	-0.4755	-0.3618	-0.1889	-0.2685	0.0204	0.6342
$\beta^{(6:7)}$	$h = 3$	-1.0994	-0.6460	-0.8264	-0.7513	-0.5930	-0.4237	-0.4041	-0.2936	-0.1155	-0.1703	0.0122	0.6016
$\beta^{(6:7)}$	$h = 12$	-1.6565	-0.9083	-1.2608	-1.1076	-0.8581	-0.5513	-0.5439	-0.3511	-0.0044	-0.0178	0.0100	0.6952
Panel C		Short-term Reversal										Top−bottom	MR
		Low	2	3	4	5	6	7	8	9	High	p-value	p-value
Average Return		0.5719	0.7780	0.7194	0.6226	0.5764	0.4955	0.4574	0.4830	0.3015	0.1794	0.0182	0.6822
For returns - $H_0 : R_{10} \geq \ldots \geq R_1$ vs $H_1 : R_{10} < \ldots < R_1$							For risk-loadings - $H_0 : \beta_{10}^{(j)} \leq \ldots \leq \beta_1^{(j)}$ vs $H_1 : \beta_{10}^{(j)} > \ldots > \beta_1^{(j)}$						
$\beta^{(6)}$	$h = 1$	-0.9308	-0.6956	-0.6245	-0.3368	-0.5560	-0.4400	-0.4034	-0.4340	-0.2983	-0.2014	0.0128	0.8368
$\beta^{(6)}$	$h = 3$	-0.8324	-0.6163	-0.5412	-0.2696	-0.4806	-0.3637	-0.3362	-0.3589	-0.2299	-0.1371	0.0140	0.8566
$\beta^{(6)}$	$h = 12$	-1.0707	-0.8151	-0.6815	-0.2608	-0.6172	-0.4075	-0.3842	-0.3818	-0.1900	0.0194	0.0280	0.8844
$\beta^{(6:7)}$	$h = 1$	-0.9351	-0.7028	-0.6727	-0.3597	-0.6193	-0.5546	-0.4947	-0.5464	-0.4792	-0.2949	0.0250	0.8074
$\beta^{(6:7)}$	$h = 3$	-0.8286	-0.6116	-0.5759	-0.2817	-0.5319	-0.4646	-0.4122	-0.4561	-0.3854	-0.2241	0.0274	0.8214
$\beta^{(6:7)}$	$h = 12$	-1.0747	-0.8353	-0.7844	-0.3036	-0.7376	-0.6326	-0.5390	-0.5534	-0.4512	-0.1171	0.0492	0.8318

Notes: This table presents the scale-specific risk exposures with respect to the factors $\Delta u_t^{(6)}$ and $\Delta u_t^{(6:7)}$ for $h = 1, 3, 12$ for various one-way portfolio sorts and the corresponding monotonicity tests. The sorting variables are: size (Panel A), long-term reversal (Panel B) and short-term reversal (Panel C). The first row in each panel reports average excess returns (in percent per month) for the test assets. The final column in each panel presents the p-value for the monotonic relation (MR) test. The penultimate column presents the bootstrap p-value for the top-minus-bottom difference in the corresponding returns and scale-wise betas.

Table 2.15b: Monotonicity tests for scale-specific risk exposures

Panel D		Book-to-Market					Top−bottom	MR
		Low	2	3	4	High	p-value	p-value
Average Return		0.4200	0.5385	0.5701	0.6902	0.8421	0.0033	0.0078
For returns - $H_0 : R_5 \leq \ldots \leq R_1$ vs $H_1 : R_5 > \ldots > R_1$								
For risk-loadings - $H_0 : \beta_5^{(j)} \geq \ldots \geq \beta_1^{(j)}$ vs $H_1 : \beta_5^{(j)} < \ldots < \beta_1^{(j)}$								
$\beta^{(6)}$	$h=1$	-0.3088	-0.5302	-0.7102	-0.8052	-0.7867	0.0112	0.0462
$\beta^{(6)}$	$h=3$	-0.2374	-0.4622	-0.6278	-0.7258	-0.7093	0.0126	0.0418
$\beta^{(6)}$	$h=12$	-0.1874	-0.5846	-0.8600	-1.0516	-1.0232	0.0142	0.0344
$\beta^{(6:7)}$	$h=1$	-0.4482	-0.5226	-0.7029	-0.7677	-0.7427	0.2038	0.0978
$\beta^{(6:7)}$	$h=3$	-0.3534	-0.4507	-0.6197	-0.6895	-0.6731	0.1716	0.0782
$\beta^{(6:7)}$	$h=12$	-0.3967	-0.5988	-0.8744	-1.0284	-1.0160	0.1292	0.0404
Panel E		Investment					Top−bottom	MR
		Low	2	3	4	High	p-value	p-value
Average Return		0.7585	0.5776	0.5203	0.5129	0.4030	0.0034	0.0240
For returns - $H_0 : R_5 \geq \ldots \geq R_1$ vs $H_1 : R_5 < \ldots < R_1$								
For risk-loadings - $H_0 : \beta_5^{(j)} \leq \ldots \leq \beta_1^{(j)}$ vs $H_1 : \beta_5^{(j)} > \ldots > \beta_1^{(j)}$								
$\beta^{(6)}$	$h=1$	-0.7509	-0.5922	-0.5566	-0.4761	-0.1936	0.0050	0.0052
$\beta^{(6)}$	$h=3$	-0.6774	-0.5274	-0.4775	-0.3953	-0.1201	0.0060	0.0034
$\beta^{(6)}$	$h=12$	-0.9480	-0.7339	-0.6222	-0.4407	0.0781	0.0076	0.0034
$\beta^{(6:7)}$	$h=1$	-0.7146	-0.6328	-0.6323	-0.5333	-0.2676	0.0394	0.0330
$\beta^{(6:7)}$	$h=3$	-0.6385	-0.5644	-0.5431	-0.4425	-0.1809	0.0336	0.0186
$\beta^{(6:7)}$	$h=12$	-0.8805	-0.8331	-0.7714	-0.5562	-0.0329	0.0294	0.0128
Panel F		Dividend Yield					Top−bottom	MR
		Low	2	3	4	High	p-value	p-value
Average Return		0.4520	0.5479	0.5028	0.6402	0.6058	0.1909	0.3302
For returns - $H_0 : R_5 \leq \ldots \leq R_1$ vs $H_1 : R_5 > \ldots > R_1$								
For risk-loadings - $H_0 : \beta_5^{(j)} \geq \ldots \geq \beta_1^{(j)}$ vs $H_1 : \beta_5^{(j)} < \ldots < \beta_1^{(j)}$								
$\beta^{(6)}$	$h=1$	0.0139	-0.4367	-0.6084	-0.6519	-1.0399	0.0002	0.0044
$\beta^{(6)}$	$h=3$	0.0670	-0.3637	-0.5436	-0.5818	-0.9337	0.0004	0.0058
$\beta^{(6)}$	$h=12$	0.3794	-0.4203	-0.7676	-0.8340	-1.3937	0.0004	0.0048
$\beta^{(6:7)}$	$h=1$	-0.1342	-0.4913	-0.5693	-0.6434	-1.0320	0.0078	0.0022
$\beta^{(6:7)}$	$h=3$	-0.0578	-0.4056	-0.5052	-0.5662	-0.9306	0.0064	0.0034
$\beta^{(6:7)}$	$h=12$	0.1636	-0.5196	-0.7459	-0.8461	-1.4417	0.0022	0.0030

Notes: This table presents the scale-specific risk exposures with respect to the factors $\Delta u_t^{(6)}$ and $\Delta u_t^{(6:7)}$ for $h = 1, 3, 12$ for various one-way portfolio sorts and the corresponding monotonicity tests. The sorting variables are: book-to-market (Panel D), investment (Panel E) and dividend-yield (Panel F). The first row in each panel reports average excess returns (in percent per month) for the test assets. The final column in each panel presents the p-value for the monotonic relation (MR) test. Similarly, the penultimate column presents the bootstrap p-value for the top-minus-bottom difference in the corresponding returns and scale-wise betas.

Appendix 2A: Results for Raw Series and Previous Studies

Table 2A.1: Cross-sectional regressions using the raw series of aggregate uncertainty

Panel A	25 FF size and book-to-market						
	λ_0		λ_u		R^2	$p\left(R^2=0\right)$	MAPE
$u_t\,(1)$	0.6038	(2.0306)	-0.1844	(-0.3039)	0.52%	0.8580	2.12%
$u_t\,(3)$	0.6091	(2.0568)	-0.1251	(-0.2883)	0.55%	0.8343	2.12%
$u_t\,(12)$	0.3370	(1.2950)	-0.2794	(-1.1998)	7.68%	0.5173	1.95%
Panel B	25 FF size and investment						
	λ_0		λ_u		R^2	$p\left(R^2=0\right)$	MAPE
$u_t\,(1)$	0.7411	(3.3525)	0.0398	(0.0828)	0.04%	0.9548	2.09%
$u_t\,(3)$	0.5821	(2.2972)	-0.1497	(-0.3915)	1.10%	0.7443	2.04%
$u_t\,(12)$	0.3729	(1.4918)	-0.2089	(-1.0464)	7.62%	0.4250	1.91%
Panel C	25 FF book-to-market and operating profitability						
	λ_0		λ_u		R^2	$p\left(R^2=0\right)$	MAPE
$u_t\,(1)$	0.4466	(1.9274)	-0.2766	(-0.6264)	0.80%	0.8515	2.72%
$u_t\,(3)$	0.7573	(3.1434)	0.1737	(0.5037)	0.66%	0.8285	2.73%
$u_t\,(12)$	0.3585	(1.6464)	-0.1667	(-1.0829)	2.76%	0.6558	2.69%
Panel D	25 FF size and variance						
	λ_0		λ_u		R^2	$p\left(R^2=0\right)$	MAPE
$u_t\,(1)$	0.8117	(3.9496)	0.1809	(0.3826)	1.04%	0.7324	2.97%
$u_t\,(3)$	0.7505	(3.7272)	0.0635	(0.1896)	0.26%	0.8617	2.95%
$u_t\,(12)$	0.5941	(3.0081)	-0.0560	(-0.3189)	0.66%	0.8042	2.86%

Notes: This table reports the estimates for the zero-beta excess return (λ_0) and the price of risk (λ_u) for the innovations in the raw series of aggregate uncertainty along with the corresponding Fama-MacBeth (1973) test statistics in parentheses. The innovations are the residuals from an AR(1) model fitted to the factor. The test assets include: the 25 FF size and book-to-market portfolios (Panel A), the 25 FF size and investment portfolios (Panel B), the 25 FF book-to-market and operating profitability portfolios (Panel C) and the 25 FF size and variance portfolios (Panel D). In addition, I report the sample R^2 for each cross-sectional regression, the p-value for the Kan et al. (2013) test of $H_0: R^2=0$ denoted as $p\left(R^2=0\right)$ and the mean absolute pricing error (MAPE) across all securities expressed in percent per year.

Table 2A.2: Long-horizon predictive regressions - forward aggregates only

		Horizon						
	q =	16	32	48	64	96	128	192
u_t (1)	β_q	-0.1226	-0.0580	0.0539	0.1835	0.5760	1.2656	2.9976
	NW t-stat	(-0.5098)	(-0.1664)	(0.1110)	(0.2624)	(0.8686)	(1.9620)	(4.0198)
	$t/\sqrt{T}$	{-0.0636}	{-0.0228}	{0.0181}	{0.0463}	{0.1219}	{0.2224}	{0.5108}
	Adj.R^2 (%)	[0.254%]	[-0.112%]	[-0.135%]	[0.063%]	[1.544%]	[5.671%]	[27.141%]
u_t (3)	β_q	-0.1284	-0.0750	0.0254	0.1473	0.5213	1.2026	2.8640
	NW t-stat	(-0.5715)	(-0.2322)	(0.0562)	(0.2255)	(0.8168)	(1.8767)	(3.9568)
	$t/\sqrt{T}$	{-0.0717}	{-0.0316}	{0.0092}	{0.0403}	{0.1196}	{0.2299}	{0.5387}
	Adj.R^2 (%)	[0.364%]	[-0.061%]	[-0.162%]	[0.006%]	[1.481%]	[6.046%]	[29.310%]
u_t (12)	β_q	-0.2248	-0.0661	0.2016	0.6129	1.4199	2.5474	5.1227
	NW t-stat	(-0.6845)	(-0.1541)	(0.3495)	(0.8109)	(1.7440)	(2.5685)	(4.4368)
	$t/\sqrt{T}$	{-0.0823}	{-0.0182}	{0.0478}	{0.1178}	{0.2322}	{0.3545}	{0.7739}
	Adj.R^2 (%)	[0.531%]	[-0.131%]	[0.077%]	[1.352%]	[5.818%]	[13.472%]	[46.187%]

Notes: This table presents the results of long-horizon predictive regressions over a horizon q using only forward aggregates, i.e. regressions of the form

$$r^e_{t+1,t+q} = a_q + \beta_q u_t + \eta_{t,t+q}$$

where $r^e_{t+1,t+q} = \sum_{i=1}^{q} r^e_{t+i}$ denotes excess market returns between $t+1$ and $t+q$ and u_t macro uncertainty at time t. For each regression, the table reports OLS estimates of the regressors, Newey-West (1987) corrected t-statistics with q lags in parentheses, Valkanov's (2003) rescaled test statistics in curly brackets and adjusted R^2 statistics in square brackets. Significance at the 5%, 2.5% and 1% level based on the rescaled t-statistic is indicated by *, ** and *** respectively. For the right-tail critical values of $t/\sqrt{T}$ at various percentiles see the Internet Appendix.

Table 2A.3: Previous studies sorted by year

Reference	Journal	Macroeconomic factor(s)
Chen, Roll, and Ross (1986)	*JB*	industrial production growth, unanticipated (*realized minus expected*) inflation
Ferson and Harvey (1991)	*JPE*	unexpected (*actual minus forecasts*) inflation, credit spread, yield spread
Cochrane (1996)	*JPE*	investment growth
Jagannathan and Wang (1996)	*JF*	real labor income growth rate
Lettau and Ludvigson (2001)	*JF*	consumption-to-wealth ratio (e.g. cay)
Vassalou (2003)	*JFE*	GDP growth news
Brennan, Wang, and Xia (2004)	*JF*	maximum Sharpe ratio
Bansal, Dittmar, and Lundblad (2005)	*JF*	long-run consumption risk
Parker and Julliard (2005)	*JPE*	long-horizon (e.g. three year) consumption growth
Hahn and Lee (2006)	*JFQA*	credit spread, yield spread
Petkova (2006)	*JF*	credit spread, yield spread
Jagannathan and Wang (2007)	*JF*	fourth-quarter year-over-year (Q4-Q4) consumption growth
Ozoguz (2009)	*RFS*	investors' uncertainty about the state of the economy extracted from a two-state regime switching model
Bali, Brown, and Caglayan (2014)	*JFE*	macroeconomic uncertainty, quantified as the time-varying conditional volatility of common macroeconomic variables
Bali and Zhou (2014)	*JFQA*	market uncertainty (e.g. variance risk premium)
Bali, Brown, and Tang (2016)	*Working Paper*	macroeconomic uncertainty, quantified as the cross-sectional dispersion in economic forecasts from the Survey of Professional Forecasters
Bandi and Tamoni (2016)	*Working Paper*	low-frequency consumption shocks
Boons and Tamoni (2016)	*Working Paper*	low-frequency shocks in industrial production growth

Notes: Overview of previous studies that explore the cross-sectional implications of various macroeconomic factors. For a full list see Harvey et al. (2016).

Appendix 2B: Robustness Checks and Additional Results

This Appendix contains additional results and robustness checks that are omitted in the main chapter for brevity.

Same burn-in period

In the main results I discard the first $2^j - 1$ observations for each scale, that is, I use a burn-in specific period for each component and rely on the maximum number of observations possible for each time-scale to conduct statistical and economic inferences. Here I adopt a different approach to initialize the filtering procedure. Specifically, I use the same burn-in period for all components which implies a reduction of the effective sample for $j \in \{1, 2, 3, 4, 5, 6\}$. Tables 2B.1 through 2B.4 present the results from the cross-sectional regressions for the same sub-period. The results for all test assets remain quantitatively similar.

Uncertainty shocks with persistence greater than 128 months

I report the results for low-frequency uncertainty shocks with persistence greater than $2^7 = 128$ months (see Table 2B.5). The factor $\Delta u_t^{(>7)}$ cannot explain the cross-sectional variation in the 25 FF size and book-to-market portfolios, the 25 FF size and investment and the 25 FF size and variance portfolios. Also, the null that the model is correctly specified (i.e., $H_0 : R^2 = 1$) is strongly rejected. In contrast, low-frequency uncertainty shocks with persistence greater than 128 months are priced in the cross-section of the 25 FF book-to-market and operating profitability portfolios. However, the estimates of the zero-beta excess return are statistically significant at the 1% level for all $h = 1, 3, 12$. Also, the factor has a higher MAPE in comparison with $\Delta u_t^{(6:7)}$ and the specification

test rejects the hypothesis of a perfect fit. In addition, the explanatory power of the factor is limited. (i.e., for $h = 1$: $se(\widehat{\mathrm{R}^2_{(>7)}}) = 0.085$, for $h = 3$: $se(\widehat{\mathrm{R}^2_{(>7)}}) = 0.084$ and for $h = 12$: $se(\widehat{\mathrm{R}^2_{(>7)}}) = 0.081$). Similar results (see Table 2B.6) hold for low-frequency uncertainty shocks with persistence ranging between 128 and 256 months (i.e., the priced factor is $\Delta u_t^{(8)}$). Also, confidence intervals for the sample cross-sectional R^2 for $\Delta u_t^{(>7)}$ and $\Delta u_t^{(8)}$ are available in Table 2B.7.

Results for the low-frequency macro volatility risk factor of Boons and Tamoni (2015) - monthly data

In line with Boons and Tamoni (2016) I extract from the volatility of monthly industrial production low-frequency shocks with persistence greater than 32 months. Note that IPVOL is estimated using an $\mathrm{AR}(1) - \mathrm{GARCH}(1,1)$ model over the full sample. Table 2B.8 reports the estimates for the zero-beta excess return and the price of risk for the innovations in macro volatility shocks with persistence greater than 32 months. The factor $\Delta IPVOL_t^{(>5)}$ is not priced in any of the test assets. From this perspective my study complements Boons and Tamoni (2016) by showing that investors care about scale-dependent economic uncertainty irrespective of their portfolio rebalancing period.

5 industry portfolios *plus* 25 FF size and book-to-market

Following the suggestion of Lewellen et al. (2010) and Daniel and Titman (2012) I relax the tight (i.e., low-dimensional) factor structure of the test assets and I use the 25 FF size and book-to-market and the 5 FF industry portfolios which are priced together. That is, I include the industry portfolios to provide a higher hurdle for the proposed factor (i.e., the cross-sectional variation in the expected returns is higher). Since the asymptotic results in Kan et al. (2013) become less reliable as the number of test assets increases (e.g. the asymptotic distribution of the sample cross-sectional R^2), I only add the 5 industry portfolios. The results in Table 2B.9 remain similar and the model with the *business-cycle uncertainty* factor is correctly specified.

Controlling for Fama-French factors

Table 3B.10 presents results from cross-sectional regressions where I control for exposure to the Fama-French's factors. The control factors include the value-weight excess return on the market portfolio (MKT), the size factor (SMB, small minus big), the value factor (HML, high minus low book-to-market), the operating profitability factor (RMW, robust minus weak profitability) and the investment factor (CMA, conservative minus aggressive investment). Except for the test assets sorted across book-to-market and operating profitability, the *business-cycle uncertainty* factor remains statistically significant in the presence of the control factors (see also the discussion in Section 3.3. of the main chapter).

Controlling for momentum, short-term reversal, long-term reversal, liquidity and portfolio characteristics

Tables 2B.11a and 2B.11b report estimates for the price of risk ($\lambda_{6:7}$) for $u_t^{(6:7)}$ after controlling for exposure to the value-weight excess return on the market portfolio (MKT), the size factor (SMB), the value factor (HML), the momentum factor (MOM), the short-term reversal factor (STR), the long-term reversal factor (LTR), the liquidity factor (LIQ), the log size ($\log(ME)$) and the log book-to-market ratio ($\log(B/M)$). I estimate the risk exposures for the MKT, SMB, HML, MOM, STR and LTR factors using the same time-series regression and the risk-loadings for the LIQ factor separately as in Pastor and Stambaugh (2003). The *business-cycle uncertainty* factor remains statistically significant in the presence of the control factors.

Residuals from an AR(1) model fitted to $u_t^{(6:7)}$

Under the one-sided, linear Haar filter used for the extraction decomposing across time-scales changes in aggregate uncertainty is equivalent to calculating changes in the scale-specific uncertainty series. Thus, in the main chapter I estimate the innovations in the scale-specific uncertainty components by first-differencing each series. For robustness, I present in Table 3B.1 the cross-

sectional estimates for the *business-cycle uncertainty* factor where the innovations are the residuals from an AR(1) model fitted to the factor $u_t^{(6:7)}$. The results remain quantitatively similar across all test assets.

Bootstrapped confidence intervals for the first and second-pass cross-sectional estimates

I calculate confidence intervals for the first-pass scale-dependent betas for $u_t^{(6:7)}$ using the bias-corrected percentile method and the stationary bootstrap procedure described in Appendix A. For a survey of bootstrap procedures for constructing confidence regions see Diciccio and Romano (1988). The results are available in Table 2B.13. Bold values denote statistically significant beta estimates at a 90% confidence level. Several of the estimated betas are individually statistical significant, that is, the bootstrap-based confidence regions do not include zero.

Moreover, for each bootstrap replication $b = 1, \ldots, 5,000$ I estimate a cross-sectional regression of average portfolio excess returns (original data) on the pseudo-sample of the scale-specific risk exposures. I report confidence intervals using the bias-corrected percentile method for the zero-beta excess return ($\lambda_{0,6:7}$), the price of risk ($\lambda_{6:7}$) and the sample R^2. The results are available in Table 2B.14. The main difference with the results in the main chapter is that for the 25 FF book-to-market and operating profitability portfolios the estimates of the zero-beta excess return remain statistically significant. Two comments are in order here. First, for these test assets the model is misspecified. Second, the scale-specific risk exposures are estimated with error in the first-pass scale-wise regression. In contrast, the popular Fama-MacBeth (1973) test-statistics reported in the main paper do not account for estimation errors in the betas or for a potentially misspecified model. Note that since the first-pass regressions are scale-wise, the Shanken (1992) correction or the misspecification-robust t-statistics of Kan et al. (2013) are not directly applicable here.

Bootstrapped confidence intervals for the scale-wise predictive regressions

Table 2B.15 reports bootstrapped confidence intervals for the scale-wise predictive regressions for $j = 6, 7$ using the bias-corrected percentile method and the stationary bootstrap of Politis and Romano (1994). In Panel A of Table 2B.15 the average block size in this case is set equal to 32 - calculated based on the Politis and White (2004) estimator. In Panel B of Table 2B.15 the block size is set equal to 2^j. For $j = 6$ the coefficients from the scale-wise predictive regressions are statistically significant.

Valkanov's (2003) rescaled t-statistic

The standard t-statistics in long-horizon regressions do not converge to well-defined distributions (for instance, see Valkanov, 2003 and Bandi and Perron, 2008). To address this inferential problem I rely on Valkanov's (2003) rescaled $t/\sqrt{T}$ statistic. In particular, as in Valkanov's framework I assume that the underlying data-generating processes are

$$r^e_{t+1} = \beta u_t + \epsilon_{1,t+1} \tag{2B.1}$$

$$u_t = \varrho u_{t-1} + \epsilon_{2,t+1} \tag{2B.2}$$

where $\rho = 1 + c/T$ and the parameter c measures deviations from unity in a decreasing (at rate T) neighbourhood of 1. Also, I assume that the vector $[\epsilon_{1,t+1}, \epsilon_{2,t+1}]$ is a vector martingale difference sequence with covariance matrix $\left[\sigma^2_{11}\, \sigma_{12}; \sigma_{21}\, \sigma^2_{22}\right]$. Following Bandi and Perron (2008) I let the portion of the overlap to be a constant fraction of the sample size, that is, $h = [\lambda T]$. Table 2B.16 reports the right-tail critical values of $t/\sqrt{T}$ at various percentiles. I simulate the distribution of $t/\sqrt{T}$ for samples of length $T = 635$. I implement 5,000 replications. It is important to highlight that I only adopt this framework to address the inferential problems that arise in predictive regressions with persistent regressors. As I demonstrate in Table 2B.17 the data-generating process for uncertainty is a multi-scale autoregressive process, i.e. a system in which high-frequency shocks are

not linear combinations of low-frequency shocks (see also the novel work of Bandi et al., 2016).

Multi-scale autoregressive system

Table 2B.17 reports the estimation results of the multi-scale autoregressive system for macro uncertainty. For $j \in \{1, 5\}$ the uncertainty components can be represented as scale-wise AR processes, i.e. $u^{(j)}_{k\times 2^j+2^j} = \rho_j u^{(j)}_{k\times 2^j} + \varepsilon^{(j)}_{k\times 2^j+2^j}$ where $k \in Z$. My results are similar with the estimates for consumption shocks in Ortu et al. (2013) (see page 2905). Note that as Bandi et al. (2016) point out the dependence ρ_j in time-scale j is significantly lower than the dependence of the raw series. Moreover, I estimate the half-life for each autoregressive component which is given by:

$$HL\left(j\right) = \frac{\ln\left(0.5\right)}{\ln\left(\left|\rho_j\right|\right)} \times 2^j. \tag{2B.3}$$

The presence of the factor 2^j is justified on the basis that the decimated component at time-scale j is defined on the grid $\left\{k \times 2^j : \ k\in \mathbb{Z}\right\}$. The estimated half-life for $j = 1$ is close to the lower bound of the corresponding interval $[2^{j-1}, 2^j)$ while for $j = 5$ lies in the middle.

In line with the novel work of Bandi et al. (2016) (see also section 1.5) these results imply a generalized Wold-type representation for the macroeconomic uncertainty series in which low-frequency macro shocks are not linear combinations of high frequency macro shocks. That is, the uncertainty shocks at each scale carry unique information.

Percentage contribution of $u_t^{(j)}$ and $IPVOL_t^{(j)}$ to total variance

Panel A of Table 2B.18 shows the percentage contribution of each individual component to the total variance of the time-series for aggregate uncertainty. Approximate confidence intervals for the variance of the components are computed based on the Chi-squared distribution with one degree of freedom (see also Percival, 1995). Note that by definition $\text{Var}\left(u_t\right) = \sum_{j=1}^{J} \text{Var}\left(u_t^{(j)}\right) + \text{Var}\left(u_t^{(>J)}\right)$. The first seven persistent components filtered out of the uncertainty index account for 74.91% of the total variance of the series. Fluctuations in uncertainty with persistence ranging between 1 and 2

months (i.e., high-frequency) account only for 0.65% of the total variance with a lower and an upper confidence bounds of 0.56% and 0.77% respectively. Low-frequency fluctuations with persistence between 32 and 64 months explain 22.89% of the total variance with a lower and an upper confidence bounds of 14.51% and 41.42% respectively. Similarly, shocks with persistence between 64 and 128 months explain 18.73% of the total variation in the series with a lower and an upper confidence bounds of 9.55% and 52.02% respectively. Figure 2B.1 depicts the scale-specific contribution of each component to the variance of the uncertainty series along with a comparison of the different methods for constructing confidence intervals.

Panel B of Table 2B.18 presents the percentage contribution of each individual component to the total variance for the volatility of industrial production. Shocks with persistence greater than 32 months (i.e., $IPVOL_t^{(>5)}$) account only for 10.45% of the total variance of the series.

Beta comparison: $\boldsymbol{\beta^{(6:7)}}$ versus $\boldsymbol{\beta^{(6)}\varpi^{(6)} + \beta^{(7)}\varpi^{(7)}}$

In Equation (2.11) $\beta^{(6:7)}$ can be viewed as a linear combination of $\beta^{(6)}$ and $\beta^{(7)}$ with weights depending on the relative contribution of the corresponding factor to total variance. The extracted components are only *nearly-uncorrelated* across scales (i.e., $Cov\left(\Delta u_t^{(6)}, \Delta u_t^{(7)}\right) \simeq 0$) and therefore this relation is not exact. In Figure 2B.2 I illustrate the difference by plotting $\beta^{(6:7)}$ versus $\beta^{(6)}\varpi^{(6)} + \beta^{(7)}\varpi^{(7)}$ for the size and book-to-market portfolios. I estimate $\beta^{(6)}$ and $\beta^{(7)}$ over the same sub-period where $\varpi^{(6)} = 0.8647$ and $\varpi^{(7)} = 1 - \varpi^{(6)}$. Note that Bandi and Tamoni (2016) follow a similar approach to calculate a business-cycle consumption factor, however, they use the decimated components which are uncorrelated across scales.

Transformations on characteristics

Size and book-to-market are not linear across portfolios (i.e., a lot of small firms - all the value in the largest-cap portfolios). For controls I use log of the book-to-market ratio and log size as a fraction of total market value (to remove the trend). Figures 2B.3 and 2B.4 depict the transformations.

Figure 2B.1: Scale-specific contribution to variance

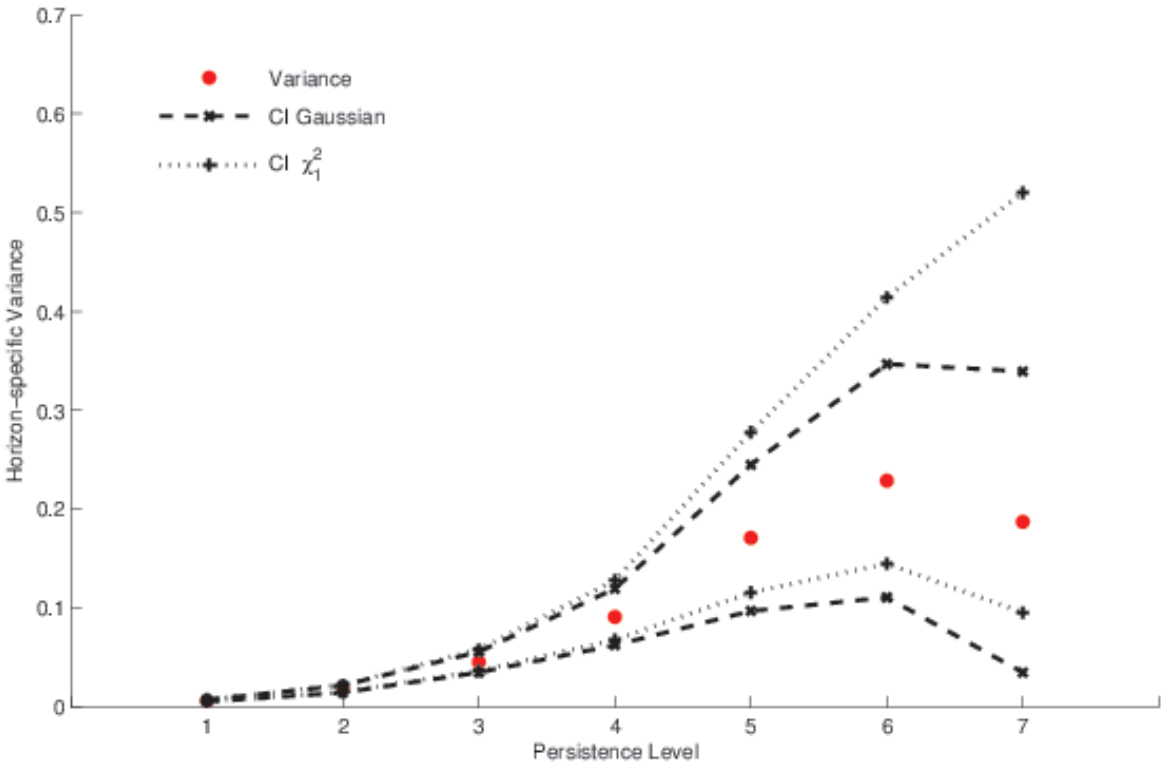

Notes: This figure plots the scale-specific contributions to the time series of aggregate uncertainty (derived from monthly forecasts) along with the relevant confidence bounds.

Figure 2B.2: Beta comparison: $\boldsymbol{\beta^{(6:7)}}$ versus $\boldsymbol{\beta^{(6)}\varpi^{(6)} + \beta^{(7)}\varpi^{(7)}}$

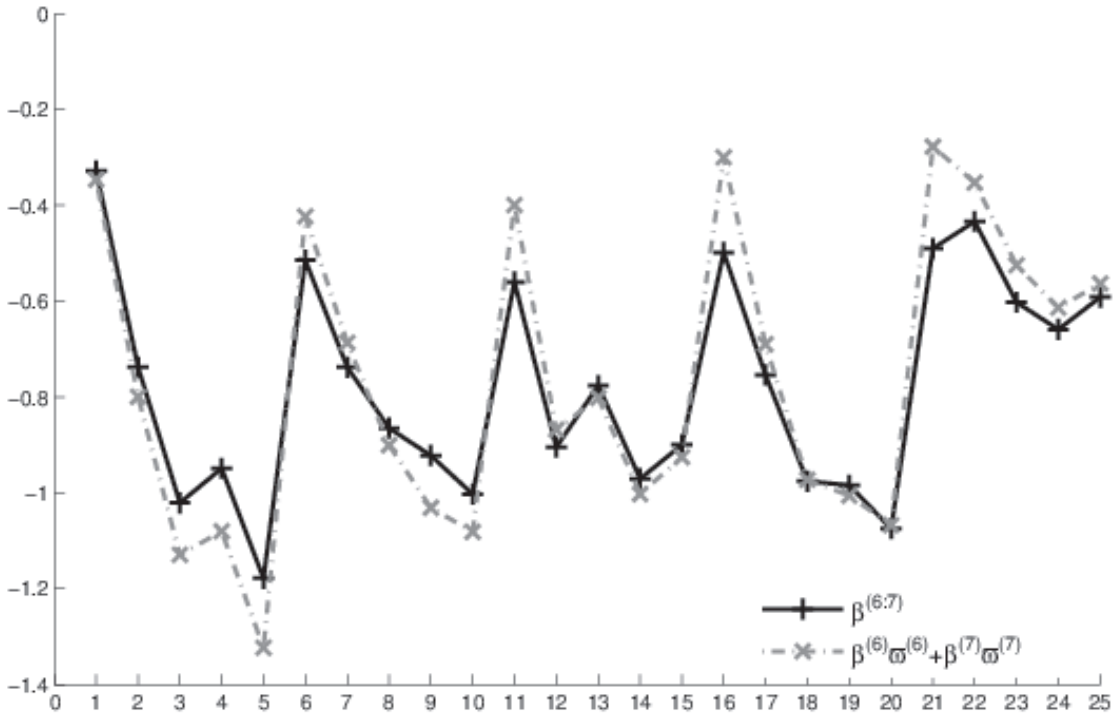

Notes: This figure plots $\beta^{(6:7)}$ versus $\beta^{(6)}\varpi^{(6)} + \beta^{(7)}\varpi^{(7)}$ for the size and book-to-market portfolios. I estimate $\beta^{(6)}$ and $\beta^{(7)}$ over the same sub-period (i.e., I discard the first $2^7 - 1$ observations) where $\varpi^{(6)} = 0.8647$ and $\varpi^{(7)} = 1 - \varpi^{(6)}$.

Figure 2B.3: Transformations on characteristics - logs

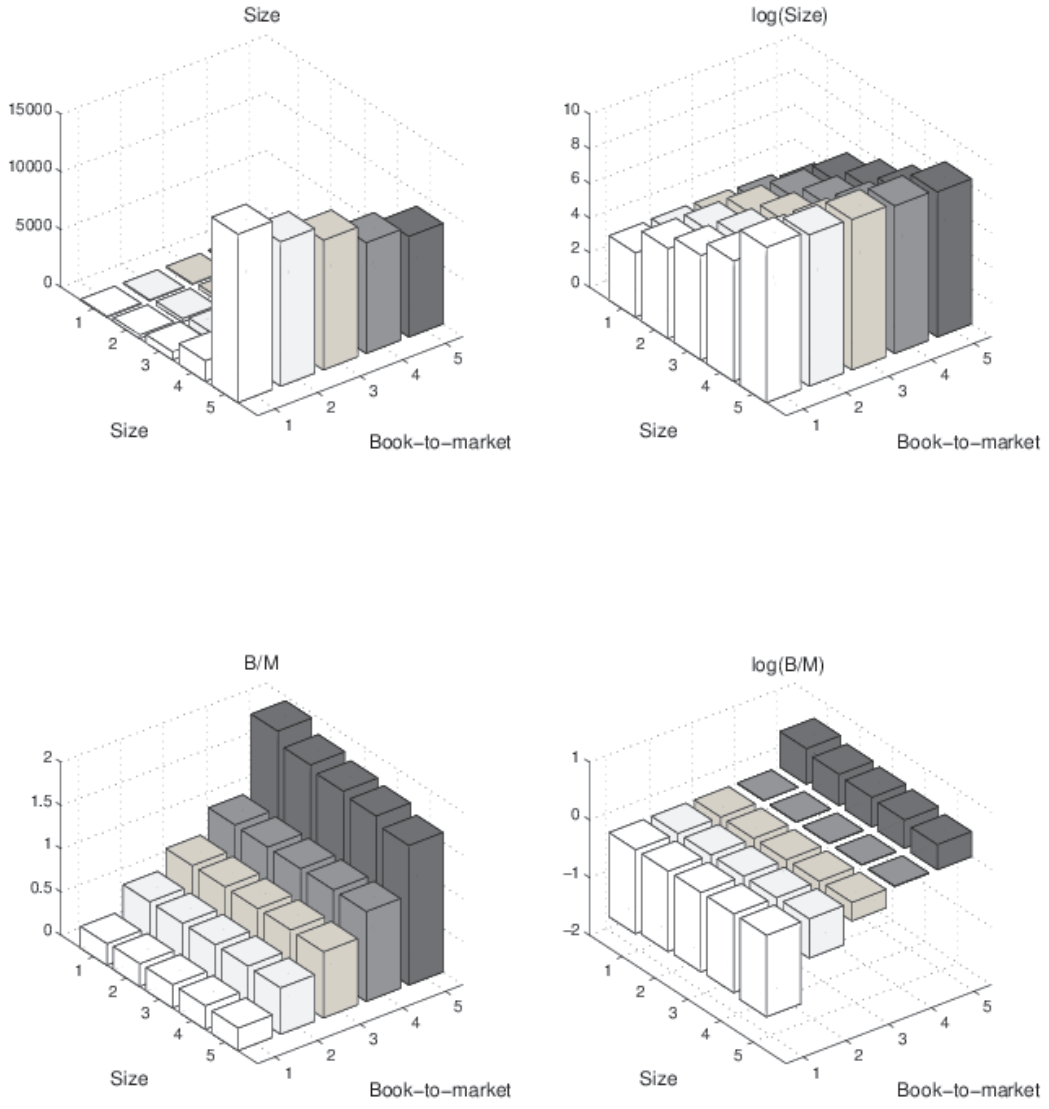

Notes: This figure plots the log transformations on the portfolio characteristics. Note that size and book-to-market are not linear across portfolios (i.e., a lot of small firms - all the value in the largest-cap portfolios).

Figure 2B.4: Transformations on characteristics - logs over time

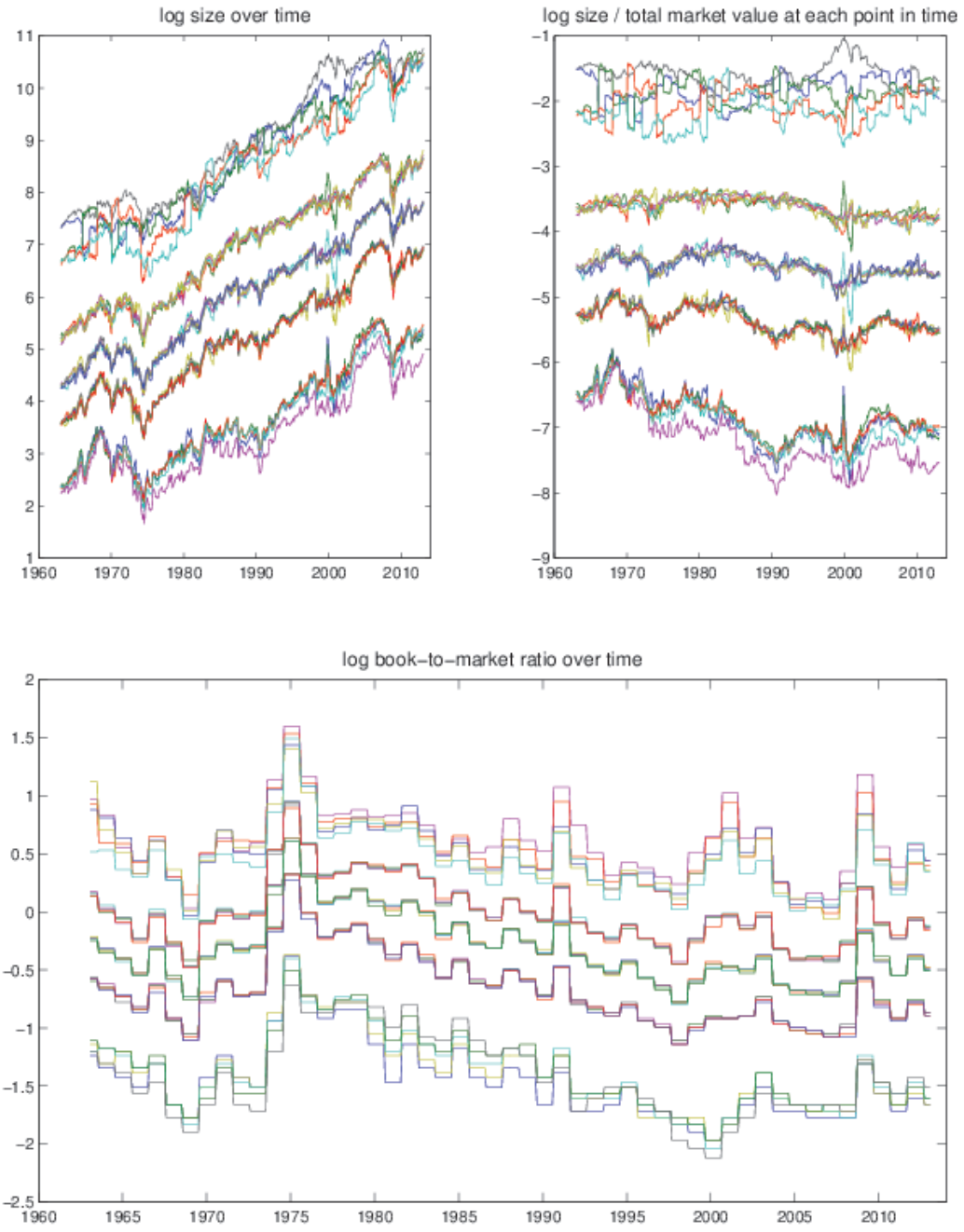

Notes: This figure plots the log transformations on the portfolio characteristics over time. For controls I use log size as a fraction of total market value (to remove the trend).

Table 2B.1: Cross-sectional regression with the same burn-in period: 25 FF size and book-to-market portfolios

	Persistence level							
$j =$	1	2	3	4	5	6	7	6:7
$u_t(1)$								
$\lambda_{0,j}$	0.8872	0.9814	1.0401	0.5502	0.3493	0.2078	0.5814	0.0581
	(2.8483)	(3.3550)	(4.1622)	(2.4048)	(1.4251)	(0.8401)	(2.3717)	(0.2083)
λ_j	0.3719	0.4399	0.5986	-0.1891	-0.3654	-0.5922	-0.4016	-0.8315
	(0.5038)	(0.8220)	(1.2698)	(-0.6207)	(-1.3914)	(-3.9006)	(-3.2124)	(-4.3264)
price of risk	0.401%	0.623%	0.939%	-0.286%	-0.844%	-2.090%	-2.295%	-2.274%
R^2	2.303%	5.547%	12.586%	1.172%	10.168%	62.416%	75.271%	73.891%
$se(\widehat{R^2})$	0.0846	0.1266	0.1681	0.0431	0.1603	0.2183	0.2375	0.1224
$p\left(R^2=1\right)$	0.0157	0.0186	0.0225	0.0175	0.0212	0.1692	0.2956	0.3139
MAPE	2.029%	2.077%	2.025%	1.949%	1.752%	1.091%	1.156%	1.114%
$u_t(3)$								
$\lambda_{0,j}$	0.8213	0.9419	1.0123	0.5725	0.3148	0.2364	0.5836	0.1109
	(2.9482)	(3.1862)	(3.8181)	(2.1542)	(1.2817)	(0.9652)	(2.4041)	(0.4097)
λ_j	0.1154	0.2264	0.4008	-0.1399	-0.4083	-0.6232	-0.4259	-0.8476
	(0.3574)	(0.6799)	(1.0331)	(-0.4201)	(-1.5297)	(-3.9064)	(-3.3841)	(-4.3044)
price of risk	0.287%	0.532%	0.801%	-0.233%	-0.950%	-2.107%	-2.340%	-2.285%
R^2	1.175%	4.037%	9.167%	0.776%	12.888%	63.443%	78.251%	74.617%
$se(\widehat{R^2})$	0.0656	0.1123	0.1586	0.0402	0.1832	0.2211	0.2066	0.1311
$p\left(R^2=1\right)$	0.0164	0.0179	0.0220	0.0167	0.0226	0.1765	0.3255	0.3229
MAPE	2.059%	2.063%	2.052%	1.965%	1.717%	1.079%	1.075%	1.079%
$u_t(12)$								
$\lambda_{0,j}$	0.7899	0.9717	1.0263	0.4595	0.2511	0.3083	0.6407	0.2278
	(3.2865)	(3.5045)	(3.8459)	(1.6573)	(1.0452)	(1.2606)	(2.6882)	(0.8350)
λ_j	0.0597	0.1283	0.1854	-0.1238	-0.2727	-0.3784	-0.2284	-0.4856
	(0.3289)	(0.8453)	(1.0747)	(-0.7572)	(-1.9470)	(-3.9801)	(-2.9019)	(-4.0302)
price of risk	0.221%	0.679%	0.835%	-0.457%	-1.223%	-2.174%	-2.182%	-2.336%
R^2	0.696%	6.587%	9.958%	2.986%	21.366%	67.543%	68.037%	77.922%
$se(\widehat{R^2})$	0.0425	0.1435	0.1654	0.0850	0.2285	0.2049	0.2665	0.1147
$p\left(R^2=1\right)$	0.0045	0.0196	0.0224	0.0168	0.0296	0.2109	0.1920	0.3653
MAPE	2.057%	2.058%	2.031%	1.880%	1.602%	1.039%	1.315%	1.029%
# observ.	507							

Notes: This table reports the estimates for the zero-beta excess return ($\lambda_{0,j}$) and the price of risk (λ_j) for each scale j along with the corresponding Fama-MacBeth (1973) test statistics in parentheses. In addition, I normalize the scale-wise risk exposures and estimate the price of risk per unit of cross-sectional standard deviation in exposure in percent per year. I also report the sample R^2 for each cross-sectional regression and its standard error, the p-value for the Kan et al. (2013) test of $H_0: R^2 = 1$ and the mean absolute pricing error (MAPE) across all securities expressed in percent per year.

Table 2B.2: Cross-sectional regression with the same burn-in period: 25 FF size and investment portfolios

	Persistence level							
$j =$	1	2	3	4	5	6	7	6:7
$u_t(1)$								
$\lambda_{0,j}$	0.9391	0.9872	1.1510	0.6117	0.2569	0.3080	0.7261	0.1923
	(4.5809)	(4.9284)	(6.3034)	(2.2124)	(0.9453)	(1.2341)	(2.9121)	(0.6872)
λ_j	0.2204	0.2402	0.6047	-0.2596	-0.6163	-0.6327	-0.4063	-0.8591
	(0.5611)	(0.7201)	(1.8107)	(-0.5637)	(-1.9119)	(-3.5367)	(-3.8261)	(-4.6799)
price of risk	0.353%	0.471%	1.037%	-0.344%	-1.227%	-2.139%	-1.927%	-2.212%
R^2	1.862%	3.312%	16.054%	1.763%	22.461%	68.268%	55.409%	73.006%
$se(\widehat{R^2})$	0.0714	0.0903	0.1607	0.0627	0.2058	0.1968	0.2299	0.0922
$p\left(R^2=1\right)$	0.0123	0.0108	0.0256	0.0079	0.0094	0.1465	0.0833	0.2508
MAPE	2.132%	2.108%	1.927%	2.088%	1.760%	0.835%	1.364%	0.985%
$u_t(3)$								
$\lambda_{0,j}$	0.7808	0.9588	1.0764	0.5910	0.2313	0.3454	0.7391	0.2531
	(3.0598)	(4.2776)	(5.7037)	(1.9993)	(0.8556)	(1.4005)	(3.0064)	(0.9309)
λ_j	-0.0250	0.1290	0.3366	-0.2447	-0.6571	-0.6545	-0.4400	-0.8672
	(-0.0857)	(0.5183)	(1.1657)	(-0.5785)	(-2.0648)	(-3.5701)	(-4.1403)	(-4.6254)
price of risk	-0.066%	0.357%	0.726%	-0.383%	-1.360%	-2.153%	-2.028%	-2.227%
R^2	0.066%	1.902%	7.868%	2.190%	27.604%	69.186%	61.365%	74.027%
$se(\widehat{R^2})$	0.0146	0.0720	0.1294	0.0746	0.2236	0.1942	0.2099	0.0934
$p\left(R^2=1\right)$	0.0114	0.0107	0.0220	0.0081	0.0104	0.1566	0.1119	0.2645
MAPE	2.151%	2.132%	2.061%	2.077%	1.668%	0.817%	1.256%	0.963%
$u_t(12)$								
$\lambda_{0,j}$	0.9459	0.9549	1.0526	0.3977	0.2035	0.4250	0.8018	0.4021
	(4.5562)	(4.4838)	(5.5522)	(1.3158)	(0.7773)	(1.7359)	(3.3523)	(1.4791)
λ_j	0.0810	0.0587	0.1352	-0.2208	-0.3997	-0.3929	-0.2238	-0.4750
	(0.5789)	(0.5494)	(1.0451)	(-1.1216)	(-2.5562)	(-3.7941)	(-3.2885)	(-4.5760)
price of risk	0.390%	0.391%	0.647%	-0.782%	-1.679%	-2.205%	-1.771%	-2.166%
R^2	2.270%	2.283%	6.248%	9.129%	42.082%	72.563%	46.790%	70.012%
$se(\widehat{R^2})$	0.0844	0.0825	0.1144	0.1505	0.2409	0.1742	0.2467	0.1424
$p\left(R^2=1\right)$	0.0116	0.0162	0.0225	0.0053	0.0176	0.2061	0.0715	0.2089
MAPE	2.126%	2.131%	2.088%	1.925%	1.401%	0.792%	1.459%	1.078%
# observ.	472							

Notes: This table reports the estimates for the zero-beta excess return ($\lambda_{0,j}$) and the price of risk (λ_j) for each scale j along with the corresponding Fama-MacBeth (1973) test statistics in parentheses. In addition, I normalize the scale-wise risk exposures and estimate the price of risk per unit of cross-sectional standard deviation in exposure in percent per year. I also report the sample R^2 for each cross-sectional regression and its standard error, the p-value for the Kan et al. (2013) test of $H_0: R^2 = 1$ and the mean absolute pricing error (MAPE) across all securities expressed in percent per year.

Table 2B.3: Cross-sectional regression with the same burn-in period: 25 FF book-to-market and operating profitability portfolios

	Persistence level							
$j =$	1	2	3	4	5	6	7	6:7
$u_t(1)$								
$\lambda_{0,j}$	0.8186	1.2477	0.8519	0.1140	0.2877	0.3041	0.6235	0.2989
	(3.3733)	(4.2837)	(3.9400)	(0.4268)	(1.2030)	(1.2003)	(2.7259)	(1.1748)
λ_j	0.2089	0.8050	0.2607	-0.7548	-0.5021	-0.5992	-0.4767	-0.6375
	(0.5940)	(1.8648)	(0.7979)	(-2.8855)	(-2.4681)	(-3.4823)	(-3.3816)	(-3.3535)
price of risk	0.267%	1.193%	0.486%	-1.584%	-1.426%	-2.638%	-2.806%	-2.322%
R^2	0.521%	10.370%	1.718%	18.290%	14.831%	50.719%	57.417%	39.300%
$se(\widehat{R^2})$	0.0177	0.0924	0.0431	0.0607	0.1043	0.1454	0.1781	0.1418
$p\left(R^2=1\right)$	0.0109	0.0059	0.0083	0.0146	0.0160	0.0252	0.0193	0.0151
MAPE	2.769%	2.734%	2.766%	2.598%	2.655%	2.068%	1.778%	2.231%
$u_t(3)$								
$\lambda_{0,j}$	1.1732	1.2312	0.8545	0.1514	0.2802	0.3314	0.6530	0.3255
	(4.7428)	(4.0781)	(3.9143)	(0.5900)	(1.1628)	(1.3229)	(2.8758)	(1.2899)
λ_j	0.4962	0.4942	0.1928	-0.6164	-0.5248	-0.6341	-0.4846	-0.6781
	(2.1715)	(1.5993)	(0.6912)	(-2.5972)	(-2.5241)	(-3.4662)	(-3.3262)	(-3.3478)
price of risk	1.402%	1.158%	0.452%	-1.397%	-1.492%	-2.647%	-2.788%	-2.376%
R^2	14.329%	9.775%	1.487%	14.221%	16.238%	51.061%	56.667%	41.156%
$se(\widehat{R^2})$	0.1086	0.1116	0.0436	0.0661	0.1091	0.1477	0.1823	0.1465
$p\left(R^2=1\right)$	0.0068	0.0065	0.0085	0.0150	0.0153	0.0226	0.0169	0.0137
MAPE	2.469%	2.675%	2.753%	2.628%	2.598%	2.062%	1.835%	2.190%
$u_t(12)$								
$\lambda_{0,j}$	0.8234	1.1336	0.9077	0.1657	0.2497	0.4047	0.6946	0.3887
	(3.4519)	(4.2409)	(4.1396)	(0.6456)	(0.9956)	(1.6534)	(3.0863)	(1.5558)
λ_j	0.0736	0.1906	0.1156	-0.2907	-0.3349	-0.3806	-0.2926	-0.4199
	(0.5681)	(1.5413)	(0.9401)	(-2.6401)	(-2.8365)	(-3.4100)	(-3.1887)	(-3.3174)
price of risk	0.317%	1.119%	0.636%	-1.462%	-1.779%	-2.662%	-2.735%	-2.499%
R^2	0.733%	9.132%	2.953%	15.590%	23.064%	51.640%	54.525%	45.510%
$se(\widehat{R^2})$	0.0275	0.1087	0.0627	0.0786	0.1244	0.1522	0.1882	0.1547
$p\left(R^2=1\right)$	0.0097	0.0061	0.0079	0.0149	0.0145	0.0184	0.0103	0.0110
MAPE	2.783%	2.682%	2.702%	2.626%	2.469%	2.050%	1.915%	2.083%
# observ.	472							

Notes: This table reports the estimates for the zero-beta excess return ($\lambda_{0,j}$) and the price of risk (λ_j) for each scale j along with the corresponding Fama-MacBeth (1973) test statistics in parentheses. In addition, I normalize the scale-wise risk exposures and estimate the price of risk per unit of cross-sectional standard deviation in exposure in percent per year. I also report the sample R^2 for each cross-sectional regression and its standard error, the p-value for the Kan et al. (2013) test of $H_0: R^2 = 1$ and the mean absolute pricing error (MAPE) across all securities expressed in percent per year.

Table 2B.4: Cross-sectional regression with the same burn-in period: 25 FF size and variance portfolios

	Persistence level							
$j =$	1	2	3	4	5	6	7	6:7
$u_t\,(1)$								
$\lambda_{0,j}$	0.9154	0.9365	0.9270	0.8118	0.9052	0.2634	0.7476	-0.1131
	(3.6746)	(4.6809)	(5.0342)	(3.8169)	(4.2425)	(1.0479)	(2.9177)	(-0.3569)
λ_j	0.2279	0.2043	0.2387	0.0327	0.1234	-0.6392	-0.3932	-1.2460
	(0.3501)	(0.4984)	(0.5191)	(0.0938)	(0.4158)	(-3.5242)	(-1.9058)	(-5.3519)
price of risk	0.365%	0.553%	0.565%	0.104%	0.484%	-2.249%	-2.054%	-2.908%
R^2	0.862%	1.987%	2.073%	0.070%	1.520%	32.819%	27.355%	54.840%
$se(\widehat{\mathrm{R}^2})$	0.0482	0.0706	0.0700	0.0150	0.0721	0.2250	0.1976	0.1644
$p\left(\mathrm{R}^2=1\right)$	0.0051	0.0033	0.0038	0.0036	0.0032	0.0265	0.0004	0.0721
MAPE	3.085%	3.051%	3.050%	3.049%	3.066%	2.070%	2.595%	1.827%
$u_t\,(3)$								
$\lambda_{0,j}$	0.8213	0.8958	0.9153	0.8214	0.8640	0.2947	0.7602	-0.0194
	(3.5579)	(4.4027)	(4.8013)	(3.8130)	(4.0972)	(1.1756)	(3.0352)	(-0.0624)
λ_j	0.0360	0.0949	0.1572	0.0375	0.0834	-0.6735	-0.4439	-1.2545
	(0.1072)	(0.3554)	(0.4577)	(0.1228)	(0.2796)	(-3.5781)	(-2.0740)	(-5.1685)
price of risk	0.117%	0.393%	0.512%	0.138%	0.321%	-2.278%	-2.186%	-2.918%
R^2	0.089%	1.003%	1.702%	0.123%	0.670%	33.656%	30.986%	55.231%
$se(\widehat{\mathrm{R}^2})$	0.0161	0.0507	0.0666	0.0202	0.0484	0.2260	0.1940	0.1699
$p\left(\mathrm{R}^2=1\right)$	0.0050	0.0045	0.0043	0.0040	0.0032	0.0271	0.0022	0.0711
MAPE	3.051%	3.058%	3.058%	3.054%	3.068%	2.054%	2.468%	1.832%
$u_t\,(12)$								
$\lambda_{0,j}$	0.7329	0.8848	0.9180	0.7619	0.7181	0.3502	0.8178	0.1788
	(4.2543)	(4.5921)	(4.7806)	(3.5566)	(3.4867)	(1.3298)	(3.5698)	(0.5214)
λ_j	-0.0279	0.0405	0.0711	-0.0099	-0.0390	-0.4407	-0.2151	-0.7293
	(-0.1798)	(0.3420)	(0.4655)	(-0.0693)	(-0.2384)	(-3.9382)	(-1.7500)	(-4.0420)
price of risk	-0.172%	0.380%	0.521%	-0.076%	-0.254%	-2.460%	-1.987%	-3.067%
R^2	0.193%	0.935%	1.763%	0.038%	0.419%	39.255%	25.623%	61.006%
$se(\widehat{\mathrm{R}^2})$	0.0218	0.0493	0.0678	0.0114	0.0379	0.2201	0.2107	0.1278
$p\left(\mathrm{R}^2=1\right)$	0.0064	0.0045	0.0043	0.0039	0.0038	0.0314	0.0004	0.0694
MAPE	2.994%	3.062%	3.061%	3.017%	2.978%	1.980%	2.654%	1.775%
# observ.	472							

Notes: This table reports the estimates for the zero-beta excess return ($\lambda_{0,j}$) and the price of risk (λ_j) for each scale j along with the corresponding Fama-MacBeth (1973) test statistics in parentheses. In addition, I normalize the scale-wise risk exposures and estimate the price of risk per unit of cross-sectional standard deviation in exposure in percent per year. I also report the sample R^2 for each cross-sectional regression and its standard error, the p-value for the Kan et al. (2013) test of $H_0: R^2 = 1$ and the mean absolute pricing error (MAPE) across all securities expressed in percent per year.

Table 2B.5: Cross-sectional regressions for $\Delta u_t^{(>7)}$

Panel A	25 FF size and book-to-market							
	$\lambda_{0,>7}$		$\lambda_{>7}$		R^2	$p\left(R^2=1\right)$	MAPE	# observ.
$h=1$	0.7020	(2.4547)	-0.0024	(-0.0247)	0.004%	0.0161	2.045%	
$h=3$	0.6924	(2.4338)	-0.0134	(-0.1271)	0.093%	0.0167	2.062%	507
$h=12$	0.6929	(2.5010)	-0.0084	(-0.1394)	0.113%	0.0166	2.065%	
Panel B	25 FF size and investment							
	$\lambda_{0,>7}$		$\lambda_{>7}$		R^2	$p\left(R^2=1\right)$	MAPE	# observ.
$h=1$	0.8998	(3.2180)	0.1006	(1.2163)	10.069%	0.0038	1.924%	
$h=3$	0.8926	(3.2023)	0.1019	(1.1443)	8.796%	0.0037	1.953%	472
$h=12$	0.8840	(3.1762)	0.0591	(1.0594)	8.341%	0.0033	1.966%	
Panel C	25 FF book-to-market and operating profitability							
	$\lambda_{0,>7}$		$\lambda_{>7}$		R^2	$p\left(R^2=1\right)$	MAPE	# observ.
$h=1$	0.4956	(2.1311)	-0.1931	(-3.6946)	21.244%	0.0115	2.771%	
$h=3$	0.4930	(2.1200)	-0.2159	(-3.7853)	22.855%	0.0123	2.755%	472
$h=12$	0.5106	(2.2299)	-0.1226	(-3.8924)	19.293%	0.0144	2.877%	
Panel D	25 FF size and variance							
	$\lambda_{0,>7}$		$\lambda_{>7}$		R^2	$p\left(R^2=1\right)$	MAPE	# observ.
$h=1$	0.6619	(2.2730)	-0.1396	(-1.7127)	19.577%	0.0076	3.002%	
$h=3$	0.6609	(2.2712)	-0.1540	(-1.7347)	20.171%	0.0077	2.997%	472
$h=12$	0.6833	(2.3682)	-0.0802	(-1.4883)	14.338%	0.0062	3.093%	

Notes: This table reports the estimates for the zero-beta excess return ($\lambda_{0,>7}$) and the price of risk ($\lambda_{>7}$) for low-frequency uncertainty shocks with persistence greater than $2^7 = 128$ months (i.e., the priced factor is $\Delta u_t^{(>7)}$) along with the corresponding Fama-MacBeth (1973) test statistics in parentheses. In addition, I report the sample R^2 for each cross-sectional regression, the p-value for the Kan et al. (2013) test of $H_0: R^2 = 1$ denoted as $p\left(R^2=1\right)$ and the mean absolute pricing error (MAPE) across all securities expressed in percent per year. The test assets include: the 25 FF size and book-to-market portfolios (Panel A), the 25 FF size and investment portfolios (Panel B), the 25 FF book-to-market and operating profitability portfolios (Panel C) and the 25 FF size and variance portfolios (Panel D).

Table 2B.6: Cross-sectional regressions for $\Delta u_t^{(8)}$

Panel A	25 FF size and book-to-market							
	$\lambda_{0,8}$		λ_8		R^2	$se(\widehat{R^2})$	MAPE	# observ.
$h=1$	0.7397	(2.5555)	-0.0618	(-0.6243)	2.627%	0.0847	2.066%	
$h=3$	0.7353	(2.5534)	-0.0768	(-0.7041)	3.349%	0.0945	2.072%	379
$h=12$	0.7475	(2.6676)	-0.0452	(-0.6743)	3.229%	0.0947	2.073%	
Panel B	25 FF size and investment							
	$\lambda_{0,8}$		λ_8		R^2	$se(\widehat{R^2})$	MAPE	# observ.
$h=1$	0.7967	(2.7041)	0.0052	(0.0639)	0.052%	0.0169	1.738%	
$h=3$	0.7947	(2.7136)	0.0023	(0.0266)	0.009%	0.0069	1.744%	344
$h=12$	0.7930	(2.7643)	-0.0007	(-0.0120)	0.002%	0.0032	1.750%	
Panel C	25 FF book-to-market and operating profitability							
	$\lambda_{0,8}$		λ_8		R^2	$se(\widehat{R^2})$	MAPE	# observ.
$h=1$	0.6304	(2.3098)	-0.1498	(-2.3513)	16.211%	0.1149	2.110%	
$h=3$	0.6333	(2.3181)	-0.1692	(-2.3330)	17.401%	0.1215	2.088%	344
$h=12$	0.6565	(2.4148)	-0.1025	(-2.2238)	14.739%	0.1116	2.136%	
Panel D	25 FF size and variance							
	$\lambda_{0,8}$		λ_8		R^2	$se(\widehat{R^2})$	MAPE	# observ.
$h=1$	0.7003	(2.3065)	-0.1446	(-1.6947)	41.160%	0.3077	2.120%	
$h=3$	0.7048	(2.3359)	-0.1591	(-1.7022)	42.254%	0.3104	2.102%	344
$h=12$	0.7299	(2.4950)	-0.0945	(-1.6421)	39.579%	0.3084	2.145%	

Notes: This table reports the estimates for the zero-beta excess return ($\lambda_{0,8}$) and the price of risk (λ_8) for low-frequency uncertainty shocks with persistence ranging between 128 and 256 months (i.e., the priced factor is $\Delta u_t^{(8)}$) along with the corresponding Fama-MacBeth (1973) test statistics in parentheses. In addition, I report the sample R^2 for each cross-sectional regression, its standard error and the mean absolute pricing error (MAPE) across all securities expressed in percent per year. The test assets include: the 25 FF size and book-to-market portfolios (Panel A), the 25 FF size and investment portfolios (Panel B), the 25 FF book-to-market and operating profitability portfolios (Panel C) and the 25 FF size and variance portfolios (Panel D).

Table 2B.7: $\Delta u_t^{(>7)}$ and $\Delta u_t^{(8)}$: Confidence intervals for R^2

	$h=1$		$h=3$		$h=12$	
	$\Delta u_t^{(>7)}$	$\Delta u_t^{(8)}$	$\Delta u_t^{(>7)}$	$\Delta u_t^{(8)}$	$\Delta u_t^{(>7)}$	$\Delta u_t^{(8)}$
Panel A						
R^2	0.004%	2.627%	0.093%	3.349%	0.113%	3.229%
$se(\widehat{R^2})$	0.0031	0.0847	0.0157	0.0945	0.0173	0.0947
2.5% CI (R^2)	0.0000	0.0000	0.0000	0.0000	0.0000	0.0000
97.5% CI (R^2)	0.0238	0.2065	0.0449	0.2308	0.0473	0.2214
Panel B						
R^2	10.069%	0.052%	8.796%	0.009%	8.341%	0.002%
$se(\widehat{R^2})$	0.1513	0.0169	0.1417	0.0069	0.1458	0.0032
2.5% CI (R^2)	0.0000	0.0000	0.0000	0.0000	0.0000	0.0000
97.5% CI (R^2)	0.3997	0.0405	0.3748	0.0230	0.3906	0.0259
Panel C						
R^2	21.244%	16.211%	22.855%	17.401%	19.293%	14.739%
$se(\widehat{R^2})$	0.0845	0.1149	0.0840	0.1215	0.0815	0.1116
2.5% CI (R^2)	0.0496	0.0000	0.0763	0.0000	0.0378	0.0000
97.5% CI (R^2)	0.3935	0.3987	0.4013	0.4121	0.3567	0.3863
Panel D						
R^2	19.577%	41.160%	20.171%	42.254%	14.338%	39.579%
$se(\widehat{R^2})$	0.2069	0.3077	0.2093	0.3104	0.1826	0.3084
2.5% CI (R^2)	0.0000	0.0000	0.0000	0.0000	0.0000	0.0000
97.5% CI (R^2)	0.6080	1.0000	0.6640	1.0000	0.5488	1.0000

Notes: This table reports the sample cross-sectional R^2, its standard error and its 95% confidence interval for low-frequency uncertainty shocks with persistence greater than $2^7 = 128$ months (i.e., the priced factor is $\Delta u_t^{(>7)}$) and for low-frequency uncertainty shocks with persistence ranging between 128 and 256 months (i.e., the priced factor is $\Delta u_t^{(8)}$). I calculate the confidence interval for the sample R^2 by pivoting the cdf. The test assets include: the 25 FF size and book-to-market portfolios (Panel A), the 25 FF size and investment portfolios (Panel B), the 25 FF book-to-market and operating profitability portfolios (Panel C) and the 25 FF size and variance portfolios (Panel D).

Table 2B.8: Cross-sectional regressions for $\Delta IPVOL_t^{(>5)}$

Panel A	25 FF size and book-to-market							
Innovations from:	λ_0		$\lambda_{\Delta IPVOL_t^{(>5)}}$		R^2	$se(\widehat{R^2})$	$p\left(R^2=1\right)$	MAPE
First-Differences	0.0989	(0.3886)	-0.0281	(-2.1067)	20.022%	0.2039	0.0114	1.782%
	95% Confidence Interval for R^2:				[0.0000, 0.6240]			
Residuals - AR(1)	0.0262	(0.1022)	-0.0302	(-2.3703)	20.165%	0.1812	0.0129	1.837%
	95% Confidence Interval for R^2:				[0.0000, 0.5975]			
Panel B	25 FF size and investment							
Innovations from:	λ_0		$\lambda_{\Delta IPVOL_t^{(>5)}}$		R^2	$se(\widehat{R^2})$	$p\left(R^2=1\right)$	MAPE
First-Differences	0.1757	(0.6162)	-0.0207	(-1.4589)	15.591%	0.2071	0.0004	1.761%
	95% Confidence Interval for R^2:				[0.0000, 0.5743]			
Residuals - AR(1)	0.1306	(0.4391)	-0.0218	(-1.5254)	15.104%	0.1932	0.0004	1.766%
	95% Confidence Interval for R^2:				[0.0000, 0.5267]			
Panel C	25 FF book-to-market and operating profitability							
Innovations from:	λ_0		$\lambda_{\Delta IPVOL_t^{(>5)}}$		R^2	$se(\widehat{R^2})$	$p\left(R^2=1\right)$	MAPE
First-Differences	0.2435	(1.1145)	-0.0150	(-1.8551)	9.399%	0.1077	0.0160	2.393%
	95% Confidence Interval for R^2:				[0.0000, 0.3134]			
Residuals - AR(1)	0.2522	(1.1398)	-0.0139	(-1.7847)	8.268%	0.1008	0.0152	2.425%
	95% Confidence Interval for R^2:				[0.0000, 0.2954]			
Panel D	25 FF size and variance							
Innovations from:	λ_0		$\lambda_{\Delta IPVOL_t^{(>5)}}$		R^2	$se(\widehat{R^2})$	$p\left(R^2=1\right)$	MAPE
First-Differences	0.7049	(3.0789)	0.0019	(0.1511)	0.161%	0.0210	0.0019	2.986%
	95% Confidence Interval for R^2:				[0.0000, 0.0533]			
Residuals - AR(1)	0.7364	(2.9672)	0.0031	(0.2282)	0.363%	0.0338	0.0018	2.987%
	95% Confidence Interval for R^2:				[0.0000, 0.0750]			

Notes: This table reports the estimates for the zero-beta excess return (λ_0) and the price of risk $\left(\lambda_{\Delta IPVOL_t^{(>5)}}\right)$ for the innovations in macro volatility shocks with persistence greater than 32 months (i.e., the priced factor is $\Delta IPVOL_t^{(>5)}$ - see Boons and Tamoni, 2016) along with the corresponding Fama-MacBeth (1973) test statistics in parentheses. In addition, I report the sample R^2 for each cross-sectional regression, its standard error, the p-value for the Kan et al. (2013) test of $H_0: R^2 = 1$ denoted as $p\left(R^2=1\right)$ and the mean absolute pricing error (MAPE) across all securities expressed in percent per year. The test assets include: the 25 FF size and book-to-market portfolios (Panel A), the 25 FF size and investment portfolios (Panel B), the 25 FF book-to-market and operating profitability portfolios (Panel C) and the 25 FF size and variance portfolios (Panel D).

Table 2B.9: Cross-sectional regression with the same burn-in period: 25 FF size and book-to-market *plus* 5 FF industry portfolios

	Persistence level							
$j =$	1	2	3	4	5	6	7	6:7
$u_t\,(1)$								
$\lambda_{0,j}$	0.6482	0.7162	0.9796	0.4788	0.3493	0.3922	0.7021	0.3296
	(2.5666)	(2.8093)	(4.1880)	(2.0995)	(1.5397)	(1.6921)	(2.9600)	(1.3127)
λ_j	-0.2164	-0.0775	0.3776	-0.3953	-0.4921	-0.4921	-0.3362	-0.6293
	(-0.4406)	(-0.1959)	(0.8865)	(-1.4694)	(-2.1747)	(-3.3567)	(-2.8454)	(-3.7462)
price of risk	-0.339%	-0.151%	0.601%	-0.694%	-1.200%	-1.965%	-1.910%	-1.926%
R^2	1.704%	0.339%	5.359%	7.146%	21.386%	57.387%	54.205%	55.111%
$se(\widehat{\mathrm{R}^2})$	0.0700	0.0308	0.1018	0.1060	0.1682	0.1909	0.2482	0.1372
$p\left(\mathrm{R}^2=1\right)$	0.0270	0.0281	0.0261	0.0213	0.0313	0.1596	0.1543	0.1734
MAPE	2.084%	2.121%	2.150%	1.973%	1.753%	1.322%	1.538%	1.473%
$u_t\,(3)$								
$\lambda_{0,j}$	0.6248	0.7137	0.8959	0.4438	0.3238	0.4143	0.7150	0.3610
	(2.3068)	(2.5563)	(3.5530)	(1.8558)	(1.4082)	(1.7974)	(3.0474)	(1.4586)
λ_j	-0.1413	-0.0513	0.1604	-0.3776	-0.5307	-0.5197	-0.3582	-0.6568
	(-0.4820)	(-0.1813)	(0.4486)	(-1.3429)	(-2.2648)	(-3.3699)	(-2.9894)	(-3.7292)
price of risk	-0.391%	-0.144%	0.333%	-0.728%	-1.315%	-1.988%	-1.983%	-1.970%
R^2	2.273%	0.308%	1.647%	7.876%	25.709%	58.707%	58.399%	57.682%
$se(\widehat{\mathrm{R}^2})$	0.0859	0.0302	0.0645	0.1233	0.1907	0.1921	0.2323	0.1402
$p\left(\mathrm{R}^2=1\right)$	0.0292	0.0302	0.0319	0.0157	0.0332	0.1690	0.1421	0.1879
MAPE	2.050%	2.125%	2.183%	1.946%	1.688%	1.297%	1.475%	1.431%
$u_t\,(12)$								
$\lambda_{0,j}$	0.6406	0.7509	0.9050	0.3587	0.2903	0.4672	0.7605	0.4553
	(2.6388)	(2.8272)	(3.5765)	(1.4524)	(1.2512)	(2.0195)	(3.2917)	(1.8065)
λ_j	-0.0780	-0.0088	0.0764	-0.2269	-0.3300	-0.3200	-0.1856	-0.3741
	(-0.4964)	(-0.0723)	(0.4799)	(-1.6604)	(-2.6141)	(-3.5016)	(-2.4855)	(-3.5451)
price of risk	-0.365%	-0.060%	0.358%	-0.967%	-1.574%	-2.041%	-1.768%	-1.956%
R^2	1.985%	0.054%	1.904%	13.883%	36.831%	61.861%	46.449%	56.873%
$se(\widehat{\mathrm{R}^2})$	0.0721	0.0133	0.0698	0.1644	0.2122	0.1778	0.2634	0.1683
$p\left(\mathrm{R}^2=1\right)$	0.0307	0.0314	0.0319	0.0192	0.0596	0.2026	0.1175	0.1733
MAPE	2.071%	2.143%	2.180%	1.825%	1.570%	1.272%	1.641%	1.444%
# observ.	507							

Notes: This table reports the estimates for the zero-beta excess return ($\lambda_{0,j}$) and the price of risk (λ_j) for each scale j along with the corresponding Fama-MacBeth (1973) test statistics in parentheses. In addition, I normalize the scale-wise risk exposures and estimate the price of risk per unit of cross-sectional standard deviation in exposure in percent per year. I also report the sample R^2 for each cross-sectional regression and its standard error, the p-value for the Kan et al. (2013) test of $H_0: R^2 = 1$ and the mean absolute pricing error (MAPE) across all securities expressed in percent per year.

Table 2B.10: Controlling for Fama-French factors

	λ_{MKT}	λ_{SMB}	λ_{HML}	λ_{RMW}	λ_{CMA}	$\lambda_{6:7}$	R^2 / MAPE
Panel A							
$h=1$	0.1881	0.1328	0.1693	0.2887	0.0536	-0.5001	85.546%
	(0.8549)	(0.9324)	(1.1591)	(1.5571)	(0.2033)	(-3.8181)	0.964%
$h=3$	0.2141	0.1229	0.1577	0.2904	0.0385	-0.5288	85.668%
	(0.9828)	(0.8560)	(1.0689)	(1.5777)	(0.1443)	(-3.7145)	0.980%
$h=12$	0.2521	0.1311	0.1021	0.2558	0.0081	-0.3484	86.244%
	(1.1774)	(0.9198)	(0.6750)	(1.3930)	(0.0302)	(-3.9708)	0.960%
Panel B							
$h=1$	0.1354	0.2019	-0.6788	0.5167	0.1285	-0.8351	85.287%
	(0.5845)	(1.3718)	(-2.2638)	(2.8650)	(1.1421)	(-5.1764)	0.726%
$h=3$	0.1761	0.1879	-0.7213	0.5301	0.1070	-0.8908	85.448%
	(0.7704)	(1.2683)	(-2.3959)	(2.9311)	(0.9240)	(-5.1083)	0.730%
$h=12$	0.2713	0.2413	-0.7833	0.4967	0.0670	-0.5324	86.016%
	(1.2165)	(1.6391)	(-2.5874)	(2.7704)	(0.5461)	(-4.9612)	0.738%
Panel C							
$h=1$	0.5365	1.2004	0.2846	0.5571	0.1401	0.2086	96.375%
	(2.3269)	(2.9695)	(1.7329)	(3.8878)	(0.6948)	(1.2954)	0.760%
$h=3$	0.5314	1.2170	0.2955	0.5578	0.1552	0.2370	96.437%
	(2.3232)	(2.9869)	(1.7752)	(3.8928)	(0.7597)	(1.3382)	0.753%
$h=12$	0.5064	1.1675	0.3099	0.5570	0.1571	0.1371	96.280%
	(2.2504)	(2.9350)	(1.7964)	(3.8854)	(0.7569)	(1.2358)	0.757%
Panel D							
$h=1$	0.0380	0.0688	-0.6081	1.0639	-0.9212	-0.9560	96.508%
	(0.1689)	(0.4504)	(-2.1305)	(5.7040)	(-3.5735)	(-7.3772)	0.787%
$h=3$	0.0891	0.0428	-0.5974	1.0479	-0.9302	-1.0085	96.548%
	(0.3989)	(0.2791)	(-2.0749)	(5.6347)	(-3.6090)	(-7.1615)	0.859%
$h=12$	0.2095	0.1135	-0.5872	1.0080	-0.9914	-0.5847	95.926%
	(0.9522)	(0.7475)	(-2.0085)	(5.4643)	(-3.8483)	(-6.7793)	0.919%

Notes: This table reports estimates for the price of risk ($\lambda_{6:7}$) for the *business-cycle uncertainty* factor (i.e., $u_t^{(6:7)}$) after controlling for exposure to the Fama-French factors. The control factors include the value-weight excess return on the market portfolio (MKT), the size factor (SMB, small minus big), the value factor (HML, high minus low book-to-market), the operating profitability factor (RMW, robust minus weak profitability) and the investment factor (CMA, conservative minus aggressive investment). The test assets include: the 25 FF size and book-to-market portfolios (Panel A), the 25 FF size and investment portfolios (Panel B), the 25 FF book-to-market and operating profitability portfolios (Panel C) and the 25 FF size and variance portfolios (Panel D).

Table 2B.11a: Controlling for UMD, STR, LTR, LIQ and portfolio characteristics

	λ_{MKT}	λ_{SMB}	λ_{HML}	λ_{MOM}	λ_{STR}	λ_{LTR}	λ_{LIQ}	$\lambda_{\log(ME)}$	$\lambda_{\log(B/M)}$	$\lambda_{6:7}$	R^2 / MAPE
Panel A											
$h=1$	0.8483	0.3581	-0.2704	2.9441	1.6270	0.2982	0.0128	0.1084	0.3373	-0.4853	89.768%
	(2.9070)	(1.1789)	(-1.0475)	(3.6185)	(1.6047)	(0.5937)	(1.7078)	(1.2886)	(2.5390)	(-2.4921)	0.762%
$h=3$	0.8621	0.3239	-0.2925	2.9541	1.6101	0.2738	0.0121	0.1023	0.3405	-0.5160	89.784%
	(2.9594)	(1.0832)	(-1.1295)	(3.6272)	(1.5896)	(0.5423)	(1.6067)	(1.2316)	(2.5679)	(-2.4652)	0.771%
$h=12$	0.8925	0.3263	-0.3818	2.9083	1.5958	0.1569	0.0093	0.1006	0.3529	-0.3553	90.812%
	(3.0708)	(1.0928)	(-1.4472)	(3.6071)	(1.5777)	(0.3058)	(1.2182)	(1.2254)	(2.6807)	(-2.7327)	0.746%
Panel B											
$h=1$	0.6637	-0.0220	-0.2501	2.3845	-1.8157	-0.5628	-0.0177	-0.0057	0.5812	-0.5666	86.993%
	(2.2317)	(-0.0959)	(-0.9503)	(3.8504)	(-2.8734)	(-1.5730)	(-2.5056)	(-0.1026)	(2.4503)	(-3.3156)	0.712%
$h=3$	0.6784	-0.0477	-0.2767	2.4009	-1.8500	-0.5796	-0.0179	-0.0103	0.5755	-0.6028	86.911%
	(2.2943)	(-0.2092)	(-1.0430)	(3.8661)	(-2.9422)	(-1.6173)	(-2.5277)	(-0.1870)	(2.4290)	(-3.2937)	0.707%
$h=12$	0.7006	-0.0397	-0.3381	2.3371	-1.7226	-0.5487	-0.0174	-0.0189	0.5489	-0.3710	86.822%
	(2.3786)	(-0.1733)	(-1.2543)	(3.8016)	(-2.7327)	(-1.5392)	(-2.4621)	(-0.3508)	(2.3012)	(-3.3926)	0.705%

Notes: This table reports estimates for the price of risk ($\lambda_{6:7}$) for the *business-cycle uncertainty* factor (i.e., $u_t^{(6:7)}$) after controlling for exposure to the value-weight excess return on the market portfolio (MKT), the size factor (SMB), the value factor (HML), the momentum factor (MOM), the short-term reversal factor (STR), the long-term reversal factor (LTR), the liquidity factor (LIQ), the log size ($\log(ME)$) and the log book-to-market ratio ($\log(B/M)$). The test assets include: the 25 FF size and book-to-market portfolios (Panel A) and the 25 FF size and investment portfolios (Panel B).

Table 2B.11b: Controlling for UMD, STR, LTR, LIQ and portfolio characteristics

	λ_{MKT}	λ_{SMB}	λ_{HML}	λ_{MOM}	λ_{STR}	λ_{LTR}	λ_{LIQ}	$\lambda_{\log(ME)}$	$\lambda_{\log(B/M)}$	$\lambda_{6:7}$	R^2 / MAPE
Panel C											
$h=1$	1.3886	1.0809	1.2605	0.3707	0.0059	1.2574	-0.0076	0.3267	-0.4150	0.2726	95.786%
	(2.8506)	(2.4337)	(3.8307)	(0.7142)	(0.0100)	(3.2085)	(-0.9084)	(2.6467)	(-2.1069)	(1.5939)	0.674%
$h=3$	1.3774	1.0710	1.2627	0.3671	0.0125	1.2581	-0.0075	0.3248	-0.4083	0.2954	95.812%
	(2.8329)	(2.4167)	(3.8157)	(0.7063)	(0.0211)	(3.2069)	(-0.8967)	(2.6331)	(-2.0891)	(1.5910)	0.669%
$h=12$	1.3663	1.0157	1.2615	0.3750	-0.0215	1.2506	-0.0076	0.3247	-0.3887	0.1837	95.811%
	(2.8148)	(2.3580)	(3.7856)	(0.7227)	(-0.0356)	(3.1986)	(-0.8897)	(2.6286)	(-2.0369)	(1.5605)	0.677%
Panel D											
$h=1$	0.9947	-0.2181	-0.0427	1.8470	-0.5911	-1.0475	-0.0181	-0.0287	1.3366	-0.3887	85.157%
	(2.9774)	(-0.9991)	(-0.1701)	(2.9666)	(-1.1518)	(-2.4757)	(-2.8742)	(-0.7801)	(3.5824)	(-2.5062)	1.065%
$h=3$	1.0001	-0.2458	-0.0568	1.8261	-0.6475	-1.0840	-0.0183	-0.0363	1.3275	-0.3906	85.080%
	(2.9980)	(-1.1289)	(-0.2257)	(2.9343)	(-1.2679)	(-2.5588)	(-2.9136)	(-0.9810)	(3.5509)	(-2.3398)	1.081%
$h=12$	1.0589	-0.2582	-0.0749	1.7541	-0.6898	-1.1317	-0.0189	-0.0430	1.3718	-0.2126	84.865%
	(3.2237)	(-1.1742)	(-0.2973)	(2.8333)	(-1.3557)	(-2.6663)	(-3.0237)	(-1.1441)	(3.7236)	(-2.0777)	1.099%

Notes: This table reports estimates for the price of risk ($\lambda_{6:7}$) for the *business-cycle uncertainty* factor (i.e., $u_t^{(6:7)}$) after controlling for exposure to the value-weight excess return on the market portfolio (MKT), the size factor (SMB), the value factor (HML), the momentum factor (MOM), the short-term reversal factor (STR), the long-term reversal factor (LTR), the liquidity factor (LIQ), the log size ($\log(ME)$) and the log book-to-market ratio ($\log(B/M)$). The test assets include: the 25 FF book-to-market and operating profitability portfolios (Panel C) and the 25 FF size and variance portfolios (Panel D).

Table 2B.12: Robustness check: Residuals from an AR(1) model fitted to $u_t^{(6:7)}$

Panel A	25 FF size and book-to-market									
	$\lambda_{0,6:7}$		$\lambda_{6:7}$		price of risk	R^2	$se(\widehat{R^2})$	$p\left(R^2=1\right)$	MAPE	# observ.
$h=1$	0.0537	(0.1916)	-0.8303	(-4.3160)	-2.272%	73.719%	0.1216	0.3107	1.120%	
$h=3$	0.1063	(0.3910)	-0.8470	(-4.2973)	-2.284%	74.497%	0.1303	0.3206	1.083%	507
$h=12$	0.2248	(0.8214)	-0.4853	(-4.0227)	-2.333%	77.775%	0.1150	0.3617	1.033%	
Panel B	25 FF size and investment									
	$\lambda_{0,6:7}$		$\lambda_{6:7}$		price of risk	R^2	$se(\widehat{R^2})$	$p\left(R^2=1\right)$	MAPE	# observ.
$h=1$	0.1861	(0.6624)	-0.8609	(-4.6863)	-2.208%	72.761%	0.0928	0.2473	0.994%	
$h=3$	0.2471	(0.9059)	-0.8694	(-4.6310)	-2.224%	73.841%	0.0936	0.2616	0.970%	472
$h=12$	0.3987	(1.4633)	-0.4756	(-4.5741)	-2.163%	69.816%	0.1430	0.1861	1.082%	
Panel C	25 FF book-to-market and operating profitability									
	$\lambda_{0,6:7}$		$\lambda_{6:7}$		price of risk	R^2	$se(\widehat{R^2})$	$p\left(R^2=1\right)$	MAPE	# observ.
$h=1$	0.2946	(1.1547)	-0.6366	(-3.3480)	-2.318%	39.183%	0.1418	0.0150	2.228%	
$h=3$	0.3213	(1.2695)	-0.6776	(-3.3437)	-2.374%	41.077%	0.1465	0.0136	2.188%	472
$h=12$	0.3853	(1.5390)	-0.4200	(-3.3149)	-2.497%	45.467%	0.1547	0.0117	2.084%	
Panel D	25 FF size and variance									
	$\lambda_{0,6:7}$		$\lambda_{6:7}$		price of risk	R^2	$se(\widehat{R^2})$	$p\left(R^2=1\right)$	MAPE	# observ.
$h=1$	-0.1248	(-0.3922)	-1.2524	(-5.3665)	-2.901%	54.610%	0.1630	0.0716	1.831%	
$h=3$	-0.0298	(-0.0957)	-1.2602	(-5.1802)	-2.913%	55.036%	0.1690	0.0706	1.837%	472
$h=12$	0.1720	(0.4994)	-0.7319	(-4.0418)	-3.063%	60.852%	0.1273	0.0689	1.780%	

Notes: This table reports the estimates for the zero-beta excess return ($\lambda_{0,6:7}$) and the price of risk ($\lambda_{6:7}$) for the innovations in the *business-cycle uncertainty* factor (i.e. $u_t^{(6:7)}$) along with the corresponding Fama-MacBeth (1973) test statistics in parentheses. The innovations are the residuals from an AR(1) model fitted to the factor. In addition, I report the sample R^2 for each cross-sectional regression, the p-value for the Kan et al. (2013) test of $H_0: R^2=1$ denoted as $p\left(R^2=1\right)$ and the mean absolute pricing error (MAPE) across all securities expressed in percent per year. The test assets include: the 25 FF size and book-to-market portfolios (Panel A), the 25 FF size and investment portfolios (Panel B), the 25 FF book-to-market and operating profitability portfolios (Panel C) and the 25 FF size and variance portfolios (Panel D).

Table 2B.13: Bias-corrected bootstrapped confidence intervals for the first-pass beta estimates

Port.	Panel A		Panel B		Panel C		Panel D	
	$\beta^{(6:7)}$	90% CI	$\beta^{(6:7)}$	90% CI	$\beta^{(6:7)}$	90% CI	$\beta^{(6:7)}$	90% CI
11	-0.3286	[-1.6027, 1.0120]	-0.8675	[-1.9345, 0.1870]	-0.1982	[-1.2600, 1.0387]	**-0.9466**	[-1.5595, -0.3810]
12	-0.7378	[-1.7181, 0.2299]	**-1.0014**	[-1.7329, -0.2513]	-0.3823	[-1.4446, 0.7233]	**-1.0397**	[-1.8286, -0.1915]
13	**-1.0207**	[-1.8518, -0.2291]	**-0.8248**	[-1.6247, -0.0670]	-0.1426	[-0.7159, 0.4913]	-0.9911	[-1.9137, 0.0305]
14	**-0.9490**	[-1.7278, -0.2357]	-0.6303	[-1.4861, 0.2202]	-0.2949	[-0.8619, 0.2911]	-0.8966	[-2.0593, 0.3862]
15	**-1.1782**	[-1.9574, -0.4303]	-0.5485	[-1.6390, 0.5995]	**-0.5698**	[-1.0627, -0.0350]	-0.4671	[-1.7534, 1.0244]
21	-0.5141	[-1.5775, 0.6269]	**-0.9057**	[-1.5789, -0.1742]	-0.4956	[-1.2812, 0.3500]	**-0.8440**	[-1.3142, -0.4496]
22	-0.7381	[-1.4826, 0.0208]	**-0.9361**	[-1.5020, -0.3696]	-0.5130	[-1.0421, 0.0346]	**-0.8386**	[-1.5425, -0.1009]
23	**-0.8648**	[-1.4052, -0.3485]	**-0.8206**	[-1.3790, -0.2605]	**-0.7192**	[-1.3226, -0.0340]	-0.7478	[-1.4718, 0.0241]
24	**-0.9221**	[-1.5378, -0.3682]	**-0.8791**	[-1.5085, -0.2627]	**-0.4553**	[-0.8676, -0.0177]	-0.7424	[-1.7635, 0.3810]
25	**-1.0029**	[-1.5739, -0.4671]	-0.2919	[-1.2129, 0.7083]	-0.4887	[-1.0455, 0.0629]	-0.5766	[-1.8003, 0.8360]
31	-0.5600	[-1.3897, 0.3336]	**-0.8393**	[-1.4075, -0.2244]	-0.7105	[-1.4017, 0.0778]	**-0.8037**	[-1.2003, -0.4840]
32	**-0.9045**	[-1.5349, -0.2718]	**-0.8773**	[-1.3146, -0.4354]	**-0.6556**	[-1.1082, -0.2134]	**-0.7994**	[-1.3110, -0.2911]
33	**-0.7760**	[-1.2942, -0.3212]	**-0.9796**	[-1.5195, -0.4053]	**-0.8639**	[-1.4533, -0.2783]	**-0.7744**	[-1.4166, -0.1084]
34	**-0.9707**	[-1.4788, -0.4748]	**-0.6984**	[-1.2806, -0.0932]	**-0.6926**	[-1.3806, -0.0011]	-0.8452	[-1.6874, 0.0775]
35	**-0.8999**	[-1.4257, -0.3849]	-0.4893	[-1.3360, 0.3395]	-0.3667	[-0.8978, 0.1341]	-0.5754	[-1.6880, 0.6378]
41	-0.4984	[-1.2933, 0.3128]	**-0.7953**	[-1.3632, -0.1944]	**-0.8006**	[-1.2247, -0.4155]	**-0.9152**	[-1.2226, -0.6508]
42	**-0.7538**	[-1.3935, -0.0875]	**-0.9537**	[-1.3890, -0.5171]	**-0.8270**	[-1.2123, -0.4275]	**-0.7400**	[-1.1413, -0.3477]
43	**-0.9759**	[-1.5840, -0.3830]	**-0.8334**	[-1.3713, -0.2435]	**-0.7247**	[-1.4072, -0.0100]	**-0.6923**	[-1.2541, -0.0906]
44	**-0.9840**	[-1.4156, -0.5527]	**-0.7393**	[-1.3485, -0.1646]	**-0.6879**	[-1.1074, -0.2504]	-0.6789	[-1.3727, 0.0934]
45	**-1.0742**	[-1.5398, -0.6118]	-0.5362	[-1.3950, 0.3350]	**-0.8108**	[-1.3952, -0.3412]	-0.7986	[-1.8772, 0.3708]
51	-0.4900	[-0.9376, 0.0447]	**-0.6866**	[-1.1940, -0.1043]	**-0.6597**	[-1.0425, -0.2343]	**-0.5785**	[-0.7678, -0.2833]
52	-0.4338	[-0.8523, 0.0256]	**-0.5334**	[-0.8745, -0.2044]	**-1.0345**	[-1.4871, -0.6401]	**-0.5307**	[-0.9657, -0.0909]
53	**-0.6023**	[-1.1265, -0.0459]	**-0.5617**	[-0.9014, -0.1779]	-0.4100	[-1.0578, 0.0742]	**-0.4467**	[-0.8131, -0.0590]
54	**-0.6590**	[-1.0403, -0.2243]	-0.4729	[-1.0086, 0.1002]	**-0.9647**	[-1.5651, -0.5452]	-0.2174	[-0.8193, 0.4297]
55	**-0.5917**	[-0.8996, -0.2459]	-0.2040	[-0.8725, 0.4780]	**-1.6050**	[-2.7376, -0.4016]	-0.4943	[-1.4090, 0.4722]

Notes: This table reports confidence intervals for the first-pass scale-dependent betas for $u_t^{(6:7)}$ using the bias-corrected percentile method and the stationary bootstrap of Politis and Romano (1994). Bold values denote statistically significant beta estimates at a 90% confidence level. The test assets include: the 25 FF size and book-to-market portfolios (Panel A), the 25 FF size and investment portfolios (Panel B), the 25 FF book-to-market and operating profitability portfolios (Panel C) and the 25 FF size and variance portfolios (Panel D).

Table 2B.14: Bias-corrected bootstrapped confidence intervals for the second-pass estimates

Panel A	25 FF size and book-to-market						
	$\lambda_{0,6:7}$	95% CI	$\lambda_{6:7}$	95% CI	R^2	95% CI	# observ.
$h = 1$	0.0581	[-0.3447, 0.1431]	**-0.8315**	[-1.0849, -0.7781]	**73.891%**	[0.6144, 0.8840]	
$h = 3$	0.1109	[-0.2595, 0.2194]	**-0.8476**	[-1.1315, -0.7648]	**74.617%**	[0.6209, 0.8878]	507
$h = 12$	0.2278	[-0.1728, 0.4402]	**-0.4856**	[-0.6952, -0.4198]	**77.922%**	[0.7046, 0.8965]	
Panel B	25 FF size and investment						
	$\lambda_{0,6:7}$	95% CI	$\lambda_{6:7}$	95% CI	R^2	95% CI	# observ.
$h = 1$	0.1923	[-0.2624, 0.4702]	**-0.8591**	[-1.0715, -0.8416]	**73.006%**	[0.6990, 0.8359]	
$h = 3$	0.2531	[-0.1928, 0.5742]	**-0.8672**	[-1.1174, -0.8213]	**74.027%**	[0.7147, 0.8400]	472
$h = 12$	0.4021	[-0.0343, 0.7801]	**-0.4750**	[-0.6338, -0.4130]	**70.012%**	[0.6089, 0.8424]	
Panel C	25 FF book-to-market and operating profitability						
	$\lambda_{0,6:7}$	95% CI	$\lambda_{6:7}$	95% CI	R^2	95% CI	# observ.
$h = 1$	**0.2989**	[0.0560, 0.3808]	**-0.6375**	[-0.7816, -0.5831]	**39.300%**	[0.0196, 0.7008]	
$h = 3$	**0.3255**	[0.0964, 0.4172]	**-0.6781**	[-0.8494, -0.6176]	**41.156%**	[0.0323, 0.7001]	472
$h = 12$	**0.3887**	[0.1291, 0.5263]	**-0.4199**	[-0.5117, -0.3975]	**45.510%**	[0.1258, 0.7112]	
Panel D	25 FF size and variance						
	$\lambda_{0,6:7}$	95% CI	$\lambda_{6:7}$	95% CI	R^2	95% CI	# observ.
$h = 1$	**-0.1131**	[-0.5922, -0.0252]	**-1.2460**	[-1.7315, -1.1387]	**54.840%**	[0.3833, 0.8143]	
$h = 3$	-0.0194	[-0.5317, 0.1141]	**-1.2545**	[-1.7906, -1.1201]	**55.231%**	[0.3932, 0.8031]	472
$h = 12$	0.1788	[-0.5455, 0.5349]	**-0.7293**	[-1.0099, -0.6378]	**61.006%**	[0.5029, 0.8201]	

Notes: This table reports bootstrapped confidence intervals for the second-pass estimates using the bias-corrected percentile method. Bold values denote statistically significant estimates at a 95% confidence level. The test assets include: the 25 FF size and book-to-market portfolios (Panel A), the 25 FF size and investment portfolios (Panel B), the 25 FF book-to-market and operating profitability portfolios (Panel C) and the 25 FF size and variance portfolios (Panel D).

Table 2B.15: Bias-corrected bootstrapped confidence intervals for the scale-wise predictive regressions

	Persistence level					
$j =$	6			7		
Panel A	β_6	95% CI	90% CI	β_7	95% CI	90% CI
$u_t\,(1)$	**3.0551**	[1.4756, 6.0636]	[1.8041, 5.3278]	0.3395	[-3.1428, 5.9147]	[-2.7186, 4.8427]
$u_t\,(3)$	**2.8094**	[1.3877, 5.5145]	[1.6605, 4.8525]	0.4748	[-2.8301, 5.3620]	[-2.4174, 4.4883]
$u_t\,(12)$	**4.2765**	[2.0514, 8.2260]	[2.5017, 7.2297]	1.2757	[-3.4772, 7.7966]	[-2.8486, 6.5519]
Panel B	β_6	95% CI	90% CI	β_7	95% CI	90% CI
$u_t\,(1)$	**3.0551**	[1.7187, 7.1527]	[1.9222, 5.8410]	0.3395	[-2.6837, 5.2625]	[-2.2762, 4.4559]
$u_t\,(3)$	**2.8094**	[1.5703, 6.5430]	[1.7769, 5.3312]	0.4748	[-2.3966, 4.7325]	[-2.0368, 4.0177]
$u_t\,(12)$	**4.2765**	[2.3730, 10.1137]	[2.7444, 8.2692]	1.2757	[-2.4808, 7.7078]	[-1.8131, 6.6627]

Notes: This table reports bootstrapped confidence intervals for the scale-wise predictive regressions for $j = 6, 7$ using the bias-corrected percentile method and the stationary bootstrap of Politis and Romano (1994). In Panel A the average block size is set equal to 32 - calculated based on the Politis and White (2004) estimator. In Panel B the block size is set equal to 2^j. Bold values denote statistically significant estimates.

Table 2B.16: Tails of $t/\sqrt{T}$ at various percentiles

		Horizon						
$q =$		16	32	48	64	96	128	192
$u_t\,(1)$		**forward aggregates only**						
	0.950	0.2665	0.3772	0.4558	0.5057	0.6005	0.6491	0.7115
	0.975	0.3234	0.4492	0.5383	0.6075	0.7201	0.7877	0.8277
$\rho = 0.9866$	**0.995**	0.4280	0.5885	0.7028	0.8024	0.9504	1.0453	1.1008
$\delta = -0.1511$		**forward/backward aggregates**						
	0.950	0.2767	0.3994	0.5128	0.6240	0.7933	0.9541	1.1051
	0.975	0.3282	0.4751	0.6092	0.7411	0.9794	1.1978	1.3902
	0.995	0.4360	0.6147	0.8306	1.0062	1.3594	1.7184	1.8800
$u_t\,(3)$		**forward aggregates only**						
	0.950	0.2742	0.3939	0.4692	0.5251	0.6379	0.7058	0.7612
	0.975	0.3310	0.4644	0.5555	0.6383	0.7588	0.8350	0.8943
$\rho = 0.9891$	**0.995**	0.4292	0.7246	0.7246	0.8331	1.0020	1.0866	1.2024
$\delta = -0.1853$		**forward/backward aggregates**						
	0.950	0.2812	0.4072	0.5169	0.6367	0.8205	0.9746	1.1388
	0.975	0.3308	0.4877	0.6249	0.7510	0.9966	1.1973	1.4137
	0.995	0.4359	0.6242	0.8474	1.0262	1.3924	1.7084	1.8487
$u_t\,(12)$		**forward aggregates only**						
	0.950	0.2848	0.4029	0.4814	0.5615	0.6783	0.7506	0.8379
	0.975	0.3342	0.4692	0.5901	0.6688	0.7955	0.8947	0.9854
$\rho = 0.9943$	**0.995**	0.4336	0.6199	0.7600	0.8968	1.0777	1.2356	1.3408
$\delta = -0.1494$		**forward/backward aggregates**						
	0.950	0.2885	0.4132	0.5317	0.6525	0.8252	1.0021	1.1553
	0.975	0.3368	0.4925	0.6352	0.7760	0.9924	1.2395	1.3988
	0.995	0.4495	0.6573	0.8381	1.0130	1.4407	1.6930	1.8793

Notes: This table reports the right-tail critical values of $t/\sqrt{T}$ at various percentiles (bold values). I simulate the distribution of $t/\sqrt{T}$ for samples of length $T = 635$. I implement 5,000 replications. The distribution depends on two nuisance parameters c and δ. The parameter $c = (\rho - 1)\,T$ measures deviations from unity in a decreasing (at rate T) neighbourhood of 1. The parameter δ measures the covariance of the innovations in Equations (2B.1) and (2B.2).

Table 2B.17: Multi-scale autoregressive process estimates

	Persistence level						
$j =$	1	2	3	4	5	6	7
$h = 1$							
ρ_j	0.2705***	0.0248	-0.0400	-0.1641	-0.3935***	-0.0754	-0.1542
Half-life (years)	0.0883	-	-	-	1.9816	-	-
NW t-stat	(3.4609)	(0.2591)	(-0.3005)	(-1.1020)	(-3.6137)	(-0.4605)	(-0.9950)
HH t-stat	(3.0862)	(0.2362)	(-0.3243)	(-1.1537)	(-4.0802)	(-0.6381)	(-1.1568)
Adj.R^2 (%)	[7.323%]	[0.062%]	[0.160%]	[2.697%]	[12.705%]	[0.411%]	[2.118%]
$h = 3$							
ρ_j	0.3374***	0.1102	0.0113	-0.1616	-0.4088***	-0.0735	-0.1585
Half-life (years)	0.1063	-	-	-	2.0663	-	-
NW t-stat	(3.6730)	(0.9750)	(0.0773)	(-1.0817)	(-3.7222)	(-0.4723)	(-1.0689)
HH t-stat	(3.2867)	(0.9118)	(0.0837)	(-1.1550)	(-4.1870)	(-0.6657)	(-1.3829)
Adj.R^2 (%)	[11.398%]	[1.224%]	[0.013%]	[2.613%]	[13.780%]	[0.402%]	[2.350%]
$h = 12$							
ρ_j	0.5237***	0.2988**	0.1783	-0.0776	-0.4668***	-0.0577	-0.1410
Half-life (years)	0.1786	0.1913	-	-	2.4262	-	-
NW t-stat	(6.5071)	(2.3747)	(1.1613)	(-0.5492)	(-4.0443)	(-0.4037)	(-0.9011)
HH t-stat	(5.6739)	(2.1486)	(1.2162)	(-0.5892)	(-4.4465)	(-0.6243)	(-2.8856)
Adj.R^2 (%)	[27.443%]	[8.990%]	[3.193%]	[0.607%]	[18.844%]	[0.271%]	[2.227%]
# observations	632	628	620	604	572	508	380

Notes: This table reports the estimation results of the multi-scale autoregressive system. For each level of persistence $j \in \{1, \ldots, 7\}$ I run a regression of the uncertainty component $u^{(j)}_{t+2^j}$ on its own lagged component $u^{(j)}_t$. For each regression, the table reports OLS estimates of the regressors, Newey-West (1987) and Hansen-Hodrick (1980) corrected t-statistics with $2^j - 1$ lags in parentheses and adjusted R^2 statistics in square brackets. ***,**,* denote statistical significance at 1%, 5% and 10% level respectively. Half-lives (in years) are obtained by $HL(j) = (\ln(0.5) / \ln(|\rho_j|)) \times 2^j/12$.

Table 2B.18: Percentage contribution to total variance

Panel A							
$u_t\,(1)$	Persistence level						
$j\,=$	1	2	3	4	5	6	7
$\text{Var}\left(u_t^{(j)}\right)$	0.0065	0.0184	0.0455	0.0912	0.1712	0.2289	0.1873
Lower confidence bound	0.0056	0.0153	0.0366	0.0682	0.1160	0.1451	0.0955
Upper confidence bound	0.0077	0.0225	0.0582	0.1283	0.2780	0.4142	0.5202
$u_t\,(3)$	Persistence level						
$j\,=$	1	2	3	4	5	6	7
$\text{Var}\left(u_t^{(j)}\right)$	0.0053	0.0154	0.0404	0.0888	0.1728	0.2357	0.1900
Lower confidence bound	0.0046	0.0128	0.0324	0.0660	0.1167	0.1485	0.0967
Upper confidence bound	0.0062	0.0188	0.0520	0.1259	0.2821	0.4305	0.5300
$u_t\,(12)$	Persistence level						
$j\,=$	1	2	3	4	5	6	7
$\text{Var}\left(u_t^{(j)}\right)$	0.0027	0.0086	0.0250	0.0644	0.1458	0.2288	0.2144
Lower confidence bound	0.0023	0.0070	0.0194	0.0466	0.0965	0.1449	0.1077
Upper confidence bound	0.0033	0.0108	0.0333	0.0949	0.2455	0.4150	0.6169
Panel B							
$IPVOL_t$	Persistence level						
$j\,=$	1	2	3	4	5	6	7
$\text{Var}\left(IPVOL_t^{(j)}\right)$	0.2043	0.2034	0.2073	0.1717	0.1088	0.0511	0.0205
Lower confidence bound	0.1826	0.1775	0.1691	0.1330	0.0768	0.0351	0.0126
Upper confidence bound	0.2301	0.2354	0.2603	0.2304	0.1660	0.0811	0.0388

Notes: Panel A presents the percentage contribution of each individual component to the total variance of the time-series for aggregate uncertainty. Panel B presents the percentage contribution of each individual component to the total variance for the volatility of industrial production. Approximate confidence intervals for the variance of the components are computed based on the Chi-squared distribution with one degree of freedom (see also - Percival, 1995).

Chapter 3

Are Low-Frequency Macroeconomic Risks Priced in Asset Prices? A Critical Appraisal of Epstein-Zin Preferences

3.1 Introduction

In a seminal paper Bansal and Yaron (2004) show that concerns about long-run[42] expected growth and time-varying uncertainty about future economic prospects drive asset prices. These two channels of macroeconomic risks (i.e., growth and volatility) can jointly explain the level and cross-sectional differences in asset prices. Recently, Dew-Becker and Giglio (2016) quantify the meaning of long-run in the content of Epstein-Zin preferences by deriving the exact weights that these preferences place upon different frequencies. They demonstrate that Epstein-Zin preferences isolate their weight almost exclusively on very low-frequencies (on cycles lasting centuries).

In this chapter, I test if the strict constraints that Epstein-Zin preferences impose in the frequency domain on asset pricing models are empirically satisfied. In particular, I examine if mac-

[42]For a review of the long-run risks literature see Bansal (2007) and for econometric estimation techniques see Constantinides and Ghosh (2011), Grammig and Schaub (2014) and Schorfheide et al. (2014). For the out-of-sample performance see Ferson et al. (2013). Long-run risk can also arise endogenously through consumption smoothing (Kaltenbrunner and Lochstoer, 2010) or via uncertainty and learning about the parameters governing the aggregate consumption process (Collin-Dufresne et al., 2016; Johannes et al., 2016).

roeconomic shocks with frequencies lower than the business-cycle are robustly priced in the cross-section of expected returns and evaluate the economic significance of the corresponding risk premia. First, I rely on the novel framework for scale-based (i.e., horizon-specific) analysis of risk as proposed in Boons and Tamoni (2016) to conduct inferences about the degree of covariability of asset returns and (innovations in) macroeconomic series across time-scales. Specifically, I decompose macro series into layers with different layers of resolution (i.e., across different frequencies) using the multiresolution-based decomposition of Ortu et al. (2013). Then, I analyse the price of risk for the scale-dependent macro shocks and their ability to explain the cross-sectional variation in asset prices. In line with Dew-Becker and Giglio (2016) I quantify low-frequency shocks as shocks that last longer than the business-cycle - rather than shocks that last hundreds of years as implied by Epstein-Zin preferences. That is, I allow fluctuations on broader ranges of frequencies to be priced when testing the theoretical predictions of Epstein-Zin preferences.

I find that macroeconomic shocks with frequencies lower than the business-cycle are not significantly priced in the equity market. That is, the price of risk for the low-frequency fluctuations is economically small and thus not in line with the theoretical predictions of Epstein-Zin preferences (i.e., the power at low frequencies does not determine risk premia). In addition, the risk premia have wrong sings and the low-frequency risk exposures cannot explain the size and value effects. These results remain similar irrespective of the type and length of the wavelet filter used in the multiresolution-based decomposition. Moreover, I draw similar conclusions if I use the econometric framework of Müller and Watson (2015) to estimate the low-frequency risk exposures (i.e., using betas from regressions of cosine transforms).

My work complements previous studies that question the key mechanism of the long-run risk (LRR) framework and its ability to explain observed features of asset market data. For instance, Beeler and Campbell (2012) document several empirical difficulties for the LRR model as calibrated by Bansal and Yaron (2004) and Bansal et al. (2012). Epstein et al. (2014) provide a quantitative assessment of how much the temporal resolution of risk matters. They show that the implied timing

premia (i.e., the fraction of the consumption stream that an agent is willing to give up in order for all risk to be resolved in the next period) required to match key moments of market returns are too large. I add to this line of research by demonstrating that the strict restrictions imposed in the frequency domain by the recursive utility are not empirically satisfied.

Instead, following Boons and Tamoni (2016) I demonstrate that the economically relevant set of frequencies for asset pricing are those that correspond to the upper bound of business-cycle length fluctuations. In particular, an asset pricing model with a single factor that captures variation in the first or second moment of macroeconomic activity at frequencies ranging from 4 to 8 years explains the cross-sectional variation in portfolio returns and is also correctly specified. Moreover, the risk loadings with respect to business-cycle frequencies match known patterns in average returns. That is, assets offer different risk compensations because they are differentially exposed to macroeconomic risks in this specific frequency range. My work builds upon the novel approach of Boons and Tamoni (2016) but it does so from a distinct perspective. That is, by showing that low-frequency macro factors have essentially no explanatory power and empirically assessing Epstein-Zin preferences. Moreover, my study is related[43] to Bandi and Tamoni (2016) who demonstrate the success of business-cycle consumption risk in explaining the cross-sectional differences in asset prices. Specifically, using a redundant - instead of a decimated - decomposition I show that the one-factor model of Bandi and Tamoni (2016) with business-cycle consumption risk is also correctly specified. Finally, my results are in line with chapter 2 in which I show that macro uncertainty shocks with persistence longer than 128 months are not robustly priced in asset prices.

In total, my work provides strong empirical support for a data generating process in the spirit of Bandi and Tamoni (2016) in which the expected return of an asset is directly related to its covariance with macro risks at horizons ranging from 4 to 8 years. Simply put, from the point of view of asset pricing business-cycle frequencies are of first-order importance. In light of these findings I argue that we need risk preferences that put more weight on business-cycles instead of

[43] Notable contributions in this branch of the literature that explores how scale-dependent shocks propagate to asset prices also include Ortu et al. (2013) and Bandi et al. (2016).

cycles lasting centuries as the recursive utility does. In addition, the conclusion of Dew-Becker and Giglio (2016) that long-run risks are significantly priced in asset prices while business-cycle fluctuations are not is drawn early. For instance, the risk loadings of the 25 FF size and book-to-market portfolio returns with respect to the low-frequency macro shocks in Dew-Becker and Giglio (2016) decrease across both directions[44] (i.e., size and value) which is difficult to justify empirically.

The remainder of this chapter is organized as follows: Section 3.2 discusses the asset pricing restrictions imposed by Epstein-Zin preferences in the frequency domain in line with the spectral decomposition of the pricing kernel by Dew-Becker and Giglio (2016). Section 3.3 provides the empirical analysis, section 3.4 contains several robustness checks, section 3.5 explains why the recursive utility fails and section 3.6 concludes.

3.2 Motivation - Spectral Decomposition of Epstein-Zin Preferences

Consider a discrete-time real endowment economy where the agent's preferences over the consumption stream C_t are described by the recursive utility function of Epstein and Zin (1989) and Weil (1989). These preferences allow for separation between the coefficient of risk aversion and the elasticity of intertemporal substitution (EIS). In particular, the utility function is defined recursively as

$$V_t = \left[(1-\delta) C_t^{\frac{1-\gamma}{\theta_0}} + \delta \left(E_t \left[V_{t+1}^{1-\gamma} \right] \right)^{\frac{1}{\theta_0}} \right]^{\frac{\theta_0}{1-\gamma}} \tag{3.1}$$

where $\delta \in (0,1)$ denotes the subjective discount factor, $\gamma > 0$ is the relative risk aversion coefficient, $\psi > 0$ is the elasticity of intertemporal substitution (EIS) and $\theta_0 = \frac{1-\gamma}{1-1/\psi}$. Note that when $\theta_0 = 1$, i.e. when $\gamma = 1/\psi$, the standard time-separable power utility is obtained as a special case.

In a recent study Dew-Becker and Giglio (2016) demonstrate that in any log-linear asset pricing

[44] See Table A2 in the internet appendix of Dew-Becker and Giglio (2016).

model the price of risk that investors assign to economic fluctuations at different frequencies can be analytically derived. Specifically, the spectral decomposition of Epstein-Zin preferences in the Bansal and Yaron (2004) model with time-varying volatility yields the following spectral weighting function for consumption:

$$Z_C^{EZ-SV}(\omega) = \gamma + 2(\gamma - \rho)\sum_{j=1}^{\infty}\theta^j \cos(\omega j) \tag{3.2}$$

where $\rho = 1/\psi$ (i.e., the inverse EIS) and θ is the parameter that comes from the Campbell and Shiller (1988) log-linearisation of the return on the agent's wealth portfolio (i.e., $\theta = \left(1 + \overline{DP}\right)^{-1}$ where $\overline{DP}$ is the dividend-price ratio for the wealth portfolio). Similarly, the spectral weighting function for consumption volatility is

$$Z_{\sigma^2}^{EZ-SV}(\omega) = \theta k_1 \frac{(\rho - \gamma)}{1 - \rho}\left(1 + 2\sum_{j=1}^{\infty}\theta^j \cos(\omega j)\right) \tag{3.3}$$

where k_1 is a constant that depends on the underlying process driving consumption growth. The frequency-specific price of risk for consumption shocks depends only on the investor's preferences. In contrast, the magnitude of $Z_{\sigma^2}^{EZ-SV}$ depends on the dynamics of the economy through k_1. That is, there is not a complete separation between preferences and consumption dynamics in this case. In addition, the shape of $Z_{\sigma^2}^{EZ-SV}$ depends only on the parameter θ.

The fraction of the mass in the range of frequencies between ω_1 and ω_2 is given by

$$\frac{\int_{\omega_1}^{\omega_2} Z(\omega)\, d\omega}{\int_0^{\pi} Z(\omega)\, d\omega}. \tag{3.4}$$

I use Equation (3.4) to estimate[45] the exact weights that Epstein-Zin preferences place in the following three economically motivated intervals: frequencies lower than the business-cycle (i.e., $\omega_1 = 0$ and $\omega_2 = 2\pi/32$), business-cycle frequencies (i.e., $\omega_1 = 2\pi/32$ and $\omega_2 = 2\pi/6$) and high-

[45] Note that $\sum_{j=0}^{\infty}\theta^j 2\cos(\omega j)$ can be simplified using Euler's formula and properties of absolutely convergent series (i.e., $\sum \Re = \Re \sum$).

frequencies (i.e., $\omega_1 = 2\pi/6$ and $\omega_2 = \pi$). Table 3.1 reports the theoretical pricing weights for these frequency ranges. The results are obtained from an annual calibration. In Panel A I set $\theta = 0.975$ which corresponds to a 2.56% annual dividend price ratio. In addition, I report the median cycle of a shock in years (i.e., the median cycle corresponds to the frequency for which the pricing weight is split into two halves). Table 3.1 demonstrates that the main effect of an increase in risk aversion is to shift the mass to low frequencies (Dew-Becker and Giglio (2016) show that the total weight placed on the spectrum is equal to $\left(\int_0^{\pi} Z_C^{EZ-SV}(\omega)\, d\omega\right)/\pi = \gamma$). Also, the median cycle of both consumption growth and volatility shocks across all calibrations is greater than 130 years.

Figure 3.1 plots the theoretical spectral weighting functions Z_C^{EZ-SV} and $Z_{\sigma^2}^{EZ-SV}$ under Epstein-Zin preferences for various parametrizations. The x-axis lists the cycle length in years. In line with the results in Table 3.1 we observe that the mass of both functions is isolated near frequency zero.

In total, these findings demonstrate that under recursive preferences low-frequencies are priced strongly while business-cycle frequencies are not quantitatively important for asset pricing. That is, around 90% of the weight that determines risk premia lies on frequencies lower than the business-cycle. In addition, these results greatly highlight the estimation problem underlying Epstein-Zin preferences, i.e. the weights lie on frequencies close to zero for which traditional inference tools of spectral analysis are not directly applicable due to the scarcity of low-information (see the discussion in the Appendix).

3.3 Empirical Analysis

3.3.1 Data

In a consumption-based asset pricing model with Epstein-Zin preferences the pricing kernel is driven by persistent shocks to consumption. Since consumption suffers from a number of measurement problems (for instance, see Savov, 2011; Qiao, 2013) and in line with Boons and Tamoni (2016) I quantify macroeconomic activity using the growth rate of industrial production[46] (IPG). Moreover,

[46] Liu and Zhang (2008) also use IPG as a common risk factor driving the pricing kernel.

I explore the robustness of all results using other macro variables such as GDP growth and volatility. This approach allows me to generalize the analysis and examine if and how the low-frequency dynamics of the economy are priced.

IPG_t is defined as $IPG_t = \log IP_t - \log IP_{t-1}$ where IP_t is the seasonally-adjusted industry production index (INDPRO series) in month t from the FRED database of the St. Louis FED. Quarterly growth rates are calculated by compounding monthly growth rates. The sample period is 1962:Q1 to 2014:Q4 (the starting period is in line with most work on cross-sectional asset pricing). In addition, to measure macro volatility I consider the following AR $(1)-$GARCH$(1,1)$ specification

$$IPG_t = \mu + \phi IPG_{t-1} + \nu_t, \tag{3.5}$$

$$\sigma_t^2 = \omega_0 + \omega_1 \nu_{t-1}^2 + \omega_2 \sigma_{t-1}^2 \tag{3.6}$$

where $IPVOL = \widehat{\sigma}_t$. I estimate Equations (3.5) and (3.6) using the full sample. Estimation results are available in Table 3.2. The estimates of ω_1 and ω_2 are both significant implying macro volatility is time varying.

My main test assets are the 5 FF industry and 25 FF size and book-to-market portfolios which are priced together. That is, in the spirit of Lewellen et al. (2010) I include the FF industry portfolios to provide a higher hurdle for the frequency-dependent macroeconomic factors. I only add the 5 industry portfolios because the asymptotic distribution of the sample cross-sectional R^2 becomes less reliable as the number of test assets increases (this approach is in line with Kan et al., 2013).

3.3.2 Econometric Framework & Cross-Sectional Analysis

I am interested in the ability of the scale-dependent macroeconomic shocks filtered out of IPG and $IPVOL$ to explain aggregate portfolio returns. I begin by decomposing the macro series of interest into layers with heterogeneous levels of persistence using the multiresolution-based decomposition of Ortu et al. (2013). In particular, let $u_t^{(j)}$ denote fluctuations of the macro series with half-life in

the interval $[2^{j-1}, 2^j)$, that is

$$u_t^{(j)} = \frac{\sum_{i=0}^{2^{(j-1)}-1} u_{t-i}}{2^{(j-1)}} - \frac{\sum_{i=0}^{2^j-1} u_{t-i}}{2^j} \equiv \pi_t^{(j-1)} - \pi_t^{(j)} \tag{3.7}$$

where $j \geq 1$, $\pi_t^{(0)} \equiv u_t$ and the moving averages $\pi_t^{(j)}$ satisfies the recursion

$$\pi_t^{(j)} = \frac{\pi_t^{(j-1)} + \pi_{t-2^{j-1}}^{(j-1)}}{2} \tag{3.8}$$

for $j = 1, 2, 3, \ldots$. The derived series $\left\{u_t^{(j)}\right\}_{t\in\mathbb{Z}}$ captures fluctuations that survive to averaging over 2^{j-1} terms but disappear when the average involves 2^j terms. For any $J \geq 1$, the original series u_t can be written as a sum of components with half-life belonging to a specific interval plus a long-run average, that is,

$$u_t = \sum_{j=1}^{J} u_t^{(j)} + \underbrace{u_t^{(>J)}}_{\equiv \pi_t^{(J)}}. \tag{3.9}$$

The decomposition of the time series is conducted using wavelet methods as in multiresolution analysis via the Maximum Overlap Discrete Wavelet Transform (MODWT). In particular, the extraction is based on the one-sided, linear Haar filter. I set $J = 5$ so that the maximum time-scale corresponds to the upper bound of business-cycle frequencies and $u_t^{(>5)}$ captures shocks lower than the business-cycle (i.e., lower than 8 years). In line with the MODWT I also extend this decomposition to allow for filters of different type and length as a robustness check (see Section 1.2 for more details).

The covariance between asset excess returns $\left(R_t^{e,i}\right)$ and innovations (i.e., the unexpected part) in macroeconomic series $(\Delta u_t \equiv u_t - u_{t-1})$[47] can be decomposed across time-scales as follows[48] (see Boons and Tamoni, 2016 or Bandi and Tamoni, 2016 for a decimated decomposition)

[47] The results are quantitatively similar if I use residuals from an AR(1) model - see Table 3B.1.

[48] This result holds irrespectively of the wavelet filter used for the decomposition. For instance, see Chapter 7 in Gençay et al. (2001).

$$Cov\left[R_t^{e,i}, \Delta u_t\right] = \sum_{j=1}^{J} Cov\left[R_t^{e,i(j)}, \Delta u_t^{(j)}\right] + Cov\left[R_t^{e,i(>J)}, \Delta u_t^{(>J)}\right] \tag{3.10}$$

and thus the scale-dependent risk exposures are defined as

$$\beta^{i(j)} \equiv \frac{Cov\left[R_t^{e,i(j)}, \Delta u_t^{(j)}\right]}{Var\left(\Delta u_t^{(j)}\right)} \quad \text{and} \quad \beta^{i(>J)} \equiv \frac{Cov\left[R_t^{e,i(>J)}, \Delta u_t^{(>J)}\right]}{Var\left(\Delta u_t^{(>J)}\right)}. \tag{3.11}$$

The approach of Boons and Tamoni (2016) for cross-sectional asset pricing differs from the standard Fama-MacBeth (1973) methodology in the first step, i.e. in the way that the risk exposures are estimated. In particular, I first run for each asset i (of size T) the following time-series regression

$$R_t^{e,i(j)} = \beta_0^{(j)} + \beta^{i(j)} \Delta u_t^{(j)} + \varepsilon_t^{(j)} \quad t = 1, \ldots, T \text{ for each } j = 1, \ldots, 5, > 5, \tag{3.12}$$

where $R_t^{e,i(j)}$ denotes the components of asset excess returns associated with scale j at time t. Then I estimate a cross-sectional regression of average portfolio returns on the estimated scale-specific risk exposures $\beta^{i(j)}$

$$\overline{R^{e,i}} = \lambda_{0,j} + \lambda_j \beta^{i(j)} + \alpha_{i,j} \quad \text{for each } j = 1, \ldots, 5, > 5, \tag{3.13}$$

where $\overline{R^{e,i}}$ denotes the average time-series excess return for asset i, $\lambda_{0,j}$ is the zero-beta excess return associated with time-scale j, λ_j is the relative price of risk for $\beta^{(j)}$ (i.e., the frequency-specific risk compensation) and $\alpha_{i,j}$ is a pricing error.

To determine whether the scale-dependent macroeconomic shocks are priced I look for an estimate $\hat{\lambda}_j$ that remains significant after using a t-statistic cutoff of three as suggested by Harvey et al. (2016), for an intercept that is small and statistically insignificant and a sample R^2 significantly different from zero. When $0 < \mathrm{R}^2 < 1$, $\widehat{\mathrm{R}^2}$ is asymptotically normally distributed around its true value and thus we cannot use $\widehat{\mathrm{R}^2} \pm 1.96 \times se(\widehat{\mathrm{R}^2})$ to obtain a 95% confidence interval. Instead, I

construct confidence intervals by pivoting[49] the cumulative distribution function (cdf). Kan and Robotti (2009) and Kan and Robotti (2015) use the same method to construct confidence intervals for the Hansen-Jagannathan distance and the Hansen-Jagannathan bound respectively.

Table 2.4 presents the scale-dependent risk exposures for business-cycle length fluctuations. I use Newey-West (1987) heteroskedasticity and autocorrelation consistent (HAC) standard errors with $2^j - 1$ lags. In the spirit of Kan and Zhang (1999) it is empirically sound to use the risk exposures from Equation (3.12) as factors in cross-sectional asset pricing (i.e., not *useless* factors). Moreover, the risk loadings with respect to macro volatility are negative, that is, assets tend to realize low returns when macro volatility is rising. This result is in line with the evidence in Boons and Tamoni (2016).

Table 3.4 reports the estimates for the zero-beta excess return and the price of risk across time-scales for innovations in macro shocks filtered out of IPG (in Panel A) and $IPVOL$ (in Panel B) along with the corresponding Fama-MacBeth (1973) test statistics in parentheses. In addition, I normalize the frequency-specific risk exposures and estimate the price of risk per unit of cross-sectional standard deviation in percent per year. I also report the p-value for the Kan et al. (2013) specification test of $H_0: \ R^2 = 1$ denoted as $p\left(\mathrm{R}^2 = 1\right)$. Innovations in low-frequency macroeconomic shocks (i.e., lower than 8 years) filtered out from the first and the second moment of industrial production are not priced in the cross-section of expected returns. In both cases the estimated risk premia are economically small and have wrong signs (i.e., $\hat{\beta}^{(>5)}_{\Delta IPG} \times \hat{\lambda}_{\Delta IPG^{(>5)}} < 0$ and $\hat{\beta}^{(>5)}_{\Delta IPVOL} \times \hat{\lambda}_{\Delta IPVOL^{(>5)}} < 0$), the estimates of the zero-beta excess returns are statistically significant and the cross-sectional R^2's are not significantly different from zero. That is, $\Delta IPG^{(>5)}$ and $\Delta IPVOL^{(>5)}$ are not priced.

On the other hand, the estimated price of risk for $\Delta IPG^{(5)}_t$ is 0.38 with a t-statistic of 2.55 while the intercept is insignificant. The coefficient of determination for this factor is equal to 56.70% and is significantly different from zero. In addition, the Kan et al. (2013) miss-specification test does

[49] For more information see section 9.2.3 in Casella and Berger (2002).

not reject the null hypothesis that the model is correctly specified. Similarly, $\Delta IPVOL_t^{(5)}$ carries a negative price of risk of -0.10 with a t-statistic of -3.26 and the intercept is insignificant (t-stat = 1.48). The cross-sectional R^2 is 60.78%, statistically significant and with lower sampling variability (i.e., $se(\widehat{\mathrm{R}^2_{(5)}}) = 0.1026$). In addition, the null hypothesis that the model is correctly specified is not rejected. Note that since $\hat{\beta}^{(5)}_{\Delta IPG} \times \hat{\lambda}_{\Delta IPG^{(5)}} > 0$ and $\hat{\beta}^{(5)}_{\Delta IPVOL} \times \hat{\lambda}_{\Delta IPVOL^{(5)}} > 0$ business-cycle growth and volatility shocks carry positive risk premia.

These results complement the earlier study of Boons and Tamoni (2016) who emphasize the importance of macro growth and volatility shocks with persistence greater than 4 years for cross-sectional asset pricing. I do not dispute the fact that the Boons and Tamoni (2016) factors are robustly priced in asset prices. Rather, I show that their pricing performance is mainly driven by a business-cycle component. That is, in contrast with the theoretical restrictions of Epstein-Zin preferences and the results in Dew-Becker and Giglio (2016) I explicitly demonstrate that low-frequency macro factors have essentially no explanatory power. Instead, business-cycle fluctuations are of first-order importance for asset pricing.

Figure 3.2 plots realized versus fitted average excess returns for the 25 size and book-to-market FF portfolios and the 5 FF industry where the priced factors are the innovations (i.e., first-differences) in the scale-specific macro shocks for $j = 5$ and $j > 5$. Each two-digit number represents a separate portfolio. The first digit refers to the size quintile of the portfolio (1 being the smallest and 5 the largest), while the second digit refers to the book-to-market quintile (1 being the lowest and 5 the highest). If the fitted and the realized returns for each portfolio are the same then they should lie on the 45-degree line from the origin.

3.4 Robustness Checks

In this section I verify the robustness of my results using several checks.

3.4.1 Leakage and other Filters

An ideal band-pass filter filter exhibits positive values only inside the desired frequency interval and is zero at all other frequencies. In contrast, the squared gain functions associated with the Haar wavelet filter at each level of resolution j (i.e., at each time-scale) do not decay rapidly outside their nominal frequency range. That is, the Haar filter is a poor approximation to an ideal band-pass filter (see Figure 3.3). To address this issue I use the least asymmetric (LA) Daubechies filter of length 8 and perform a similar multiresolution-based decomposition. The LA(8) wavelet suffers from less leakage at the edge of each frequency band and hence is a much better approximation to an ideal band-pass filter than the Haar (see Figure 3.4). At each time-scale I estimate the unexpected part of the scale-specific macroeconomic shocks using the residuals from an AR(1) model. Table 3.5 provides the cross-sectional estimates. The results for $IPVOL$ remain quantitatively similar.

The preferred decomposition is the one used by Ortu et al. (2013) and Boons and Tamoni (2016) since under the one-sided, linear Haar filter used for the extraction there is a close relation between scale-specific and long-horizon betas (see also Bandi and Tamoni, 2016). In addition, for macroeconomic series that are less volatile (e.g., IPG or GDP Growth) wavelet filters of length 4 or less are more appropriate (see Crowley, 2007).

3.4.2 Comparison: Business-Cycle Frequencies ($j = 5$) vs Low-Frequencies ($j > 5$)

I compare the two factors that capture variation in macro activity at frequencies ranging between 4 and 8 years (i.e., $j = 5$) and frequencies lower than 8 years (i.e., $j > 5$) by estimating the following cross-sectional regression

$$\overline{R^{e,i}} = \lambda_0 + \lambda_5 \beta^{i(5)} + \lambda_{>5} \beta^{i(>5)} + \alpha_i \tag{3.14}$$

where the scale-specific risk loadings are estimated from two separate time-series regressions as in Equation (3.12). Table 3.6 reports the cross-sectional estimates. Adding the low-frequency macro

factor does not improve the cross-sectional fit relative to a model with a single business-cycle factor. In particular, the risk premium associated with the low-frequency macro shocks is not statistically significant. This result remains similar irrespective of the type and length of the wavelet filter used for the multi-resolution based decomposition.

3.4.3 Consumption Growth

The results remain similar if I replace industrial production growth with consumption measured as the growth rate in real per capita non-durable consumption (seasonally adjusted at annual rates) from the Bureau of Economic Analysis. Panel A of Table 3.7 presents the cross-sectional estimates. The sampling period is quarterly from 1952:Q2 to 2012:Q4. The results for $j = 5$ are in line with Bandi and Tamoni (2016) who use a decimated decomposition (i.e., they sample the scale-dependent macro shocks every $k \times 2^j, k \in \mathbb{Z}$ times) while for $j > 5$ the consumption shocks are not priced. Also, I cannot reject the null that the one-factor model with business-cycle consumption risk of Bandi and Tamoni (2016) is correctly specified[50].

3.4.4 GDP Growth and Volatility

Panels B and C of Table 3.7 present the results for GDP growth and volatility respectively. GDP growth is the growth rate in the Real Gross Domestic Product (seasonally adjusted at annual rates) from the Bureau of Economic Analysis (series GDPC96) while GDP VOL is estimated using an AR(1)-GARCH(1,1) model over the full sample. The sampling period is from 1962:Q1 to 2014:Q4. The cross-sectional fit of a business-cycle factor filtered out of GDP growth and volatility remains similar.

[50] If I exclude the 5 FF industry portfolios the sample R^2 is equal to 65.725%, $se(\widehat{R^2})$=0.1844 and $p\left(R^2 = 1\right)$ is 0.1165.

3.4.5 Monotonicity in Risk Loadings

Moreover, I examine if the frequency-specific risk exposures match known patters in average returns. That is, I test if the risk loadings are monotonically increasing (or decreasing) across portfolios using the monotonic relation (MR) test of Patton and Timmermann (2010). The MR test is designed so that the alternative hypothesis is the one that we want to prove and therefore a monotonic relation is confirmed only if there is sufficient evidence in the data to reject the null. For example, for assets sorted on portfolios across book-to-market the null and alternative hypothesis for the MR tests are the following: for portfolio returns $H_0 : R_5 \leq \ldots \leq R_1$ vs $H_1 : R_5 > \ldots > R_1$, for risk loadings with respect to $\Delta IPG_t^{(j)}$ $H_0 : \beta_5^{(j)} \leq \ldots \leq \beta_1^{(j)}$ vs $H_1 : \beta_5^{(j)} > \ldots > \beta_1^{(j)}$ and for risk-loadings with respect to $\Delta IPVOL_t^{(j)}$ $H_0 : \beta_5^{(j)} \geq \ldots \geq \beta_1^{(j)}$ vs $H_1 : \beta_5^{(j)} < \ldots < \beta_1^{(j)}$ where the direction is reversed because the risk price is negative. I implement the MR test using the stationary bootstrap of Politis and Romano (1994) where the average block size is calculated based on the Politis and White (2004) estimator[51]. For all MR test I use 5,000 replications.

Table 2.15b presents the frequency-specific risk exposures with respect to the factors $\Delta IPG_t^{(j)}$ and $\Delta IPVOL_t^{(j)}$ for $j = 5$ (i.e., business-cycle frequencies) and $j > 5$ (i.e., frequencies lower than 8 years) for one-way portfolio sorts and the corresponding monotonicity tests. Only the risk loadings at business-cycle frequencies match the size and values effects. That is, asset offer different risk compensations because they are differentially exposed to macro risks at this frequency range. Similar results hold for consumption growth (see Table 3B.9).

3.4.6 Low-Frequency Betas from OLS Regressions of Cosine Transforms

Furthermore, I rely on the econometric approach of Müller and Watson (2015) to conduct inferences about the degree of covariability between (innovations) in macro shocks and asset excess returns in frequencies lower than the business cycle. Then, I use the low-frequency betas as regressors in the second-pass of the Fama-MacBeth (1973) methodology. In particular, I extract low-frequency

[51] For details on how to test for monotonic patterns in risk exposures see Appendix A.

information by computing a finite number (q) of weighted averages of the original data where the weights are known and deterministic low-frequency trigonometric series (i.e., discrete cosine transforms)[52]. Within this framework estimation and inference about the low-frequency covariability of the series is based only on the properties of the q weighted averages which are approximately multivariate normal. That is, the inference problem is solved by classic results about inference in small Gaussian samples.

Low-Frequency Weighted Averages: Let x_t denote the economic variable of interest that is observed for $t = 1, \ldots, T$. Following Müller and Watson (2008, 2015) I isolate[53] the low-frequency information in x_t using weights associated with the cosine transform, where the $n-$th weight is given by

$$\Psi_n(s) = \sqrt{2}\cos(n\pi s) \qquad \text{for } n = 1, \ldots, q, \tag{3.15}$$

so that $\Psi_n(t/T)$ has period $2T/n$. The $n-$th weighted average is then denoted by

$$X_{Tn} = \int_0^1 \Psi_n(s)\, x_{\lfloor sT \rfloor + 1} ds = \iota_{nT} T^{-1} \sum_{t=1}^{T} \Psi_n\left(\frac{t-1/2}{T}\right) x_t \tag{3.16}$$

where $\iota_{nT} = (2T/n\pi)\sin(n\pi/2T)$ for all fixed $n \geq 1$ and $\lfloor sT \rfloor$ denotes the integer part of $sT \in \mathbb{R}$. The weighted averages X_{Tn}, $n = 1, \ldots, q$, capture variation in x_t corresponding to frequencies lower than $q\pi/T$. The weights Ψ_n add to zero and therefore X_{Tn} is invariant to location shifts of the sample.

Asymptotic Approximations and Inference in a $I(0)$ Model: Müller and Watson (2008) demonstrate that suitably scaled partial sums of the weighted averages are normally distributed in large samples if x_t satisfies certain persistence properties. That is, for a model-specific κ: $T^{1-\kappa} X_T \overset{a}{\sim}$

[52] For a thorough discussion regarding the choice of weights for extracting the low-frequency components see Müller and Watson (2008). Similar properties hold for other transforms such as discrete Fourier or sine.

[53] I would like to thank Mark Watson for making the code available in his personal website: https://www.princeton.edu/~mwatson/.

$\mathcal{N}(0, \Sigma)$ where $X_T = (X_{T1}, \ldots, X_{Tq})'$ and the covariance matrix Σ depends on the specific model of low-frequency variability (i.e., Σ is determined by the parameters characterizing the persistence of x_t). In particular for the $I(0)$ case, $T^{-1/2} X_T \overset{a}{\sim} \mathcal{N}\left(0, \omega^2 I_q\right)$ where ω^2 is the long-run variance.

Low-Frequency Risk Exposures in a Multivariate $I(0)$ Model: Now, let x_t denote an $h \times 1$ vector of time series. Partition x_t into a scalar r_t and a $k \times 1$ vector z_t where $k = h - 1$ with corresponding cosine transforms

$$\sqrt{T} \begin{pmatrix} R_{Tn} \\ Z_{Tn} \end{pmatrix} \Rightarrow \begin{pmatrix} R_n \\ Z_n \end{pmatrix} \sim \mathcal{N}\left(0, \underbrace{\begin{pmatrix} \Omega_{rr} & \Omega_{rz} \\ \Omega_{zr} & \Omega_{zz} \end{pmatrix}}_{\equiv \Omega}\right) \tag{3.17}$$

where Ω is the long-run covariance matrix of x_t. Standard statistical theory concerning *i.i.d.* multivariate normal samples can be used to obtain inference. In particular, $\varepsilon_n = R_n - Z_n' \beta$ is *i.i.d.* $\mathcal{N}\left(0, \sigma^2\right)$ where $\sigma^2 = \Omega_{rr} - \Omega_{rz}\Omega_{zz}^{-1}\Omega_{zr}$ and $\beta = \Omega_{zz}^{-1}\Omega_{zr}$ is the population regression coefficient in a regression of R_n on Z_n, $n = 1, \ldots, q$. The R^2 in this regression measures the fraction in the low-frequency variability in r_t that can be explained by the low-frequency variability in z_t. Moreover as long as $k < q$, $\hat{\beta} = \left(\sum_{n=1}^{q} Z_n Z_n'\right)^{-1} \left(\sum_{n=1}^{q} Z_n Z_n'\right)$. For scalar elements of β usual t-statistic inference is applicable. In particular, $\hat{\beta}$ follows a student-t distribution with $q-k$ degrees of freedom.

Choice of q: For 53 years of data ($T = 212$ quarters) a small number of projection coefficients ($q = 13$) capture variability lower than the business cycle regardless of the sampling frequency, that is, the cut-off periodicity is equal to $\frac{2*T}{q} = 32.62$ quarters or approximately 8.15 years.

The $I(0)$ Assumption and Inference about Persistence: In general, the low-frequency methods described in this section are appropriate for both weakly and highly persistent processes. However, the $I(0)$ assumption is crucial for conducting statistical inference about β. For inference in the cointegrated case see Müller and Watson (2013) and for the large size distortions that arise in

the local-to-unity case see Elliott (1998). To conduct inference about the persistence parameters I use three optimal tests that direct power to different alternatives. First, I consider the low-frequency versions of the point optimal (i.e., best power against the alternative) unit root and stationarity tests derived in Müller and Watson (2008). In particular, I test the $I(0)$ null hypothesis against the point alternative of a local-level model with parameter $b = b_a > 0$ using the low-frequency stationarity test (LFST)

$$\text{LFST} = \frac{\sum_{n=1}^{q} X_{Tn}^2}{\sum_{n=1}^{q} X_{Tn}^2 \left(1 + b_a / (n\pi)^2\right)^{-1}} \tag{3.18}$$

where b_a is a parameter that governs the relative importance of the $I(1)$ component in the local-level model[54]. For $b_a = 10$ the test exhibits near optimality for a wide range of values of b (see Müller and Watson, 2013). In addition, I test the unit root model using the likelihood ratio statistic

$$\text{LFUR} = \frac{X_T' \Sigma(c_0)^{-1} X_T}{X_T' \Sigma(c_a)^{-1} X_T} \tag{3.19}$$

where $X_T = (X_{T1}, \ldots, X_{Tq})'$, $\Sigma(c_0)$ is the covariance matrix under the null (i.e., the $I(1)$ model with $c_0 = 0$), $\Sigma(c_a)$ is the covariance matrix under the alternative and the statistic is labelled low-frequency unit root (LFUR). Following Müller and Watson (2015) and Elliott (1999) I set $c_a = 10$.

Also, I consider a weighted average power (WAP) optimal test. That is, I use a point-optimal test for the null ($H_0 : d = d_0$) versus the alternative ($H_a : d = d_a$) and construct a confidence set by collecting the values of d_0 that are not rejected. In line with Müller and Watson (2015) I use a weighting function that is uniform on $-0.5 < d < 1.5$. This approach allows a generalization of the $I(0)$ and $I(1)$ dichotomy in the spirit of the fractionally integrated model $I(d)$ where d is not restricted to take on integer values (for instance, see Baillie, 1996).

[54] The local-level model decomposes x_t into an $I(0)$ and $I(1)$ component, that is, $x_t = e_{1t} + (b/T)\sum_{s=1}^{T} e_{2s}$ where $\{e_{1t}\}$ and $\{e_{2t}\}$ are mutually uncorrelated $I(0)$ processes with the same long-run variance. $I(0)$ behaviour follows when $b = 0$. For more information see Harvey (1990).

Panel A of Table 3.10 reports the results for the persistence tests. The low-frequency variability in the macro series is consistent with the $I(0)$ model. Hence, it is empirically sound to conduct inference about the degree of low-frequency covariability between asset returns and these variables using the Müller and Watson (2015) approach. Table 3.9 presents the low-frequency betas from OLS regressions of cosine transforms. In particular, for each asset i I estimate the risk exposures in a regression of $R_n^{e,i}$ on Z_n, that is,

$$R_n^{e,i} = \beta Z_n \quad n = 1, \ldots, q. \tag{3.20}$$

where $R_n^{e,i}$ and Z_n denote the low-frequency weighted averages constructed from asset's i excess returns and innovations (i.e., residuals from an AR(1) model) in macro series respectively. Panel B of Table 3.10 presents the cross-sectional estimates for three different frequency cut-offs (i.e., $q = 11, 12, 13$). In line with the results from the multiresolution-based decompositions I find that the low-frequency macro shocks are not priced.

3.4.7 Frequency Domain Risk Exposures

Finally, in the spirit of Kalyvitis and Panopoulou (2013) I calculate the gain[55] between asset returns and the macro series (i.e., IPG or $IPVOL$) at a specific frequency and then use the estimates as regressors in the second step of the Fama-MacBeth (1973) methodology. In particular, the gain between portfolio's i excess returns $R^{e,i}$ and industrial production at frequency ω is defined as the ratio between the co-spectra of the series and the spectrum of IPG given by

$$G_{R^{e,i},IPG}(\omega) = \frac{|f_{R^{e,i},IPG}(\omega)|}{f_{IPG,IPG}(\omega)} \tag{3.21}$$

where $f_{R^{e,i},IPG}$ is the cross-spectrum of the two-series and is complex-valued and $f_{IPG,IPG}$ is the

[55] I use demeaned series to estimate the spectral measures based on Welch's (1967) method with a Hamming window and 50% overlap. For details regarding window designs see Chapter 2 in Stoica and Moses (2005). Note that while I use this approach as a robustness check the transition between the frequency domain and the time domain is ad hoc.

spectrum of IPG. The gain can be considered as the frequency domain analogue of the regression coefficient (for instance, see Engle, 1974) and is always positive.

The results in Table 3.11 remain quantitatively similar. At business-cycle frequencies $\hat{G}_{R^{e,i},IPG} \times \hat{\lambda} > 0$ and $\hat{G}_{R^{e,i},IPVOL} \times \hat{\lambda} > 0$ and hence the estimated macro growth and volatility risk premia are positive. In contrast, for frequencies lower than 8 years the risk premia have wrong signs and the corresponding factors are not robustly priced. Similar results hold for GDP growth and volatility (see Table 3B.11). Figure 3.5 presents the price of risk in percent per year across all frequencies. There is a clear pick in the risk prices at frequencies close to the upper bound of the business-cycle.

3.5 Why Do Epstein-Zin Preferences Fail?

To understand why the recursive utility does not work and give some economic meaning to its failure consider the innovations in the log stochastic discount factor (for details see Dew-Becker and Giglio, 2016)

$$\begin{aligned} \Delta E_{t+1} m_{t+1} \approx & -\gamma \Delta E_{t+1} \left(\Delta C_{t+1}\right) - (\gamma - \rho) \sum_{j=1}^{\infty} \theta^j \Delta E_{t+1} \left(\Delta C_{t+1+j}\right) \\ & - \theta k_1 \frac{(\rho - \gamma)}{1 - \rho} \left(\Delta E_{t+1} \left(\sigma^2_{t+1}\right) + \sum_{j=1}^{\infty} \theta^j \Delta E_{t+1} \left(\sigma^2_{t+1+j}\right) \right) \end{aligned} \tag{3.22}$$

where $\Delta E_{t+1} = E_{t+1} - E_t$ denotes the change in expectations. In Equation (3.22), $\Delta E_{t+1} \left(\Delta C_{t+1}\right)$ captures current consumption conditions while $\sum_{j=1}^{\infty} \Delta E_{t+1} \left(\Delta C_{t+1+j}\right)$ news about long-run future consumption growth. Similarly, $\sum_{j=1}^{\infty} \Delta E_{t+1} \left(\sigma^2_{t+1+j}\right)$ captures news about long-run future consumption volatility. In essence, under Epstein-Zin preferences what drives the theoretical pricing weights and hence risk premia are news about shocks in consumption growth and volatility that last centuries (i.e., with a median cycle greater than 130 years) and are orthogonal (i.e., not related) to current conditions. Assuming that investors are endowed with this amount of news and allowing

this information to drive asset prices is unrealistic and very hard to justify empirically.

3.6 Conclusions

In this chapter, I examine whether the strict conditions that Epstein-Zin preferences impose in the frequency domain on asset pricing models are empirically satisfied. I find that macroeconomic shocks with frequencies lower than the business-cycle are not robustly priced in asset prices. In addition, the estimated risk premia are economically small, carry wrong signs and the low-frequency risk exposures fail to match known patterns in average returns (i.e., size and value effects). Instead, I demonstrate that the economic relevant frequencies for asset pricing are mainly those that correspond to the upper bound of business-cycle frequencies (i.e., 4 to 8 years). In this frequency range the theoretical pricing weights that Epstein-Zin preferences place are only around 4%. My results remain robust and quantitatively similar irrespective of how macro growth and volatility are quantified or how the frequency-specific risk exposures are estimated.

Overall, my work highlights the need for risk preferences that put less weight on cycles lasting centuries and allow investors to be more risk averse to business-cycle frequencies. An alternative approach is to specify risk preferences with a flat weighting function in the frequency domain (e.g., power utility or external habit formation - Campbell and Cochrane, 1999) and use scale-dependent consumption components to drive the pricing kernel and thus generate business-cycle correlated risk premia (for instance, see Bandi and Tamoni, 2016).

Figure 3.1: Theoretical pricing weighting functions for Epstein-Zin preferences

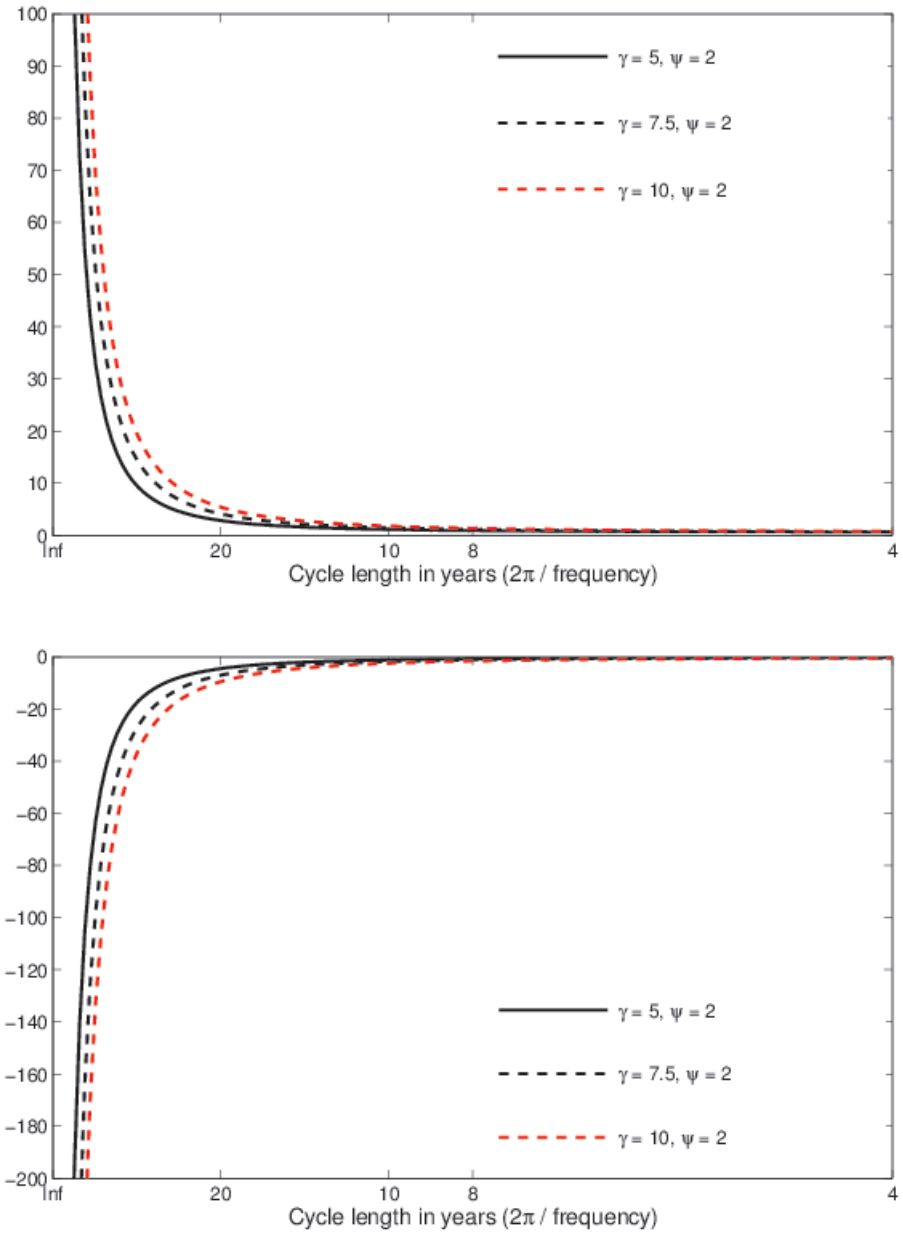

Notes: This figure plots the theoretical spectral weighting functions for consumption (Panel A) and consumption volatility (Panel B) under Epstein-Zin preferences. γ is the relative risk aversion coefficient and ψ the elasticity of intertemporal substitution (EIS). The results are obtained from an annual calibration with $\theta = 0.975$ which corresponds to a 2.56% annual dividend price ratio (i.e., $\theta = \left(1 + \overline{DP}\right)^{-1}$). The x-axis lists the cycle length in years (given a frequency of ω the corresponding cycle has length $2\pi/\omega$ periods).

Figure 3.2: Cross-sectional fit

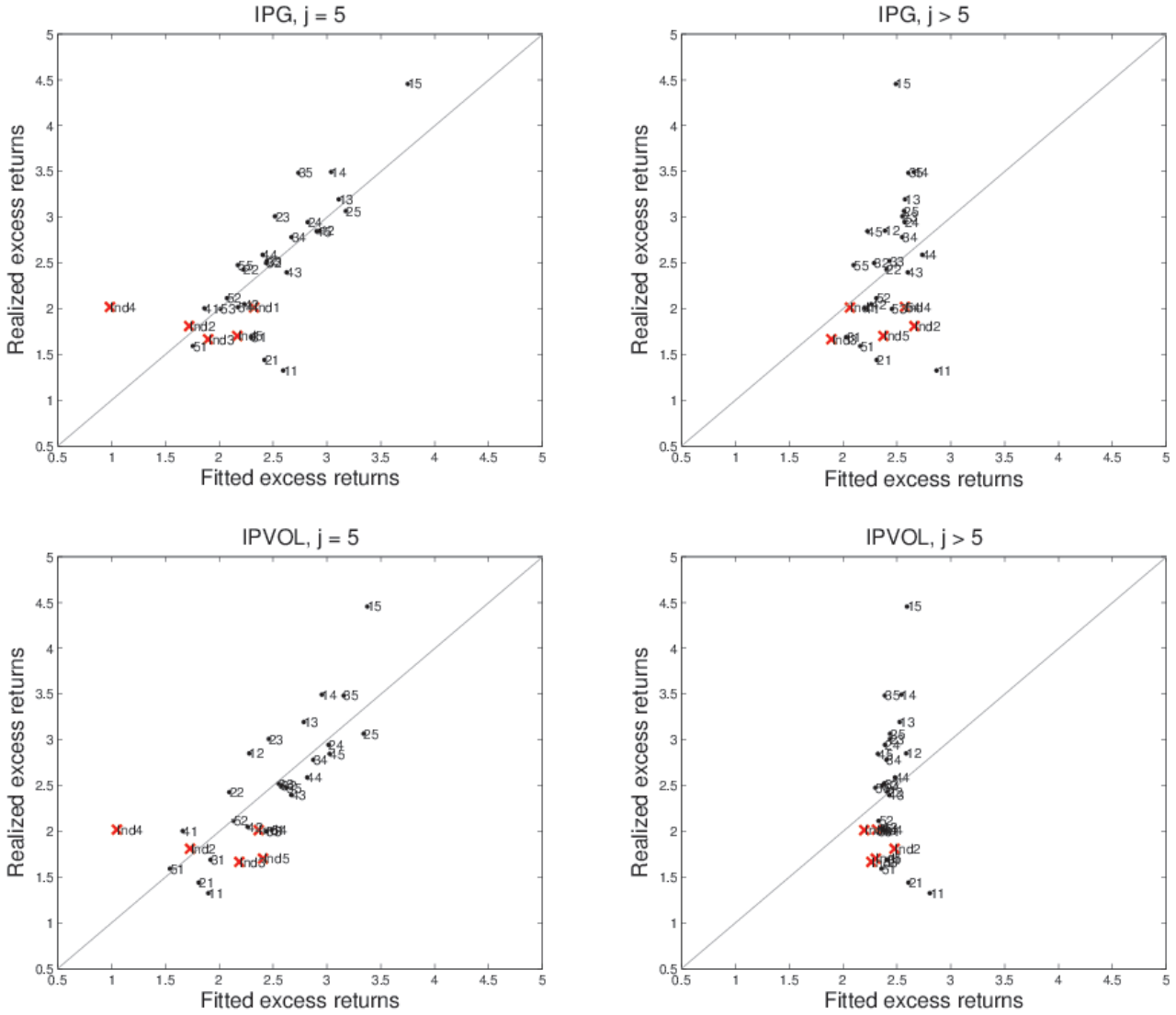

Notes: This figure plots realized versus fitted excess returns for the 25 size and book-to-market Fama and French (1993) portfolios and the 5 FF industry where the priced factors are the innovations (i.e., first-differences) in the scale-specific macro shocks for $j = 5$ and $j > 5$. Each two-digit number represents a separate portfolio. The first digit refers to the size quintile of the portfolio (1 being the smallest and 5 the largest), while the second digit refers to the book-to-market quintile (1 being the lowest and 5 the highest). The straight line is the 45-degree line from the origin.

Figure 3.3: Frequency domain representation: Haar wavelet filter

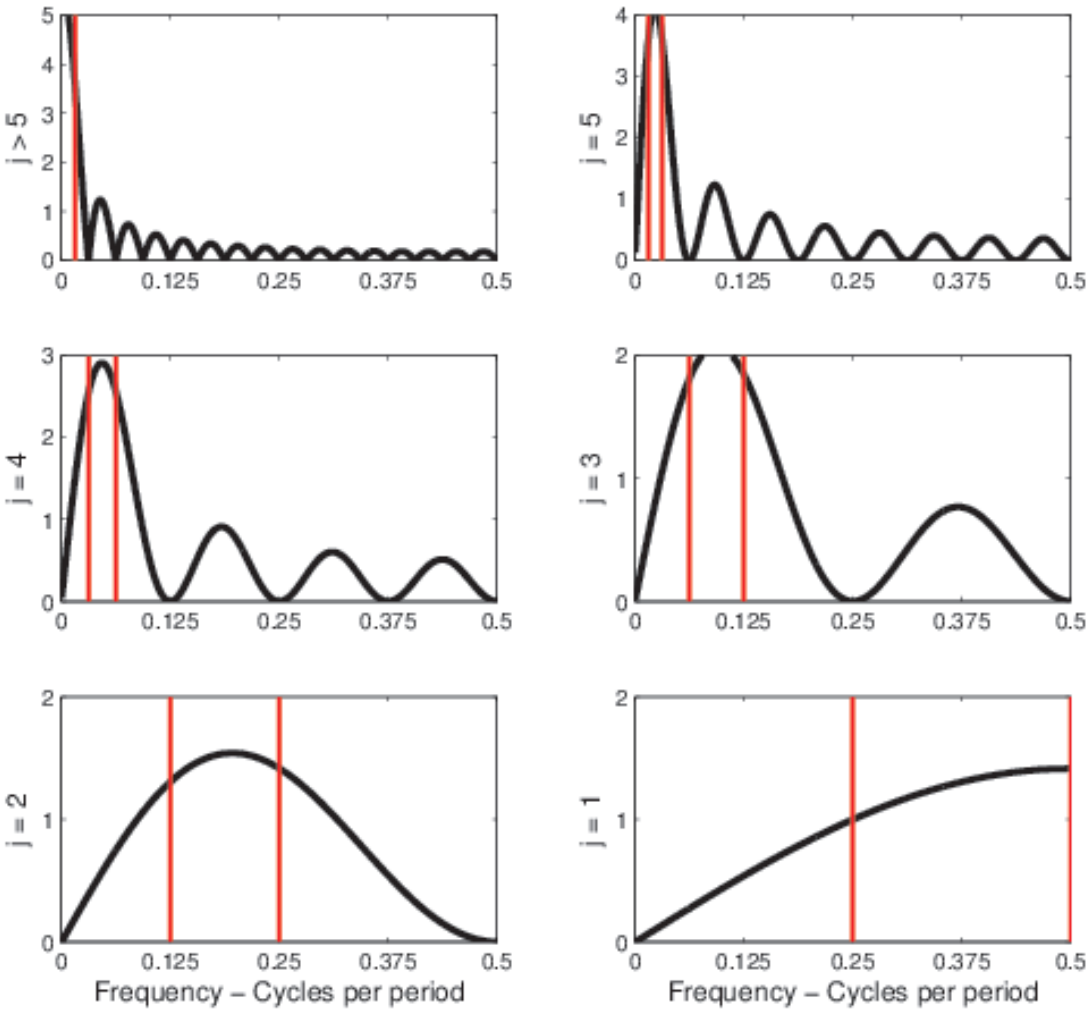

Notes: This figure plots the frequency response (i.e., the squared gained function) of the Haar filter at levels of resolution $j = 1, \ldots, 5, > 5$. Frequencies with positive weights outside of the nominal range (i.e., the vertical red lines) correspond to the leakage associated with this approximation to an ideal band-pass filter. Frequency is in units of cycles per period, which is radian frequency normalized by 2π.

Figure 3.4: Frequency domain representation: LA(8) wavelet filter

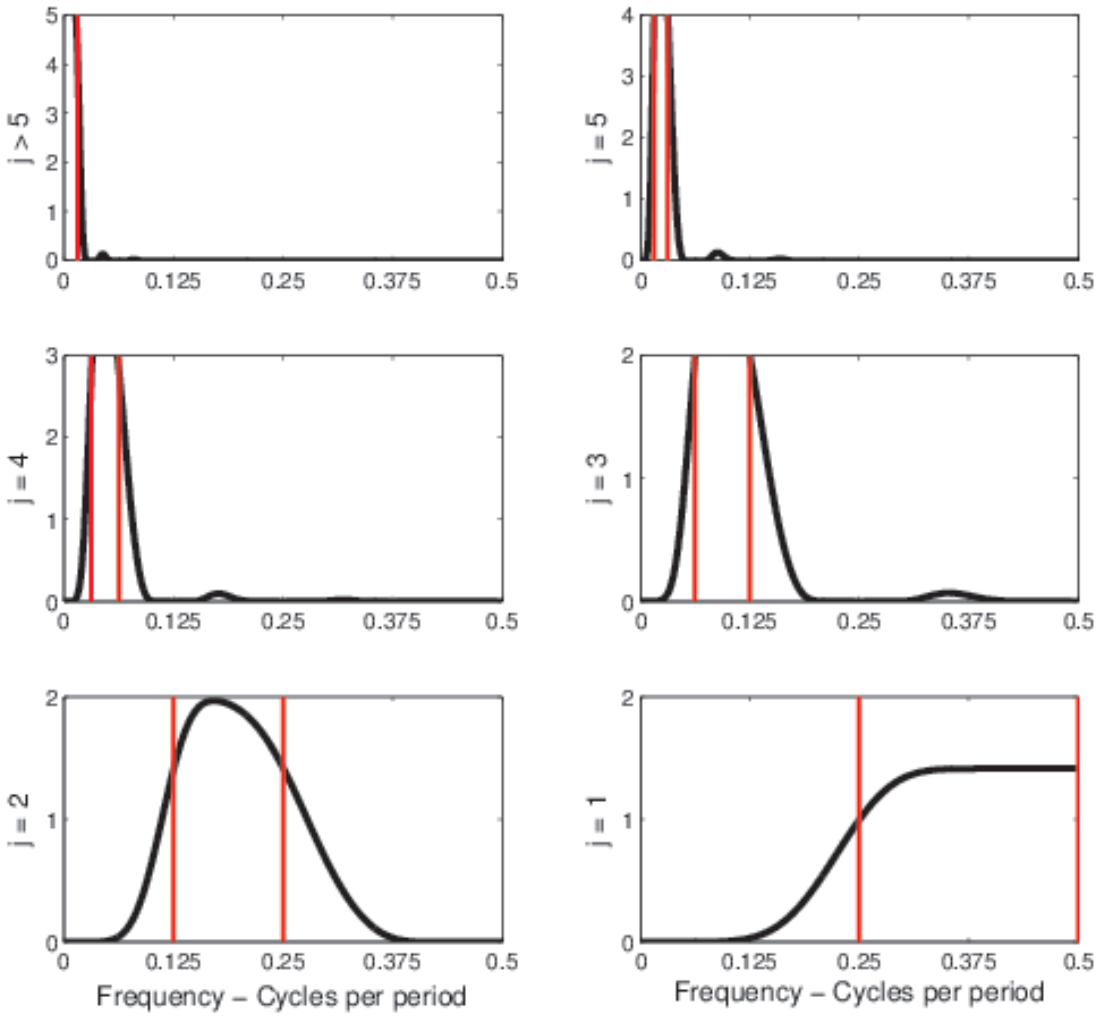

Notes: This figure plots the frequency response (i.e., the squared gained function) of the Daubechies Least Asymmetric filter of length 8 (LA(8)) at levels of resolution $j = 1, \ldots, 5, > 5$. Frequencies with positive weights outside of the nominal range (i.e., the vertical red lines) correspond to the leakage associated with this approximation to an ideal band-pass filter. Frequency is in units of cycles per period, which is radian frequency normalized by 2π.

Figure 3.5: Price of risk from frequency domain risk exposures

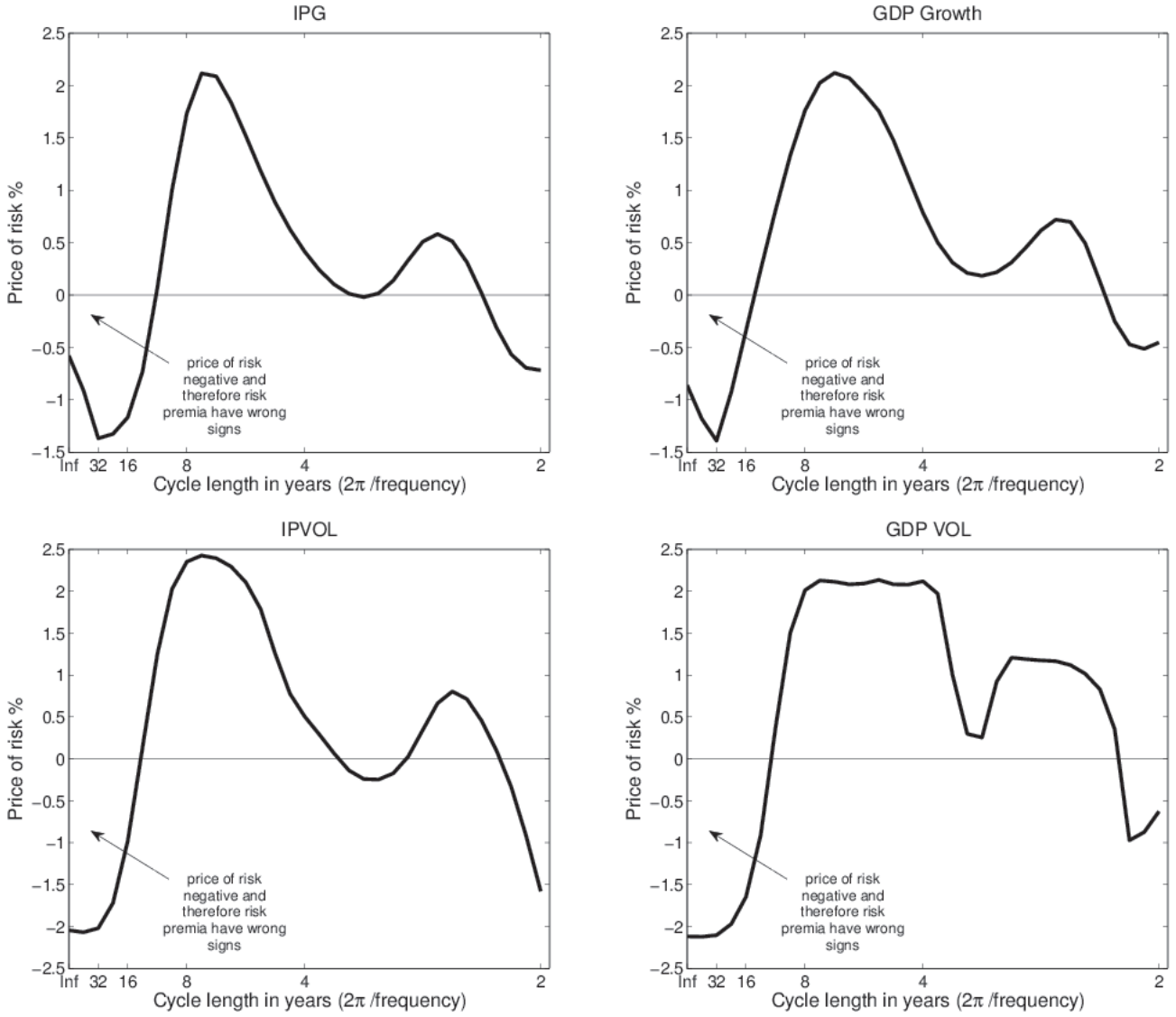

Notes: This figure plots the price of risk in percent per year for the macro shocks across frequencies. To estimate the risk prices I use the normalized gains between asset returns and the macro series at each frequency as regressors in the second pass of the Fama-MacBeth (1973) methodology. The frequency specific risk exposures are always positive - see Equation (3.21) - and therefore the low frequency risk premia carry wrong signs. The x-axis lists the cycle length in years (given a frequency of ω the corresponding cycle has length $2\pi/\omega$ periods). I use demeaned series to estimate the spectral measures based on Welch's (1967) method with a Hamming window and 50% overlap.

Table 3.1: Theoretical pricing weights for Epstein-Zin preferences

Panel A - Z_C^{EZ-SV}		Weight (%) in Frequencies			Median Cycle	Weight (%) in
γ	ψ (EIS)	$>$ 8 years	1.5 - 8 years	$<$ 1.5 years	(in years)	4 - 8 years
2.5	1.5	69.03%	12.17%	18.80%	138.24	4.67%
2.5	2	74.74%	10.81%	14.45%	167.55	4.52%
5	1.5	80.45%	9.45%	10.10%	195.43	4.38%
5	2	83.30%	8.78%	7.92%	208.95	4.31%
7.5	1.5	84.25%	8.55%	7.20%	213.42	4.28%
7.5	2	86.16%	8.10%	5.75%	222.26	4.24%
10	2	87.58%	7.76%	4.66%	228.81	4.20%
Panel B - $Z_{\sigma^2}^{EZ-SV}$		Weight (%) in Frequencies			Median Cycle	Weight (%) in
θ	$\overline{DP}$	$>$ 8 years	1.5 - 8 years	$<$ 1.5 years	(in years)	4 - 8 years
0.960	4.17%	86.99%	10.76%	2.25%	153.96	6.50%
0.965	3.63%	88.61%	9.43%	1.96%	176.39	5.70%
0.970	3.09%	90.23%	8.09%	1.68%	206.31	4.90%
0.975	2.56%	91.86%	6.74%	1.40%	248.20	4.09%
0.980	2.04%	93.49%	5.39%	1.11%	311.03	3.28%

Notes: This table reports the theoretical pricing weights for consumption (Panel A) and consumption volatility (Panel B) under Epstein-Zin preferences in different frequency ranges. γ is the relative risk aversion coefficient, ψ the elasticity of intertemporal substitution (EIS) and $\theta = \left(1 + \overline{DP}\right)^{-1}$ where $\overline{DP}$ is the dividend-price ratio for the wealth portfolio. In Panel A the results are obtained from an annual calibration with $\theta = 0.975$ which corresponds to a 2.56% annual dividend price ratio. In Panel B the shape of $Z_{\sigma^2}^{EZ-SV}$ (and hence the weights) depends only on θ. Also, I report the median cycle in years (i.e., the median cycle corresponds to the frequency for which the pricing weight is split into two halves).

Table 3.2: AR(1)-GARCH(1,1) fit

	μ	ϕ	ω_0	ω_1	ω_2
Estimate	**0.0047**	**0.4914**	**7.96E-05**	**0.3040**	**0.3517**
Std. Error	0.0012	0.0794	2.49E-05	0.0818	0.1631

Notes: This table reports the estimates for the following specification: $IPG_t = \mu + \phi IPG_{t-1} + \nu_t$, where $\sigma_t^2 = \omega_0 + \omega_1 \nu_{t-1}^2 + \omega_2 \sigma_{t-1}^2$. The sample period is 1962:Q1 to 2014:Q4. Bold values denote statistically significant estimates at a 95% confidence level.

Table 3.3: Scale-specific risk exposures

Size	Book-to-market	Panel A - IPG		Panel B - IPVOL	
Small	LowBM	**4.0615**	(2.3587)	-7.1271	(-0.5163)
	2BM	**4.9565**	(3.4651)	-11.0553	(-1.0944)
	3BM	**5.4196**	(3.9546)	-16.2839	(-1.7211)
	4BM	**5.2345**	(3.5456)	**-18.0221**	(-2.0146)
	HighBM	**7.1047**	(4.0767)	**-22.3852**	(-2.4101)
2	LowBM	**3.6032**	(2.7275)	-6.2003	(-0.5440)
	2BM	**3.0875**	(3.8597)	-9.1357	(-1.1931)
	3BM	**3.8616**	(4.3223)	**-12.9265**	(-2.2168)
	4BM	**4.6606**	(5.8665)	**-18.6692**	(-3.2022)
	HighBM	**5.5915**	(3.8623)	**-22.0407**	(-2.9285)
3	LowBM	**3.2898**	(2.7561)	-7.3420	(-0.7343)
	2BM	**3.6470**	(4.5451)	**-14.1497**	(-1.9788)
	3BM	**3.6631**	(6.2559)	**-13.8604**	(-2.7438)
	4BM	**4.2653**	(3.6623)	**-17.1972**	(-2.6265)
	HighBM	**4.4334**	(3.9634)	**-20.1132**	(-3.5106)
4	LowBM	**2.1394**	(2.4089)	-4.6602	(-0.5660)
	2BM	**3.1143**	(3.7338)	-10.9030	(-1.5701)
	3BM	**4.1466**	(3.1829)	-15.0852	(-1.7441)
	4BM	**3.5600**	(3.6093)	**-16.6233**	(-3.0151)
	HighBM	**4.8815**	(3.6945)	**-18.7705**	(-2.8532)
Big	LowBM	**1.8552**	(2.2206)	-3.4436	(-0.4933)
	2BM	**2.6870**	(3.4145)	-9.5265	(-1.7591)
	3BM	**2.5276**	(3.2209)	**-12.6822**	(-2.2650)
	4BM	**2.9551**	(3.5861)	**-13.2140**	(-2.2243)
	HighBM	**2.9540**	(6.1883)	**-14.6385**	(-5.5588)
Industry 1	Consum.	**3.3498**	(5.4492)	**-11.9538**	(-2.6403)
Industry 2	Manuf.	**1.7633**	(3.4149)	-5.3715	(-1.2556)
Industry 3	HiTech	**2.2295**	(2.7424)	**-10.1037**	(-2.4871)
Industry 4	Health	-0.1721	(-0.1862)	1.6506	(0.2781)
Industry 5	Other	**2.9394**	(3.1315)	-12.3844	(-1.6416)
	Wald-stat	225.66		172.24	
	p-value	0.0000		0.0000	

Notes: This table reports first-pass beta estimates for the Fama and French (1993) 25 size and book-to-market portfolios (indexed by Small to Big and LowBM to HighBM) and the 5 FF industry. The betas are estimated component-wise that is regressing scale-specific components of returns on the scale-specific components of macro shocks. The associated t-statistics are based on Newey-West standard errors with $2^j - 1$ lags. The last rows of the table present the Wald test-statistics and their corresponding p-values from testing the joint hypothesis that all component-wise exposures are equal to zero, i.e. $H_0: \beta^{1(j)} = \ldots = \beta^{30(j)} = 0$ for $j = 5$. The initial sample period is 1962:Q1 to 2014:Q4. Bold values denote statistically significant beta estimates at a 95% confidence level.

Table 3.4: Cross-sectional regressions: 5 FF industry and 25 FF size and book-to-market portfolios

	Persistence level / Time-scale						
$j =$	1	2	3	4	5	> 4	> 5
Horizon in quarters	1 - 2	2 - 4	4 - 8	8 - 16	16 - 32	> 16	> 32
Panel A - IPG							
$\lambda_{0,j}$	3.3538	2.0587	1.5998	0.8166	1.0522	0.4911	3.2058
	(3.6105)	(3.6436)	(2.4106)	(1.0952)	(1.4964)	(0.7158)	(3.4181)
λ_j	1.8642	0.3317	0.2108	0.3190	0.3796	0.5028	-0.1860
	(2.4274)	(1.0623)	(1.0671)	(1.6752)	(2.5545)	(2.8691)	(-2.0738)
price of risk	1.865%	0.988%	0.996%	1.606%	2.131%	1.981%	-0.917%
R^2	39.501%	10.645%	10.583%	29.808%	56.695%	45.387%	10.493%
$se(\widehat{R^2})$	(0.2171)	(0.1716)	(0.1681)	(0.2593)	(0.2513)	(0.1318)	(0.1002)
2.5% CI (R^2)	0.0000	0.0000	0.0000	0.0000	0.1117	0.1999	0.0000
97.5% CI (R^2)	0.8113	0.4420	0.4707	0.7925	1.0000	0.7193	0.3113
$p\,(R^2 = 1)$	0.0185	0.0094	0.0111	0.0064	0.0894	0.0452	0.0449
MAPE	1.855%	2.254%	2.325%	1.849%	1.297%	1.709%	2.041%
Panel B - IPVOL							
$\lambda_{0,j}$	1.9246	2.2404	2.3416	1.6946	1.2109	1.1536	2.6466
	(3.3524)	(3.8338)	(3.0952)	(1.9639)	(1.4831)	(1.2143)	(2.4610)
λ_j	0.2644	0.0473	-0.0937	-0.0844	-0.0966	-0.0846	0.0152
	(1.8358)	(0.4964)	(-1.5971)	(-2.2113)	(-3.2556)	(-2.5505)	(0.5667)
price of risk	1.631%	0.414%	-1.047%	-1.195%	-2.207%	-1.487%	0.489%
R^2	30.217%	1.867%	11.707%	16.514%	60.781%	25.569%	2.980%
$se(\widehat{R^2})$	(0.2512)	(0.0728)	(0.1474)	(0.0821)	(0.1026)	(0.1422)	(0.0983)
2.5% CI (R^2)	0.0000	0.0000	0.0000	0.0115	0.4208	0.0000	0.0000
97.5% CI (R^2)	0.7898	0.1544	0.4208	0.3449	0.8154	0.5512	0.2421
$p\,(R^2 = 1)$	0.0088	0.0168	0.0346	0.0156	0.1561	0.0361	0.0167
MAPE	1.963%	2.455%	2.288%	2.114%	1.403%	1.939%	2.157%
# observ.	210	208	204	196	180	196	180

Notes: This table reports the estimates for the zero-beta excess return ($\lambda_{0,j}$) and the price of risk (λ_j) for each scale j along with the corresponding Fama-MacBeth (1973) test statistics in parentheses. The priced factors are the innovations (i.e., first-differences) in the scale-specific components filtered out of IPG (Panel A) and IPVOL (Panel B). In addition, I normalize the scale-wise risk exposures and estimate the price of risk per unit of cross-sectional standard deviation in exposure in percent per year. I also report the sample R^2 for each cross-sectional regression and its standard error, the 95% confidence interval for R^2 which is obtained by pivoting the cdf, the p-value for the Kan et al. (2013) test of $H_0: R^2 = 1$ and the mean absolute pricing error (MAPE) across all securities expressed in percent per year. The initial sample period is 1962:Q1 to 2014:Q4.

Table 3.5: Robustness: Multiresolution decomposition with a LA(8) wavelet filter

	Time-scale						
$j =$	1	2	3	4	5	4:5	> 5
Frequency Resolution in quarters	1 - 2	2 - 4	4 - 8	8 - 16	16 - 32	8 - 32	> 32
Panel A - IPG							
$\lambda_{0,j}$	0.8392	2.5063	1.5282	0.4927	1.7243	0.6186	2.8500
	(1.2119)	(3.4513)	(2.1473)	(0.6631)	(2.1529)	(0.8321)	(3.1814)
λ_j	-0.4532	0.4842	0.1570	0.2388	0.0837	0.2235	-0.0306
	(-1.7793)	(1.4364)	(1.0454)	(2.0496)	(3.4240)	(2.3302)	(-2.2260)
price of risk	-1.287%	1.148%	0.940%	1.779%	2.347%	1.962%	-1.792%
R^2	18.821%	14.384%	9.434%	36.577%	68.717%	48.064%	40.056%
$se(\widehat{R^2})$	(0.1534)	(0.1635)	(0.1617)	(0.2225)	(0.0711)	(0.2615)	(0.2669)
2.5% CI (R^2)	0.0000	0.0000	0.0000	0.0000	0.5658	0.0000	0.0000
97.5% CI (R^2)	0.4797	0.4801	0.4325	0.7763	0.8304	1.0000	0.9109
$p\,(R^2 = 1)$	0.0104	0.0072	0.0125	0.0107	0.2227	0.0598	0.0208
MAPE	1.988%	2.150%	2.380%	1.774%	1.281%	1.467%	1.544%
Panel B - IPVOL							
$\lambda_{0,j}$	3.3873	2.6769	2.4595	1.4778	1.1172	0.9728	2.9092
	(3.8158)	(4.5119)	(3.4852)	(1.9498)	(1.4158)	(1.2990)	(2.9405)
λ_j	0.1869	-0.0330	-0.0077	-0.0597	-0.0370	-0.0639	0.0079
	(2.6515)	(-0.5554)	(-0.1920)	(-3.2623)	(-3.4294)	(-2.9875)	(1.5647)
price of risk	1.599%	-0.452%	-0.145%	-1.409%	-2.383%	-2.004%	1.308%
R^2	29.040%	2.229%	0.225%	22.946%	70.882%	50.133%	21.346%
$se(\widehat{R^2})$	(0.1174)	(0.0825)	(0.0246)	(0.0451)	(0.1358)	(0.1517)	(0.2213)
2.5% CI (R^2)	0.0835	0.0000	0.0000	0.1525	0.4539	0.1996	0.0000
97.5% CI (R^2)	0.5206	0.1987	0.0599	0.3264	0.9604	0.7896	0.6739
$p\,(R^2 = 1)$	0.0259	0.0217	0.0225	0.0281	0.2437	0.0756	0.0100
MAPE	2.029%	2.394%	2.474%	1.953%	1.237%	1.528%	1.841%
# observ.	210	208	204	196	180	180	180

Notes: This table reports the estimates for the zero-beta excess return ($\lambda_{0,j}$) and the price of risk (λ_j) for each scale j along with the corresponding Fama-MacBeth (1973) test statistics in parentheses. The priced factors are the residuals from an AR(1) model fitted to the frequency-specific components filtered out of IPG (Panel A) and IPVOL (Panel B). In addition, I normalize the scale-wise risk exposures and estimate the price of risk per unit of cross-sectional standard deviation in exposure in percent per year. I also report the sample R^2 for each cross-sectional regression and its standard error, the 95% confidence interval for R^2 which is obtained by pivoting the cdf, the p-value for the Kan et al. (2013) test of $H_0 : R^2 = 1$ and the mean absolute pricing error (MAPE) across all securities expressed in percent per year. The initial sample period is 1962:Q1 to 2014:Q4 and the test assets are the 5 FF industry and the 25 FF size and book-to-market portfolios which are priced together.

Table 3.6: Comparison: Business-cycle frequencies vs low-frequencies

Panel A - IPG									
Filter:	Innovations:	λ_0		$\lambda_{\Delta IPG_t^{(5)}}$		$\lambda_{\Delta IPG_t^{(>5)}}$		R^2	MAPE
Haar	First-Diff.	1.4164	(2.2748)	0.3622	(2.5413)	-0.0711	(-1.1215)	58.109%	1.214%
Haar	AR(1) Resid.	1.0111	(1.4136)	0.3790	(2.7478)	-0.0532	(-0.8194)	55.449%	1.344%
D(4)	AR(1) Resid.	1.7480	(1.7078)	0.0827	(2.6433)	-0.0083	(-0.5324)	73.938%	1.120%
D(6)	AR(1) Resid.	1.9198	(1.8723)	0.0740	(2.5300)	-0.0112	(-0.7090)	74.101%	1.129%
LA(8)	AR(1) Resid.	2.0290	(1.9838)	0.0689	(2.4556)	-0.0133	(-0.8433)	73.923%	1.135%
LA(12)	AR(1) Resid.	2.1533	(2.1184)	0.0633	(2.3690)	-0.0160	(-1.0073)	73.625%	1.142%
LA(16)	AR(1) Resid.	2.2143	(2.1874)	0.0607	(2.3265)	-0.0175	(-1.0871)	73.567%	1.146%
LA(20)	AR(1) Resid.	2.2443	(2.2224)	0.0594	(2.3061)	-0.0182	(-1.1241)	73.650%	1.146%
C(6)	AR(1) Resid.	1.7645	(1.7226)	0.0817	(2.6306)	-0.0086	(-0.5497)	73.961%	1.121%
C(12)	AR(1) Resid.	2.0497	(2.0057)	0.0679	(2.4411)	-0.0138	(-0.8695)	73.883%	1.137%
Panel B - IPVOL									
Filter:	Innovations:	λ_0		$\lambda_{\Delta IPVOL_t^{(5)}}$		$\lambda_{\Delta IPVOL_t^{(>5)}}$		R^2	MAPE
Haar	First-Diff.	1.3997	(1.2999)	-0.0958	(-3.2693)	0.0118	(0.4425)	62.567%	1.322%
Haar	AR(1) Resid.	1.3273	(1.2117)	-0.0980	(-3.2331)	0.0122	(0.4962)	60.330%	1.373%
D(4)	AR(1) Resid.	0.9626	(0.8868)	-0.0391	(-3.4139)	-0.0007	(-0.1302)	69.829%	1.233%
D(6)	AR(1) Resid.	1.1175	(1.0127)	-0.0371	(-3.3595)	0.0001	(0.0275)	71.663%	1.202%
LA(8)	AR(1) Resid.	1.2469	(1.1196)	-0.0359	(-3.3161)	0.0009	(0.1595)	72.708%	1.180%
LA(12)	AR(1) Resid.	1.4220	(1.2656)	-0.0342	(-3.2618)	0.0018	(0.3298)	73.643%	1.160%
LA(16)	AR(1) Resid.	1.5160	(1.3423)	-0.0332	(-3.2371)	0.0022	(0.4086)	73.998%	1.148%
LA(20)	AR(1) Resid.	1.5634	(1.3789)	-0.0325	(-3.2299)	0.0024	(0.4367)	74.182%	1.139%
C(6)	AR(1) Resid.	0.9762	(0.8978)	-0.0389	(-3.4095)	-0.0006	(-0.1168)	70.022%	1.229%
C(12)	AR(1) Resid.	1.2744	(1.1425)	-0.0356	(-3.3080)	0.0010	(0.1858)	72.892%	1.175%

Notes: This table reports the estimates for the zero-beta excess return and the price of risk for innovations in macro shocks with business-cycle frequencies and frequencies lower than then business-cycle filtered out of IPG (Panel A) and IPVOL (Panel B) along with the corresponding Fama-MacBeth (1973) test statistics in parentheses. I also report the sample R^2 for each cross-sectional regression and the mean absolute pricing error (MAPE) across all securities expressed in percent per year. The scale-specific risk loadings are estimated from two separate time-series regressions as in Equation (3.12). The first column specifies the filter used for the decomposition and the second how the innovations are quantified. The test assets are the 5 FF industry and the 25 FF size and book-to-market portfolios which are priced together.

Table 3.7: Robustness: Consumption and GDP

	Filter-Innovations:	$\lambda_{0,j}$	λ_j	price of risk	R^2	95% CI (R^2)		$p\,(R^2=1)$	MAPE
Panel A - CG									
$j=5$	Haar-First-Diff.	0.8552	0.2268	1.832%	50.950%	0.1683	0.8629	0.0652	1.442%
		(1.3545)	(2.9644)		(0.1852)				
	Haar-AR(1) Resid.	0.7543	0.2010	1.843%	51.554%	0.1251	0.9145	0.0606	1.418%
		(1.1774)	(2.8973)		(0.2023)				
$j>5$	Haar-First-Diff.	1.7764	0.0380	0.312%	1.477%	0.0000	0.1243	0.0242	2.131%
		(3.1917)	(0.5804)		(0.0483)				
	Haar-AR(1) Resid.	1.5341	0.0592	0.607%	5.591%	0.0000	0.2580	0.0203	2.027%
		(2.7531)	(1.0536)		(0.0996)				
Panel B - GDP Growth									
	Filter-Innovations:	$\lambda_{0,j}$	λ_j	price of risk	R^2	95% CI (R^2)		$p\,(R^2=1)$	MAPE
$j=5$	Haar-First-Diff.	1.1484	0.2038	2.185%	59.588%	0.1446	1.0000	0.1003	1.299%
		(1.6476)	(2.6726)		(0.2449)				
	Haar-AR(1) Resid.	0.8232	0.1998	2.200%	60.402%	0.1705	1.0000	0.1082	1.324%
		(1.1209)	(2.8049)		(0.2217)				
$j>5$	Haar-First-Diff.	1.8843	0.0730	0.483%	2.905%	0.0000	0.1177	0.0484	2.194%
		(2.4412)	(2.1737)		(0.0359)				
	Haar-AR(1) Resid.	1.8353	0.0792	0.532%	3.539%	0.0000	0.1293	0.0487	2.186%
		(2.3384)	(2.3858)		(0.0408)				
Panel C - GDP VOL									
	Filter-Innovations:	$\lambda_{0,j}$	λ_j	price of risk	R^2	95% CI (R^2)		$p\,(R^2=1)$	MAPE
$j=5$	Haar-First-Diff.	1.2689	-0.0313	-2.286%	65.204%	0.4752	0.8326	0.1775	1.347%
		(1.5553)	(-3.2918)		(0.1043)				
	Haar-AR(1) Resid.	1.2246	-0.0314	-2.256%	63.492%	0.4512	0.8438	0.1633	1.390%
		(1.4848)	(-3.2750)		(0.1003)				
$j>5$	Haar-First-Diff.	2.5006	0.0038	0.476%	2.824%	0.0000	0.2267	0.0165	2.132%
		(2.7871)	(0.5125)		(0.1010)				
	Haar-AR(1) Resid.	2.5037	0.0039	0.496%	3.071%	0.0000	0.2359	0.0162	2.123%
		(2.7908)	(0.5326)		(0.1073)				

Notes: This table reports the estimates for the zero-beta excess return ($\lambda_{0,j}$) and the price of risk (λ_j) for $j=5$ and $j>5$ along with the corresponding Fama-MacBeth (1973) test statistics in parentheses for consumption growth (Panel A), GDP growth (Panel B) and GDP volatility (Panel C). In addition, I normalize the scale-wise risk exposures and estimate the price of risk per unit of cross-sectional standard deviation in exposure in percent per year. I also report the sample R^2 for each cross-sectional regression and its standard error, the 95% confidence interval for R^2 which is obtained by pivoting the cdf, the p-value for the Kan et al. (2013) test of $H_0: R^2=1$ and the mean absolute pricing error (MAPE) across all securities expressed in percent per year. The test assets are the 5 FF industry and the 25 FF size and book-to-market portfolios which are priced together.

Table 3.8: Monotonicity tests for scale-specific risk exposures

Panel A		Size					Top−bottom	MR
		Low	2	3	4	High	p-value	p-value
Average Return		2.4179	2.3523	2.2285	2.0582	1.4224	**0.0605**	0.1096
Factor:	Innovations:							
IPG, $j=5$	First-Diff.	4.2226	3.3879	3.1681	2.7663	1.9246	**0.0466**	**0.0638**
	AR(1) Resid.	4.9743	4.1516	3.9305	3.5817	2.9966	**0.0708**	**0.0576**
IPG, $j>5$	First-Diff.	2.1038	3.9455	5.2230	4.4296	5.1834	0.8526	0.8524
	AR(1) Resid.	2.2378	3.9573	5.1772	4.4781	5.4797	0.8674	0.8298
IPVOL, $j=5$	First-Diff.	-14.4232	-11.3900	-11.3147	-10.5324	-7.3189	0.1334	0.2616
	AR(1) Resid.	-15.1306	-12.4025	-12.3119	-12.1835	-9.5072	0.1912	0.2510
IPVOL, $j>5$	First-Diff.	-4.7783	-13.8111	-18.2973	-16.8347	-22.7112	0.9394	0.9212
	AR(1) Resid.	-4.1431	-12.9705	-17.9019	-17.5293	-24.5734	0.9640	0.9140
Null and Alternative Hypotheses for Monotonicity Test								
For returns:		$H_0: R_5 \geq \ldots \geq R_1$ vs $H_1: R_5 < \ldots < R_1$						
For IPG risk-loadings:		$H_0: \beta_5^{(j)} \geq \ldots \geq \beta_1^{(j)}$ vs $H_1: \beta_5^{(j)} < \ldots < \beta_1^{(j)}$						
For IPVOL risk-loadings:		$H_0: \beta_5^{(j)} \leq \ldots \leq \beta_1^{(j)}$ vs $H_1: \beta_5^{(j)} > \ldots > \beta_1^{(j)}$ (price of risk negative)						

Panel B		Book-to-Market					Top−bottom	MR
		Low	2	3	4	High	p-value	p-value
Average Return		1.4157	1.6715	1.7245	2.1067	2.6175	**0.0084**	**0.0178**
Factor:	Innovations:							
IPG, $j=5$	First-Diff.	1.6775	2.3736	2.8378	2.7424	3.2512	**0.0286**	0.1638
	AR(1) Resid.	2.5485	3.2639	3.8851	3.6583	4.1725	**0.0246**	0.3546
IPG, $j>5$	First-Diff.	5.6696	4.8496	3.7237	2.8250	4.6462	0.7044	0.7092
	AR(1) Resid.	6.0051	4.8577	3.8964	3.0853	4.7825	0.7406	0.6654
IPVOL, $j=5$	First-Diff.	-2.8198	-9.1464	-12.6079	-12.8469	-16.5351	**0.0020**	**0.0104**
	AR(1) Resid.	-4.6676	-10.9427	-14.6865	-14.1683	-17.4667	**0.0010**	0.1340
IPVOL, $j>5$	First-Diff.	-20.9278	-18.9825	-17.8095	-15.0369	-20.4243	0.5544	0.6070
	AR(1) Resid.	-23.1213	-19.9025	-18.7947	-15.6145	-20.1773	0.6944	0.6754
Null and Alternative Hypotheses for Monotonicity Test								
For returns:		$H_0: R_5 \leq \ldots \leq R_1$ vs $H_1: R_5 > \ldots > R_1$						
For IPG risk-loadings:		$H_0: \beta_5^{(j)} \leq \ldots \leq \beta_1^{(j)}$ vs $H_1: \beta_5^{(j)} > \ldots > \beta_1^{(j)}$						
For IPVOL risk-loadings:		$H_0: \beta_5^{(j)} \geq \ldots \geq \beta_1^{(j)}$ vs $H_1: \beta_5^{(j)} < \ldots < \beta_1^{(j)}$ (price of risk negative)						

Notes: This table presents the frequency-specific risk exposures with respect to the factors $\Delta IPG_t^{(j)}$ and $\Delta IPVOL_t^{(j)}$ for $j=5$ (i.e., business-cycle frequencies) and $j>5$ (i.e., frequencies lower than 8 years) for one-way portfolio sorts and the corresponding monotonicity tests. The sorting variables are size (Panel A) and book-to-market (Panel B). The first row in each panel reports average excess returns (in percent per quarter) for the test assets. The final column in each panel presents the p-value for the monotonic relation (MR) test. Similarly, the penultimate column presents the bootstrap p-value for the top-minus-bottom difference in the corresponding returns and scale-wise betas.

Table 3.9: Low-frequency risk exposures from OLS regressions of cosine transforms

Size	Book-to-market	Panel A - IPG		Panel B - IPVOL	
Small	LowBM	1.6246	(0.4567)	1.7353	(0.1518)
	2BM	0.9550	(0.2994)	-0.6212	(-0.0608)
	3BM	1.8573	(0.6362)	-3.0890	(-0.3277)
	4BM	2.8741	(0.9701)	-4.7059	(-0.4842)
	HighBM	3.4190	(1.1434)	-5.5335	(-0.5580)
2	LowBM	0.7756	(0.2928)	-2.7807	(-0.3294)
	2BM	0.7183	(0.3693)	-2.5494	(-0.4115)
	3BM	1.2848	(0.6331)	-5.4391	(-0.8511)
	4BM	2.8759	(1.4325)	-6.3927	(-0.9571)
	HighBM	2.7748	(1.3353)	-2.9972	(-0.4251)
3	LowBM	1.0272	(0.4622)	-6.0646	(-0.8746)
	2BM	1.1654	(0.6031)	-4.9715	(-0.8164)
	3BM	1.4443	(0.8183)	-2.6021	(-0.4536)
	4BM	2.1598	(1.1630)	-6.9731	(-1.1788)
	HighBM	1.4852	(0.7633)	-3.2755	(-0.5211)
4	LowBM	0.1775	(0.0988)	-7.7922	(-1.4784)
	2BM	1.8113	(1.0612)	**-9.0789**	(-1.7959)
	3BM	**3.0282**	(1.8326)	**-9.7109**	(-1.8451)
	4BM	**2.9081**	(2.3629)	**-9.1506**	(-2.3165)
	HighBM	**2.9749**	(2.0998)	-4.6433	(-0.9083)
Big	LowBM	2.1240	(1.3457)	**-11.6802**	(-2.7682)
	2BM	1.9703	(1.2880)	**-9.9237**	(-2.2828)
	3BM	**3.3404**	(2.0422)	**-12.4262**	(-2.5462)
	4BM	**3.2330**	(2.7110)	**-9.6730**	(-2.4541)
	HighBM	2.4956	(1.6988)	-5.4032	(-1.0848)
Industry 1	Consum.	1.4603	(0.9905)	**-8.2829**	(-1.9413)
Industry 2	Manuf.	1.7613	(1.5073)	**-8.3192**	(-2.5366)
Industry 3	HiTech	3.0380	(1.4763)	-7.7019	(-1.1359)
Industry 4	Health	2.7236	(1.3275)	**-14.2207**	(-2.5035)
Industry 5	Other	**4.5623**	(2.7788)	**-13.7929**	(-2.5515)

Notes: This table reports low-frequency risk-exposures from a time-series regression between $q = 13$ weighted averages constructed from asset excess returns and (innovations) in macro series based on the Müller and Watson (2015) framework. Note that the low-frequency betas follow a Student-t distribution with 12 degrees of freedom ($q - k = 13 - 1$). Bold values denote statistically significant beta estimates at a 90% confidence level.

Table 3.10: Persistence tests and cross-sectional regressions

Panel A	AR(1) Resid. from IPG		AR(1) Resid. from IPVOL	
q	13	12	13	12
Cut-off periodicity (in years)	8.1538	8.8333	8.1538	8.8333
LFST p-values	0.2671	0.2919	0.4326	0.3663
LFUR p-values	0.0087	0.0077	0.0034	0.0238
MLE for d	0.0500	0.0300	0.0400	0.0900
C.I. for d				
67% level	(-0.14, 0.37)	(-0.16, 0.37)	(-0.17, 0.36)	(-0.12, 0.44)
90% level	(-0.49, 0.58)	(-0.49, 0.57)	(-0.33, 0.55)	(-0.32, 0.66)
95% level	(-0.49, 0.69)	(-0.49, 0.69)	(-0.49, 0.65)	(-0.49, 0.77)

Panel B	Test assets: 5 FF industry and the 25 FF size and book-to-market portfolios				
AR(1) Resid. from	λ_0	λ	price of risk	R^2	MAPE
IPG, $q = 13$	2.0947	0.1300	0.520%	3.019%	2.432%
	(2.4246)	(1.1286)		cut-off periodicity = 8.1538	
IPG, $q = 12$	2.2451	0.0630	0.267%	0.794%	2.434%
	(2.6152)	(0.5743)		cut-off periodicity = 8.8333	
IPG, $q = 11$	2.0194	0.1628	0.681%	5.176%	2.406%
	(2.4077)	(1.5986)		cut-off periodicity = 9.6364	
IPVOL, $q = 13$	2.8709	0.0755	1.155%	14.885%	2.085%
	(3.0138)	(1.4927)		cut-off periodicity = 8.1538	
IPVOL, $q = 12$	2.8302	0.0726	1.402%	21.928%	1.957%
	(3.1730)	(1.7804)		cut-off periodicity = 8.8333	
IPVOL, $q = 11$	2.7825	0.0520	0.792%	6.995%	2.230%
	(2.8230)	(1.1199)		cut-off periodicity = 9.6364	

Notes: Panel A reports the results of the low-frequency persistence tests for the innovations in the macro series. LFST and LFUR are low-frequency point-optimal tests for the $I(0)$ and $I(1)$ models. In addition, I report the maximum likelihood estimate (MLE) of d in the $I(d)$ model and confidence intervals which are constructed by inverting weighted average power (WAP) tests. Panel B reports the estimates for the zero-beta excess return (λ_0) and the price of risk (λ) for low-frequency macro shocks along with the corresponding Fama-MacBeth (1973) test statistics in parentheses. In addition, I report the sample R^2 for each cross-sectional regression and the mean absolute pricing error (MAPE) across all securities expressed in percent per year. The test assets are the 5 FF industry and the 25 Fama and French (1993) size and book-to-market portfolios priced together. The sample period is 1962:Q1 to 2014:Q4.

Table 3.11: Cross-sectional regressions using frequency domain risk exposures

Panel A - IPG						
Freq. (ω)	Cycle length in years	λ_0	λ	price of risk	R^2	MAPE
0.0491	32.00	2.8145	-0.4311	-1.368%	20.889%	2.144%
		(3.4329)	(-2.6219)			
0.0982	16.00	3.1191	-0.4538	-1.168%	15.216%	2.127%
		(3.2217)	(-2.1607)			
0.1963	8.00	0.5828	0.9445	1.735%	33.588%	1.916%
		(0.6617)	(3.9770)			
0.2209	7.11	0.2304	1.0646	2.115%	49.912%	1.601%
		(0.3142)	(4.1554)			
0.2454	6.40	0.3608	0.9152	2.088%	48.638%	1.625%
		(0.5437)	(3.2099)			
0.3927	4.00	1.9556	0.1284	0.413%	1.906%	2.382%
		(2.7175)	(0.4823)			
0.7854	2.00	3.0728	-0.1135	-0.718%	5.750%	2.323%
		(4.4563)	(-0.8933)			
Panel B - IPVOL						
Freq. (ω)	Cycle length in years	λ_0	λ	price of risk	R^2	MAPE
0.0491	32.00	3.2545	-0.2956	-2.020%	45.525%	1.604%
		(3.6134)	(-3.0562)			
0.0982	16.00	3.0655	-0.1644	-0.978%	10.675%	2.159%
		(2.7367)	(-1.3242)			
0.1963	8.00	0.3675	0.3635	2.352%	61.697%	1.393%
		(0.4621)	(4.5846)			
0.2209	7.11	0.5606	0.3364	2.426%	65.682%	1.299%
		(0.7647)	(4.4432)			
0.2454	6.40	0.7956	0.3020	2.393%	63.886%	1.309%
		(1.1396)	(4.2552)			
0.3927	4.00	1.9216	0.0532	0.504%	2.838%	2.341%
		(3.1052)	(0.6159)			
0.7854	2.00	4.2950	-0.1539	-1.581%	27.869%	1.997%
		(6.0026)	(-2.6338)			

Notes: This table reports the estimates for the zero-beta excess return (λ_0) and the price of risk (λ) for the frequency-specific macro shocks along with the corresponding Fama-MacBeth (1973) test statistics in parentheses. The regressors are the estimated gains between asset returns and the macro series at frequency ω. In addition, I report the sample R^2 for each cross-sectional regression and the mean absolute pricing error (MAPE) across all securities expressed in percent per year. The test assets are the 5 FF industry and the 25 Fama and French (1993) size and book-to-market portfolios priced together. The sample period is 1962:Q1 to 2014:Q4. I use demeaned series to estimate the spectral measures based on Welch's (1967) method with a Hamming window and 50% overlap.

Appendix 3A: Scarcity of Low-Frequency Information

I explore the frequency-domain properties of the time series of interest (i.e., IPG or $IPVOL$) using their periodograms. A periodogram is a representation of a time-series as a superposition of sinusoidal waves of various frequencies. Figure 3A.1 plots the periodograms for the macro series. The shaded areas represent frequencies lower than the business-cycle. The very small number of periodogram ordinates in the low-frequency region (i.e., 6 points) reflects the scarcity of information about low-frequency phenomena in the data and highlights the estimation problem underlying Epstein-Zin preferences. That is, the weight that determines risk premia in asset pricing models based on recursive preferences lies on frequencies about which we have limited information.

Since the estimation of the spectral density of a series $\{x_t\}_1^T$ depends heavily on the asymptotic distribution[56] as $T \to \infty$ of the periodogram ordinates, Figure 3A.1 greatly highlights the core intuition behind the work of Müller and Watson (2008, 2015). That is, given the limited number of periodogram ordinates in the low-frequency region inference about the value of the spectral density based on averaging periodogram ordinates is not applicable here (i.e., the asymptotics are based on the assumption that the spectrum is fixed and continuous). Even with a lag window estimator inference about the value of the long-run variance (i.e., spectral density at zero) of a series like consumption growth that contains a highly persistent component is not trivial. In particular, a persistent trend in a series induces a peak in its spectral density around frequency zero and thus the confidence intervals from many estimators have poor coverage. For a thorough discussion see Dew-Becker (2016). This point raises concerns regarding the infinite-horizon results in Kalyvitis and Panopoulou (2013) who estimate the degree of covariability between portfolio returns and consumption growth at zero.

[56] For an introduction to spectral analysis see Chapter 6 in Hamilton (1994) and for a more formal treatment Chapters 4 and 10 in Brockwell and Davis (2009). For the asymptotic properties of the periodogram and the asymptotic behaviour of discrete spectral average estimators see Sections 10.3 and 10.4 in Brockwell and Davis (2009).

Figure 3A.1: Periodograms

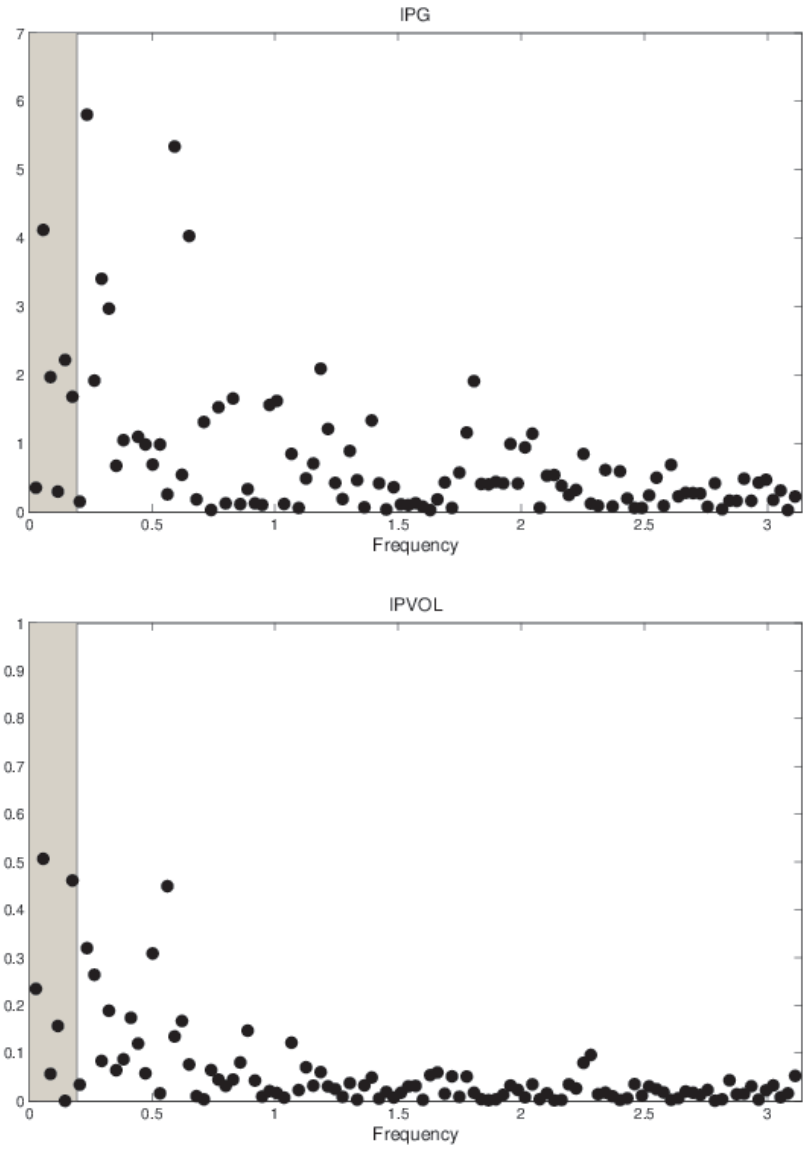

Notes: This figure plots the periodograms for industrial production growth (Panel A) and industrial production volatility (Panel B). The shaded areas represent frequencies lower than the business-cycle. The limited number of periodogram ordinates in the shaded areas reflects the scarcity of information about low-frequency phenomena in the data (i.e., traditional inference tools of spectral analysis are not directly applicable at frequencies close to zero) and highlights the estimation problem underlying Epstein-Zin preferences.

Appendix 3B: Robustness Checks and Additional Results

This Appendix contains additional results and robustness checks that are omitted in the main chapter for brevity.

Residuals from an AR(1) model

Table 3B.1 presents the cross-sectional estimates for the scale-specific macro shocks filtered out of IPG and IPVOL where the innovations are the residuals from an AR(1) model fitted to the factor. The results remain quantitatively similar.

Cross-sectional regressions with different filters

I examine whether the choice of the wavelet filter affects the pricing of the frequency-specific macroeconomic shocks. I use Daubechies Extremal Phase (denoted as D), Daubechies Least Asymmetric (denoted as LA) and Coiflet (denoted as C) types of filters which are the most widely used orthogonal and compactly supported families of filters (see Percival and Walden, 2000). In addition I allow the length of each filter to vary. I refer to each wavelet type and length together, for instance LA(12) refers to the Daubechies Least Asymmetric filter that has a length of 12. The results in Tables 3B.2 - 3B.8 remain similar.

Table 3B.1: Robustness check: Residuals from an AR(1) model

	Persistence level / Time-scale						
j =	1	2	3	4	5	> 4	> 5
Horizon in quarters	1 - 2	2 - 4	4 - 8	8 - 16	16 - 32	> 16	> 32
Panel A - IPG							
$\lambda_{0,j}$	1.9087	2.3529	1.4803	0.6737	0.7305	0.2091	3.1792
	(2.8542)	(3.5492)	(2.1944)	(0.8476)	(0.9775)	(0.2836)	(3.2821)
λ_j	-0.2664	0.5213	0.2496	0.3333	0.3915	0.5070	-0.1772
	(-0.6234)	(1.2959)	(1.1951)	(1.7005)	(2.6520)	(2.9895)	(-1.9279)
price of risk	-0.369%	1.122%	1.086%	1.604%	2.092%	2.025%	-0.877%
R^2	1.550%	13.736%	12.583%	29.755%	54.624%	47.395%	9.604%
$se(\widehat{\mathrm{R}^2})$	(0.0427)	(0.1730)	(0.1782)	(0.2556)	(0.2303)	(0.1090)	(0.1022)
2.5% CI (R^2)	0.0000	0.0000	0.0000	0.0000	0.1373	0.2826	0.0000
97.5% CI (R^2)	0.1051	0.4833	0.5146	0.8088	1.0000	0.6949	0.2846
$p\left(\mathrm{R}^2 = 1\right)$	0.0139	0.0086	0.0112	0.0061	0.0753	0.0528	0.0477
MAPE	2.342%	2.232%	2.324%	1.869%	1.408%	1.755%	2.032%
Panel B - IPVOL							
$\lambda_{0,j}$	2.3672	2.2193	2.5245	1.9856	1.0728	1.2629	2.6556
	(3.5881)	(3.8070)	(3.7130)	(2.2357)	(1.2306)	(1.2231)	(2.5077)
λ_j	0.1545	0.0400	-0.0438	-0.0582	-0.1013	-0.0748	0.0157
	(1.5042)	(0.5440)	(-0.6930)	(-1.4138)	(-3.1984)	(-2.1085)	(0.6282)
price of risk	1.336%	0.476%	-0.515%	-0.804%	-2.098%	-1.291%	0.560%
R^2	20.276%	2.476%	2.831%	7.476%	54.925%	19.277%	3.912%
$se(\widehat{\mathrm{R}^2})$	(0.2247)	(0.0892)	(0.0835)	(0.0794)	(0.0853)	(0.1586)	(0.1147)
2.5% CI (R^2)	0.0000	0.0000	0.0000	0.0000	0.4030	0.0000	0.0000
97.5% CI (R^2)	0.6270	0.2129	0.1885	0.2473	0.7135	0.5300	0.2951
$p\left(\mathrm{R}^2 = 1\right)$	0.0117	0.0161	0.0267	0.0160	0.1187	0.0344	0.0136
MAPE	2.129%	2.444%	2.408%	2.200%	1.511%	2.030%	2.118%
# observ.	210	208	204	196	180	196	180

Notes: This table reports the estimates for the zero-beta excess return ($\lambda_{0,j}$) and the price of risk (λ_j) for each scale j along with the corresponding Fama-MacBeth (1973) test statistics in parentheses. The priced factors are the residuals from an AR(1) model fitted to the scale-specific components filtered out of IPG (Panel A) and IPVOL (Panel B). In addition, I report the sample R^2 for each cross-sectional regression and its standard error, the 95% confidence interval for R^2 which is obtained by pivoting the cdf, the p-value for the Kan et al. (2013) test of $H_0: R^2 = 1$ denoted as $p\left(\mathrm{R}^2 = 1\right)$ and the mean absolute pricing error (MAPE) across all securities expressed in percent per year. The initial sample period is 1962:Q1 to 2014:Q4 and the test assets are the 5 FF industry and the 25 FF size and book-to-market portfolios which are priced together.

Table 3B.2: Multiresolution decomposition with a D(4) wavelet filter

	Time-scale						
$j =$	1	2	3	4	5	4:5	> 5
Frequency Resolution in quarters	1 - 2	2 - 4	4 - 8	8 - 16	16 - 32	8 - 32	> 32
Panel A - IPG							
$\lambda_{0,j}$	0.8226	2.5302	1.5292	0.4938	1.5343	0.5984	2.8222
	(1.1293)	(3.4283)	(2.1396)	(0.6411)	(1.9721)	(0.7958)	(3.1738)
λ_j	-0.4677	0.4907	0.1581	0.2358	0.0949	0.2245	-0.0300
	(-1.6969)	(1.3349)	(1.0348)	(1.9460)	(3.4063)	(2.2757)	(-2.2127)
price of risk	-1.255%	1.097%	0.934%	1.748%	2.409%	1.948%	-1.789%
R^2	17.896%	13.125%	9.316%	35.316%	72.418%	47.376%	39.938%
$se(\widehat{R^2})$	(0.1565)	(0.1611)	(0.1614)	(0.2421)	(0.1292)	(0.2696)	(0.2684)
2.5% CI (R^2)	0.0000	0.0000	0.0000	0.0000	0.4913	0.0000	0.0000
97.5% CI (R^2)	0.4865	0.4692	0.4321	0.8462	0.9709	0.9988	0.9312
$p\,(R^2 = 1)$	0.0096	0.0080	0.0123	0.0094	0.2741	0.0587	0.0201
MAPE	1.997%	2.191%	2.375%	1.773%	1.181%	1.466%	1.556%
Panel B - IPVOL							
$\lambda_{0,j}$	3.3573	2.5299	2.4725	1.4331	1.0013	0.9186	2.8584
	(3.7292)	(4.3140)	(3.5591)	(1.8861)	(1.3167)	(1.2238)	(2.9323)
λ_j	0.1904	-0.0080	-0.0132	-0.0648	-0.0384	-0.0655	0.0076
	(2.4873)	(-0.1284)	(-0.3092)	(-3.2067)	(-3.2159)	(-2.9331)	(1.5150)
price of risk	1.564%	-0.109%	-0.233%	-1.420%	-2.350%	-2.008%	1.287%
R^2	27.769%	0.129%	0.579%	23.310%	68.927%	50.312%	20.664%
$se(\widehat{R^2})$	(0.1311)	(0.0204)	(0.0386)	(0.0457)	(0.1555)	(0.1683)	(0.2227)
2.5% CI (R^2)	0.0409	0.0000	0.0000	0.1533	0.4260	0.1772	0.0000
97.5% CI (R^2)	0.5462	0.0512	0.0884	0.3337	1.0000	0.8226	0.6352
$p\,(R^2 = 1)$	0.0227	0.0196	0.0233	0.0279	0.1919	0.0731	0.0103
MAPE	2.057%	2.445%	2.465%	1.967%	1.242%	1.519%	1.841%
# observ.	210	208	204	196	180	180	180

Notes: This table reports the estimates for the zero-beta excess return ($\lambda_{0,j}$) and the price of risk (λ_j) for each scale j along with the corresponding Fama-MacBeth (1973) test statistics in parentheses. The priced factors are the residuals from an AR(1) model fitted to the frequency-specific components filtered out of IPG (Panel A) and IPVOL (Panel B). In addition, I normalize the scale-wise risk exposures and estimate the price of risk per unit of cross-sectional standard deviation in exposure in percent per year. I also report the sample R^2 for each cross-sectional regression and its standard error, the 95% confidence interval for R^2 which is obtained by pivoting the cdf, the p-value for the Kan et al. (2013) test of $H_0 : R^2 = 1$ and the mean absolute pricing error (MAPE) across all securities expressed in percent per year. The initial sample period is 1962:Q1 to 2014:Q4 and the test assets are the 5 FF industry and the 25 FF size and book-to-market portfolios which are priced together.

Table 3B.3: Multiresolution decomposition with a D(6) wavelet filter

	Time-scale						
$j =$	1	2	3	4	5	4:5	> 5
Frequency Resolution in quarters	1 - 2	2 - 4	4 - 8	8 - 16	16 - 32	8 - 32	> 32
Panel A - IPG							
$\lambda_{0,j}$	0.8286	2.5187	1.5272	0.4952	1.6491	0.6103	2.8385
	(1.1745)	(3.4418)	(2.1420)	(0.6569)	(2.0809)	(0.8172)	(3.1771)
λ_j	-0.4578	0.4892	0.1575	0.2370	0.0879	0.2238	-0.0301
	(-1.7524)	(1.4017)	(1.0424)	(2.0031)	(3.4380)	(2.3075)	(-2.2163)
price of risk	-1.279%	1.132%	0.939%	1.765%	2.380%	1.957%	-1.789%
R^2	18.578%	13.981%	9.407%	36.041%	70.668%	47.788%	39.937%
$se(\widehat{R^2})$	(0.1550)	(0.1636)	(0.1617)	(0.2316)	(0.0899)	(0.2649)	(0.2678)
2.5% CI (R^2)	0.0000	0.0000	0.0000	0.0000	0.5540	0.0000	0.0000
97.5% CI (R^2)	0.5140	0.4416	0.4110	0.8323	0.8749	0.9578	0.9300
$p\,(R^2 = 1)$	0.0101	0.0071	0.0124	0.0094	0.2541	0.0583	0.0204
MAPE	1.989%	2.163%	2.378%	1.775%	1.240%	1.466%	1.550%
Panel B - IPVOL							
$\lambda_{0,j}$	3.3972	2.6275	2.4641	1.4543	1.0617	0.9499	2.8880
	(3.8071)	(4.4529)	(3.5161)	(1.9234)	(1.3682)	(1.2700)	(2.9383)
λ_j	0.1885	-0.0240	-0.0096	-0.0619	-0.0375	-0.0642	0.0078
	(2.6260)	(-0.3958)	(-0.2359)	(-3.2499)	(-3.3469)	(-2.9530)	(1.5471)
price of risk	1.585%	-0.327%	-0.178%	-1.421%	-2.376%	-2.005%	1.302%
R^2	28.516%	1.167%	0.339%	23.350%	70.431%	50.166%	21.162%
$se(\widehat{R^2})$	(0.1172)	(0.0601)	(0.0302)	(0.0430)	(0.1604)	(0.1612)	(0.2223)
2.5% CI (R^2)	0.0696	0.0000	0.0000	0.1536	0.3974	0.1931	0.0000
97.5% CI (R^2)	0.5168	0.1410	0.0661	0.3327	1.0000	0.8138	0.6608
$p\,(R^2 = 1)$	0.0256	0.0209	0.0228	0.0282	0.2257	0.0739	0.0106
MAPE	2.038%	2.419%	2.471%	1.955%	1.239%	1.522%	1.840%
# observ.	210	208	204	196	180	180	180

Notes: This table reports the estimates for the zero-beta excess return ($\lambda_{0,j}$) and the price of risk (λ_j) for each scale j along with the corresponding Fama-MacBeth (1973) test statistics in parentheses. The priced factors are the residuals from an AR(1) model fitted to the frequency-specific components filtered out of IPG (Panel A) and IPVOL (Panel B). In addition, I normalize the scale-wise risk exposures and estimate the price of risk per unit of cross-sectional standard deviation in exposure in percent per year. I also report the sample R^2 for each cross-sectional regression and its standard error, the 95% confidence interval for R^2 which is obtained by pivoting the cdf, the p-value for the Kan et al. (2013) test of $H_0 : R^2 = 1$ and the mean absolute pricing error (MAPE) across all securities expressed in percent per year. The initial sample period is 1962:Q1 to 2014:Q4 and the test assets are the 5 FF industry and the 25 FF size and book-to-market portfolios which are priced together.

Table 3B.4: Multiresolution decomposition with a LA(12) wavelet filter

	Time-scale						
$j =$	1	2	3	4	5	4:5	> 5
Frequency Resolution in quarters	1 - 2	2 - 4	4 - 8	8 - 16	16 - 32	8 - 32	> 32
Panel A - IPG							
$\lambda_{0,j}$	0.8458	2.4926	1.5351	0.4842	1.8120	0.6291	2.8661
	(1.2469)	(3.4598)	(2.1614)	(0.6628)	(2.2391)	(0.8506)	(3.1905)
λ_j	-0.4522	0.4744	0.1555	0.2419	0.0785	0.2232	-0.0314
	(-1.8178)	(1.4675)	(1.0426)	(2.1187)	(3.3675)	(2.3639)	(-2.2510)
price of risk	-1.301%	1.161%	0.936%	1.797%	2.294%	1.972%	-1.801%
R^2	19.234%	14.717%	9.345%	37.359%	65.690%	48.521%	40.478%
$se(\widehat{R^2})$	(0.1520)	(0.1643)	(0.1607)	(0.2118)	(0.0522)	(0.2579)	(0.2653)
2.5% CI (R^2)	0.0000	0.0000	0.0000	0.0000	0.5675	0.0000	0.0000
97.5% CI (R^2)	0.4964	0.4666	0.4187	0.7644	0.7669	1.0000	0.9381
$p\,(R^2 = 1)$	0.0097	0.0073	0.0127	0.0138	0.1907	0.0553	0.0217
MAPE	1.984%	2.140%	2.383%	1.768%	1.332%	1.466%	1.532%
Panel B - IPVOL							
$\lambda_{0,j}$	3.3414	2.7232	2.4550	1.5144	1.2033	1.0054	2.9393
	(3.7847)	(4.5573)	(3.4447)	(1.9780)	(1.4946)	(1.3336)	(2.9402)
λ_j	0.1847	-0.0420	-0.0054	-0.0568	-0.0359	-0.0638	0.0081
	(2.6169)	(-0.7251)	(-0.1396)	(-3.2529)	(-3.4965)	(-3.0578)	(1.5817)
price of risk	1.617%	-0.580%	-0.106%	-1.382%	-2.377%	-2.005%	1.310%
R^2	29.709%	3.671%	0.119%	22.092%	70.529%	50.185%	21.401%
$se(\widehat{R^2})$	(0.1261)	(0.1048)	(0.0179)	(0.0477)	(0.0975)	(0.1356)	(0.2191)
2.5% CI (R^2)	0.0836	0.0000	0.0000	0.1325	0.5522	0.2617	0.0000
97.5% CI (R^2)	0.5324	0.2539	0.0467	0.3277	0.9055	0.7796	0.6186
$p\,(R^2 = 1)$	0.0248	0.0238	0.0222	0.0276	0.2457	0.0791	0.0103
MAPE	2.021%	2.360%	2.477%	1.961%	1.238%	1.535%	1.843%
# observ.	210	208	204	196	180	180	180

Notes: This table reports the estimates for the zero-beta excess return ($\lambda_{0,j}$) and the price of risk (λ_j) for each scale j along with the corresponding Fama-MacBeth (1973) test statistics in parentheses. The priced factors are the residuals from an AR(1) model fitted to the frequency-specific components filtered out of IPG (Panel A) and IPVOL (Panel B). In addition, I normalize the scale-wise risk exposures and estimate the price of risk per unit of cross-sectional standard deviation in exposure in percent per year. I also report the sample R^2 for each cross-sectional regression and its standard error, the 95% confidence interval for R^2 which is obtained by pivoting the cdf, the p-value for the Kan et al. (2013) test of $H_0 : R^2 = 1$ and the mean absolute pricing error (MAPE) across all securities expressed in percent per year. The initial sample period is 1962:Q1 to 2014:Q4 and the test assets are the 5 FF industry and the 25 FF size and book-to-market portfolios which are priced together.

Table 3B.5: Multiresolution decomposition with a LA(16) wavelet filter

	Time-scale						
$j =$	1	2	3	4	5	4:5	> 5
Frequency Resolution in quarters	1 - 2	2 - 4	4 - 8	8 - 16	16 - 32	8 - 32	> 32
Panel A - IPG							
$\lambda_{0,j}$	0.8400	2.4894	1.5445	0.4745	1.8546	0.6346	2.8775
	(1.2514)	(3.4617)	(2.1756)	(0.6554)	(2.2826)	(0.8604)	(3.1989)
λ_j	-0.4551	0.4669	0.1538	0.2444	0.0757	0.2229	-0.0322
	(-1.8503)	(1.4796)	(1.0342)	(2.1668)	(3.3234)	(2.3896)	(-2.2757)
price of risk	-1.317%	1.166%	0.927%	1.811%	2.264%	1.980%	-1.811%
R^2	19.699%	14.840%	9.167%	37.944%	63.960%	48.929%	40.951%
$se(\widehat{R^2})$	(0.1517)	(0.1640)	(0.1618)	(0.2063)	(0.0575)	(0.2550)	(0.2641)
2.5% CI (R^2)	0.0000	0.0000	0.0000	0.0051	0.5333	0.0277	0.0000
97.5% CI (R^2)	0.4806	0.4619	0.4029	0.7688	0.7706	1.0000	0.9412
$p\,(R^2 = 1)$	0.0099	0.0073	0.0128	0.0079	0.1746	0.0573	0.0251
MAPE	1.977%	2.137%	2.386%	1.760%	1.357%	1.462%	1.520%
Panel B - IPVOL							
$\lambda_{0,j}$	3.2988	2.7454	2.4531	1.5410	1.2564	1.0292	2.9611
	(3.7514)	(4.5786)	(3.4203)	(1.9925)	(1.5479)	(1.3550)	(2.9370)
λ_j	0.1831	-0.0461	-0.0042	-0.0549	-0.0350	-0.0639	0.0082
	(2.5695)	(-0.8075)	(-0.1094)	(-3.2246)	(-3.5096)	(-3.1151)	(1.5884)
price of risk	1.628%	-0.640%	-0.083%	-1.360%	-2.369%	-2.007%	1.307%
R^2	30.092%	4.475%	0.073%	21.403%	70.028%	50.253%	21.316%
$se(\widehat{R^2})$	(0.1348)	(0.1150)	(0.0140)	(0.0548)	(0.0782)	(0.1236)	(0.2172)
2.5% CI (R^2)	0.0531	0.0000	0.0000	0.1108	0.5696	0.2835	0.0000
97.5% CI (R^2)	0.5814	0.2842	0.0394	0.3281	0.8603	0.7299	0.6338
$p\,(R^2 = 1)$	0.0250	0.0249	0.0220	0.0227	0.2490	0.0819	0.0105
MAPE	2.018%	2.341%	2.478%	1.967%	1.239%	1.540%	1.845%
# observ.	210	208	204	196	180	180	180

Notes: This table reports the estimates for the zero-beta excess return ($\lambda_{0,j}$) and the price of risk (λ_j) for each scale j along with the corresponding Fama-MacBeth (1973) test statistics in parentheses. The priced factors are the residuals from an AR(1) model fitted to the frequency-specific components filtered out of IPG (Panel A) and IPVOL (Panel B). In addition, I normalize the scale-wise risk exposures and estimate the price of risk per unit of cross-sectional standard deviation in exposure in percent per year. I also report the sample R^2 for each cross-sectional regression and its standard error, the 95% confidence interval for R^2 which is obtained by pivoting the cdf, the p-value for the Kan et al. (2013) test of $H_0 : R^2 = 1$ and the mean absolute pricing error (MAPE) across all securities expressed in percent per year. The initial sample period is 1962:Q1 to 2014:Q4 and the test assets are the 5 FF industry and the 25 FF size and book-to-market portfolios which are priced together.

Table 3B.6: Multiresolution decomposition with a LA(20) wavelet filter

	Time-scale						
$j =$	1	2	3	4	5	4:5	> 5
Frequency Resolution in quarters	1 - 2	2 - 4	4 - 8	8 - 16	16 - 32	8 - 32	> 32
Panel A - IPG							
$\lambda_{0,j}$	0.8298	2.4911	1.5542	0.4647	1.8744	0.6374	2.8863
	(1.2433)	(3.4610)	(2.1881)	(0.6452)	(2.3036)	(0.8654)	(3.2062)
λ_j	-0.4586	0.4613	0.1521	0.2464	0.0741	0.2227	-0.0329
	(-1.8780)	(1.4847)	(1.0238)	(2.2027)	(3.2994)	(2.4108)	(-2.2980)
price of risk	-1.332%	1.168%	0.916%	1.823%	2.249%	1.988%	-1.821%
R^2	20.160%	14.895%	8.959%	38.414%	63.136%	49.302%	41.393%
$se(\widehat{R^2})$	(0.1520)	(0.1638)	(0.1600)	(0.2027)	(0.0616)	(0.2521)	(0.2630)
2.5% CI (R^2)	0.0000	0.0000	0.0000	0.0222	0.5341	0.0012	0.0000
97.5% CI (R^2)	0.5031	0.4757	0.4028	0.7706	0.7589	1.0000	0.9444
$p\,(R^2 = 1)$	0.0100	0.0074	0.0129	0.0145	0.1655	0.0590	0.0260
MAPE	1.970%	2.136%	2.389%	1.753%	1.367%	1.456%	1.509%
Panel B - IPVOL							
$\lambda_{0,j}$	3.2660	2.7597	2.4521	1.5626	1.2865	1.0479	2.9785
	(3.7268)	(4.5954)	(3.4040)	(2.0030)	(1.5819)	(1.3704)	(2.9328)
λ_j	0.1819	-0.0483	-0.0034	-0.0535	-0.0344	-0.0639	0.0083
	(2.5321)	(-0.8541)	(-0.0894)	(-3.1893)	(-3.5092)	(-3.1588)	(1.5910)
price of risk	1.634%	-0.674%	-0.068%	-1.342%	-2.365%	-2.007%	1.303%
R^2	30.337%	4.958%	0.049%	20.819%	69.808%	50.278%	21.200%
$se(\widehat{R^2})$	(0.1445)	(0.1226)	(0.0114)	(0.0588)	(0.0742)	(0.1146)	(0.2157)
2.5% CI (R^2)	0.0388	0.0000	0.0000	0.0973	0.5625	0.2974	0.0000
97.5% CI (R^2)	0.5912	0.3039	0.0346	0.3361	0.8524	0.7420	0.6431
$p\,(R^2 = 1)$	0.0238	0.0256	0.0219	0.0222	0.2353	0.0923	0.0107
MAPE	2.016%	2.328%	2.480%	1.973%	1.236%	1.543%	1.846%
# observ.	210	208	204	196	180	180	180

Notes: This table reports the estimates for the zero-beta excess return ($\lambda_{0,j}$) and the price of risk (λ_j) for each scale j along with the corresponding Fama-MacBeth (1973) test statistics in parentheses. The priced factors are the residuals from an AR(1) model fitted to the frequency-specific components filtered out of IPG (Panel A) and IPVOL (Panel B). In addition, I normalize the scale-wise risk exposures and estimate the price of risk per unit of cross-sectional standard deviation in exposure in percent per year. I also report the sample R^2 for each cross-sectional regression and its standard error, the 95% confidence interval for R^2 which is obtained by pivoting the cdf, the p-value for the Kan et al. (2013) test of $H_0 : R^2 = 1$ and the mean absolute pricing error (MAPE) across all securities expressed in percent per year. The initial sample period is 1962:Q1 to 2014:Q4 and the test assets are the 5 FF industry and the 25 FF size and book-to-market portfolios which are priced together.

Table 3B.7: Multiresolution decomposition with a C(6) wavelet filter

	Time-scale						
$j =$	1	2	3	4	5	4:5	> 5
Frequency Resolution in quarters	1 - 2	2 - 4	4 - 8	8 - 16	16 - 32	8 - 32	> 32
Panel A - IPG							
$\lambda_{0,j}$	0.8220	2.5297	1.5293	0.4936	1.5454	0.5996	2.8238
	(1.1323)	(3.4294)	(2.1402)	(0.6422)	(1.9826)	(0.7980)	(3.1742)
λ_j	-0.4669	0.4906	0.1579	0.2359	0.0941	0.2244	-0.0300
	(-1.7039)	(1.3416)	(1.0352)	(1.9515)	(3.4118)	(2.2790)	(-2.2132)
price of risk	-1.259%	1.100%	0.934%	1.750%	2.407%	1.949%	-1.789%
R^2	17.998%	13.211%	9.318%	35.395%	72.318%	47.423%	39.944%
$se(\widehat{R^2})$	(0.1564)	(0.1612)	(0.1614)	(0.2414)	(0.1251)	(0.2692)	(0.2684)
2.5% CI (R^2)	0.0000	0.0000	0.0000	0.0000	0.4854	0.0000	0.0000
97.5% CI (R^2)	0.4736	0.4811	0.4321	0.8579	0.9714	1.0000	0.9311
$p\,(R^2 = 1)$	0.0097	0.0080	0.0124	0.0095	0.2726	0.0590	0.0202
MAPE	1.996%	2.188%	2.375%	1.773%	1.186%	1.465%	1.555%
Panel B - IPVOL							
$\lambda_{0,j}$	3.3626	2.5405	2.4715	1.4353	1.0065	0.9216	2.8614
	(3.7381)	(4.3301)	(3.5546)	(1.8900)	(1.3214)	(1.2284)	(2.9329)
λ_j	0.1902	-0.0097	-0.0128	-0.0645	-0.0383	-0.0653	0.0076
	(2.5032)	(-0.1553)	(-0.3007)	(-3.2113)	(-3.2286)	(-2.9345)	(1.5184)
price of risk	1.566%	-0.131%	-0.227%	-1.420%	-2.353%	-2.008%	1.288%
R^2	27.858%	0.187%	0.548%	23.317%	69.104%	50.296%	20.719%
$se(\widehat{R^2})$	(0.1300)	(0.0246)	(0.0376)	(0.0457)	(0.1538)	(0.1679)	(0.2227)
2.5% CI (R^2)	0.0564	0.0000	0.0000	0.1510	0.3814	0.1739	0.0000
97.5% CI (R^2)	0.5155	0.0641	0.0862	0.3338	0.9855	0.8239	0.6185
$p\,(R^2 = 1)$	0.0230	0.0198	0.0232	0.0279	0.1948	0.0732	0.0103
MAPE	2.055%	2.443%	2.466%	1.966%	1.242%	1.519%	1.841%
# observ.	210	208	204	196	180	180	180

Notes: This table reports the estimates for the zero-beta excess return ($\lambda_{0,j}$) and the price of risk (λ_j) for each scale j along with the corresponding Fama-MacBeth (1973) test statistics in parentheses. The priced factors are the residuals from an AR(1) model fitted to the frequency-specific components filtered out of IPG (Panel A) and IPVOL (Panel B). In addition, I normalize the scale-wise risk exposures and estimate the price of risk per unit of cross-sectional standard deviation in exposure in percent per year. I also report the sample R^2 for each cross-sectional regression and its standard error, the 95% confidence interval for R^2 which is obtained by pivoting the cdf, the p-value for the Kan et al. (2013) test of $H_0 : R^2 = 1$ and the mean absolute pricing error (MAPE) across all securities expressed in percent per year. The initial sample period is 1962:Q1 to 2014:Q4 and the test assets are the 5 FF industry and the 25 FF size and book-to-market portfolios which are priced together.

Table 3B.8: Multiresolution decomposition with a C(12) wavelet filter

	Time-scale						
$j =$	1	2	3	4	5	4:5	> 5
Frequency Resolution in quarters	1 - 2	2 - 4	4 - 8	8 - 16	16 - 32	8 - 32	> 32
Panel A - IPG							
$\lambda_{0,j}$	0.8401	2.5042	1.5294	0.4910	1.7388	0.6203	2.8527
	(1.2176)	(3.4528)	(2.1497)	(0.6625)	(2.1671)	(0.8351)	(3.1829)
λ_j	-0.4529	0.4825	0.1567	0.2394	0.0828	0.2235	-0.0307
	(-1.7860)	(1.4417)	(1.0449)	(2.0607)	(3.4179)	(2.3358)	(-2.2301)
price of risk	-1.290%	1.150%	0.939%	1.782%	2.339%	1.964%	-1.793%
R^2	18.901%	14.438%	9.418%	36.716%	68.287%	48.144%	40.124%
$se(\widehat{R^2})$	(0.1533)	(0.1634)	(0.1615)	(0.2212)	(0.0669)	(0.2608)	(0.2666)
2.5% CI (R^2)	0.0000	0.0000	0.0000	0.0000	0.5706	0.0143	0.0000
97.5% CI (R^2)	0.4868	0.4537	0.4196	0.7970	0.8168	0.9876	0.9753
$p\,(R^2 = 1)$	0.0105	0.0072	0.0125	0.0110	0.2094	0.0602	0.0209
MAPE	1.987%	2.148%	2.380%	1.773%	1.289%	1.467%	1.542%
Panel B - IPVOL							
$\lambda_{0,j}$	3.3808	2.6853	2.4586	1.4842	1.1304	0.9780	2.9142
	(3.8119)	(4.5209)	(3.4784)	(1.9553)	(1.4280)	(1.3048)	(2.9405)
λ_j	0.1866	-0.0345	-0.0072	-0.0592	-0.0368	-0.0638	0.0079
	(2.6482)	(-0.5844)	(-0.1826)	(-3.2624)	(-3.4430)	(-2.9984)	(1.5677)
price of risk	1.602%	-0.474%	-0.138%	-1.405%	-2.384%	-2.005%	1.308%
R^2	29.163%	2.453%	0.204%	22.813%	70.901%	50.150%	21.360%
$se(\widehat{R^2})$	(0.1182)	(0.0864)	(0.0234)	(0.0458)	(0.1298)	(0.1485)	(0.2209)
2.5% CI (R^2)	0.0769	0.0000	0.0000	0.1481	0.4702	0.2340	0.0000
97.5% CI (R^2)	0.5277	0.2075	0.0523	0.3234	0.9573	0.7872	0.6766
$p\,(R^2 = 1)$	0.0258	0.0221	0.0225	0.0280	0.2443	0.0762	0.0100
MAPE	2.027%	2.389%	2.474%	1.954%	1.236%	1.529%	1.841%
# observ.	210	208	204	196	180	180	180

Notes: This table reports the estimates for the zero-beta excess return ($\lambda_{0,j}$) and the price of risk (λ_j) for each scale j along with the corresponding Fama-MacBeth (1973) test statistics in parentheses. The priced factors are the residuals from an AR(1) model fitted to the frequency-specific components filtered out of IPG (Panel A) and IPVOL (Panel B). In addition, I normalize the scale-wise risk exposures and estimate the price of risk per unit of cross-sectional standard deviation in exposure in percent per year. I also report the sample R^2 for each cross-sectional regression and its standard error, the 95% confidence interval for R^2 which is obtained by pivoting the cdf, the p-value for the Kan et al. (2013) test of $H_0 : R^2 = 1$ and the mean absolute pricing error (MAPE) across all securities expressed in percent per year. The initial sample period is 1962:Q1 to 2014:Q4 and the test assets are the 5 FF industry and the 25 FF size and book-to-market portfolios which are priced together.

Table 3B.9: Monotonicity tests - risk exposures with respect to consumption growth

Panel A		Size					Top−bottom	MR
		Low	2	3	4	High	p-value	p-value
Average Return		2.5273	2.4643	2.3596	2.1788	1.6142	**0.0540**	0.1052
Factor:	Innovations:							
CG, $j = 5$	First-Diff.	7.5269	5.9658	5.4755	4.9459	3.6878	**0.0968**	**0.0664**
	AR(1) Resid.	9.2826	7.3213	6.6320	6.0459	4.6809	**0.0590**	**0.0298**
CG, $j > 5$	First-Diff.	11.5480	10.3283	9.7070	8.6477	8.7718	0.2796	0.2604
	AR(1) Resid.	13.7571	10.9536	9.5592	9.1356	9.0241	0.1620	0.1768
Null and Alternative Hypotheses for Monotonicity Test								
For returns:		$H_0 : R_5 \geq \ldots \geq R_1$ vs $H_1 : R_5 < \ldots < R_1$						
For CG risk-loadings:		$H_0 : \beta_5^{(j)} \geq \ldots \geq \beta_1^{(j)}$ vs $H_1 : \beta_5^{(j)} < \ldots < \beta_1^{(j)}$						
Panel B		Book-to-Market					Top−bottom	MR
		Low	2	3	4	High	p-value	p-value
Average Return		1.6029	1.7924	1.9863	2.2214	2.6464	**0.0121**	**0.0006**
Factor:	Innovations:							
CG, $j = 5$	First-Diff.	3.4811	4.3839	5.2996	5.5229	6.2314	**0.0468**	**0.0102**
	AR(1) Resid.	4.2415	5.3141	6.4794	6.8205	7.6033	**0.0194**	**0.0026**
CG, $j > 5$	First-Diff.	9.0839	7.8512	8.8235	8.1679	10.1217	0.3716	0.3420
	AR(1) Resid.	9.6880	7.3403	9.0684	8.9702	10.0594	0.4750	0.6882
Null and Alternative Hypotheses for Monotonicity Test								
For returns:		$H_0 : R_5 \leq \ldots \leq R_1$ vs $H_1 : R_5 > \ldots > R_1$						
For CG risk-loadings:		$H_0 : \beta_5^{(j)} \leq \ldots \leq \beta_1^{(j)}$ vs $H_1 : \beta_5^{(j)} > \ldots > \beta_1^{(j)}$						

Notes: This table presents the frequency-specific risk exposures with respect to the factors $\Delta CG_t^{(j)}$ for $j = 5$ (i.e., business-cycle frequencies) and $j > 5$ (i.e., frequencies lower than 8 years) for one-way portfolio sorts and the corresponding monotonicity tests. The sorting variables are size (Panel A) and book-to-market (Panel B). The first row in each panel reports average excess returns (in percent per quarter) for the test assets. The final column in each panel presents the p-value for the monotonic relation (MR) test. Similarly, the penultimate column presents the bootstrap p-value for the top-minus-bottom difference in the corresponding returns and scale-wise betas.

Table 3B.10: Controlling for Fama-French factors and momentum

Factor	Innovations	λ_{MKT}	λ_{SMB}	λ_{HML}	λ_{MOM}	λ_5	R^2 / MAPE
Panel A							
IPG, $j = 5$	First-Diff.	1.3701	0.2798	0.7306	2.5117	0.2753	78.801%
		(1.9164)	(0.6286)	(1.3944)	(2.0315)	(2.3715)	1.282%
	AR(1) Resid.	1.3214	0.4438	0.8626	2.2230	0.2062	77.944%
		(1.7596)	(1.0093)	(1.6624)	(1.8511)	(1.9115)	1.289%
IPVOL, $j = 5$	First-Diff.	1.4931	0.6055	0.5558	2.4288	-0.0577	78.175%
		(2.1318)	(1.3239)	(0.9650)	(2.0357)	(-2.2178)	1.255%
	AR(1) Resid.	1.4423	0.6409	0.6091	2.2352	-0.0553	78.030%
		(2.0333)	(1.3972)	(1.0710)	(1.8800)	(-2.1063)	1.265%
Panel B							
GDP Growth, $j = 5$	First-Diff.	1.3620	0.1812	0.6463	2.6037	0.1735	80.812%
		(1.9757)	(0.3983)	(1.2976)	(2.0962)	(3.5020)	1.239%
	AR(1) Resid.	1.1602	0.2937	0.6818	2.2164	0.1432	80.157%
		(1.6162)	(0.6562)	(1.3524)	(1.8480)	(3.1015)	1.255%
GDP VOL, $j = 5$	First-Diff.	1.4134	0.5217	0.3096	2.1640	-0.0237	79.330%
		(2.0257)	(1.1662)	(0.5243)	(1.8154)	(-2.6770)	1.257%
	AR(1) Resid.	1.4151	0.5551	0.4043	2.1091	-0.0217	78.798%
		(2.0147)	(1.2410)	(0.6905)	(1.7734)	(-2.4755)	1.274%

Notes: This table reports estimates for the price of risk (λ_5) for the business-cycle macro factors filtered out of industrial production (Panel A) and GDP (Panel B) after controlling for exposure to the value-weight excess return on the market portfolio (MKT), the size factor (SMB), the value factor (HML) and the momentum factor (MOM). The test assets include the 5 FF industry and the 25 FF size and book-to-market portfolios which are priced together.

Table 3B.11: Cross-sectional regressions using frequency domain risk exposures

Panel A - GDP Growth						
Freq. (ω)	Cycle length in years	λ_0	λ	price of risk	R^2	MAPE
0.0491	32.00	2.8896	-0.2652	-1.391%	21.600%	2.117%
		(3.3915)	(-2.4715)			
0.0982	16.00	2.6431	-0.0840	-0.339%	1.283%	2.383%
		(2.4777)	(-0.5946)			
0.1963	8.00	0.4125	0.5561	1.762%	34.653%	1.856%
		(0.5347)	(3.9909)			
0.2209	7.11	0.4441	0.5431	2.026%	45.776%	1.660%
		(0.6402)	(3.8300)			
0.2454	6.40	0.6391	0.4706	2.120%	50.145%	1.599%
		(0.9861)	(3.3822)			
0.3927	4.00	1.7051	0.0899	0.784%	6.856%	2.295%
		(2.5707)	(0.8736)			
0.7854	2.00	2.7572	-0.0311	-0.453%	2.294%	2.364%
		(4.2272)	(-0.5499)			
Panel B - GDP VOL						
Freq. (ω)	Cycle length in years	λ_0	λ	price of risk	R^2	MAPE
0.0491	32.00	3.2282	-0.3992	-2.105%	49.434%	1.376%
		(3.6847)	(-3.3270)			
0.0982	16.00	3.4116	-0.3211	-1.646%	30.227%	1.817%
		(3.2594)	(-2.3097)			
0.1963	8.00	-0.1535	0.2522	2.012%	45.184%	1.780%
		(-0.1976)	(3.7791)			
0.2209	7.11	0.0572	0.1953	2.127%	50.466%	1.599%
		(0.0773)	(3.1904)			
0.2454	6.40	0.4022	0.1475	2.113%	49.814%	1.586%
		(0.5727)	(2.8684)			
0.3927	4.00	-0.7051	0.1058	2.119%	50.071%	1.533%
		(-0.7635)	(3.1131)			
0.7854	2.00	3.2335	-0.0210	-0.628%	4.395%	2.378%
		(4.5048)	(-0.9133)			

Notes: This table reports the estimates for the zero-beta excess return (λ_0) and the price of risk (λ) for the frequency-specific macro shocks along with the corresponding Fama-MacBeth (1973) test statistics in parentheses. The regressors are the estimated gains between asset returns and the macro series at frequency ω. In addition, I report the sample R^2 for each cross-sectional regression and the mean absolute pricing error (MAPE) across all securities expressed in percent per year. The test assets are the 5 FF industry and the 25 Fama and French (1993) size and book-to-market portfolios priced together. The sample period is 1962:Q1 to 2014:Q4. I use demeaned series to estimate the spectral measures based on Welch's (1967) method with a Hamming window and 50% overlap.

Table 3B.12: Low-frequency risk exposures from OLS regressions of cosine transforms - GDP

Size	Book-to-market	Panel A - GDP Growth		Panel B - GDP VOL	
Small	LowBM	2.0258	(0.4119)	8.4167	(0.2030)
	2BM	1.1926	(0.2707)	-22.2232	(-0.6089)
	3BM	2.9100	(0.7255)	-27.2278	(-0.8140)
	4BM	4.5945	(1.1387)	-31.4923	(-0.9146)
	HighBM	5.1223	(1.2531)	-44.5065	(-1.3049)
2	LowBM	-1.1114	(-0.3041)	-13.4946	(-0.4422)
	2BM	0.4423	(0.1640)	-21.0920	(-0.9673)
	3BM	1.5700	(0.5584)	-39.4870	(-1.8819)
	4BM	4.1186	(1.4959)	-39.5256	(-1.7639)
	HighBM	4.0290	(1.4158)	-31.3226	(-1.2976)
3	LowBM	-0.6267	(-0.2029)	-26.9639	(-1.0892)
	2BM	0.7483	(0.2772)	-31.4754	(-1.5129)
	3BM	1.4402	(0.5833)	-30.7453	(-1.6161)
	4BM	2.7385	(1.0590)	**-43.8356**	(-2.3299)
	HighBM	2.5043	(0.9436)	-39.0487	(-1.9407)
4	LowBM	-1.1933	(-0.4859)	-28.9536	(-1.5206)
	2BM	1.6259	(0.6721)	**-44.4465**	(-2.7444)
	3BM	3.4850	(1.4665)	**-42.7529**	(-2.4055)
	4BM	3.6513	(2.0677)	**-39.5180**	(-3.0562)
	HighBM	3.7022	(1.8310)	**-36.4998**	(-2.2782)
Big	LowBM	0.9841	(0.4242)	-33.5944	(-1.9725)
	2BM	1.5272	(0.6912)	**-45.7457**	(-3.3864)
	3BM	3.3373	(1.3690)	**-53.0754**	(-3.3685)
	4BM	3.5614	(1.9566)	**-41.6802**	(-3.2701)
	HighBM	2.1647	(0.9973)	**-41.9540**	(-2.8815)
Industry 1	Consum.	1.2474	(0.5981)	**-37.5885**	(-2.6765)
Industry 2	Manuf.	1.3935	(0.8137)	**-35.5437**	(-3.3543)
Industry 3	HiTech	1.8326	(0.6024)	-30.3834	(-1.2472)
Industry 4	Health	1.4692	(0.4892)	-28.0008	(-1.1613)
Industry 5	Other	4.7552	(1.8569)	-43.7766	(-2.1018)

Notes: This table reports low-frequency risk-exposures from a time-series regression between $q = 13$ weighted averages constructed from asset excess returns and (innovations) in macro series based on the Müller and Watson (2015) framework. Note that the low-frequency betas follow a Student-t distribution with 12 degrees of freedom ($q - k = 13 - 1$). Bold values denote statistically significant beta estimates at a 95% confidence level. Note that the low-frequency betas for GDP Growth are not statistically significant (i.e., *useless factor*).

Table 3B.13: Cross-sectional regressions using low-frequency betas based on the Müller and Watson (2015) framework - GDP

Test assets: 5 FF industry and the 25 FF size and book-to-market portfolios					
AR(1) Resid. from	λ_0	λ	price of risk	R^2	MAPE
GDP Growth, $q = 13$	1.8108	0.2582	1.715%	32.830%	1.956%
	(2.3935)	(3.3193)	cut-off periodicity = 8.1538		
GDP Growth, $q = 12$	1.8764	0.2465	1.620%	29.273%	2.023%
	(2.4731)	(3.2129)	cut-off periodicity = 8.8333		
GDP Growth, $q = 11$	1.9890	0.2084	1.326%	19.617%	2.183%
	(2.5744)	(2.6681)	cut-off periodicity = 9.6364		
GDP VOL, $q = 13$	1.9564	-0.0123	-0.574%	3.678%	2.388%
	(1.8045)	(-0.8121)	cut-off periodicity = 8.1538		
GDP VOL, $q = 12$	2.1468	-0.0068	-0.329%	1.206%	2.416%
	(1.9704)	(-0.4473)	cut-off periodicity = 8.8333		
GDP VOL, $q = 11$	2.7747	0.0138	1.021%	11.623%	2.107%
	(2.8850)	(1.1726)	cut-off periodicity = 9.6364		

Notes: This table reports the estimates for the zero-beta excess return (λ_0) and the price of risk (λ) for low-frequency macro shocks along with the corresponding Fama-MacBeth (1973) test statistics in parentheses. In addition, I report the sample R^2 for each cross-sectional regression and the mean absolute pricing error (MAPE) across all securities expressed in percent per year. The test assets are the 5 FF industry and the 25 Fama and French (1993) size and book-to-market portfolios priced together. The sample period is 1962:Q1 to 2014:Q4.

Table 3B.14: Comparison for other macro factors: Business-cycle frequencies vs low-frequencies

Panel A - GDP Growth									
Filter:	Innovations:	λ_0		$\lambda_{\Delta GDPG_t^{(5)}}$		$\lambda_{\Delta GDPG_t^{(>5)}}$		R^2	MAPE
Haar	First-Diff.	1.3941	(1.9512)	0.2121	(2.5430)	-0.0408	(-0.8339)	60.397%	1.221%
Haar	AR(1) Resid.	0.9685	(1.2773)	0.2082	(2.5819)	-0.0344	(-0.6635)	61.016%	1.260%
D(4)	AR(1) Resid.	2.3833	(2.2030)	0.0445	(2.6593)	-0.0132	(-1.2298)	78.043%	1.041%
D(6)	AR(1) Resid.	2.6485	(2.4217)	0.0390	(2.4423)	-0.0164	(-1.5062)	76.351%	1.086%
LA(8)	AR(1) Resid.	2.8242	(2.5809)	0.0358	(2.3092)	-0.0187	(-1.7057)	74.868%	1.109%
C(6)	AR(1) Resid.	2.4094	(2.2233)	0.0439	(2.6370)	-0.0135	(-1.2557)	77.913%	1.046%
C(12)	AR(1) Resid.	2.8602	(2.6142)	0.0352	(2.2827)	-0.0192	(-1.7468)	74.540%	1.115%
Panel B - GDP VOL									
Filter:	Innovations:	λ_0		$\lambda_{\Delta GDPVOL_t^{(5)}}$		$\lambda_{\Delta GDPVOL_t^{(>5)}}$		R^2	MAPE
Haar	First-Diff.	1.3175	(1.3953)	-0.0310	(-3.3000)	0.0016	(0.2219)	65.722%	1.309%
Haar	AR(1) Resid.	1.2806	(1.3424)	-0.0310	(-3.2725)	0.0018	(0.2509)	64.181%	1.343%
D(4)	AR(1) Resid.	1.5884	(1.5622)	-0.0224	(-3.1267)	0.0023	(0.4603)	62.007%	1.413%
D(6)	AR(1) Resid.	1.7207	(1.6904)	-0.0215	(-3.0502)	0.0031	(0.6049)	60.458%	1.452%
LA(8)	AR(1) Resid.	1.7941	(1.7642)	-0.0211	(-3.0107)	0.0035	(0.6824)	59.536%	1.478%
C(6)	AR(1) Resid.	1.6016	(1.5749)	-0.0223	(-3.1194)	0.0024	(0.4742)	61.866%	1.416%
C(12)	AR(1) Resid.	1.8051	(1.7757)	-0.0210	(-3.0065)	0.0035	(0.6915)	59.413%	1.482%
Panel C - CG									
Filter:	Innovations:	λ_0		$\lambda_{\Delta CG_t^{(5)}}$		$\lambda_{\Delta CG_t^{(>5)}}$		R^2	MAPE
Haar	First-Diff.	1.6156	(2.8788)	0.2923	(3.4397)	-0.1185	(-1.6714)	61.077%	1.246%
Haar	AR(1) Resid.	1.2466	(2.1466)	0.2401	(3.2805)	-0.0936	(-1.4366)	59.188%	1.265%

Notes: This table reports the estimates for the zero-beta excess return and the price of risk for innovations in macro shocks with business-cycle frequencies and frequencies lower than then business-cycle filtered out of GDP growth (Panel A), GDP volatility (Panel B) and consumption growth (Panel C) along with the corresponding Fama-MacBeth (1973) test statistics in parentheses. I also report the sample R^2 for each cross-sectional regression and the mean absolute pricing error (MAPE) across all securities expressed in percent per year. The scale-specific risk loadings are estimated from two separate time-series regressions as in Equation (3.12). The first column specifies the filter used for the decomposition and the second how the innovations are quantified. The test assets are the 5 FF industry and the 25 FF size and book-to-market portfolios which are priced together.

Conclusion to Thesis

In this thesis, I analyze how scale-dependent macroeconomic shocks propagate to asset prices. Chapter 1 provides an introduction to time-series modelling with multiple scales and scale-wise heterogeneity building mainly upon the studies of Ortu et al. (2013), Bandi et al. (2016) and Bandi and Tamoni (2016). While chapter 1 serves as introduction to the topic, I contribute in the existing literature in the following ways: First, I present new results for the power and size properties of the modified multi-scale variance ratio test of Ortu et al. (2013). Second, I demonstrate theoretically and via simulations that there is a close one-to-one mapping between scale-specific predictability and two-way aggregation irrespective of whether the scale-wise regressor is autoregressive.

In chapter 2, I show that a single factor that captures assets' exposure to business-cycle variation in macroeconomic uncertainty can explain the level and cross-sectional differences of asset returns. In particular, based on portfolio-level tests I demonstrate that uncertainty shocks with persistence ranging from 32 to 128 months carry a negative price of risk of about -2% annually. The price of risk for innovations in the raw series of aggregate uncertainty and for high-frequency fluctuations is not significant. Also, equity exposures are negative and hence risk premia are positive. I quantify macroeconomic uncertainty using the model-free index of Jurado et al. (2015) and my results remain quantitatively similar irrespective of whether uncertainty is derived from monthly, quarterly or annual forecasts..

In chapter 3, I test if the theoretical conditions that Epstein-Zin preferences impose in the frequency domain for asset pricing models are empirically satisfied. My work is motivated by the

spectral decomposition of the pricing kernel under recursive preferences by Dew-Becker and Giglio (2016). I find that macroeconomic shocks with frequencies lower than the business-cycle are not robustly priced in the cross-section of expected returns. In addition, the estimated risk premia are economically small, have wrong signs and the low-frequency risk exposures fail to match known patters in average returns. In total, this chapter highlights the need for risk preferences that allow investors to be more risk averse to business-cycle frequencies and put less weight on cycles lasting centuries.

Overall, the central recommendation of my work is that empirical studies should pay more attention to the information content of scale-specific macroeconomic shocks. Furthermore, my thesis demonstrates that - in contrast with the conventional wisdom of the long-run risks literature - business-cycle length fluctuations are of first-order importance for asset pricing and hence stabilisation and monetary policies should focus at this specific frequency range. That is, in line with mainstream macroeconomic theory central banks should aim the effects of their policies (e.g., smoothing out output and consumption) primarily at business-cycle frequencies - rather than trying to reduce uncertainty about very long-run growth rates.

Limitations and Directions for Future Work

In chapter 1, the modified multi-scale variance ratio tests demonstrate modest power in small samples when there is a persistent component in the time-series localized at low-frequencies. Deriving the asymptotic joint distribution of these tests could allow to gain power. In chapters 2 and 3 my analysis is purely non-structural and lacks a formal theoretical set-up. What is more, the empirical evidence in these chapters cannot be nested within standard asset pricing models. From this perspective, promising directions for future work include risk preferences with horizon dependent risk aversion (as a starting point see Andries et al., 2015) or asset pricing models that incorporate multi-scale pricing kernels. Moreover, in chapter 3 the exact theoretical mapping (or potential differences in power) between the three econometric techniques is not clear. Finally, on

the empirical front two interesting extensions include: i) performing a scale-by-scale decomposition of the risk exposures with respect to the market factor to investigate scale-dependent downside risk (for instance, see Lettau et al. 2014 and Dobrynskaya, 2014) and ii) modelling the dependence of macro uncertainty and volatility shocks across different time horizons via wavelet-based hidden Markov trees. In the spirit of Gençay et al. (2010), I expect that a state (regime) with low macro uncertainty at a long time horizon is most likely followed by low macro uncertainty states at shorter time horizons. In contrast, a high macro uncertainty state at long time horizons will not necessarily imply a high macro uncertainty state at shorter time horizons (i.e., I expect macro uncertainty to exhibit asymmetric vertical dependence across different time horizons).

Additional Appendices

Appendix A: Monotonicity in Factor Loadings

I present how to implement the monotonic relation (MR) test of Patton and Timmermann (2010) to test for monotonicity in factor loadings. The MR test specifies a flat or weakly pattern under the null hypothesis and a strictly monotonic relation under the alternative[57]. The main advantage of the test is that it makes no parametric assumptions on the distribution from which the data are drawn. Below I describe the MR methodology for the general case with the extension for horizon-specific exposures being straightforward (for instance, using component-wise regressions as in Equation (3.12)).

Let $\{r_{i,t},\, i = 1, \ldots, N; t = 1, \ldots, T\}$ be the set of returns recorded for N assets over T time periods which is regressed on K risk factors $\boldsymbol{F}_t = (F_{1,t}, \ldots, F_{K,t})^{'}$, that is,

$$r_{i,t} = \boldsymbol{\beta}_i \boldsymbol{F}_t + e_{i,t} \tag{A.1}$$

where $\boldsymbol{\beta}_i = (\beta_{1,i}, \ldots, \beta_{K,i})$. The associated hypotheses[58] on the $j - th$ parameter $(1 \leq j \leq K)$ in the above regression is

[57] I would like to thank Andrew Patton for making the code available in his personal website: http://public.econ.duke.edu/~ap172/

[58] To test for monotonically decreasing patters the order of the assets is simply reversed.

$$H_0 : \ \beta_{j,N} \leq \beta_{j,N-1} \leq \ldots \leq \beta_{j,1} \text{ versus} \tag{A.2}$$

$$H_1 : \ \beta_{j,N} > \beta_{j,N-1} > \ldots > \beta_{j,1}. \tag{A.3}$$

The alternative hypotheses can be rewritten as

$$H_1 : \ \min_{i=1,\ldots,N} \{\beta_{j,i} - \beta_{j,i-1}\} > 0 \tag{A.4}$$

that is if the smallest value of $\{\beta_{j,i} - \beta_{j,i-1}\} > 0$ then it must be that $\{\beta_{j,i} - \beta_{j,i-1}\} > 0$ for all $i = 1, \ldots, N$.

Patton and Timmermann (2010) use the stationary bootstrap of Politis and Romano (1994) to randomly draw a new sample of returns and factors $\left\{\tilde{r}^{(b)}_{i,\tau(t)},\ i = 1, \ldots, N; \tau(1), \ldots, \tau(T)\right\}$ and $\left\{\boldsymbol{F}^{(b)}_{\tau(t)},\ \tau(1), \ldots, \tau(T)\right\}$ where $\tau(t)$ is the new time index which is a random draw from the original set $\{1, \ldots, T\}$ and b is an indicator for the bootstrap number which runs from $b = 1$ to $b = B$. To preserve any cross-sectional dependencies in returns the randomized time index $\tau(t)$ is common across portfolios. Moreover, observations are re-sampled in blocks - to preserve the dependence in the original series - where the size of each block is random and determined by a geometric distribution. The bootstrap regression takes the form

$$\tilde{r}^{(b)}_{i,\tau(t)} = \boldsymbol{\beta}^{(b)}_i \boldsymbol{F}^{(b)}_{\tau(t)} + e^{(b)}_{i,\tau(t)}. \tag{A.5}$$

The null hypothesis is imposed by subtracting the estimated parameter $\hat{\boldsymbol{\beta}}_i$ from the parameter estimate obtained on the bootstrapped series $\hat{\boldsymbol{\beta}}^{(b)}_i$. The test statistic for the bootstrap sample - motivated by Equation (A.4) - is computed as

$$J^{(b)}_{j,T} \equiv \min_{i=1,\ldots,N} \left\{ \left(\hat{\beta}^{(b)}_{j,i} - \hat{\beta}_{j,i} \right) - \left(\hat{\beta}^{(b)}_{j,i-1} - \hat{\beta}_{j,i-1} \right) \right\}. \tag{A.6}$$

Patton and Timmermann (2010) then count the number of times a pattern at least as unfavourable against the null as that observed in the real sample emerges. An estimate of the p-value for the null hypothesis is given by

$$\hat{p} = \frac{1}{B}\sum_{b=1}^{B} \mathbf{1}\left\{J_{j,T}^{(b)} > J_{j,T}\right\} \tag{A.7}$$

where the indicator $\mathbf{1}\left\{J_{j,T}^{(b)} > J_{j,T}\right\}$ is one if $J_{j,T}^{(b)} > J_{j,T}$ and otherwise zero. When the bootstrap p-value is less than 0.05 there are significant evidence against the null in favor of a monotonically increasing relation. To eliminate the impact of cross-sectional heteroskedasticity Patton and Timmermann (2010) suggest implementing a studentized version of the bootstrap in line with Hansen (2005) and Romano and Wolf (2005).

Appendix B: Asymptotic Distribution of R^2

Let f be a $K-$vector of factors , R a vector of returns on N assets with mean μ_R and covariance matrix V_R and β the $N \times K$ matrix of regression betas. The $K-$factor beta pricing model is given by $\mu_R = X\gamma$ where $X = [1_N, \beta]$ and $\gamma = [\gamma_0, \gamma_1]$. The pricing errors of the N assets are given by $e = \mu_R - X\gamma$ and the cross-sectional R^2 is defined as

$$R^2 = 1 - \frac{Q}{Q_0} \tag{B.1}$$

where $Q = \acute{e}We$ denotes the aggregate pricing-error measure, $Q_0 = \acute{e_0}We_0$ the cross-sectional variance of mean returns, $e_0 = \left[I_N - 1_N\left(1_N^{'}W1_N\right)^{-1}1_N^{'}W\right]\mu_R$ deviations of mean returns from their cross-sectional average and W is an $N \times N$ weighting matrix (throughout this thesis I assume that $W = I_N$ - OLS case).

When $0 < R^2 < 1$, the asymptotic distribution of R^2 is given by

$$\sqrt{T}\left(\widehat{\mathrm{R}^2}-\mathrm{R}^2\right)\xrightarrow{a}\mathcal{N}\left(0,\sum_{j=-\infty}^{\infty}E[n_t n_{t+j}]\right) \tag{B.2}$$

where $n_t = 2\left[-u_t y_t + (1-\mathrm{R}^2)v_t\right]/Q_0$, $u_t = \acute{e}W\left(R_t-\mu_R\right)$, $v_t = \acute{e}_0 W\left(R_t-\mu_R\right)$ and y_t is the normalized stochastic discount factor.

When the model is correctly specified (i.e., $\mathrm{R}^2=1$)

$$\sqrt{T}\left(\widehat{\mathrm{R}^2}-1\right)\xrightarrow{a}\sum_{j=1}^{N-K-1}\frac{\xi_j}{Q_0}x_j \tag{B.3}$$

where the x_j's are independent χ^2_1 random variables and the ξ_j's are the eigenvalues of $P'W^{\frac{1}{2}}SW^{\frac{1}{2}}P$ where P is an $N\times(N-K-1)$ orthonormal matrix with columns orthogonal to $W^{\frac{1}{2}}C$, S is the asymptotic covariance matrix of $\frac{1}{\sqrt{T}}\sum_{t=1}^{T}\epsilon_t y_t$, $\epsilon_t = R_t-\mu_R-\beta\left(f_t-\mu_f\right)$. Equation (B.3) can be used as a specification test.

Pivoting the cdf

Plot the $100(a/2)$ and $100(1-a/2)$ percentiles of the distribution of $\widehat{\mathrm{R}^2}$ for different values of R^2. Draw a horizontal line at the observed value of $\widehat{\mathrm{R}^2}$. The horizontal line will intersect first the $100(1-a/2)$ percentile line and then the $100(a/2)$ line. The interval between these two intersection points gives a $100(1-a)\%$ confidence interval.

Bibliography

Andries, Marianne, Thomas M. Eisenbach, and Martin Schmalz, 2015, Asset pricing with horizon-dependent risk aversion, Working Paper, Available at SSRN: http://ssrn.com/abstract=2535919.

Baillie, Richard T., 1996, Long memory processes and fractional integration in econometrics, *Journal of Econometrics* 73, 5–59.

Baker, Scott R., Nicholas Bloom, and Steven J. Davis, 2013, Measuring economic policy uncertainty, Working Paper, Available at SSRN: http://ssrn.com/abstract=2198490.

Bali, Turan G., Stephen Brown, and Yi Tang, 2016, Is economic uncertainty priced in the cross-section of stock returns?, *Journal of Financial Economics,* Forthcoming.

Bali, Turan G., Stephen J. Brown, and Mustafa O Caglayan, 2014, Macroeconomic risk and hedge fund returns, *Journal of Financial Economics* 114, 1–19.

Bali, Turan G., and Hao Zhou, 2014, Risk, uncertainty, and expected returns, *Journal of Financial and Quantitative Analysis,* Forthcoming.

Bandi, Federico M., Benoit Perron, Andrea Tamoni, and Claudio Tebaldi, 2016, The scale of predictability, Working Paper, Available at SSRN: http://ssrn.com/abstract=2184260.

Bandi, Federico M., and Benoît Perron, 2008, Long-run risk-return trade-offs, *Journal of Econometrics* 143, 349–374.

Bandi, Federico M., and Andrea Tamoni, 2016, The horizon of systematic risk: A new beta representation, Working Paper, Available at SSRN: http://ssrn.com/abstract=2337973.

Bansal, Ravi, 2007, Long-run risks and financial markets, Working Paper 13196, National Bureau of Economic Research.

Bansal, Ravi, Robert F. Dittmar, and Christian T. Lundblad, 2005, Consumption, dividends, and the cross section of equity returns, *Journal of Finance* 60, 1639–1672.

Bansal, Ravi, Dana Kiku, Ivan Shaliastovich, and Amir Yaron, 2014, Volatility, the macroeconomy, and asset prices, *Journal of Finance* 69, 2471–2511.

Bansal, Ravi, Dana Kiku, and Amir Yaron, 2012, An empirical evaluation of the long-run risks model for asset prices, *Critical Finance Review* 1, 183–221.

Bansal, Ravi, and Amir Yaron, 2004, Risks for the long run: A potential resolution of asset pricing puzzles, *Journal of Finance* 59, 1481–1509.

Baxter, Marianne, and Robert G. King, 1999, Measuring business cycles: Approximate band-pass filters for economic time series, *Review of Economics and Statistics* 81, 575–593.

Beeler, Jason, and John Y. Campbell, 2012, The long-run risks model and aggregate asset prices: An empirical assessment, *Critical Finance Review* 1, 141–182.

Bekaert, Geert, Eric Engstrom, and Yuhang Xing, 2009, Risk, uncertainty, and asset prices, *Journal of Financial Economics* 91, 59–82.

Beveridge, Stephen, and Charles R. Nelson, 1981, A new approach to decomposition of economic time series into permanent and transitory components with particular attention to measurement of the 'business cycle', *Journal of Monetary Economics* 7, 151–174.

Black, Fischer, 1972, Capital market equilibrium with restricted borrowing, *Journal of Business* 45, 444–455.

Bloom, Nicholas, 2009, The impact of uncertainty shocks, *Econometrica* 77, 623–685.

Bloom, Nicholas, 2014, Fluctuations in uncertainty, *Journal of Economic Perspectives* 28, 153–176.

Bloom, Nicholas, Max Floetotto, Nir Jaimovich, Itay Saporta-Eksten, and Stephen J. Terry, 2012, Really Uncertain Business Cycles, NBER Working Papers 18245, National Bureau of Economic Research, Inc.

Bloom, Nick, Stephen Bond, and John Van Reenen, 2007, Uncertainty and investment dynamics, *Review of Economic Studies* 74, 391–415.

Boguth, Oliver, and Lars-alexander Kuehn, 2013, Consumption volatility risk, *Journal of Finance* 68, 2589–2615.

Boons, Martijn, 2016, State variables, macroeconomic activity and the cross-section of individual stocks, *Journal of Financial Economics* 119, 489–511.

Boons, Martijn, and Andrea Tamoni, 2016, Horizon-specific macroeconomic risks and the cross-section of expected returns, Working Paper, Available at SSRN: http://ssrn.com/abstract=2516251.

Boudoukh, Jacob, Matthew Richardson, and Robert F. Whitelaw, 2008, The myth of long-horizon predictability, *Review of Financial Studies* 21, 1577–1605.

Box, George E. P., and David A. Pierce, 1970, Distribution of residual autocorrelations in autoregressive-integrated moving average time series models, *Journal of the American Statistical Association* 65, 1509–1526.

Brennan, Michael J., Ashley W. Wang, and Yihong Xia, 2004, Estimation and test of a simple model of intertemporal capital asset pricing, *Journal of Finance* 59, 1743–1776.

Brockwell, Peter J., and Richard A. Davis, 2009, *Time Series: Theory and Methods*, Springer Series in Statistics (Springer).

Burns, Arthur F., and Wesley C. Mitchell, 1946, *Measuring Business Cycles*, number burn46-1 in NBER Books (National Bureau of Economic Research, Inc).

Campbell, John Y., 1993, Intertemporal asset pricing without consumption data, *American Economic Review* 83, 487–512.

Campbell, John Y., 1996, Understanding risk and return, *Journal of Political Economy* 104, 298–345.

Campbell, John Y., and John H. Cochrane, 1999, By force of habit: A consumption-based explanation of aggregate stock market behavior, *Journal of Political Economy* 107, 205–251.

Campbell, John Y., Stefano Giglio, Christopher Polk, and Robert Turley, 2014, An intertemporal capm with stochastic volatility, Working Paper, Available at SSRN: http://ssrn.com/abstract=2021846.

Campbell, John Y., and Rober J. Shiller, 1988, The dividend-price ratio and expectations of future dividends and discount factors, *Review of Financial Studies* 1, 195–228.

Campbell, John Y., and Motohiro Yogo, 2006, Efficient tests of stock return predictability, *Journal of Financial Economics* 81, 27–60.

Casella, George, and Roger L. Berger, 2002, *Statistical Inference*, Duxbury advanced series in statistics and decision sciences (Thomson Learning).

Chen, Hui, 2010, Macroeconomic conditions and the puzzles of credit spreads and capital structure, *Journal of Finance* 65, 2171–2212.

Chen, Joseph, 2002, Intertemporal capm and the cross-section of stock returns, Working paper, Available at SSRN: http://ssrn.com/abstract=301918.

Chen, Nai-Fu, Richard Roll, and Stephen A. Ross, 1986, Economic forces and the stock market, *Journal of Business* 59, 383–403.

Cochrane, John H., 1996, A cross-sectional test of an investment-based asset pricing model, *Journal of Political Economy* 104, 572–621.

Cochrane, John H., 2005, *Asset Pricing: Revised Edition* (Princeton University Press).

Cochrane, John H., 2008, The dog that did not bark: A defense of return predictability, *Review of Financial Studies* 21, 1533–1575.

Cogley, Timothy, 2001, Alternative definitions of the business cycle and their implications for business cycle models: A reply to Torben Mark Pederson, *Journal of Economic Dynamics and Control* 25, 1103–1107.

Cogley, Timothy, and James M. Nason, 1995, Effects of the hodrick-prescott filter on trend and difference stationary time series implications for business cycle research, *Journal of Economic Dynamics and Control* 19, 253–278.

Coifman, Ronald R., and David L. Donoho, 1995, Translation-invariant de-noising, in Anestis Antoniadis, and Georges Oppenheim, eds., *Wavelets and Statistics*, volume 103 of *Lecture Notes in Statistics*, 125–150 (Springer New York).

Collin-Dufresne, Pierre, Michael Johannes, and Lars A. Lochstoer, 2016, Parameter learning in general equilibrium: The asset pricing implications, *American Economic Review* 106, 664–98.

Comin, Diego, and Mark Gertler, 2006, Medium-term business cycles, *American Economic Review* 96, 523–551.

Constantinides, George M., and Anisha Ghosh, 2011, Asset pricing tests with long-run risks in consumption growth, *Review of Asset Pricing Studies* 1, 96–136.

Crowley, Patrick M., 2007, A guide to wavelets for economists, *Journal of Economic Surveys* 21, 207–267.

Daniel, Kent, and Sheridan Titman, 2012, Testing factor-model explanations of market anomalies, *Critical Finance Review* 1, 103–139.

Daubechies, Ingrid, 1990, The wavelet transform, time-frequency localization and signal analysis, *IEEE Transactions on Information Theory* 36, 961–1005.

Dew-Becker, Ian, 2016, How risky is consumption in the long-run? benchmark estimates from a robust estimator, *Review of Financial Studies,* Forthcoming.

Dew-Becker, Ian, and Stefano Giglio, 2016, Asset Pricing in the Frequency Domain: Theory and Empirics, *Review of Financial Studies,* Forthcoming.

Diciccio, Thomas J., and Joseph P. Romano, 1988, A review of bootstrap confidence intervals, *Journal of the Royal Statistical Society. Series B (Methodological)* 50, 338–354.

Dickey, David A., and Wayne A. Fuller, 1979, Distribution of the estimators for autoregressive time series with a unit root, *Journal of the American Statistical Association* 74, 427–431.

Diebold, Francis X., 1998, The past, present, and future of macroeconomic forecasting, *Journal of Economic Perspectives* 12, 175–192.

Diebold, Francis X., and Glenn D. Rudebusch, 1996, Measuring business cycles: A modern perspective, *Review of Economics and Statistics* 78, 67–77.

Dijkerman, Robert W., and Ravi R. Mazumdar, 1994, Wavelet representations of stochastic processes and multiresolution stochastic models, *IEEE Transactions on Signal Processing* 42, 1640–1652.

Dobrynskaya, Victoria, 2014, Downside market risk of carry trades, *Review of Finance* 18, 1885–1913.

Duchesne, Pierre, 2006, On testing for serial correlation with a wavelet-based spectral density estimator in multivariate time series, *Econometric Theory* 22, 633–676.

Elliott, Graham, 1998, On the robustness of cointegration methods when regressors almost have unit roots, *Econometrica* 66, 149–158.

Elliott, Graham, 1999, Efficient tests for a unit root when the initial observation is drawn from its unconditional distribution, *International Economic Review* 40, 767–784.

Engle, Robert F., 1974, Interpreting spectral analyses in terms of time-domain models, Working Paper 37, National Bureau of Economic Research.

Epstein, Larry G., Emmanuel Farhi, and Tomasz Strzalecki, 2014, How much would you pay to resolve long-run risk?, *American Economic Review* 104, 2680–2697.

Epstein, Larry G., and Stanley E. Zin, 1989, Substitution, risk aversion, and the temporal behavior of consumption and asset returns: A theoretical framework, *Econometrica* 57, 937–969.

Estrella, Arturo, and Gikas A. Hardouvelis, 1991, The term structure as a predictor of real economic activity, *Journal of Finance* 46, 555–576.

Fama, Eugene F., and Kenneth R. French, 1989, Business conditions and expected returns on stocks and bonds, *Journal of Financial Economics* 25, 23–49.

Fama, Eugene F., and Kenneth R. French, 1993, Common risk factors in the returns on stocks and bonds, *Journal of Financial Economics* 33, 3–56.

Fama, Eugene F., and Kenneth R. French, 2015, A five-factor asset pricing model, *Journal of Financial Economics* 116, 1–22.

Fama, Eugene F., and Kenneth R. French, 2016, Dissecting anomalies with a five-factor model, *Review of Financial Studies* 29, 69–103.

Fama, Eugene F., and James D. MacBeth, 1973, Risk, return, and equilibrium: Empirical tests, *Journal of Political Economy* 81, 607–636.

Ferson, Wayne, Suresh Nallareddy, and Biqin Xie, 2013, The out-of-sample performance of long run risk models, *Journal of Financial Economics* 107, 537–556.

Ferson, Wayne E., and Campbell R. Harvey, 1991, The variation of economic risk premiums, *Journal of Political Economy* 99, 385–415.

Ferson, Wayne E., Sergei Sarkissian, and Timothy T. Simin, 2003, Spurious regressions in financial economics?, *Journal of Finance* 58, 1393–1414.

Frisch, Ragnar, 1933, Propagation problems and impulse problems in dynamic economics, Economic Essays in Honour of Gustav Cassel.

Gençay, Ramazan, Nikola Gradojevic, Faruk Selçuk, and Brandon Whitcher, 2010, Asymmetry of information flow between volatilities across time scales, *Quantitative Finance* 10, 895–915.

Gençay, Ramazan, Faruk Selçuk, and Brandon Whitcher, 2001, *An Introduction to Wavelets and Other Filtering Methods in Finance and Economics* (Elsevier Science).

Gençay, Ramazan, and Daniele Signori, 2015, Multi-scale tests for serial correlation, *Journal of Econometrics* 184, 62–80.

Ghosh, Anisha, and George M. Constantinides, 2014, Prices, consumption, and dividends over the business cycle: A tale of two regimes, Working Paper 20678, National Bureau of Economic Research.

Gospodinov, Nikolay, Raymond Kan, and Cesare Robotti, 2014, Misspecification-robust inference in linear asset-pricing models with irrelevant risk factors, *Review of Financial Studies* 27, 2139–2170.

Goyal, Amit, 2012, Empirical cross-sectional asset pricing: a survey, *Financial Markets and Portfolio Management* 26, 3–38.

Grammig, Joachim, and Eva-Maria Schaub, 2014, Give me strong moments and time: Combining gmm and smm to estimate long-run risk asset pricing models, Working Paper, Available at SSRN: http://ssrn.com/abstract=2386094.

Guay, Alain, and Pierre St.-Amant, 2005, Do the hodrick-prescott and baxter-king filters provide a good approximation of business cycles?, *Annales d'Économie et de Statistique* 133–155.

Hahn, Jaehoon, and Hangyong Lee, 2006, Yield spreads as alternative risk factors for size and book-to-market, *Journal of Financial and Quantitative Analysis* 41, 245–269.

Hamilton, James D., 1994, *Time Series Analysis* (Princeton University Press).

Hansen, Lars Peter, John C. Heaton, and Nan Li, 2008, Consumption strikes back? measuring long-run risk, *Journal of Political Economy* 116, 260–302.

Hansen, Lars Peter, and Robert J Hodrick, 1980, Forward Exchange Rates as Optimal Predictors of Future Spot Rates: An Econometric Analysis, *Journal of Political Economy* 88, 829–853.

Hansen, Peter Reinhard, 2005, A test for superior predictive ability, *Journal of Business & Economic Statistics* 23, 365–380.

Harvey, Andrew C., 1990, *Forecasting, Structural Time Series Models and the Kalman Filter* (Cambridge University Press).

Harvey, Andrew C., and Albert Jaeger, 1993, Detrending, stylized facts and the business cycle, *Journal of Applied Econometrics* 8, 231–247.

Harvey, Campbell R., Yan Liu, and Heqing Zhu, 2016, ... and the cross-section of expected returns, *Review of Financial Studies* 29, 5–68.

Hayashi, Fumio, 2000, *Econometrics* (Princeton University Press).

Hodrick, Robert J., and Edward C. Prescott, 1997, Postwar u.s. business cycles: An empirical investigation, *Journal of Money, Credit and Banking* 29, 1–16.

Hou, Kewei, Chen Xue, and Lu Zhang, 2015, Digesting anomalies: An investment approach, *Review of Financial Studies* 28, 650–705.

Jagannathan, Ravi, and Yong Wang, 2007, Lazy investors, discretionary consumption, and the cross-section of stock returns, *Journal of Finance* 62, 1623–1661.

Jagannathan, Ravi, and Zhenyu Wang, 1996, The conditional capm and the cross-section of expected returns, *Journal of Finance* 51, 3–53.

Jarque, Carlos M., and Anil K. Bera, 1980, Efficient tests for normality, homoscedasticity and serial independence of regression residuals, *Economics Letters* 6, 255–259.

Johannes, Michael, Lars A. Lochstoer, and Yiqun Mou, 2016, Learning about consumption dynamics, *Journal of Finance* 71, 551–600.

Jurado, Kyle, Sydney C. Ludvigson, and Serena Ng, 2015, Measuring uncertainty, *American Economic Review* 105, 1177–1216.

Kaltenbrunner, Georg, and Lars A. Lochstoer, 2010, Long-run risk through consumption smoothing, *Review of Financial Studies* 23, 3190–3224.

Kalyvitis, Sarantis, and Ekaterini Panopoulou, 2013, Estimating C-CAPM and the equity premium over the frequency domain, *Studies in Nonlinear Dynamics & Econometrics* 17, 551–571.

Kamara, Avraham, Robert A. Korajczyk, Xiaoxia Lou, and Ronnie Sadka, 2015, Horizon pricing, Forthcoming, Journal of Financial and Quantitative Analysis. Available at SSRN: http://ssrn.com/abstract=2114987.

Kan, Raymond, and Cesare Robotti, 2009, Model comparison using the Hansen-Jagannathan distance, *Review of Financial Studies* 22, 3449–3490.

Kan, Raymond, and Cesare Robotti, 2015, The exact distribution of the Hansen-Jagannathan bound, Working paper, Available at SSRN: http://ssrn.com/abstract=1076687.

Kan, Raymond, Cesare Robotti, and Jay Shanken, 2013, Pricing model performance and the two-pass cross-sectional regression methodology, *Journal of Finance* 68, 2617–2649.

Kan, Raymond, and Chu Zhang, 1999, Two-pass tests of asset pricing models with useless factors, *Journal of Finance* 54, 203–235.

Krishnamurthy, Arvind, and Annette Vissing-Jorgensen, 2012, The Aggregate Demand for Treasury Debt, *Journal of Political Economy* 120, 233–267.

Kwiatkowski, Denis, Peter C.B. Phillips, Peter Schmidt, and Yongcheol Shin, 1992, Testing the null hypothesis of stationarity against the alternative of a unit root: How sure are we that economic time series have a unit root?, *Journal of Econometrics* 54, 159–178.

Lahiri, Soumendra N., 1999, Theoretical comparisons of block bootstrap methods, *Annals of Statistics* 27, 386–404.

Lee, Jin, and Yongmiao Hong, 2001, Testing for serial correlation of unknown form using wavelet methods, *Econometric Theory* 17, 386–423.

Lettau, Martin, and Sydney Ludvigson, 2001, Consumption, aggregate wealth, and expected stock returns, *Journal of Finance* 56, 815–849.

Lettau, Martin, and Sydney C. Ludvigson, 2010, Measuring and modeling variation in the risk-return trade-off, in Yacine Ait-Sahalia, and Lars Peter Hansen, eds., *Handbook of Financial Econometrics: Tools and Techniques*, volume 1 of *Handbooks in Finance*, 617–690 (North-Holland, San Diego).

Lettau, Martin, Matteo Maggiori, and Michael Weber, 2014, Conditional risk premia in currency markets and other asset classes, *Journal of Financial Economics* 114, 197–225.

Lewellen, Jonathan, 2004, Predicting returns with financial ratios, *Journal of Financial Economics* 74, 209–235.

Lewellen, Jonathan, Stefan Nagel, and Jay Shanken, 2010, A skeptical appraisal of asset pricing tests, *Journal of Financial Economics* 96, 175–194.

Liu, Laura Xiaolei, and Lu Zhang, 2008, Momentum profits, factor pricing, and macroeconomic risk, *Review of Financial Studies* 21, 2417–2448.

Ljung, G. M., and G. E. P. Box, 1978, On a measure of lack of fit in time series models, *Biometrika* 65, 297–303.

Ludvigson, Sydney C., and Serena Ng, 2007, The empirical risk-return relation: A factor analysis approach, *Journal of Financial Economics* 83, 171–222.

Ludvigson, Sydney C., and Serena Ng, 2009, A factor analysis of bond risk premia, NBER Working Papers 15188, National Bureau of Economic Research, Inc.

Maio, Paulo, and Pedro Santa-Clara, 2012, Multifactor models and their consistency with the ICAPM, *Journal of Financial Economics* 106, 586–613.

Mallat, Stephane G., 1989a, Multiresolution approximations and wavelet orthonormal bases of L2(R), *Transactions of the American Mathematical Society* 315, 69–87.

Mallat, Stephane G., 1989b, A theory for multiresolution signal decomposition: the wavelet representation, *IEEE Transactions on Pattern Analysis and Machine Intelligence* 11, 674–693.

Merton, Robert C., 1973, An intertemporal capital asset pricing model, *Econometrica* 41, 867–887.

Müller, Ulrich K., and Mark W. Watson, 2008, Testing models of low-frequency variability, *Econometrica* 76, 979–1016.

Müller, Ulrich K., and Mark W. Watson, 2013, Low-frequency robust cointegration testing, *Journal of Econometrics* 174, 66–81.

Müller, Ulrich K., and Mark W. Watson, 2015, Low-frequency econometrics, Working Paper 21564, National Bureau of Economic Research.

Murray, Christian J., 2003, Cyclical Properties of Baxter-King Filtered Time Series, *Review of Economics and Statistics* 85, 472–476.

Nason, Guy P., and Bernard W. Silverman, 1995, The stationary wavelet transform and some statistical applications, in Anestis Antoniadis, and Georges Oppenheim, eds., *Wavelets and Statistics*, volume 103 of *Lecture Notes in Statistics*, 281–299 (Springer New York).

Newey, Whitney, and Kenneth D. West, 1987, A simple, positive semi-definite, heteroskedasticity and autocorrelation consistent covariance matrix, *Econometrica* 55, 703–708.

Nordman, Daniel J., 2009, A note on the stationary bootstrap's variance, *Annals of Statistics* 37, 359–370.

Novy-Marx, Robert, 2013, The other side of value: The gross profitability premium, *Journal of Financial Economics* 108, 1–28.

Ortu, Fulvio, Federico Severino, Andrea Tamoni, and Claudio Tebaldi, 2016, A persistence-based wold-type decomposition for stationary time series, Working Paper, Available at SSRN: http://ssrn.com/abstract=1973049.

Ortu, Fulvio, Andrea Tamoni, and Claudio Tebaldi, 2013, Long-run risk and the persistence of consumption shocks, *Review of Financial Studies* 26, 2876–2915.

Ozoguz, Arzu, 2009, Good times or bad times? investors' uncertainty and stock returns, *Review of Financial Studies* 22, 4377–4422.

Parker, Jonathan A., and Christian Julliard, 2005, Consumption risk and the cross section of expected returns, *Journal of Political Economy* 113, 185–222.

Pastor, Lubos, and Robert F. Stambaugh, 2003, Liquidity risk and expected stock returns, *Journal of Political Economy* 111, 642–685.

Patton, Andrew, Dimitris N. Politis, and Halbert White, 2009, Correction to "automatic block-length selection for the dependent bootstrap", *Econometric Reviews* 28, 372–375.

Patton, Andrew J., and Allan Timmermann, 2010, Monotonicity in asset returns: New tests with applications to the term structure, the CAPM, and portfolio sorts, *Journal of Financial Economics* 98, 605–625.

Percival, Donald, and Andrew Walden, 2000, *Wavelet Methods for Time Series Analysis* (Cambridge University Press).

Percival, Donald P., 1995, On estimation of the wavelet variance, *Biometrika* 82, 619–631.

Pesquet, Jean-Christophe, Hamid Krim, and Hervé Carfantan, 1996, Time-invariant orthonormal wavelet representations, *IEEE Transactions on Signal Processing* 44, 1964–1970.

Petkova, Ralitsa, 2006, Do the fama-french factors proxy for innovations in predictive variables?, *Journal of Finance* 61, 581–612.

Phillips, Peter C. B., and Pierre Perron, 1988, Testing for a unit root in time series regression, *Biometrika* 75, 335–346.

Politis, Dimitris N., and Joseph P. Romano, 1994, The stationary bootstrap, *Journal of the American Statistical Association* 89, 1303–1313.

Politis, Dimitris N., and Halbert White, 2004, Automatic block-length selection for the dependent bootstrap, *Econometric Reviews* 23, 53–70.

Qiao, Xiao, 2013, Cross-sectional evidence in consumption mismeasurement, Working Paper, Available at SSRN: http://ssrn.com/abstract=2317486.

Ramsey, James B., 1999, The contribution of wavelets to the analysis of economic and financial data, *Philosophical Transactions of the Royal Society of London A: Mathematical, Physical and Engineering Sciences* 357, 2593–2606.

Ravn, Morten O., and Harald Uhlig, 2002, On adjusting the Hodrick-Prescott filter for the frequency of observations, *Review of Economics and Statistics* 84, 371–375.

Renaud, Olivier, Jean-Luc Starck, and Fionn Murtagh, 2005, Wavelet-based combined signal filtering and prediction, *IEEE Transactions on Systems, Man, and Cybernetics, Part B: Cybernetics,* 35, 1241–1251.

Romano, Joseph P., and Michael Wolf, 2005, Stepwise multiple testing as formalized data snooping, *Econometrica* 73, 1237–1282.

Savov, Alexi, 2011, Asset pricing with garbage, *Journal of Finance* 66, 177–201.

Schorfheide, Frank, Dongho Song, and Amir Yaron, 2014, Identifying long-run risks: A bayesian mixed-frequency approach, Working Paper 20303, National Bureau of Economic Research.

Shanken, Jay, 1992, On the estimation of beta-pricing models, *Review of Financial Studies* 5, 1–33.

Slutzky, Eugen, 1937, The summation of random causes as the source of cyclic processes, *Econometrica* 5, 105–146.

Stock, James H, and Mark W Watson, 2002, Macroeconomic forecasting using diffusion indexes, *Journal of Business & Economic Statistics* 20, 147–162.

Stoica, Petre, and Randolph Moses, 2005, *Spectral Analysis of Signals* (Pearson Prentice Hall).

Subrahmanyam, Avanidhar, 2010, The cross-section of expected stock returns: What have we learnt from the past twenty-five years of research?, *European Financial Management* 16, 27–42.

Tédongap, Roméo, 2015, Consumption volatility and the cross-section of stock returns, *Review of Finance* 19, 367–405.

Valkanov, Rossen, 2003, Long-horizon regressions: theoretical results and applications, *Journal of Financial Economics* 68, 201–232.

Vassalou, Maria, 2003, News related to future GDP growth as a risk factor in equity returns, *Journal of Financial Economics* 68, 47–73.

Vuong, Quang H., 1989, Likelihood ratio tests for model selection and non-nested hypotheses, *Econometrica* 57, 307–333.

Wang, Huijun, and Jianfeng Yu, 2015, Dissecting the profitability premium, Working Paper, Available at SSRN: http://ssrn.com/abstract=1711856.

Weil, Philippe, 1989, The equity premium puzzle and the risk-free rate puzzle, *Journal of Monetary Economics* 24, 401–421.

Welch, Ivo, and Amit Goyal, 2008, A comprehensive look at the empirical performance of equity premium prediction, *Review of Financial Studies* 21, 1455–1508.

Welch, Peter, 1967, The use of fast fourier transform for the estimation of power spectra: A method based on time averaging over short, modified periodograms, *IEEE Transactions on Audio and Electroacoustics* 15, 70–73.

Wong, Ping Wah, 1993, Wavelet decomposition of harmonizable random processes, *IEEE Transactions on Information Theory* 39, 7–18.

Yu, Jianfeng, 2012, Using long-run consumption-return correlations to test asset pricing models, *Review of Economic Dynamics* 15, 317–335.

Yule, G. Udny, 1927, On a method of investigating periodicities in disturbed series, with special reference to wolfer's sunspot numbers, *Philosophical Transactions of the Royal Society of London A: Mathematical, Physical and Engineering Sciences* 226, 267–298.